IN-91

24806

P128

[illegible]378

[illegible]ghness Project

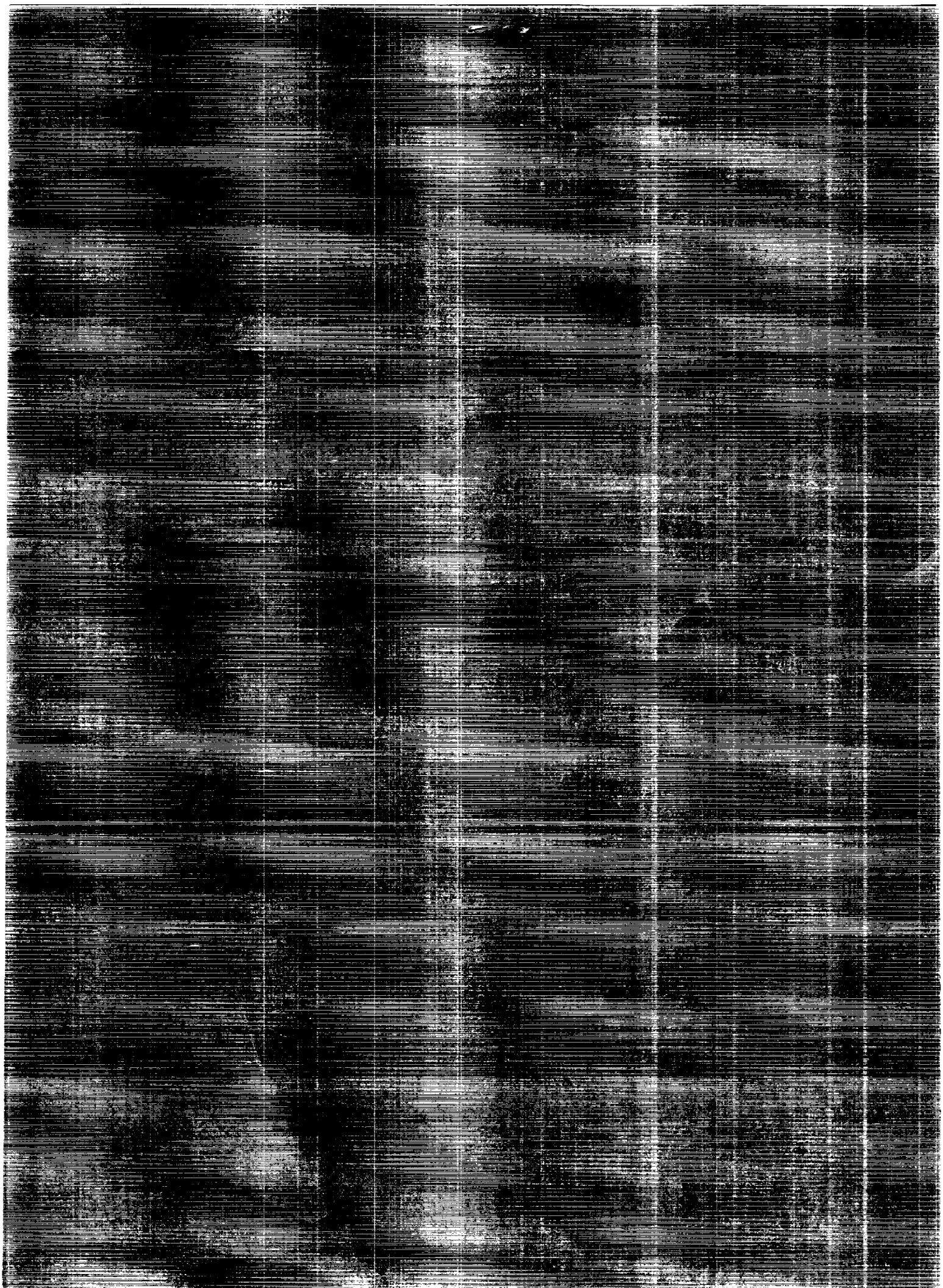

NASA Contractor Report 4378

Radar-Aeolian Roughness Project

R. Greeley, A. Dobrovolskis, and L. Gaddis
Arizona State University
Tempe, Arizona

J. Iversen
Iowa State University
Ames, Iowa

N. Lancaster and R. Leach
Arizona State University
Tempe, Arizona

K. Rasnussen
Aarhus University
Aarhus C, Denmark

S. Saunders, J. VanZyl, and S. Wall
Jet Propulsion Laboratory
Pasadena, California

B. White
University of California
Davis, California

H. Zebker
Jet Propulsion Laboratory
Pasadena, California

Prepared for
NASA Office of Space Science and Applications
under Grant NSG-7415

National Aeronautics and
Space Administration

Office of Management

Scientific and Technical
Information Program

1991

Table of Contents

Abstract

The objective of this project is to establish an empirical relationship between measurements of radar, aeolian, and surface roughness on a variety of natural surfaces and to understand the underlying physical causes. This relationship will form the basis for developing a predictive equation to derive aeolian roughness from radar backscatter. Preliminary studies and first principles support the existence of such a relationship at L_{HH}. To increase the confidence in the observed preliminary correlation and to extend the application of the technique to future studies involving regional aeolian dynamics, the study will be expanded by: 1) defining the empirical relationship between the radar backscatter and aeolian roughness, 2) investigating the sensitivity of the relationship to microwave parameters using calibrated multiple wavelength, polarization, and incidence angle aircraft and Shuttle Imaging Radar (SIR-C) data, and 3) applying the results to models to gain an understanding of the physical properties which produce the relationship. The approach will combine the measurement, analysis, and interpretation of radar SIR-C data with field investigations of aeolian processes and surface roughness, and incorporate results from laboratory simulations.

This report gives results from investigations carried out in 1989 on the principal elements of the project, with separate sections on field studies, radar data analysis, laboratory simulations, and development of theory for planetary applications.

1.0 INTRODUCTION

R. Greeley, N. Lancaster, and L. Gaddis

The Radar Aeolian Roughness Project (RARP) focuses on the use of multiparameter radar data to assess aeolian roughness, which is an important factor in determining aeolian sand transport. Determination of valid transport rates is necessary for studies of regional sediment budgets, the evolution of sand seas, and desertification. Because aeolian roughness is difficult to measure, conventional methods of calculating potential sand transport assume a smooth surface composed of like particles which may lead to inaccurate estimates of sand movement. Radar backscatter can provide an indication of surface roughness, and thus aeolian roughness, if the effects of local slope and dielectric constant are minor. Preliminary studies of desert surfaces suggest that a relationship exists between radar backscatter (σ^{o}) and aeolian roughness (z_o) (Fig. 1.1 and Greeley et al., 1988). More work is needed to define this relationship and to establish which combination of radar parameters (angle, polarization, and wavelength) provides backscatter functions that are the most useful indicators of aeolian roughness.

The specific objective is to develop a technique for deriving aeolian roughness (z_o) for different geologic surfaces from calibrated radar (SAR) measurements of backscatter at multiple frequencies, polarizations, and incidence angles. The scale of roughness on surfaces important for aeolian studies varies from < cm to several meters. Multifrequency SAR may be able to obtain roughness values representative of different scales of roughness; but before this is possible, the proper combination of wavelength, polarization state, and incidence angle must be determined. Such data will be supplied by aircraft systems and the Shuttle Imaging Radar (SIR-C). Technique development using SIR-C data will form the basis for extending our results to regional and global investigations of aeolian environments with future spaceborne imaging radar systems planned as part of EOS for Earth and Magellan for Venus. This extension can be done with confidence only if models having a physical basis exist and agree with empirical data.

A combination of radar analysis and field investigations are being employed to determine the relationship between radar backscatter and aeolian roughness and to develop a technique by which radar backscatter can be used to derive a roughness parameter for input to wind profile equations. Development of a model, based on boundary layer theory, from which aeolian roughness can be extracted from surface roughness is a fundamental problem and an ongoing area of research.

The relationship between backscatter and aeolian parameters on land appears to be similar to those governing backscatter from the ocean surface, as measured by Seasat and other oceanographic radar systems (e.g., Krishen, 1971; Jones and Schroeder, 1978; Moore and Fung, 1979; Jones et al., 1981; Liu and Large, 1981; and others). Although the roughness of the air-sea interface depends on wind conditions, the successful recovery of wind and wave patterns at sea from radar data encourages an analogous approach to remote sensing of aeolian roughness over land.

1.1 Significance and Derivation of Aeolian Roughness

In many regions, wind can transport large amounts of sand over long distances, linking zones of deflation and sand supply to depositional areas. Sand accumulations cover 10 to 30% of the surface in many deserts, and constitute important sedimentary systems both today and in the geologic past. Regional or subcontinental aeolian transport systems have been assessed from wind data by Dubief (1952), Brookfield (1970), Wilson (1971), Lancaster (1985), and others and confirmed by studies of Landsat and Meteosat images (e.g., El Baz and Wolfe, 1982; Mainguet, 1984). Within these systems, sand is transported over surfaces of different roughness characteristics, including river valleys, sand sheets, dunes, and rock and gravel plains (Breed et al., 1979; Fryberger and Ahlbrandt, 1979; Mainguet, 1978, 1984).

In many arid regions, the mobilization of silt and clay-sized particles by the wind generates dust storms, the occurrence of which may have important environmental and economic impacts (Morales, 1979; Cooke et al., 1982; Goudie, 1983; Middleton et al., 1986). Dust deposition is also important to soil and desert varnish formation in arid regions (McFadden et al., 1984). Middleton et al. (1986) indicate that agricultural development of alluvial plains and soils developed on Quaternary alluvial and lacustrine deposits is a major source of dust. Widespread desertification is the result of over-utilization of these areas.

With increasing development of desert regions, windblown sand and dust are a significant hazard to human activity (Embabi, 1982; Cooke et al., 1982; Watson, 1985). Mitigation of existing hazards and prevention of future impacts require recognition and characterization of active aeolian surfaces. Prediction of areas of potential sand transport and dust generation from SIR-C, Magellan, and future EOS data will contribute to the environmental assessment of desert regions.

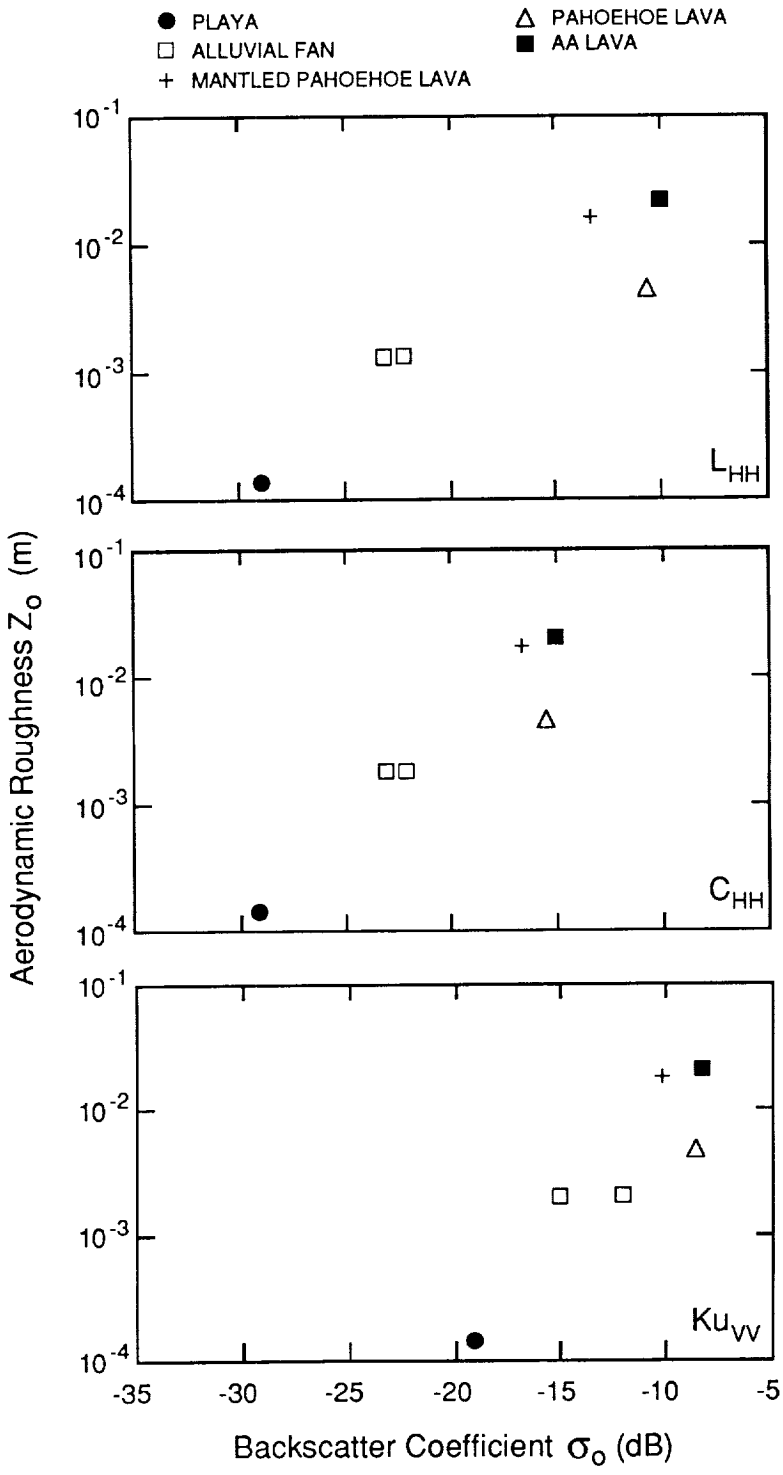

Figure 1.1. Plots of aeolian roughness (z_o) versus radar backscatter coefficient for three typical desert surfaces including bare playa, alluvial fan, and lava flow. Backscatter values for L_{HH}, C_{HH}, and Ku_{VV} data are for 35° incidence angle. Both aeolian roughness and radar backscatter increase with the surface roughness.

Estimates of sand transport rates in desert regions by Finkel (1959), Wilson (1971), Fryberger and Ahlbrandt (1979), and Lancaster (1985) are based on equations developed by Bagnold (1941, 1953) or Lettau and Lettau (1978). These assume a linear relationship between surface shear stress, as expressed by surface friction speed, u_*, and wind velocity, U, for a *constant value for aerodynamic roughness height*, z_o (symbols defined in Table 1.1). Use of such assumptions makes it possible to calculate sand transport rates from standard meteorological observations at a single height above the ground. However, such calculated rates may be in error by an order of magnitude because of variations in surface roughness which affect z_o and u_*. RARP involves assessing techniques to use SAR data to produce an aeolian roughness parameter which can be used to obtain valid estimates of potential sand transport rates.

Aeolian transport of sand results from the drag or shear stress imparted by the wind to the surface. Shear stress causes an increase in wind velocity with height in the turbulent atmospheric boundary layer, and can be written:

$$\tau = \rho u_*^2 \qquad (1.1)$$

where τ is surface shear stress, ρ is air density and u_* is friction speed, determined from the nature of the wind velocity profile. Following mixing length theory, time averaged wind speed profiles over a natural surface under conditions of neutral stability can be expressed by:

$$U = u_*/0.4 \, (\ln ((z - D)/z_o)) \qquad (1.2)$$

where U is wind velocity, z is a reference height, and D is the zero plane displacement.

Aeolian roughness is a function of the size and spacing of roughness elements on the surface (Iversen et al., 1973; Lyles et al., 1974; Greeley and Iversen, 1985). For closely packed objects, such as sand grains, z_o is approximately 1/30 their reference height (h). A maximum value of z_o, equal to 1/8 h, is obtained when the roughness elements are spaced at twice their height. As roughness element

Table 1.1 Symbols And Abbreviations

A	Site area
C	Mass transport coefficient
D	Zero plane displacement
D_p	Particle diameter
EOS	Earth Observing System
g	Gravitational acceleration
h	Reference height of roughness elements
n	Number of individual roughness elements
q	Mass transport flux of sand
q_o	Mass transport in absence of nonerodible roughness elements
q_r	Mass transport in presence of nonerodible roughness elements
Ri	Bulk Richardson number
Ri_g	Richardson number or gradient Richardson number
s	Silhouette area of roughness element
SAR	Synthetic Aperture Radar
TM	Thematic mapper
u_*	Wind friction speed
u_{*t}	Threshold friction speed
u_{*to}	Threshold friction speed for sand sheet
u_{*tr}	Threshold friction speed in presence of non-erodible roughness elements
U	Wind velocity
z	Height above surface
z_o	Aeolian roughness height
L-,C-,Ku-band	Radar frequencies with wavelengths of ~25, 3.8-7.5, and 1.7–2.4 cm respectively
HH	Horizontal transmit, horizontal receive polarization
VV	Vertical transmit, vertical receive polarization
HV	Horizontal transmit, vertical receive polarization
VH	Vertical transmit, horizontal receive polarization
θ	Incidence angle (angle between the surface normal and the incoming radar wave)
τ	Surface shear stress
ρ	Air density
σ°	Radar backscatter coefficient

spacing is increased from the closely packed situation, z_o increases to a maximum at a certain spacing, then decreases as spacing is increased still further.

Measurements of z_o on geologic surfaces range from 0.02 cm on a playa surface to 1-2 cm on rough lava flows with a local relief of 80 cm (Greeley and Iversen, 1987; Appendix II). On sand surfaces z_o is typically on the order of 0.0008-0.0010 cm when no sand transport is taking place, but rises to 0.3-0.8 cm when active sand transport by saltation is occurring (Bagnold, 1941).

Potential sand transport rates can be calculated from wind data using a variety of formulae which are summarized in Greeley and Iversen (1985). Sand transport rates vary between surfaces of different roughness heights because threshold friction speed, u_{*t}, varies with the ratio of the average particle diameter, D_p, to equivalent roughness height, D_p/z_o. It is assumed here that the effect of roughness on the saltation threshold is approximately given by:

$$u_{*tr}/u_{*to} = 2(D_p/z_o)^{-1/5} \qquad (1.3)$$

where u_{*to} is threshold friction speed in the absence of non-erodible roughness elements and u_{tr} is the threshold friction-speed in the presence of non-erodible roughness elements. If, for example, the mass transport rate, q, is expressed as:

$$q = C\rho u_*^2 (u_* - u_{*t}) / g \qquad (1.4)$$

where ρ is air density, g is gravitational acceleration, and C is a mass transport coefficient, then the effect of non-erodible roughness on mass transport can be estimated by assuming that the effect is due only to the increase in threshold friction speed. Defining q_r as the mass transport in the presence of non-erodible roughness elements and q_o as the mass transport rate in the absence of non-erodible roughness elements,

$$q_r/q_o = (u_* - u_{*to}(z_o/D_p)^{-1/5}) / (u_* - u_{*to}) \qquad (1.5)$$

For given values of u_*, the effect of increase in roughness is to decrease the mass transport rate, until a roughness level is reached at which sand transport is no longer possible (Fig. 1.2).

It should be noted, however, for a given synoptic wind system, that an aerodynamically rougher surface exhibits a larger value of surface friction speed, so that mass transport may be larger or smaller on the rougher surface, depending on the relative values of u_*, u_{*to}, and u_{*tr}. Greeley and Iversen (1987) compared sand transport rates on an alluvial

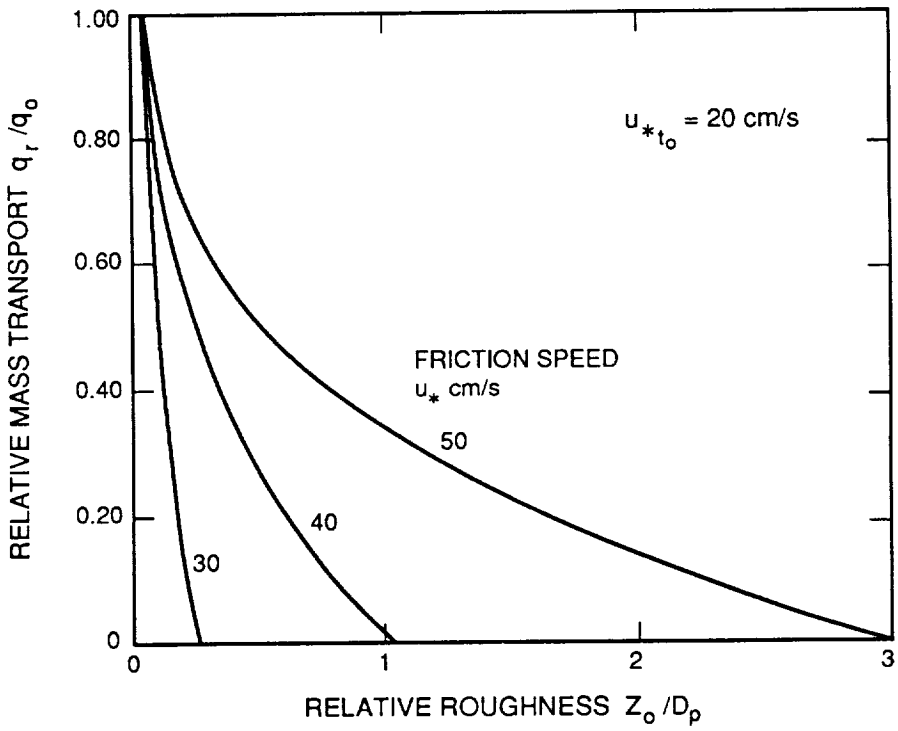

Figure 1.2. The influence of surface roughness on aeolian mass transport. Equation 1.5 was used to produce this plot. Symbols defined in the text and in Table 1.1.

fan and lava flow and showed that sand transport occurs only on the smoother alluvial fan surface at low wind velocities; at intermediate wind velocities, transport occurred on both surfaces, with greater sand transport on the alluvial fan; however, at high wind velocities, sand transport rates possibly could be higher on the rough lava surface.

It is clear that aeolian roughness (z_o) is an important quantity which strongly influences the absolute and relative rates of sand transport by the wind. Limited data on aeolian roughness on different surfaces have been derived from field measurements of wind velocity profiles. Typically, many hours of data recording are necessary to obtain representative wind profiles, and consequently the existing data set is very small and covers a limited number of surface types. Wind profile measurements are not a part of routine meteorological observations and there is a need to develop a technique for deriving aeolian roughness from remotely sensed data. Radar interacts with roughness elements at the scale of the wavelength and may be useful in obtaining an aeolian roughness parameter. These values can then be used to assess aeolian sand transport potential on a regional scale.

1.2 Surface Roughness Information from Radar Backscatter

When microwave radiation is directed at a target surface, the strength of the returned signal depends on the properties of the surface and the characteristics of the radar system. Surface properties affecting the backscatter include: 1) the roughness of the surface at the scale of the radiation's wavelength, 2) the local incidence angle (angle between the surface normal and the incoming radiation) averaged over the spatial extent of the target, and 3) the complex dielectric constant of the target. For surfaces with modest topography at the scale resolvable by the sensor and whose electromagnetic properties are similar, the first effect dominates and the returned signal strength can be taken as a measure of the surface roughness at or near the wavelength scale (Farr and Engheta, 1983; Blom et al., 1987). The dielectric constant influences the magnitude of the backscatter coefficient and for naturally occurring particulate surfaces is primarily a function of soil moisture content. The variation of radar backscatter with dielectric constant is beyond the scope of this project and data used will be constrained to a narrow range of "dry" conditions. Important characteristics of the radar system include polarization, wavelength, and incidence angle.

Interactions of microwaves with geologic surfaces consist of coherent and noncoherent surface scattering and volume scattering. Theoretical models employing idealized surface roughness elements are used to relate radar backscatter to surface roughness (e.g., Ulaby et al., 1982). For all of the models, the size and spacing of the roughness elements responsible for backscatter are dependent on radar wavelength and incidence angle.

Understanding the quantitative relationship between radar backscatter coefficient and surface roughness requires statistical descriptions of the surface and calibrated backscatter values (Farr and Engheta, 1983). Although the lack of calibrated radar data has hindered efforts to develop a quantitative relationship, some correlations have been reported. Statistical measures of roughness which are used in conjunction with various theoretical models include standard deviation of height (rms, root mean square height), correlation length, power density spectra, and rms slopes (e.g., Schaber et al., 1980a,b; Ulaby et al., 1982; Farr and Engheta, 1983). Schaber et al. (1976) and Evans (1978) found a correlation between a single parameter combining different aspects of surface roughness and relative returned power. Using externally calibrated SIR-B images, Wang et al. (1986) also found a strong relationship between rms height and the scattering coefficient.

Multifrequency and multipolarization data sets increase the ability to discriminate and interpret surface roughness and, in many cases, geologic units (Dellwig and Moore, 1966; Dellwig, 1969; Schaber et al., 1976; Daily et al., 1978a,b; Evans, 1978; Malin et al., 1978; Schaber et al., 1980a; Evans et al., 1986). Because the radar interacts with the roughness elements at the scale of the radar wavelength, the amount of backscatter is strongly dependent on the radar frequency (Dellwig, 1969; Elachi et al., 1980; Farr and Engheta, 1983; Blom et al., 1987; Blom, 1987). Using the Rayleigh criterion and a Bragg scattering model, the dominant and overall roughness spectrum of a surface can be predicted by comparing and ratioing multiple frequency and polarization data sets (Schaber et al., 1976; Daily et al., 1978a; Evans, 1978; Malin et al., 1978). Comparison of multifrequency, multipolarization radar data also yields information on the effects of the topography, dielectric constant, and subsurface penetration (Daily et al., 1978a). It is anticipated that SIR-C will provide calibrated data at multiple frequencies and polarizations which will allow better discrimination of units and interpretation of the roughness spectrum of the surface of each unit.

The influence of the incidence angle on radar backscatter for surfaces of different roughness is shown by theoretical backscatter curves in Figure 1.3. Reversal in relative magnitude of radar returns

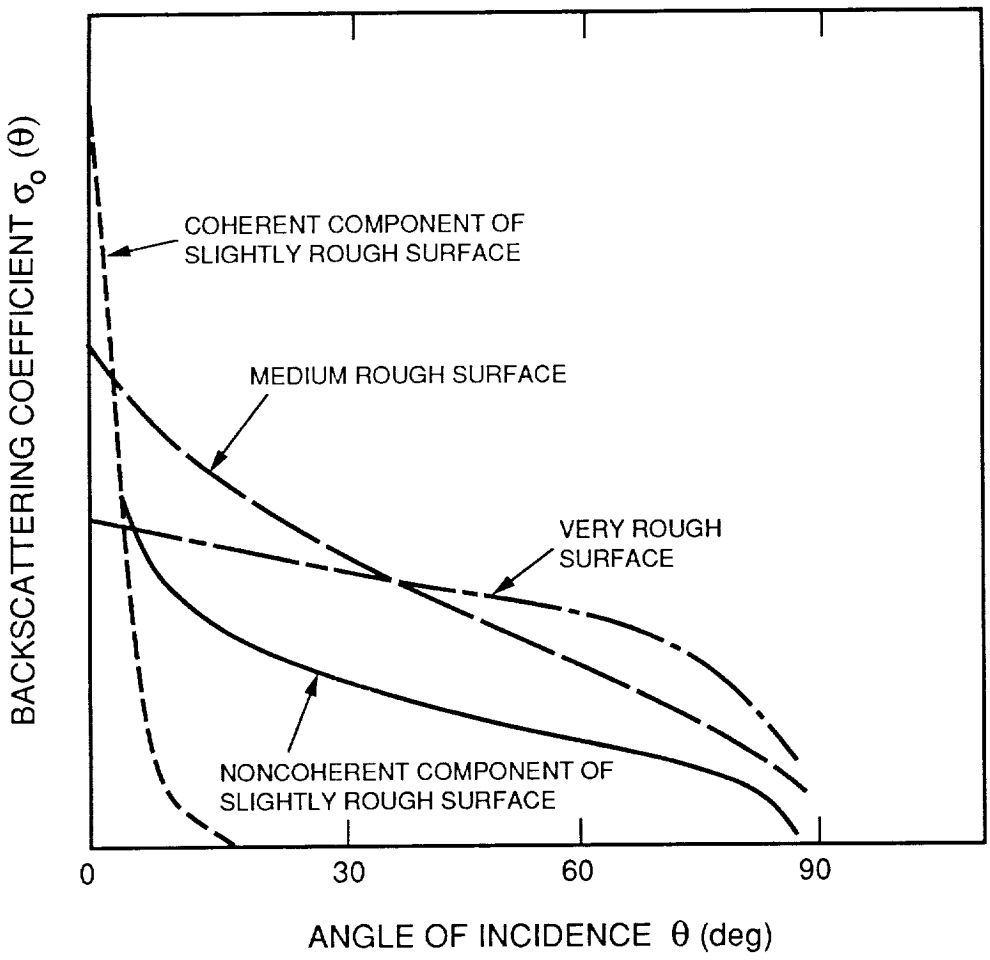

Figure 1.3. Idealized backscatter curves for a slightly rough, medium rough, and very rough surface. From Ulaby et al., 1982.

occurs between 5° and 30° and affects the ability to discriminate between surfaces of different roughnesses. Above 30° increased separation between the curves suggests better discrimination of units. However, the decrease in the return signal with increasing angle for slight to medium rough targets suggests that increased discrimination of these surfaces could be gained using several incidence angles. Comparative studies of SAR data support the roughness reversal and variation of effective roughness with incidence angle (Elachi et al., 1980; Schaber et al., 1980a; Blom, 1987). Backscatter curves from field studies produced similar variations of radar return versus incidence angles (Ulaby et al., 1978). Radar data and the future SIR-C mission provide the opportunity to acquire multiple incidence angle data to better discriminate slightly rough to medium surfaces and to determine at which angles the radar and aeolian roughness correlate the best. Derivation of techniques to extract surface roughness from radar data are currently under development (VanZyl et al., 1987; Zebker et al., 1987).

1.3 Correlation of Aeolian Roughness and Radar Backscatter

Preliminary studies indicate that there is a relationship between aeolian roughness and radar backscatter (Fig. 1.1 and Greeley et al., 1988). Three surface types were assessed, a smooth playa, an alluvial fan, and a rough lava flow. Calibrated values of backscatter coefficients were obtained from scatterometer data for Pisgah lava field, California. Data were acquired in L-, C-, and Ku-band by the NASA/JSC (Johnson Space Center) Scatterometer. The L- and C-band data are HH polarized and the Ku-band data are VV polarized. Surface units were identified from aerial photographs and geologic maps and an average backscatter coefficient was obtained for each. A discriminant analysis technique was used to determine which incidence angles provided the best discrimination between the units.

Aeolian roughness values were derived from wind velocity profiles recorded for comparable surfaces. Wind measurements for three lava flow

textures were collected on the Pisgah lava field. Wind data for a bare playa were measured at Lucerne Dry Lake (Sullivan, unpublished data) and for an alluvial fan at a site adjacent to Amboy lava field (Greeley and Iversen, 1987). Because of the variation in surface roughness which exists on alluvial fans (Schaber et al., 1976), the wind data from Amboy was compared to two alluvial fan surfaces at Pisgah. At both locations the sites tested are in the distal parts of young fans and do not contain large boulders and incised channels typical of proximal fan surfaces.

Plots of aeolian roughness heights (z_o) versus radar backscatter coefficients (σ^o) are shown in Figure 1.1 for L-, C-, and Ku-band at 35° incidence. The aeolian roughness height and backscatter coefficient both increase with the increase in surface roughness from smooth playa to rough lava flow. Plots using 30°, 40°, and 45° incidence angle data yielded similar results. The preliminary results show great promise but wind and radar data from the same locations are needed to define and validate the relationship. To do this, calibrated radar data at different frequencies, polarizations, and incidence angles are required to cover a wider range of surfaces.

1.4 Site Selection

The sites selected for detailed field investigations of aeolian and radar roughness characteristics would satisfy the following criteria:

1. Contain a range of commonly occurring desert surfaces which are important sources for sand and dust or over which sand transport takes place.
2. Each surface type should be sufficiently extensive to be identified in the radar data and to allow enough fetch for the wind.
3. Vegetation should be sparse or absent and the surface flat or with low relief.
4. The sites should be easily accessible.

The percentage of the surface area of desert regions covered by different surface types is summarized by Clements et al. (1957) and shown in Table 1.2 below. Major sources of dust and sand for aeolian transport are desert flats, alluvial fans, and playas (Clements et al., 1963). Lyles et al. (1974) indicate that surfaces composed of more than 40% sand-sized particles are most easily erodible. Gillette et al. (1980) found that, for undisturbed surfaces, threshold velocity for particle movement increased from sand dunes through sandy soils of aeolian and fluvial origins, playas, and desert pavement surfaces. Surfaces proposed for this study are, therefore, sandy alluvial fans and desert flats, agricultural fields; sand sheets and low dunes; rocky desert areas, including lava flows and bedrock surfaces; desert pavement surfaces, and playas.

Prior to radar data analysis, the targeted sites are studied using TM images, aerial photographs, and geologic maps to identify the important geologic/geomorphic units. Each unit is mapped by 1) surface type (alluvial fan, playa, etc.), 2) aeolian regime (source, transportation, or depositional area), 3) vegetation, and 4) regional slope. These maps are then used to identify the geomorphic units on the radar images and as a means to assess potential anomalies in radar backscatter.

1.5 Radar Data Requirements and Analysis

Data Requirements. The RARP requires calibrated radar backscatter coefficients at direct and cross polarizations and multiple incidence angles to discriminate between surface roughness units and to better define the overall roughness of the surface. For future applications of the technique, the best radar parameters for defining a roughness parameter which can be used in aeolian transport rate equations need to be defined. Listed in descending order of priority are the specific radar requirements:

Table 1.2 Percent of desert area covered by different surface types

	SW USA	Saharan-Arabian Region
Playas	1.1	1.0
Bedrock	0.7	5.7
Desert flats	20.5	14.7
Fans and bajadas	31.4	2.0
Dunes	0.6	25.0
Dry washes	3.6	1.0
Badlands	2.6	3.0
Volcanic fields	0.2	2.0
Desert mountains	38.1	43.0

1. Calibrated data as backscatter coefficients
2. Dual frequency: P-, L-, and C-band
3. Quad or dual polarization
4. Dynamic range greater than 20 dB
5. Multiple incidence angles
6. Exact resolutions, bits per sample, and swath widths to be determined to optimize the above requirements and the ability to discriminate and characterize surface units

Although it is possible to develop a technique relating only relative return power to aeolian roughness, the results would be site- and image-specific and would not be applicable to future regional studies. As discussed above, it is necessary to obtain P-, L-, and C-band data in at least dual polarization to discriminate surface roughness units and to relate the radar return to surface roughness. Backscatter curves in the preliminary study (Greeley et al., 1988) indicate a range of σ^o for playa to extremely rough lava flows of greater than 20 dB. This indicates a need for either the 8 bps (bits per sample) or (8,4) BFPQ (Block Floating Point Quantizer) data available from SIR-C. Although preliminary studies suggest that the best incidence angles for discriminating between surfaces of different roughness are 30° to 45°, other studies have shown the utility of different angles for identifying geologic units (e.g., Blom et al., 1987). Thus, it would be desirable to obtain SAR data at several incidence angles. The extent of the areas to be studied will be used to determine the tradeoffs to be made concerning swath width, resolution, and dynamic range.

Radar Analysis. Primary radar analysis consists of extracting average backscatter coefficient values for each surface. Digital image processing enables the determination of average backscatter coefficients for each surface on each image. Values of σ^o in the unfiltered calibrated data are averaged over each unit defined on the radar data for all combinations of frequency, polarization, and incidence angle acquired. An average value is derived to represent the surface being sampled by the wind and is used for comparison with aeolian roughness.

1.6 Measurement of Surface Roughness

Radar backscatter is a function of incidence angle, wavelength, polarization, and dielectric constant as well as surface texture. In contrast, the aeolian roughness is a single parameter characteristic of the site and insensitive to conditions. Thus, several sites of distinct radar characteristics can have the same value of z_o. Though not likely, it also may be possible for two surfaces with different z_o to exhibit similar backscatter behavior.

In order to gain physical understanding of the aeolian roughness parameter and to guide our interpretation of the radar returns, we are measuring and analyzing surface texture on at least two scales. Large-scale profiles, tens of meters long, are surveyed both parallel and perpendicular to the dominant wind direction using an electronic distance meter with vertical accuracy of a few centimeters over a 500 m distance. Small-scale profiles a few meters long are measured at intervals along the survey lines. Microrelief at a spacing of 0.01 m are recorded in the field for later analysis.

Lettau (1969) has discussed the relationships between aeolian roughness and the nature of surface roughness elements and suggests that z_o is related to both the effective height, h, of the surface roughness elements as well as their silhouette area, s, measured in the vertical plane across the wind. This relationship is approximately

$$z_o = 0.5\ nhs/A \qquad (1.6)$$

where A is the site area and n is the number of roughness elements in that area. These parameters will also be measured for each site to obtain an objective characterization of surface roughness and to test Lettau's model.

From the measured topographic profiles, statistical descriptions of the surface are extracted, including root mean square (rms) heights, slope distributions, correlation lengths, and power spectra. These will be related to the radar scattering characteristics using models currently under development at Jet Propulsion Laboratory (VanZyl et al., 1987; see also Schaber et al., 1976). The profiles will also be used to quantify the relationship between the distribution of roughness elements and the aeolian roughness as given by boundary-layer theory. The results will help clarify the relations among all three observables (radar backscatter, aeolian roughness, and surface relief) and will be useful in determining the radar parameters most suitable for predicting aeolian roughness.

1.7 Determination of Aeolian Roughness Height, z_o

The goal of the wind measurements is to characterize wind profiles over surfaces of different radar roughness to obtain values for aeolian roughness height (z_o), wind friction speed (u_*), and zero plane displacement (D).

The selection of sites for wind profile measurements take into account the need for an adequate fetch of the wind across the surface so that the boundary layer will be fully developed. An upwind distance of approximately 1000 roughness element heights is suggested by Counihan (1971) from

wind tunnel studies and of 200 roughness elements by Bradley (1968) from field measurements. Wind profile measurements are made with a 9.6 m high field-portable mast, equipped with six cup anemometers. Temperature measurements are made to calculate the Richardson number (Ri) as an index of atmospheric stability.

Data are recorded with a microcomputer data-logging system and reduced at Arizona State University. Criteria for determining the validity and quality of the wind profile data include: 1) constant winds for a period of at least one hour from the dominant wind direction as determined from previous observations, analysis of field data, and aerial photographs; 2) conditions of neutral atmospheric stability, as indicated by the bilk Richardson number (Ri); and 3) wind velocities in excess of the threshold velocity.

Wind data are reduced following the methods employed by Greeley and Iversen (1987). Following mixing length theory, time averaged wind speed profiles over a natural surface in a neutrally stable boundary layer are given by Equation 1.2. An iterative procedure is used to calculate u_* and z_o from the wind profile data. This procedure finds values of z_o and u_* using successive values of D to obtain the best least squares fit to a logarithmic profile.

Values of z_o and u_* for each surface tested are plotted against backscatter coefficients and surface roughness parameters to determine the relationship between the three measurements of roughness. The nature of the empirical relationship is determined by regression analysis.

1.8 Summary

In the chapters that follow, individual reports are given on the principal elements of the project as outlined above.

1.9 References Cited

Bagnold, R.A. 1941. *The Physics of Blown Sand and Desert Dunes*. London: Chapman and Hall, 265 pp.

Bagnold, R.A. 1953. Forme des dunes de sable et regime des vents. Actions Eoliennes, Centre National de Recherches Scientifiques, Colloques Internationaux 35, 23-32.

Blom, R.G. 1987. Effects of variation in incidence angle and wavelength in radar images of volcanic and aeolian terranes. To be submitted to *Int. J. Rem. Sens.*

Blom, R.G., L.R. Schenck, and R.E. Alley, 1987. What are the best radar wavelengths, incidence angles, and polarizations for discrimination among lava flows and sedimentary rocks? A statistical approach. *IEEE Trans. Geosci. and Rem. Sens. GE-25*, 208-213.

Bradley, E.F. 1968. A micrometeorological study of velocity profiles and surface drag in the region modified by a change in surface roughness. *Quar. J. of the Royal Meteor. Soc. 94*, 361-379.

Breed, C.S., S.C. Fryberger, S. Andrews, C. McCauley, F. Lennartz, D. Geber, and K. Horstman, 1979. Regional studies of sand seas using LANDSAT (ERTS) imagery. In E.D. McKee (ed.), A Study of Global Sand Seas. *U.S. Geol. Surv. Prof. Paper 1052*, 305-398.

Brookfield, M., 1970. Dune trend and wind regime in central Australia. *Zeitschrift für Geomorphologie, Supp. 10*, 121-158.

Clements, T. *et al.*, 1957. A study of desert surface conditions. Headquarters Quartermaster Research and Development Command, Environmental Protection Research Division, Technical Report, EP3, 110 pp.

Clements, T., R.O. Stone, J.F. Mann, and J.L. Eyman, 1963. A study of windborne sand and dust in desert areas. U.S. Army Natick Laboratories, Earth Sciences Division, Technical Report ES-8, 61 pp.

Cooke, R.U., D. Brunsden, J.C. Doornkamp, and D.K.C. Jones, 1982. *Urban Geomorphology in Deserts*. Oxford University Press, 324 pp.

Counihan, J. 1971. Wind tunnel determination of the roughness length as a function of three dimensional roughness elements. *Atmos. Envir. 5*, 637-642.

Daily, M., C. Elachi, T. Farr, W. Stromberg, S. Williams, and G. Schaber, 1978a. Application of multispectral radar and Landsat imagery to geologic mapping in Death Valley. Jet Prop. Lab. Publ. 78-19, 47 pp.

Daily, M., C. Elachi, T. Farr, and G. Schaber, 1978b. Discrimination of geologic units in Death Valley using dual frequency and polarization imaging radar data. *Geophys. Res. Lett. 5*, 889–892.

Dellwig, L.F. 1969. An evaluation of multifrequency radar imagery of the Pisgah Crater area, California. *Mod. Geol. 1*, 65-73.

Dellwig, L.F. and R.K. Moore, 1966. The geological value of simultaneously produced like- and cross-polarized radar imagery. *J. Geophys. Res. 71*, 3597-3601.

Dubief, J. 1952. Le vent et la deplacement du sable au Sahara. *Travaux, Institute de Recherches Sahariennes, 8*, 123-162.

El Baz, F. and R.W. Wolfe, 1982. Wind patterns in the Western Desert. *In* F. El Baz *et al.* (eds.), *Desert Landforms of Southwestern Egypt: a basis for comparison with Mars*, National Aeronautics and Space Administration, Contractor Rep. 3611, 119-140.

Elachi, C., R. Blom, M. Daily, T. Farr, and R.S. Saunders, 1980. Radar imaging of volcanic fields and sand dune fields: Implications for VOIR. *In Radar Geology: An assessment*, Jet Prop. Lab. Pub. 80-61, 114-150.

Embabi, N.S. 1982. Barchans of the Kharga Depression. *In* E. El Baz *et al.* (eds.), *Desert Landforms of Southwestern Egypt: a basis for comparison with Mars*, National Aeronautics and Space Administration, Contractor Rep. 3611, 141-155.

Evans, D.L., 1978. Radar observations of a volcanic terrain: Askja Caldera, Iceland. Jet Propulsion Lab. Publ. 78-81, 39 pp.

Evans, D.L., T.G. Farr, J.P. Ford, T.W. Thompson, and C.L. Werner, 1986. Multipolarization radar images for geologic mapping and vegetation discrimination. *IEEE Trans. Geosci. and Rem. Sens. GE-24*, 246-257.

Farr, T.G. and N. Engheta, 1983. Quantitative comparisons of radar image, scatterometer, and surface roughness data

from Pisgah Crater, CA. *In Proc. Int. Geosci. Remote Sensing Symp.*, San Francisco, CA, 2.1-2.6.

Finkel, H.J. 1959. The barchans of southern Peru. *J. Geol. 67*, 614-647.

Fryberger, S.G. and T.S. Ahlbrandt, 1979. Mechanisms for the formation of eolian sand seas. *Z. Geomorph. 23*, 440-460.

Gaddis, L., P. Mouginis-Mark, R. Singer, and V. Kaupp, 1987. Geologic analyses of Shuttle Imaging Radar (SIR-B) data of Kilauea Volcano, Hawaii. Submitted to *Geol. Soc. Amer. Bull.*

Gillette, D.A., J. Adams, A. Endo, D. Smith, and R. Kihl, 1980. Threshold velocities for the input of soil particles into the air by desert soils. *J. Geophys. Res. 85*, 5621-5630.

Goudie, A.S. 1983. Dust storms in space and time. *Prog. Phys. Geog. 7*, 502-530.

Greeley, R. and J.D. Iversen, 1985. *Wind as a Geological Process on Earth, Mars, Venus and Titan.* Cambridge Univ. Press, Cambridge, 333 pp.

Greeley, R. and J.D. Iversen, 1987. Measurements of wind friction speeds over lava surfaces and assessment of sediment transport. *Geophys. Res. Lett., 14*, 925-928.

Greeley, R., N. Lancaster, R.J. Sullivan, R.S. Saunders, E. Theilig, S. Wall, A. Dobrovolskis, B.R. White, and J.D. Iversen, 1988. A relationship between radar backscatter and aerodynamic roughness: Preliminary results. *Geophys. Res. Letts., 5*, 565-568.

Haralick, R.M., K. Shanmugam, and I. Dinstein, 1973. Textural features of image classification. *IEEE Trans, Systems, Man, and Cybernetics SMC-3*, 610-621.

Iversen, J.D., R. Greeley, J.B. Pollack, and B.R. White, 1973. Simulation of martian eolian phenomena in the atmospheric wind tunnel. Space Simulation. NASA Special Publication, 36, 191–213.

Jones, W.L. and L.C. Schroeder, 1978. Radar backscatter from the ocean: Dependence on surface friction velocity. *Boundary Layer Meteorology 13*, 133-149.

Jones, W.L., D.H. Boggs, E.M. Bracalente, R.A. Brown, T.H. Guymer, D. Shelton, and L.C. Schroeder, 1981. Evaluation of the Seasat wind scatterometer. *Nature 294*, 704-707.

Krishen, K. 1971. Correlation of radar backscattering cross sections with ocean wave height and wind velocity. *J. Geophys. Res. 76*, 6528-6539.

Lancaster, N., 1985. Winds and sand movements in the Namib sand sea. *Earth Surface Processes and Landforms 10*: 607-619.

Lettau, H., 1969. Note on aerodynamic roughness-parameter estimation on the basis of roughness-element description, *J. Appl. Meteor. 8*, 828-832.

Lettau, H. and K. Lettau, 1978. Experimental and micrometeorological studies of dune migration. *In* Lettau, H. and K. Lettau (eds.), *Exploring the world's driest climate*, University of Wisconsin-Madison, Institute for Environmental Studies Report 101, 101-147.

Liu, W.T. and W.G. Large, 1981. Determination of surface stress by Seasat-SASS: A case study with JASIN data. *J. Phys. Oceanography 11*, 1603-1611.

Lyles, L., R.L. Schrandt, and N.F. Schneidler, 1974. How aerodynamic roughness elements control sand movement. *Trans. Amer. Soc. Ag. Eng. 17*, 134-139.

Mainguet, M. 1978. The influence of trade winds, local air masses and topographic obstacles on the aeolian movement of sand particles and the origin and distribution of ergs in the Sahara and Australia. *Geoforum 9*, 17-28.

Mainguet, M., 1984. Space observations of Saharan aeolian dynamics. *In* F. El Baz (ed.), *Deserts and Arid Lands*, Martinus Nyhoff Publ., The Hague, 31-58.

Malin, M.C., D. Evans, and C. Elachi, 1978. Imaging radar observations of Askja Caldera, Iceland. *Geophys. Res. Lett. 5*, 931-934.

McFadden, L.D., S. Wells, J.C. Dohrenwend, and B. Turrin, 1984. Cumulic soil development in eolian parent materials on flows of the Cima volcanic field, Mojave Desert, California. *In* J.C. Dohrenwend (ed.), *Surficial Geology of the Eastern Mojave Desert, California*, Geological Society of America, Reno Meeting, 134-149.

Middleton, N.J., A.S. Goudie, and G.L. Wells, 1986. The frequency and sources areas of desert dust. *In* Nickling, W.G. (ed.), *Aeolian Geomorphology*, Allen and Unwin, 237-260.

Moore, R.K. and A.K. Fung, 1979. Radar determination of winds at sea. *Proc. IEEE 67*, 1504–1521.

Morales, C. (ed.), 1979. *Saharan Dust.* John Wiley and Sons, Chichester, 297 pp.

Schaber, G.G., G.L. Berlin, and W.E. Brown, Jr., 1976. Variations in surface roughness within Death Valley, California: Geological evaluation of 25-cm-wavelength radar images. *Geol. Soc. Amer. Bull. 87*, 29-41.

Schaber, G.G., C. Elachi, and T.G. Farr, 1980a. Remote sensing data of SP Mountain and SP lava flow in north-central Arizona. *Rem. Sens. of Envir. 9*, 149-170.

Schaber, G.G., G.L. Berlin, and R.J. Pike, 1980b. Terrain analysis procedures for modeling radar backscatter. *In Radar Geology: An Assessment*, Jet Prop. Lab. Publ. 80-61, 168-181.

Ulaby, F.T., P.P. Batlivala, and M.C. Dobson, 1978. Microwave backscatter dependence on surface roughness, soil moisture, and soil texture, Part I: Bare soil. *IEEE Trans, Geosci. Electr. GE-16*, 286-295.

Ulaby, F.T., R.K. Moore, and A.K. Fung, 1982. *Microwave Remote Sensing, Active and Passive, Volume 2, Radar Remote Sensing and Surface Scattering and Emission Theory.* Addison-Wesley Publishing Co., Reading, Massachusetts.

VanZyl, J.J., H.A. Zebker, and C. Elachi, 1987. Imaging Radar Polarization Signatures: Theory and Observations. *Radio Science 22*, 529-543.

Wang, J.R., E.T. Englman, J.C. Shiue, M. Rusek, and C. Steinmeier, 1986. The SIR-B observations of microwave backscatter dependence on soil moisture, surface roughness, and vegetation covers. *IEEE Trans. Geosci. and Rem. Sens. GE-24*, 510-516.

Watson, A. 1985. The control of windblown sand and moving dunes: a review of the methods of sand control in deserts with observations from Saudi Arabia. *Quar. J. Eng. Geo. 18*, 237–252.

Wilson, I.E., 1971. Desert sandflow basins and a model for the development of ergs. *Geogr. J. 137*, 180-197.

Zebker, H.A., J.J. VanZyl and D.N. Held, 1987. Imaging radar polarimetry from wave synthesis, *J. Geophys. Res. 92*, 638-2701.

2.0 SIR-C RARP FIELDWORK IN DEATH VALLEY, 1989

N. Lancaster, K. Rasmussen, L. Gaddis, and R. Greeley

2.1 Introduction

This section describes field measurements carried out at five sites in Death Valley during March-June 1989, and presents preliminary results of these studies. Studies at each site comprised: 1) measurements of boundary layer wind profiles, 2) general characterization of site topography and surface particle size and distribution, 3) measurements of micro-topography using template and laser methods. The investigations were conducted as part of an ongoing series of field, wind tunnel, and theoretical studies of the relationship between aerodynamic roughness and radar backscatter of surfaces over which aeolian sediment transport takes place.

Studies were carried out at the following sites in Death Valley National Monument: Stovepipe Wells, Kit Fox Fan, Trail Canyon Fan, Golden Canyon Fan, and Confidence Mill Playa (Fig. 2.1, Table 2.1).

2.2 The Study Sites

Stovepipe Wells

This site (Fig. 2.2) is located on a flat to gently undulating sand and gravel surface (reg) on the distal part of an alluvial fan that heads in the Kit Fox Hills and extends west beneath the Stovepipe Wells dune field. Small (10-20 cm deep, 1-2 m wide) washes cross the surface, which, at the time of investigations, was completely unvegetated. Average slope (determined with an Abney Level) is < 1° to the south, and 1-2° from east to west. Active transport of sand across this surface is evidenced by 10-20 cm high sand drifts with wind ripples in the washes. In addition, active transport of both sand and dust was observed. Some of the clasts on the surface show evidence of wind facetting.

Kit Fox Fan

This site (Fig. 2.3) is located on the active mid- to proximal-part of the same fan as the Stovepipe Wells site. Its surface consists of gravel to cobble sized clasts, with a sandy matrix. Average slope of the site is 0.5° to the southeast and 3° to the west. Multiple small channels (5-10 cm deep, 1-2 m wide) floored with sand and granules cross the site from east to west. Water flow occurred in some of the channels following rain in early May. Scattered dead ephemeral herbs spaced >1 m apart were observed at this site. Scattered brittlebush plants occur outside a radius of 25 m from the anemometer sites. Active sand transport is evidenced by ventifacted clasts and was observed in the field.

Golden Canyon Fan

This site (Fig. 2.4) is on an active alluvial fan/mudflow surface and has a well developed bar and swale topography with a 20-50 cm relief. Channels (swales) are generally covered by sandy or silty material. Bars are composed of gravel to small boulders of a variety of lithologies (Paleozoic sedimentary rocks, Tertiary to Quaternary tuffs, vesicular basalts, and fanglomerates set in a sandy silt matrix). Average slopes are <1° to the southeast and 2° downfan (west). There was no vegetation at this site.

Trail Canyon Fan

This site (Fig. 2.5) is on a well-developed desert pavement on the lower part of the Trail Canyon large alluvial fan that heads in the Panamint Range. The surface consists of interlocking oblate gravel to cobble-sized clasts, with scattered boulders. A well-developed desert varnish coats all of the clasts. Clast lithology appears to be mainly sandstones, shales, and limestones of Precambrian to lower Paleozoic age. The surface is gently undulating to flat and is incised by 1.5 m deep washes. Spacing of washes is more than 100-200 m. Bar and swale

Table 2.1 Site locations

Site	Latitude (N)	Longitude (W)	USGS 7.5' quad
Stovepipe Wells	36° 39'	117° 4'	Stovepipe Wells NE
Kit Fox Fan	36° 37'	117° 2'	Stovepipe Wells NE
Golden Canyon Fan	36° 25'	116° 51'	Furnace Creek
Trail Canyon Fan	36° 18'	116° 53'	Devils Speedway
Confidence Mill Playa	35° 48'	116° 33'	Confidence Hills

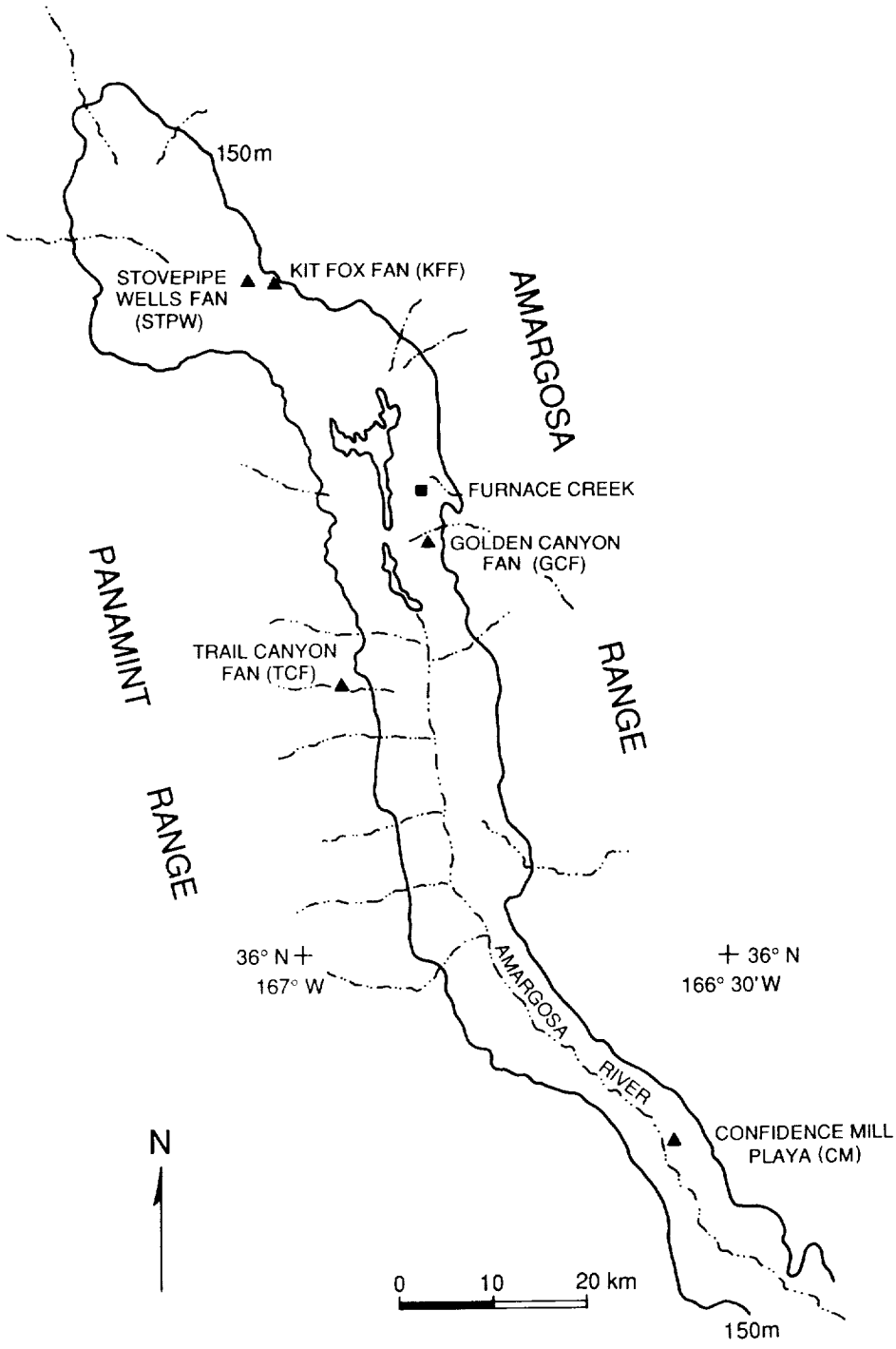

Figure 2.1. Sketch map to show the location of the study sites in Death Valley National Monument.

Figure 2.2. Stovepipe Wells: view southwest toward edge of Stovepipe Wells dune field. Note thin sand cover and small shadow dune in wash in center of view.

Figure 2.3. Kit Fox Fan: view west (down fan) to Stovepipe Wells dune field. Note rough surface of fan, and anastomosing washes.

Figure 2.4. Golden Canyon Fan: view southeast across fan. Note large cobbles and boulders on bars, with coarse sand and gravel in swales.

Figure 2.5. Trail Canyon Fan: view north across fan. Note well-developed desert pavement surface.

Figure 2.6. Confidence Mill playa: view north toward main part of Death Valley. Note puffy surface of playa.

topography is evident in places. Average slopes are < 1° to the north and 3.5° to the east (down fan). There is no vegetation except along the washes where scattered creosote bushes occur.

Confidence Mill Playa

This site (Fig. 2.6) is on a clay-silt playa that forms the terminus of the Amargosa River. The surface is flat with a soft to locally hard puffy clay-rich crust. There are numerous water escape structures formed by rapid dewatering of soft sediment and scattered south-north trending "channels" 5-10 cm deep.

2.3 Boundary Layer Wind Profile Studies

Measurements of surface winds and boundary layer profiles were carried out at each site for the periods shown in Table 2.2.

2.3.1 Instrumentation

General description

Boundary layer wind profiles were measured using field-portable anemometer masts with a height of 9.8 m. Figure 2.7 shows the general instrument set-up; Figures 2.8 and 2.9 show the equipment in the field. Cup anemometers (Tradewinds) were placed at the following heights with a logarithmic spacing: 0.75, 1.25, 2.07, 3.44, 5.72, and 9.5 m. Pairs of AD590 temperature sensors were placed in a shielded and ventilated mounting at heights of 1.3 and 9.6 m. Wind directions were measured with wind vanes (WD1 instruments from Remote Measurement Systems) at heights of 9.7 m and 1.5 m. At sites that were considered to be topographically rough (Golden Canyon Fan, Kit Fox Fan), an additional mast with four anemometers at heights of 1.0, 2.11, 4.49 and 9.5 m was sited 80 m upslope

Table 2.2 Duration of wind measurements

Site	Surface Type	Start Date	End Date
Stovepipe Wells	Gravel reg	30 March 1989	21 April 1989
Kit Fox Fan	Alluvial fan	3 May 1989	23 May 1989
Golden Canyon Fan	Alluvial fan	31 March 1989	2 May 1989
Trail Canyon Fan	Alluvial fan	29 March 1989	1 May 1989
Confidence Mill Playa	Playa	2 May 1989	3 June 1989

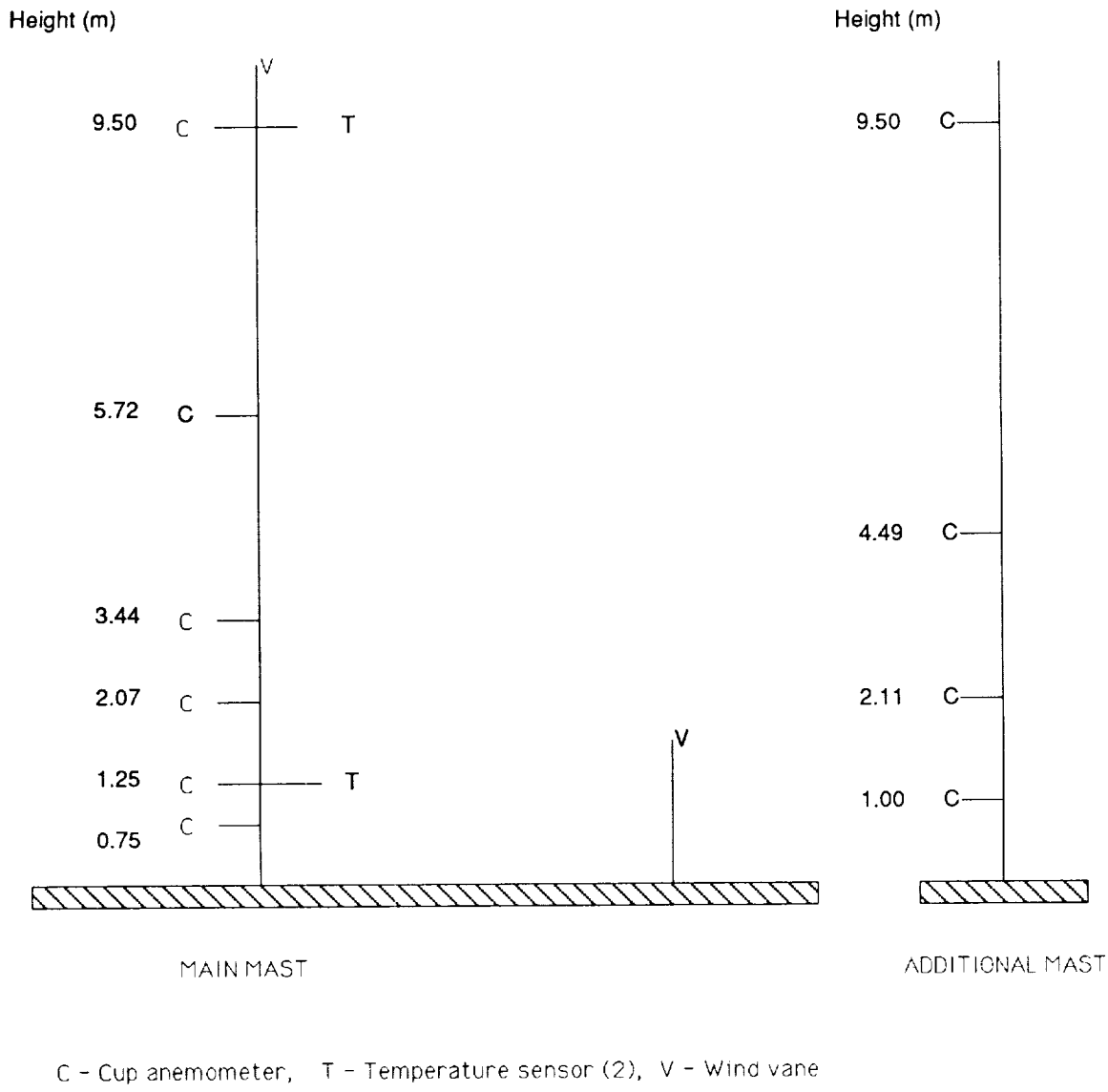

Figure 2.7. Instrument configuration used in Death Valley, 1989.

from the main mast. Data were recorded using an ADC-1 analog-to-digital converter and a Tandy 102 laptop computer as a data logger, and were located 10-15 m from the base of the mast. The anemometers and temperature sensors were sampled by the data logger every 25 seconds. Data were averaged for a 20 minute period and these values were stored in the field on cassette tapes. Each cassette tape lasted 14-17 days. The data were then transferred to a Macintosh computer in the laboratory. The system was powered by a 12 volt deep-cycle battery. Calibration procedures are described in appendix I.

Accuracy and precision of instruments

The Tradewinds anemometers were determined during calibration to have an accuracy of ± 5-10 cm/sec. The temperature sensors are rated as accurate to 0.1° C by the manufacturer (Analog Devices). The WD1 wind vanes are rated accurate to ± 3°.

2.3.2 Wind data reduction and analysis procedures

The following procedures were adopted for data reduction and analysis.

After data were transferred to the Macintosh and archived on 3.5" disks, they were converted to an Excel worksheet format. This allowed derivation of intermediate and final profile parameters, as well as sorting of data.

Data were initially sorted by the wind speed at the anemometer closest to the ground (0.75 m). A subset of the data was extracted in which wind speeds at all anemometers were above 4 m/sec. These data were used for subsequent analysis. Use

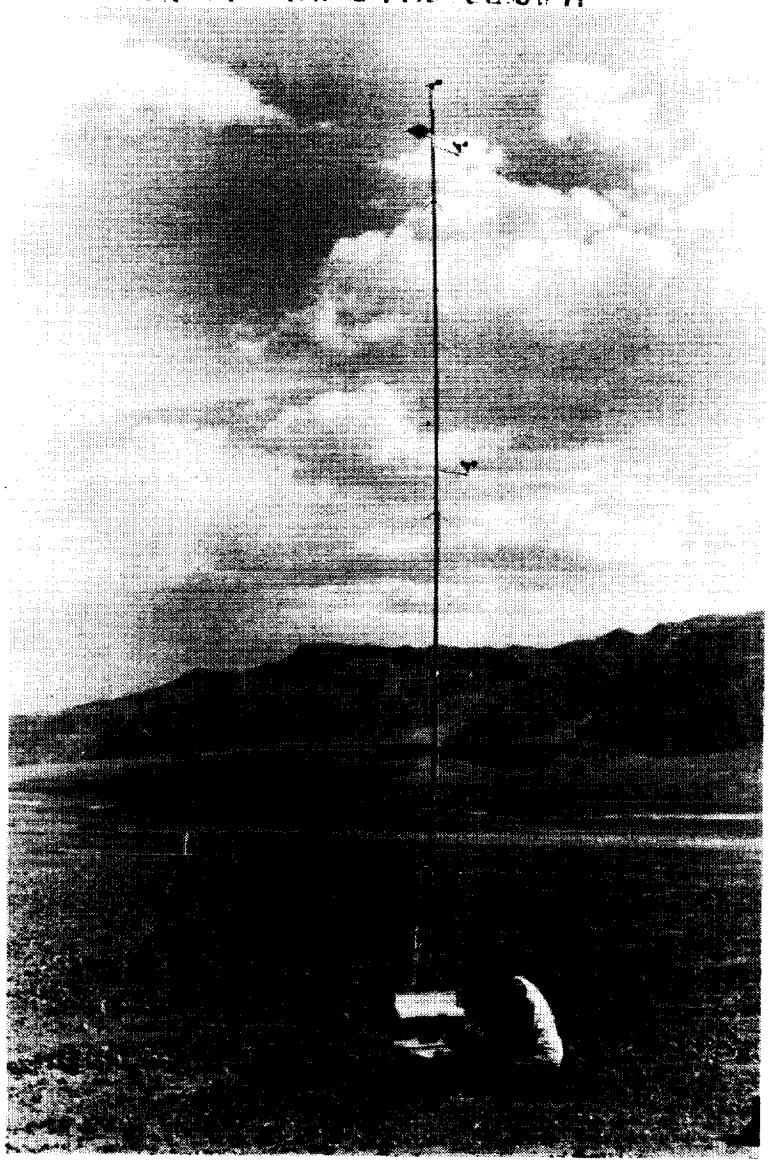

Figure 2.8. Anemometer mast at Kit Fox Fan.

of data for relatively high wind speeds had the effect of offsetting the relatively poor accuracy of the temperature sensors in correcting the profiles for atmospheric stability conditions. A large amount of data were collected that satisfy these criteria (Table 2.3).

Richardson Number

The Richardson number (or a.k.a. gradient Richardson) is proportional to the ratio of flow energy derived from buoyant gas forces to flow energy obtained solely from the shear of the wind over the surface. The Richardson number provides quantitative data on the destabilizing effect of buoyancy and the stabilizing effect of large scale wind. The Richardson number is defined as

$$Ri = \frac{g\partial t}{\overline{T}\cdot\partial z} \Big/ \left(\frac{\partial u}{\partial z}\right)^2 \text{ where } u = u(z,x).$$

The Richardson number may be approximated by the bulk Richardson number which is given by

$$Ri = \frac{g}{T_o}\,\frac{z\Delta T}{u^2}$$

where ΔT is the potential temperature difference between the lower and upper temperature sensors, T_o is the mean temperature between the two sensor heights and ΔH is the mean wind speed between the sensor heights.

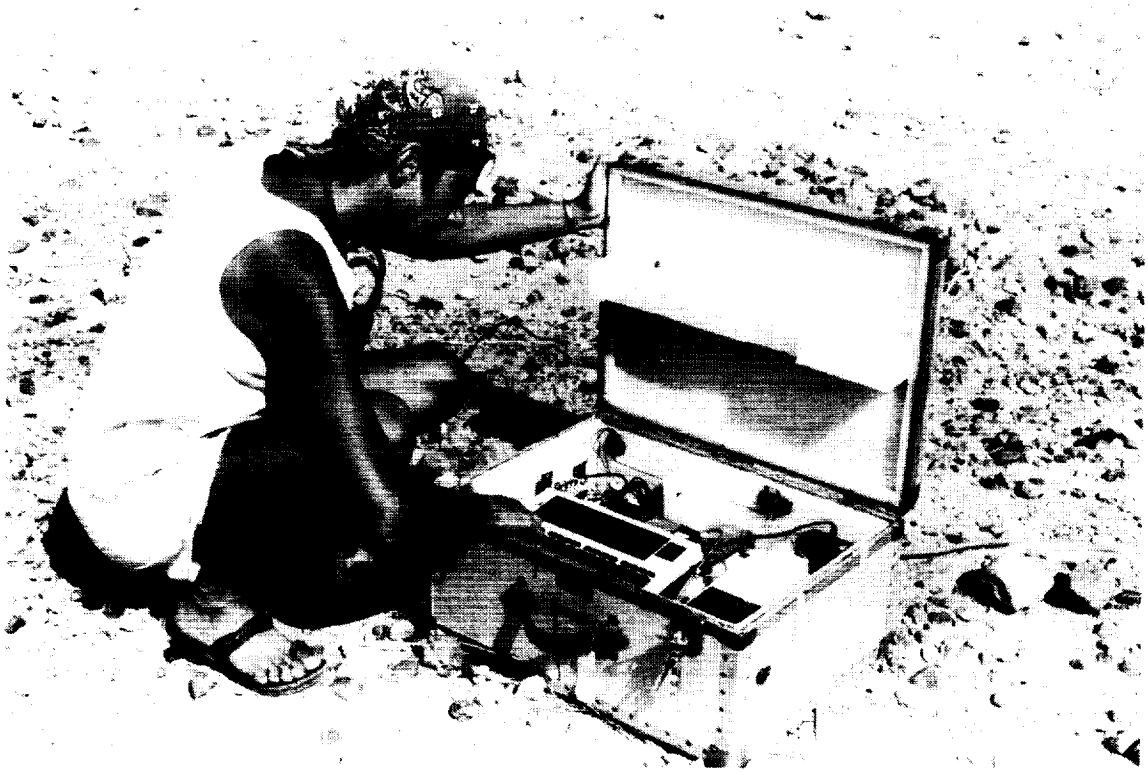

Figure 2.9. Close-up of Tandy 102 computer, analog to digital converter and cassette recorder in the field.

Table 2.3 Wind data for periods when wind speed at lowest anemometer exceeded 4 m/sec

Site	Hours of data	Number of profiles
Stovepipe Wells	71	214
Kit Fox Fan	80	238
Golden Canyon Fan	129	387
Trail Canyon Fan	178	533
Confidence Mill Playa	190	571

Pairs of temperature sensors were installed at heights of 1.3 and 9.6 m to ensure that temperature data were recorded in the event of failure of one of the sensors. Selection of pairs of sensors for calculation of the bulk Richardson number (Ri) was done on the basis of the smallest consistent difference between sensors and checked against periods of strong winds at night when differences between upper and lower sensors should be at a minimum. The bulk Richardson number (Ri) was calculated for all 20 minute periods as:

$$Ri = g\,\Delta T\, z / T_o \Delta u^2 \qquad (2.1)$$

where g = gravitational acceleration (9.81 m/sec/sec); ΔT = the temperature difference between the lower and upper temperature sensors, expressed as a potential temperature; z = the geometric mean height of the temperature sensors; T_o = the surface reference temperature in K (approximated by the lower temperature sensor reading); and Δu is the difference in wind speeds between the anemometers at 0.75 and 9.6 m.

The Monin-Obukhov stability length was determined using the following approximation for L. For unstable conditions:

$$Ri \sim z/L \qquad (2.2)$$

$$\text{and } L = z/Ri \qquad (2.3)$$

where L = the Monin-Obukhov stability length and z = the geometric mean of the anemometer heights. For stable conditions, the stability parameter (ξ) is defined by:

$$\xi = z/L = Ri/(1\text{-}5\,Ri) \qquad (2.4)$$

$$\text{and } L = z(1\text{-}5\,Ri)/Ri \qquad (2.5)$$

The stability correction of the profiles was based on:

$$u_{(z)} = u_*/k\,[\ln z/z_o + \psi] \quad (2.6)$$

$$\text{and } u_{(z)} = u_*/k\,[\ln z + \psi] - [u_*/k \ln z_o] \quad (2.7)$$

where $u_{(z)}$ wind speed at height z, u_* = friction speed, k = Von Karmann's constant, ψ = stability function, and z_o = aerodynamic roughness length. For each height z_i, the stability function y is given by:

$$y\,(z_i/L) \quad (2.8)$$

$$\text{where } y\,(z_i/L) = 1.1.(-z_i/L)^{0.5} \text{ (unstable)} \quad (2.9)$$

$$\text{and } y\,(z_i/L) = -4.8\,(-z_i/L) \text{ (stable)} \quad (2.10)$$

Corrections were made so that:

$$z' = \ln z_i - \psi \text{ (unstable)} \quad (2.11)$$

$$\text{and } z' = \ln z_i + \psi \text{ (stable).} \quad (2.12)$$

U_* and z_o were then determined by a least squares fit to the relationship between the corrected height (z') and $u_{(z)}$ using an iterative procedure in which a "seed" z_o was inserted and successively modified so that the mean value of the constant term in the regression was minimized.

Several checks were placed on the data to ensure the reliability and consistency of the estimates of wind profile parameters. Plots of u_* versus wind speed at 9.5 m height show that in all cases friction speed increases with wind speed (Figs. 2.10-2.14). Plots of z_o versus bulk Richardson number (Figs. 2.15-2.19) show that there were no trends, indicating that stability corrections were made correctly. Plots of z_o versus wind direction (Figs. 2.20-2.24) indicate that, in most cases, z_o varies within 10-20% for each directional sector.

2.3.3 Wind profile data

Appendix II contains a complete listing of wind speed, temperature, and wind direction for each site for periods when the mean wind speed at the lowest anemometer was above 4 m/sec. The raw data are stored in Macintosh format on disk at ASUIPF.

At all sites, winds greater than 4 m/sec were from two main directions: north to northwest and south through southeast. At Confidence Mill and Trail Canyon, periods of winds from the west to northwest were also recorded. Winds from the south were dominant in April, whereas winds from the north and northwest were more common in May (Table 2.4). The pattern of wind directions observed reflects the topography of Death Valley: winds blow up or down the valley, which is oriented approximately NW-SE. Westerly winds at Trail Canyon are down-canyon winds, whereas winds from a similar direction at Confidence Mill reflect the generally more open aspect of this site which lies outside the main part of Death Valley.

Periods of winds >4 m/sec had no clear diurnal pattern and occurred at all times of the day. Many periods of strong winds occurred at night. There was a major wind event on April 21-25, when winds from the south blew almost continuously for 96 hours with speeds of >4 m/sec. Another major southerly wind storm occurred between May 17 and 22.

Periods of strong winds can be correlated with the passage of frontal systems to the north of Death Valley, thus increasing regional pressure gradients. Diurnal heating effects seem to be a minor influence on the pattern of wind speeds >4 m/sec, although there does appear to be a slight increase in mean wind speed during afternoon hours (Fig. 2.25).

Temperatures recorded at a height of 1.5 m above ground level varied from a minimum of 8.32° C to a maximum of 44.92° C during the course of the field experiment. The maximum 20 minute average of wind speed recorded was 17.09 m/sec on May 9 at Confidence Mill.

Selected wind profiles for near-neutral conditions (Ri < 0.01) for each major direction recorded at each site are given in Figures 2.26-2.30. The profiles are, in most cases, quite regular and indicate that confidence can be placed in the estimates of z_o and u_* that were derived from the profiles. They show that aerodynamic roughness

Table 2.4 Percentage of winds >4 m/sec from different directional sectors

Site	N-NE	SE-S	W-NW
Stovepipe Wells	11	89	
Kit Fox Fan	46.5	49.1	4.4
Golden Canyon Fan	9.4	86.7	4.8
Trail Canyon Fan		85.4	14.6
Confidence Mill Playa	35	72	3

Note: these stations were in operation at different times.

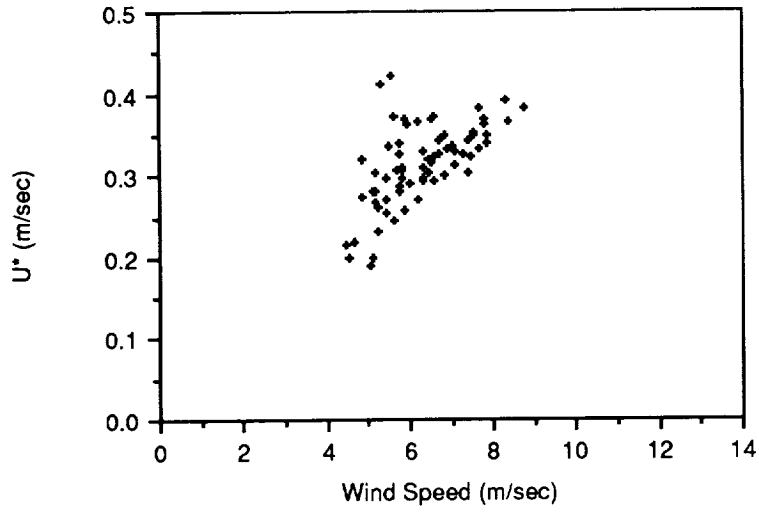

Figure 2.10a. Stovepipe Wells: northerly winds. Relationship between friction speed (U_*) and wind speed at 5.72 m.

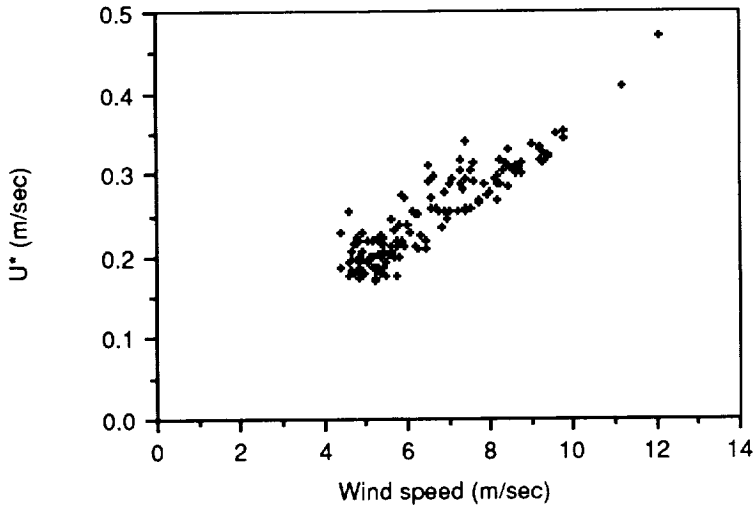

Figure 2.10b. Stovepipe Wells: southerly winds. Relationship between friction speed (U_*) and wind speed at 5.72 m.

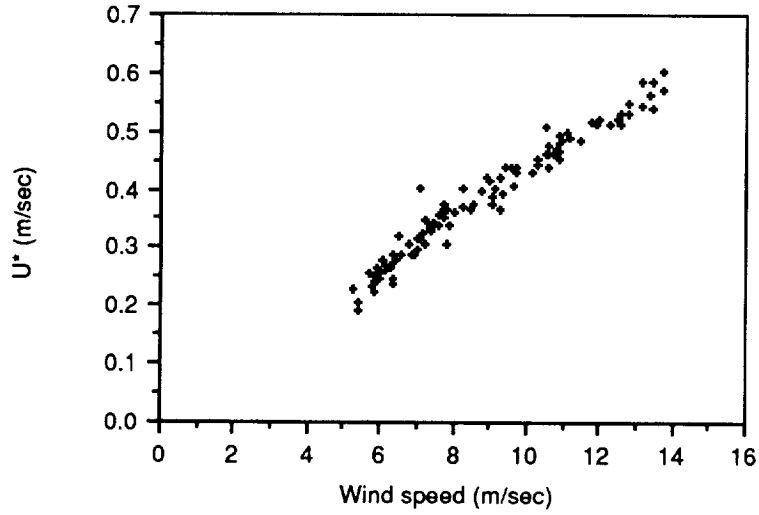

Mast 1 (downfan)

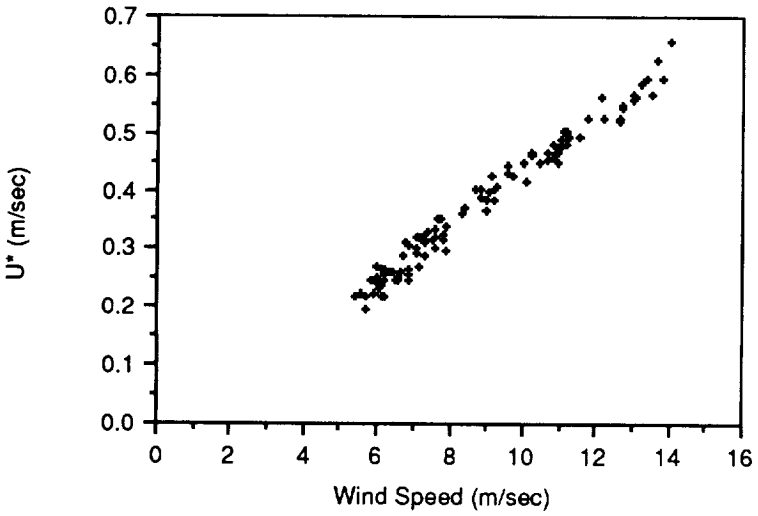

Mast 2 (upfan)

Figure 2.11a. Kit Fox Fan: northerly winds. Relationship between friction speed (u_*) and wind speed at 9.5 m.

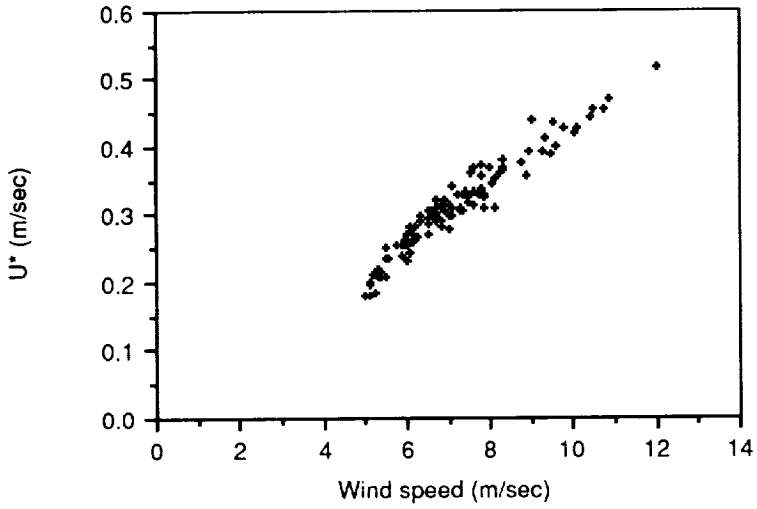

Mast 1 (downfan)

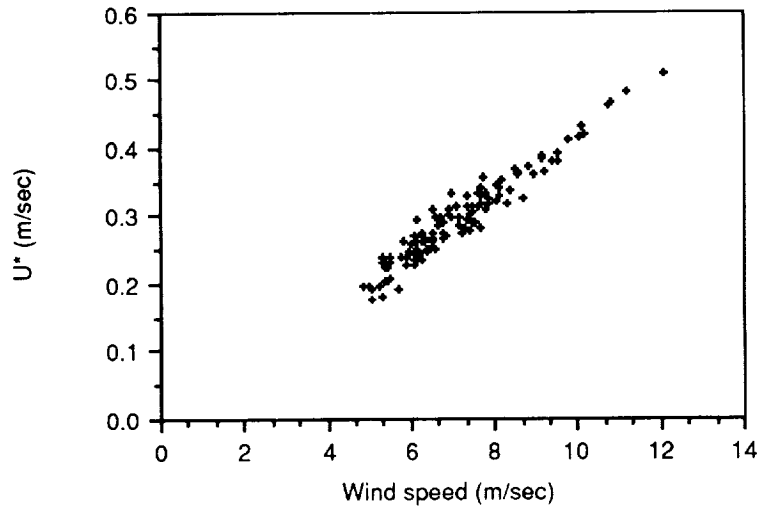

Mast 2 (upfan)

Figure 2.11b. Kit Fox Fan: southerly winds. Relationship between friction speed (u_*) and wind speed at 9.5 m.

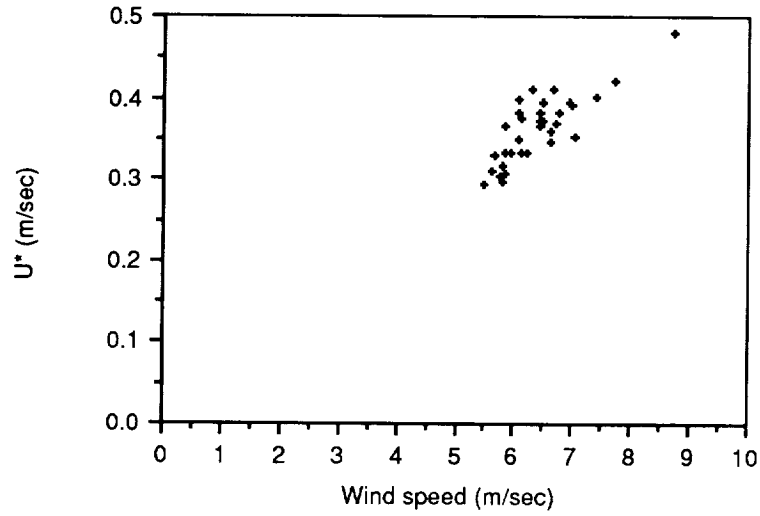

Mast 1 (upfan)

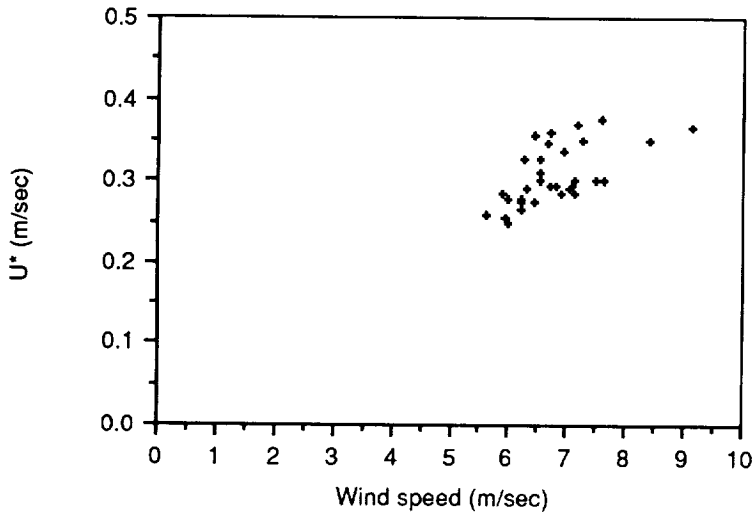

Mast 2 (downfan)

Figure 2.12a. Golden Canyon Fan: northerly winds. Relationship between friction speed (u_*) and wind speed at 9.5 m.

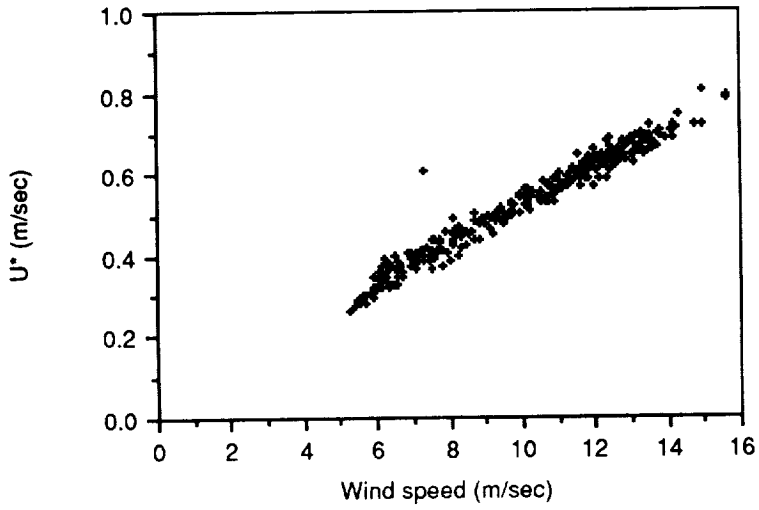

Mast 1 (upfan)

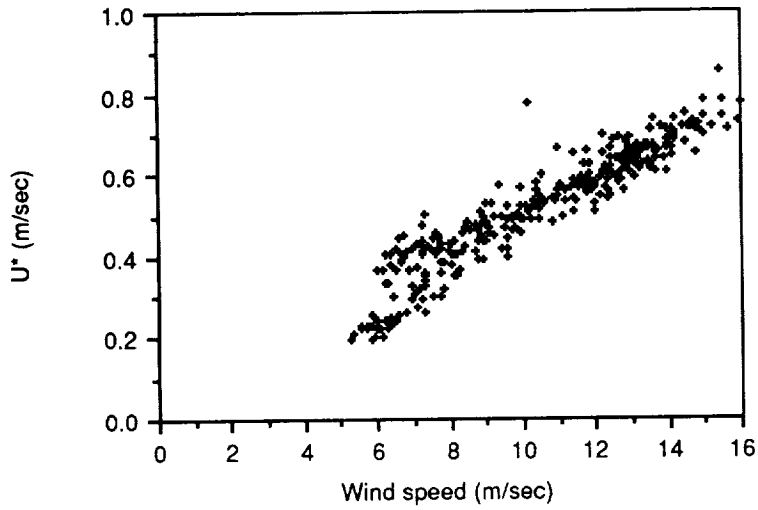

Mast 2 (downfan)

Figure 2.12b. Golden Canyon Fan: southerly winds. Relationship between friction speed (u_*) and wind speed at 9.5 m.

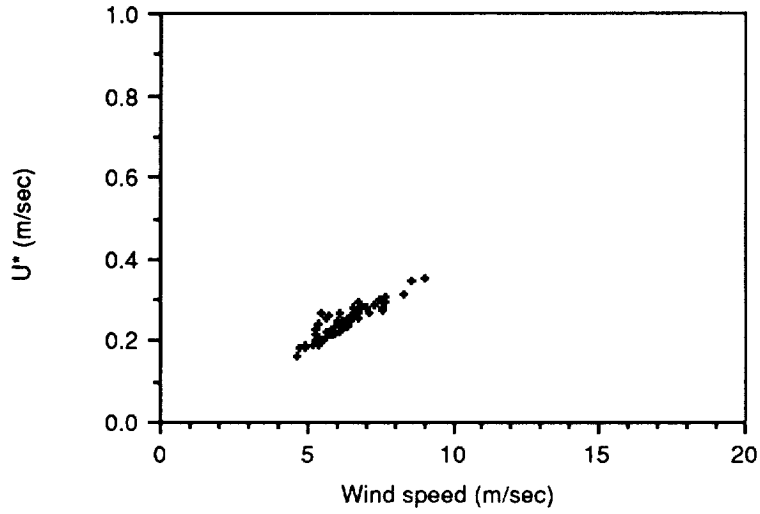

Figure 2.13a. Trail Canyon Fan: northerly winds. Relationship between friction speed (u_*) and wind speed at 5.72 m.

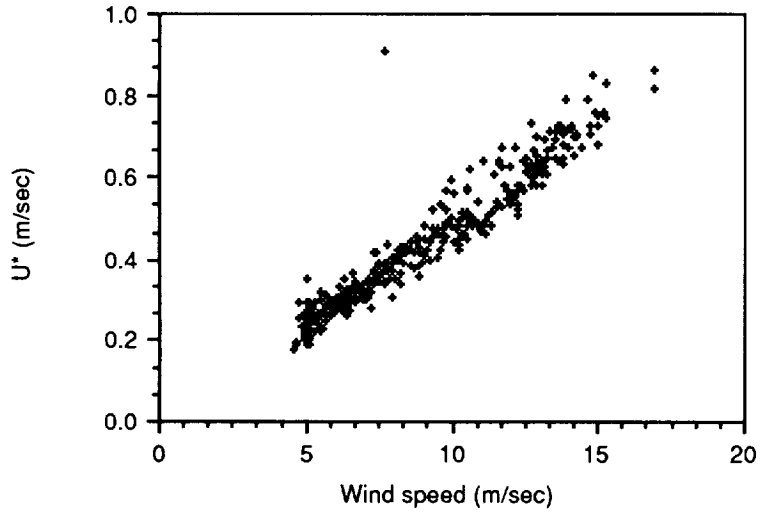

Figure 2.13b. Trail Canyon Fan: southerly winds. Relationship between friction speed (u_*) and wind speed at 5.72 m.

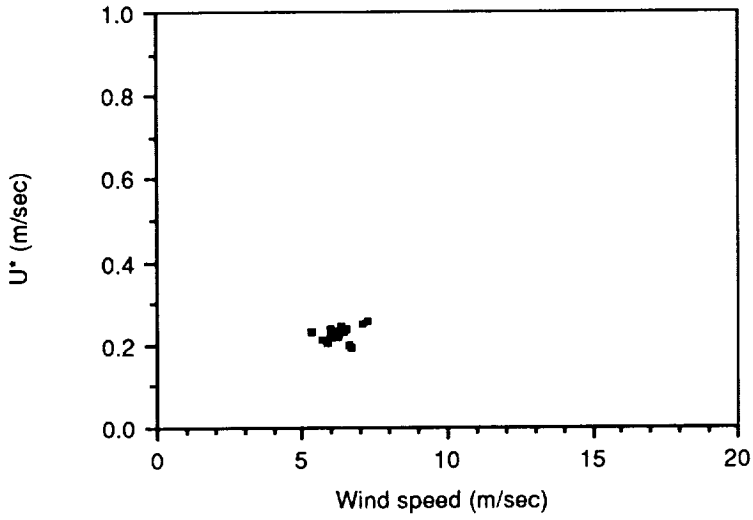

Figure 2.14a. Confidence Mill Playa: northerly winds. Relationship between friction speed (u_*) and wind speed at 9.5 m.

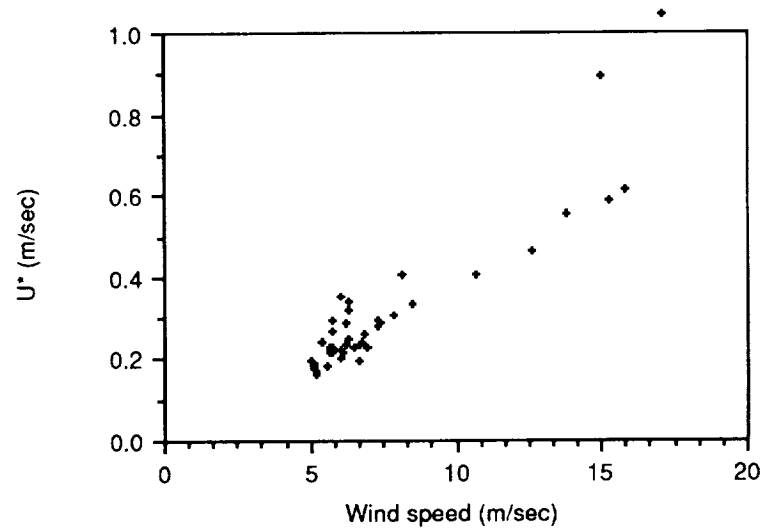

Figure 2.14b. Confidence Mill Playa: southerly winds. Relationship between friction speed (u_*) and wind speed at 9.5 m.

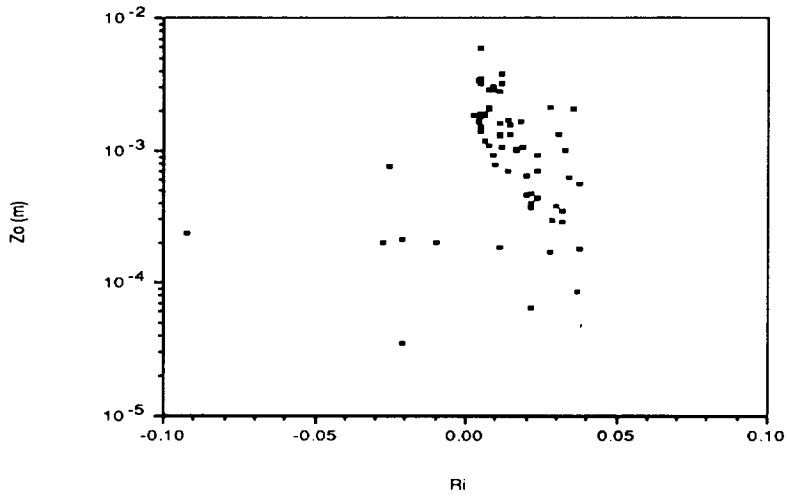

Figure 2.15a. Stovepipe Wells: northerly winds. Relationship between aerodynamic roughness (z_o) and bulk Richardson number (Ri).

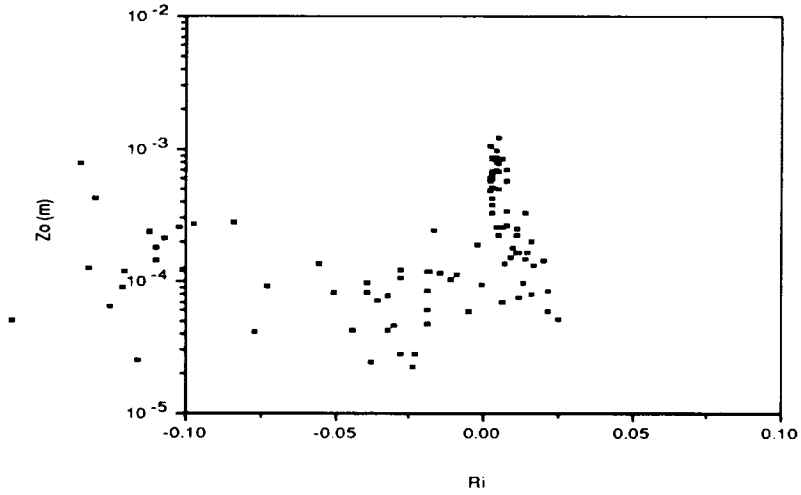

Figure 2.15b. Stovepipe Wells: southerly winds. Relationship between aerodynamic roughness (z_o) and bulk Richardson number (Ri).

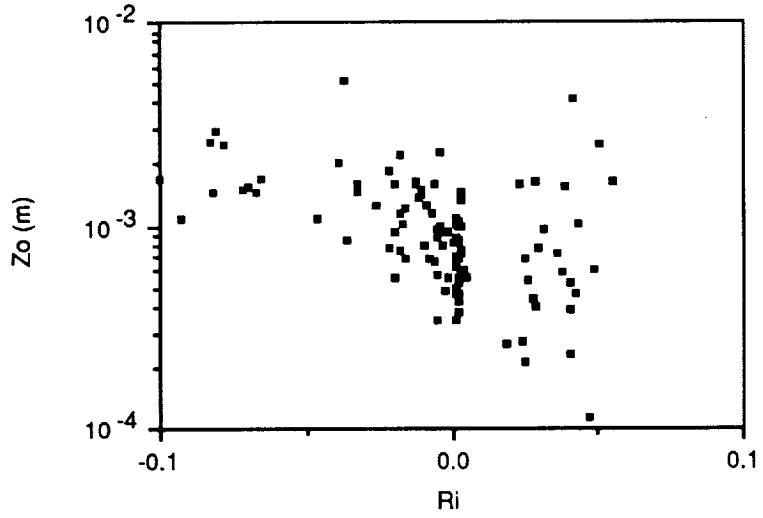

Mast 1

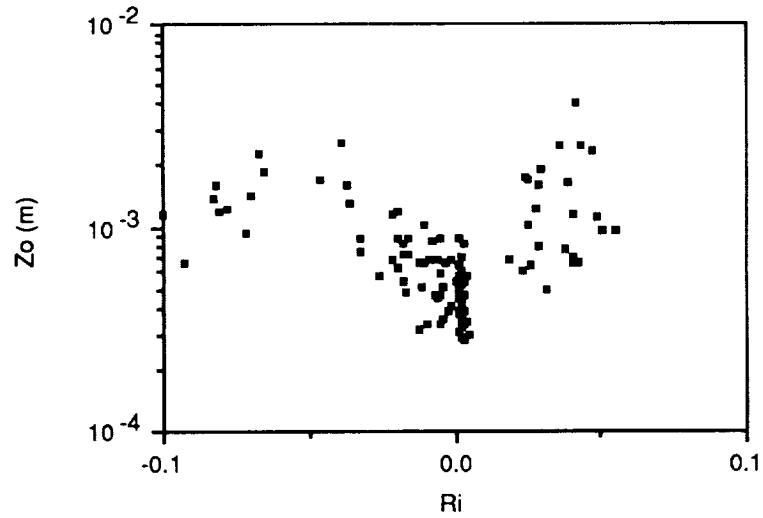

Mast 2

Figure 2.16a. Kit Fox Fan: northerly winds. Relationship between aerodynamic roughness (z_o) and bulk Richardson number (Ri).

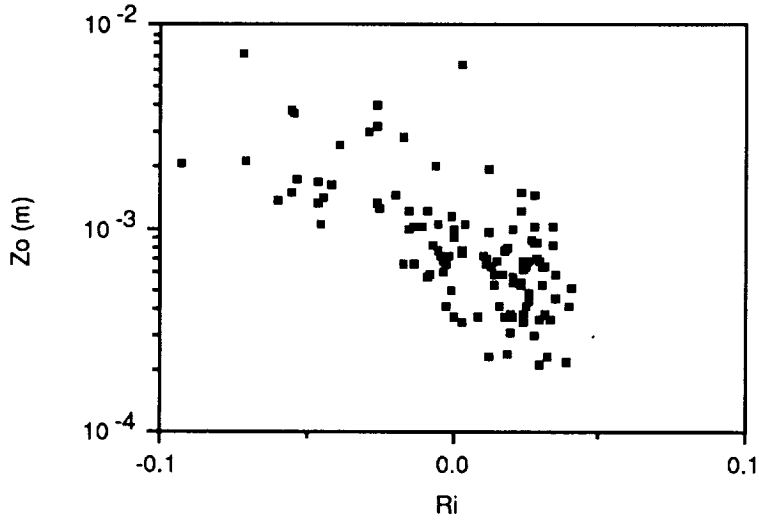

Mast 1

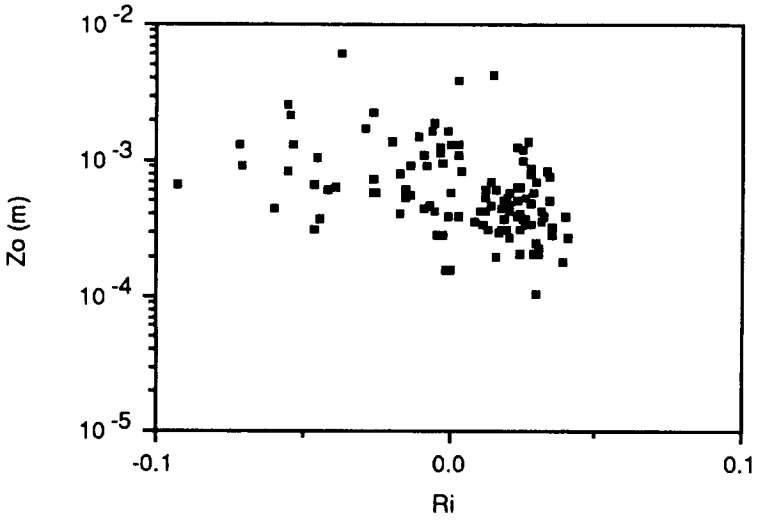

Mast 2

Figure 2.16b. Kit Fox Fan: southerly winds. Relationship between aerodynamic roughness (z_o) and bulk Richardson number (Ri).

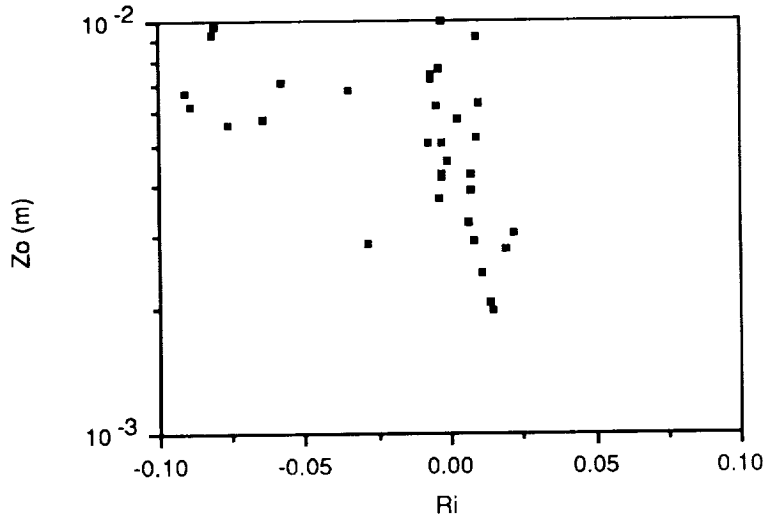

Mast 1

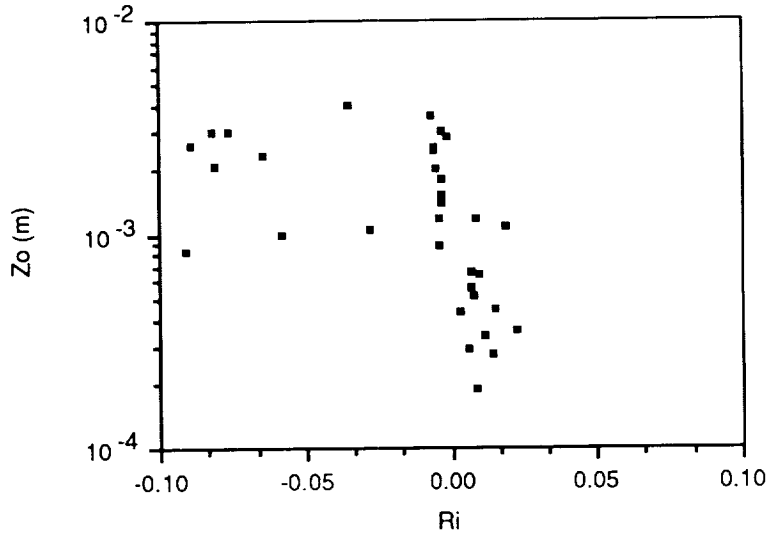

Mast 2

Figure 2.17a. Golden Canyon Fan: northerly winds. Relationship between aerodynamic roughness (z_o) and bulk Richardson number (Ri).

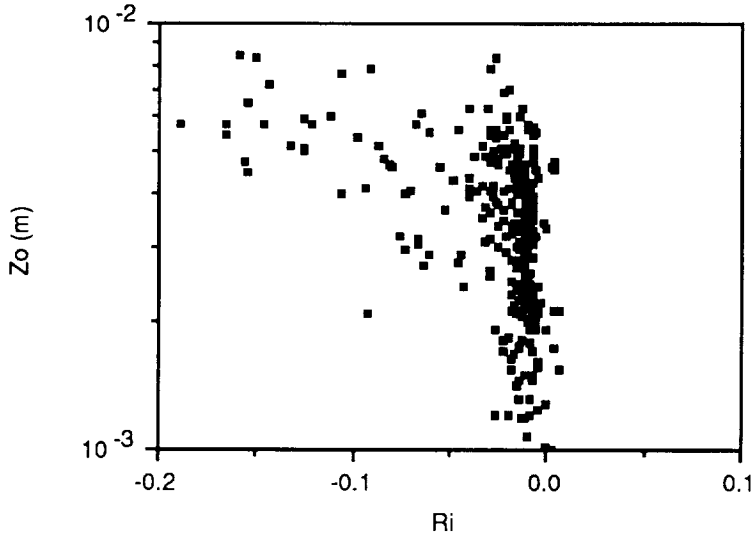

Mast 1

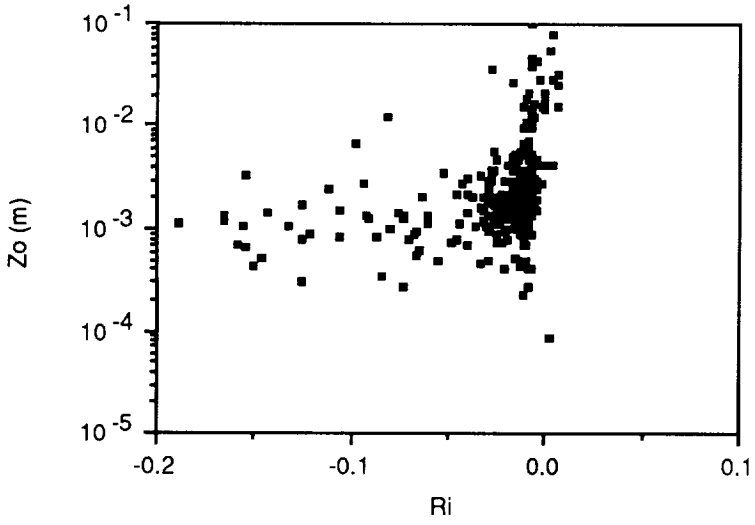

Mast 2

Figure 2.17b. Golden Canyon Fan: southerly winds. Relationship between aerodynamic roughness (z_o) and bulk Richardson number (Ri).

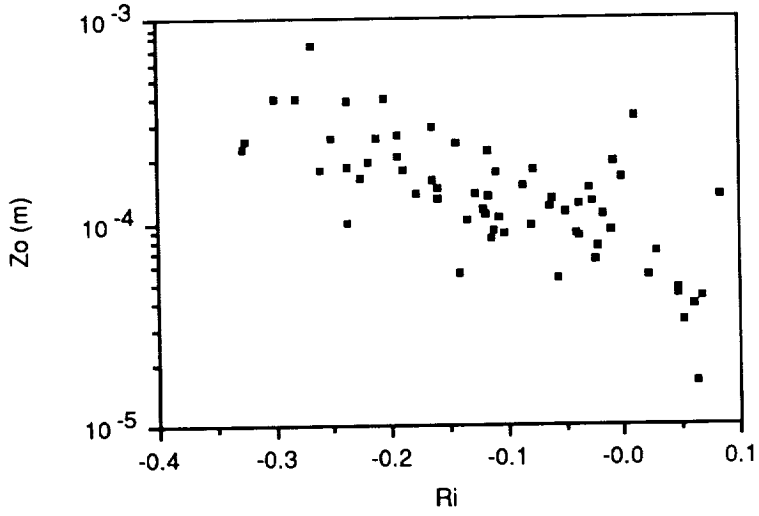

Figure 2.18a. Trail Canyon Fan: northerly winds. Relationship between aerodynamic roughness (z_o) and bulk Richardson number (Ri).

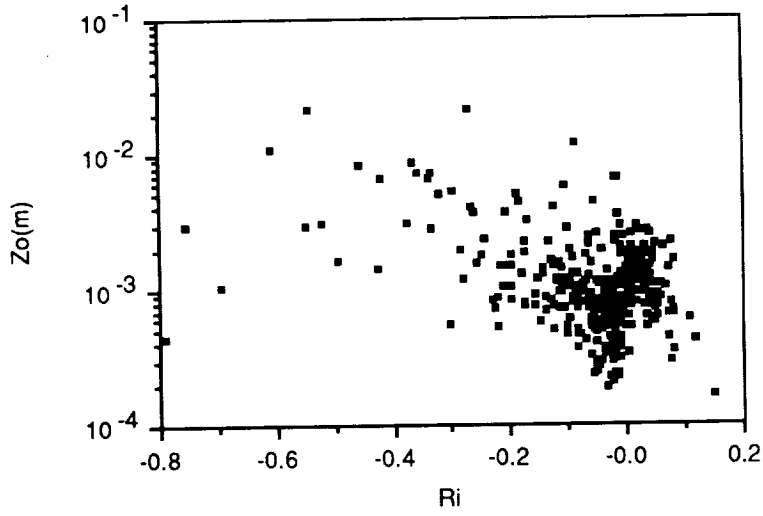

Figure 2.18b. Trail Canyon Fan: southerly winds. Relationship between aerodynamic roughness (z_o) and bulk Richardson number (Ri).

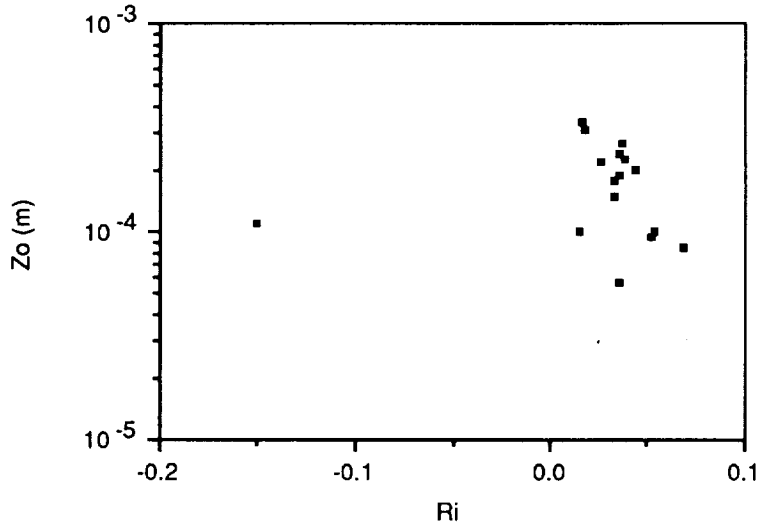

Figure 2.19a. Confidence Mill Playa: northerly winds. Relationship between aerodynamic roughness (z_o) and bulk Richardson number (Ri).

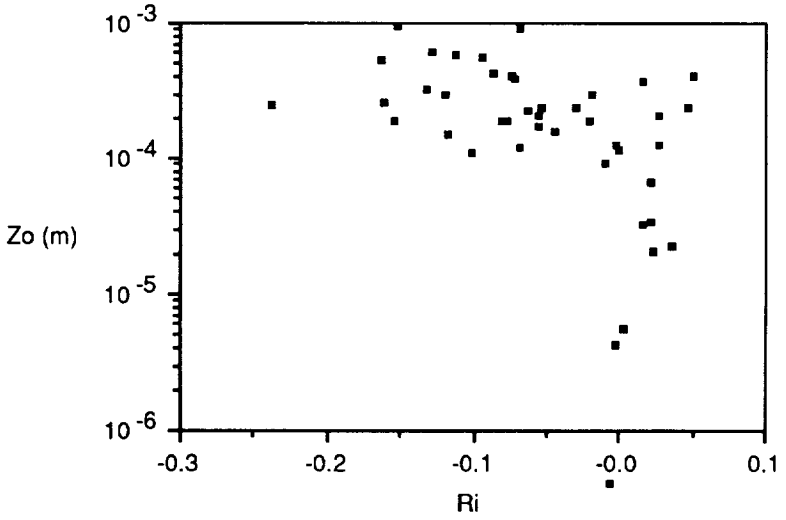

Figure 2.19b. Confidence Mill Playa: southerly winds. Relationship between aerodynamic roughness (z_o) and bulk Richardson number (Ri).

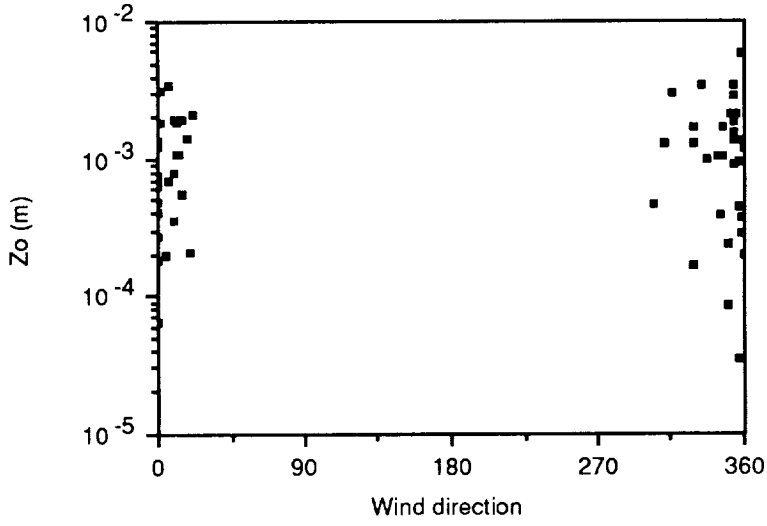

Fure 2.20a. Stovepipe Wells: northerly winds. Relationship between aerodynamic roughness (z_o) and wind azimuth direction (°).

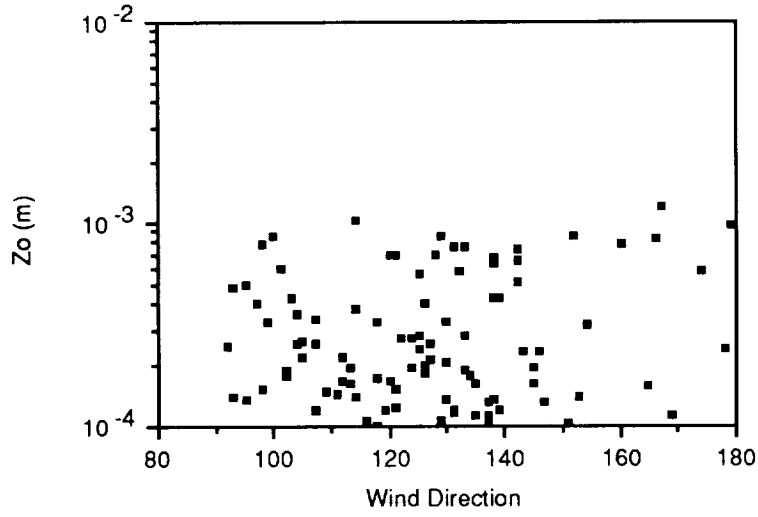

Figure 2.20b. Stovepipe Wells: southerly winds. Relationship between aerodynamic roughness (z_o) and wind azimuth direction (°).

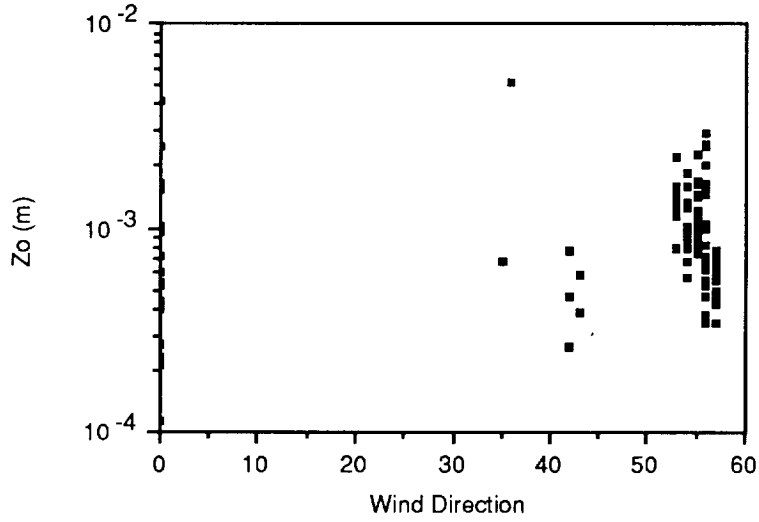

Mast 1

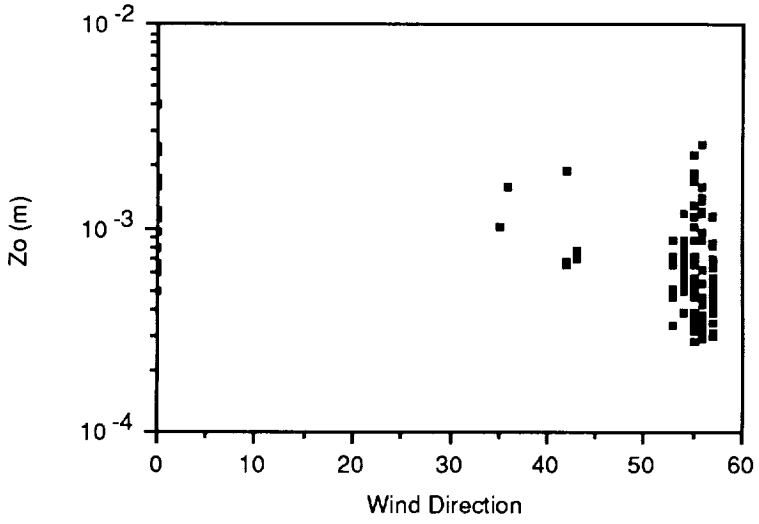

Mast 2

Figure 2.21a. Kit Fox Fan: northerly winds. Relationship between aerodynamic roughness (z_o) and wind azimuth direction (°).

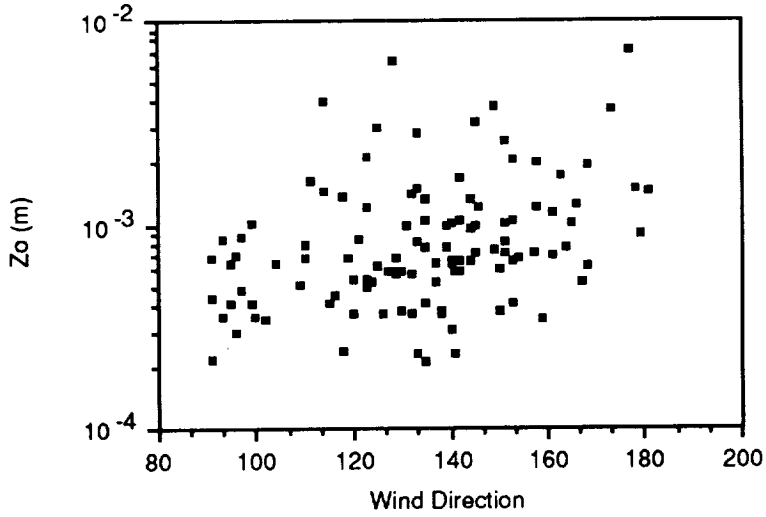

Mast 1

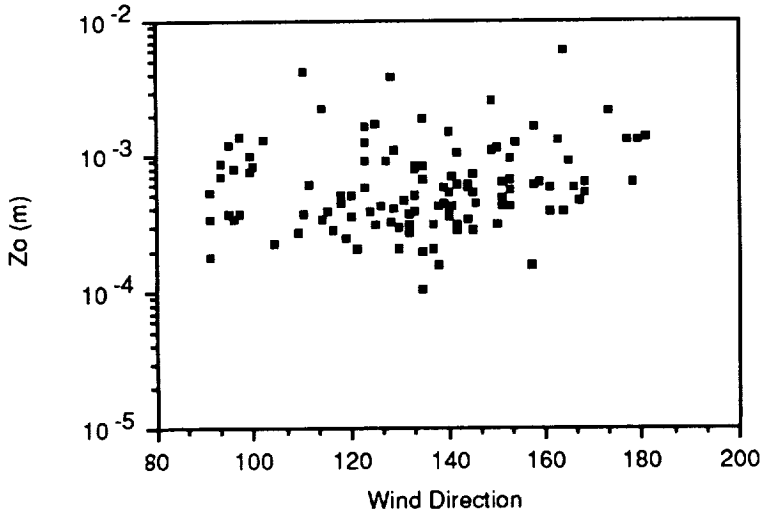

Mast 2

Figure 2.21b. Kit Fox Fan: southerly winds. Relationship between aerodynamic roughness (z_o) and wind azimuth direction (°).

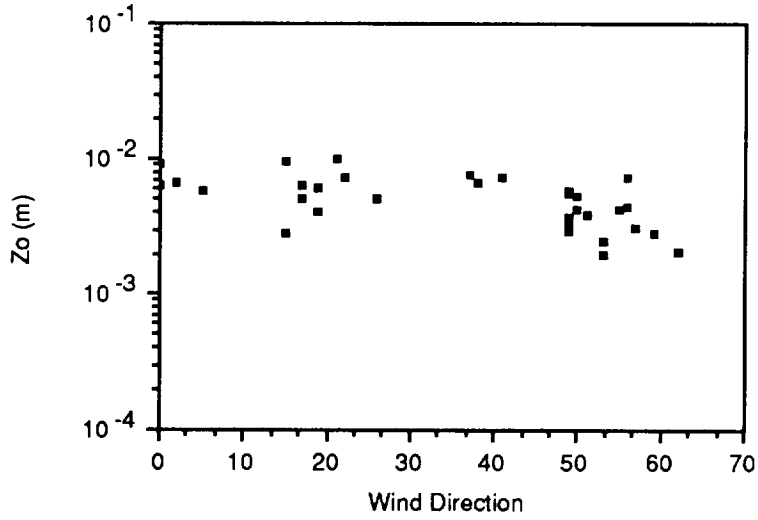

Mast 1

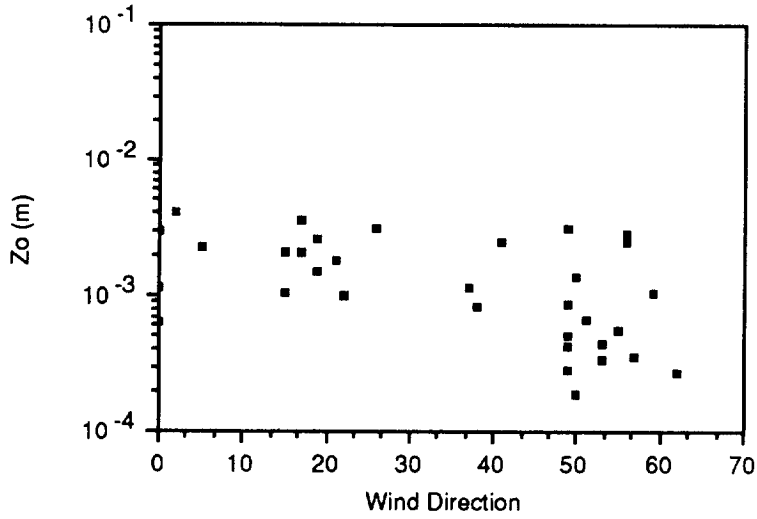

Mast 2

Figure 2.22a. Golden Canyon Fan: northerly winds. Relationship between aerodynamic roughness (z_o) and wind azimuth direction (°).

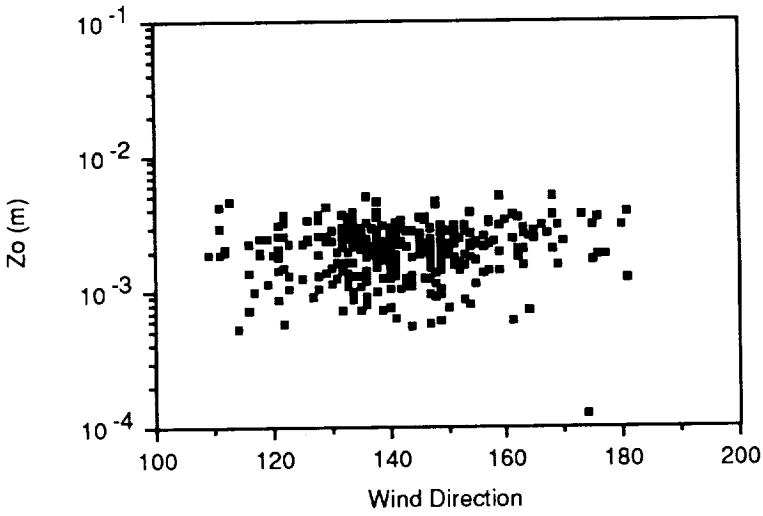

Mast 1

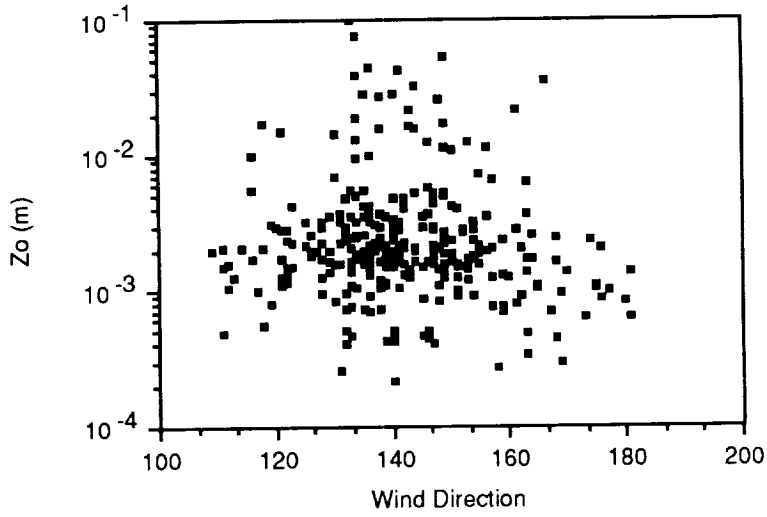

Mast 2

Figure 2.22b. Golden Canyon Fan: southerly winds. Relationship between aerodynamic roughness (z_o) and wind azimuth direction (°).

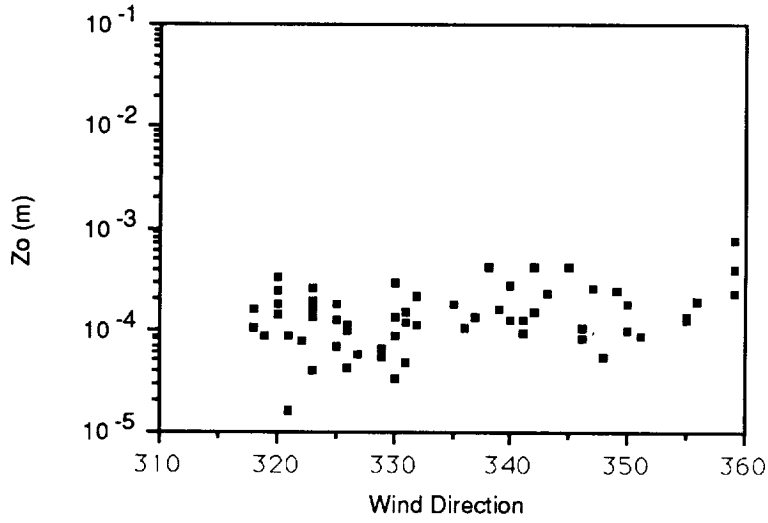

Figure 2.23a. Trail Canyon Fan: northerly winds. Relationship between aerodynamic roughness (z_o) and wind azimuth direction (°).

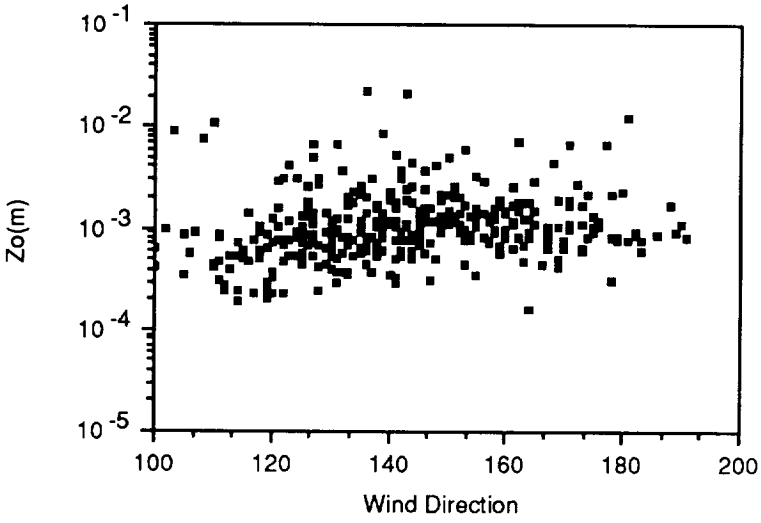

Figure 2.23b. Trail Canyon Fan: southerly winds. Relationship between aerodynamic roughness (z_o) and wind azimuth direction (°).

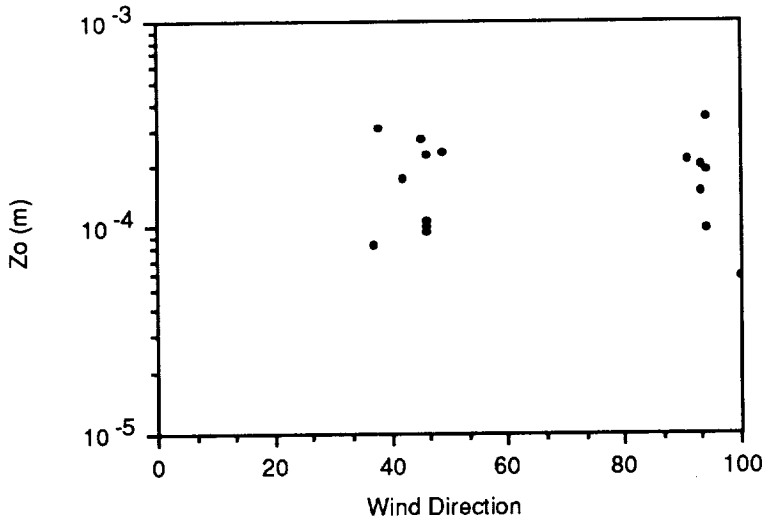

Figure 2.24a. Confidence Mill Playa: northeasterly winds. Relationship between aerodynamic roughness (z_o) and wind azimuth direction (°).

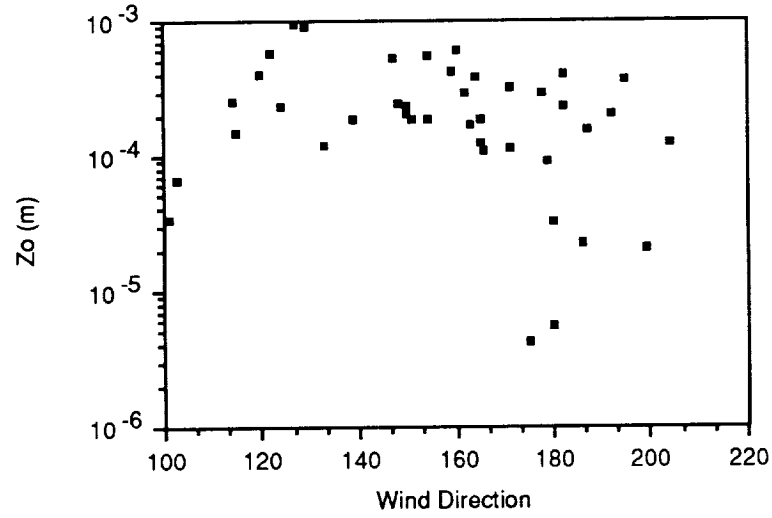

Figure 2.24b. Confidence Mill Playa: southerly winds. Relationship between aerodynamic roughness (z_o) and wind azimuth direction (°).

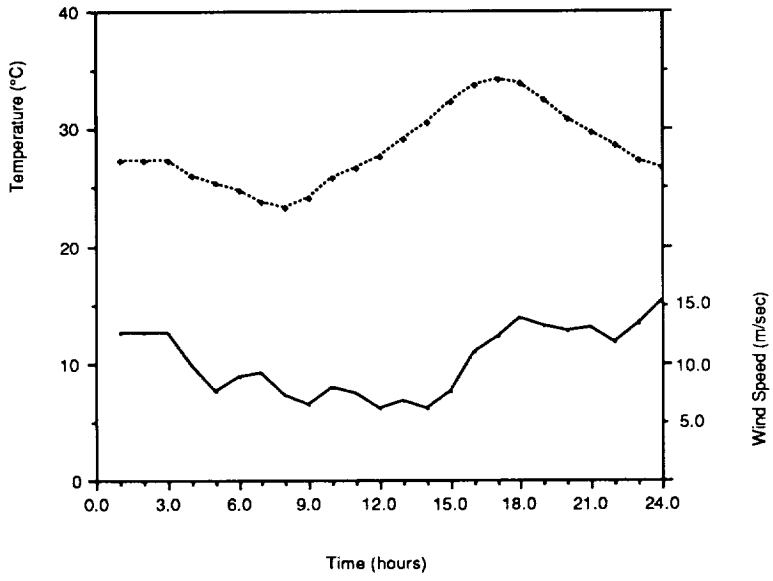

Figure 2.25. Diurnal variation of temperature and wind speed at Golden Canyon on April 22, 1989.

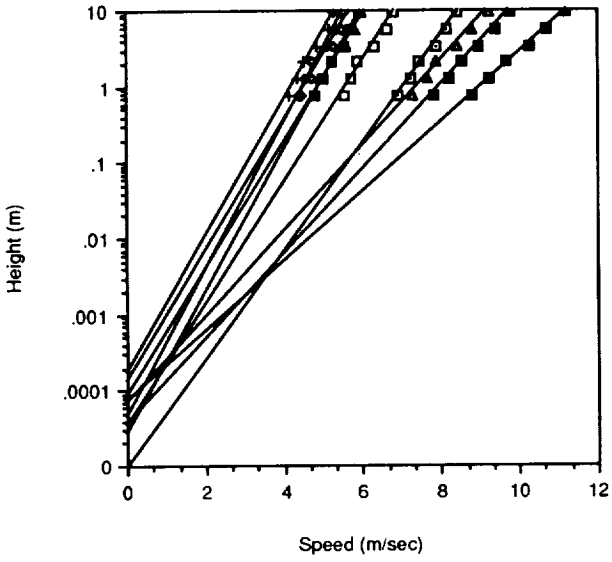

Figure 2.26. Stovepipe Wells: selected wind profiles for near neutral conditions. Southerly winds.

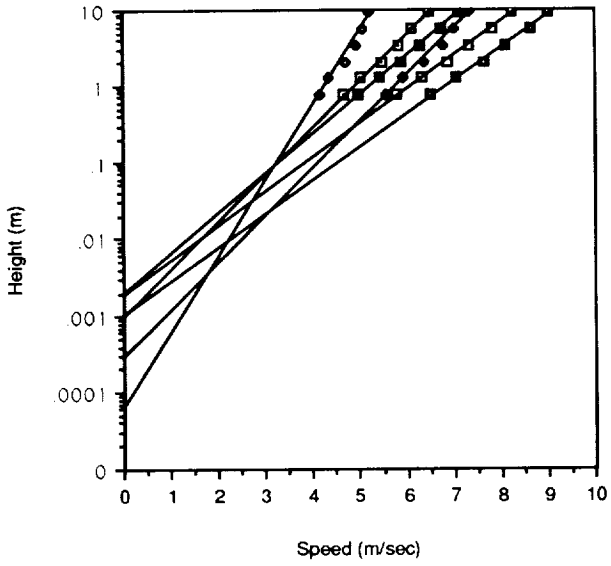

Figure 2.27. Kit Fox Fan: selected wind profiles for near neutral conditions. Southerly winds.

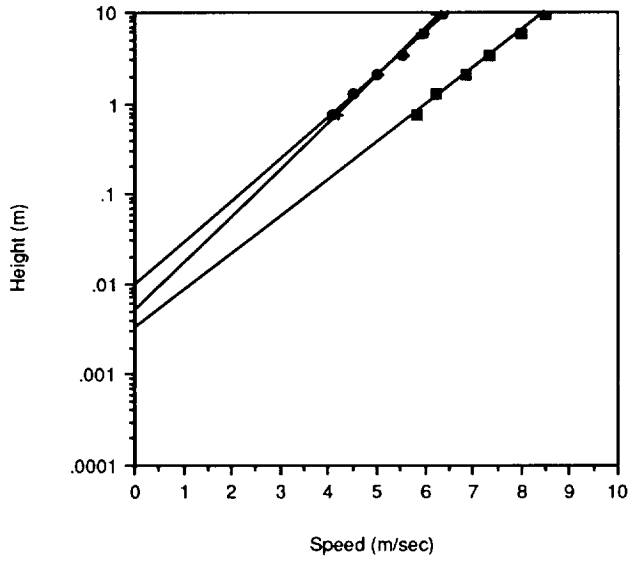

Mast 1

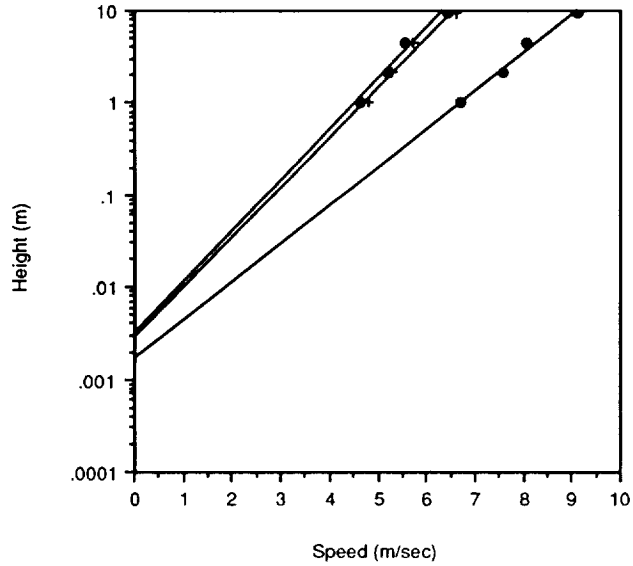

Mast 2

Figure 2.28. Golden Canyon Fan: selected wind profiles for neutral conditions. Southerly winds.

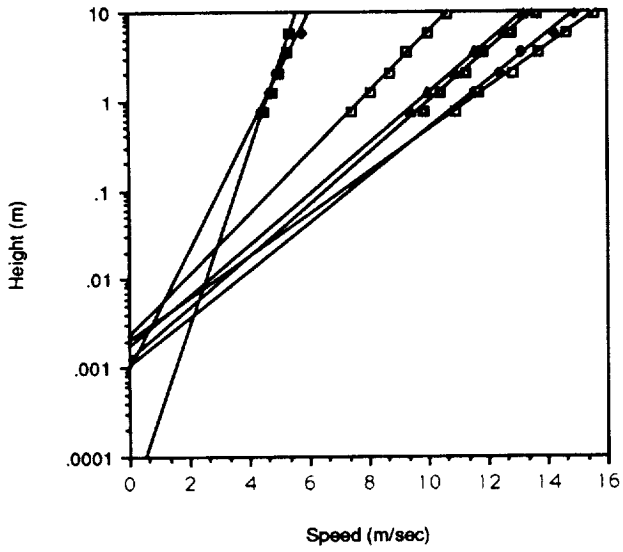

Figure 2.29. Trail Canyon Fan: selected wind profiles for neutral conditions. Southerly winds.

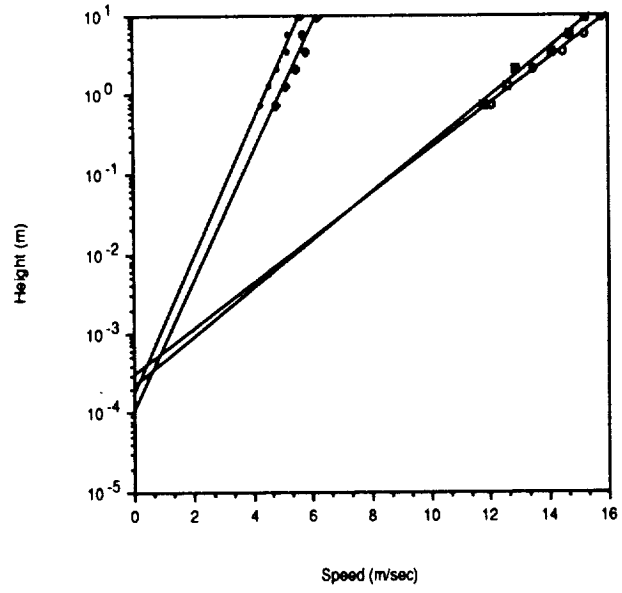

Figure 2.30. Confidence Mill Playa: selected wind profiles for neutral conditions. Southerly winds.

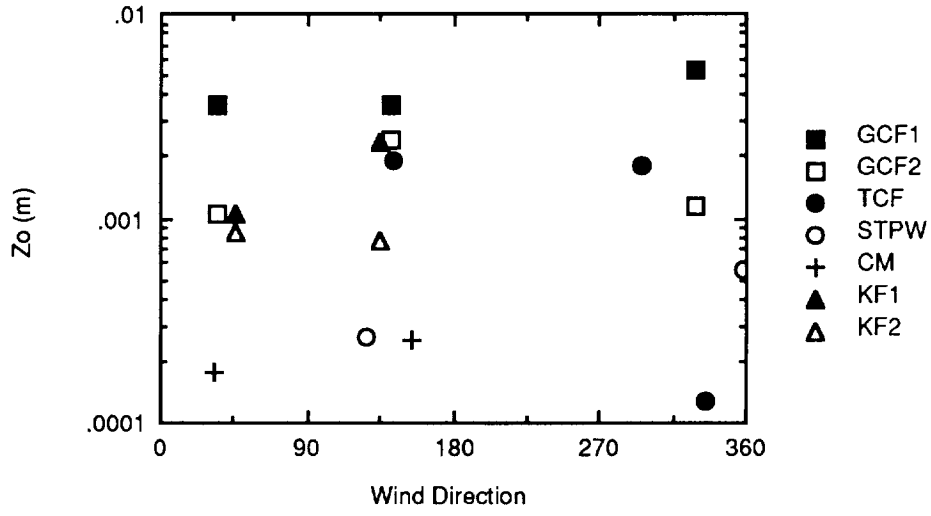

Figure 2.31a. Comparison between mean values of estimates of aerodynamic roughness (z_o) for sites studied in Death Valley.

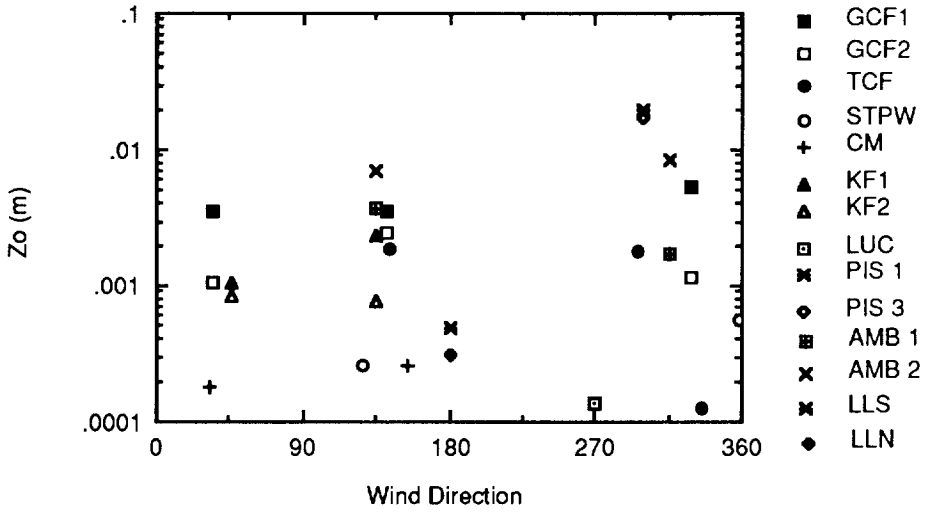

Figure 2.31b. Comparison between mean values of estimates of aerodynamic roughness (z_o) for sites studied in Death Valley and sites at Amboy, Pisgah, and Lunar Lake.

Table 2.5 Mean values of friction speed ratio ($u_*/u_{(9.5\,m)}$)

Site	Wind Direction			
	N-NE	SE-S	W-NW	NW-NNW
Stovepipe Wells		0.0385		0.0412
Kit Fox Fan				
Mast 1	0.0437	0.0405		
Mast 2	0.0427	0.0413		
Golden Canyon Fan				
Mast 1	0.0528	0.0524		0.0571
Mast 2	0.0435	0.0497		0.0449
Trail Canyon Fan		0.0467	0.0502	0.0374
Confidence Mill Playa	0.0412	0.0385		

Table 2.6 Arithmetic mean values of aerodynamic roughness (z_o)

Site	Wind Direction			
	N-NE	SE-S	W-NW	NW-NNW
Stovepipe Wells		0.00026	0.00055	
Kit Fox Fan				
Mast 1	0.00107	0.00237		
Mast 2	0.00085	0.00078		
Golden Canyon Fan				
Mast 1	0.00356	0.00360	0.00537	
Mast 2	0.00110	0.00245	0.00113	
Trail Canyon Fan		0.00190	0.00182	0.00012
Confidence Mill Playa	0.00063	0.00018		

varies from one site to another and, in some cases, from one direction to another at the same site.

2.3.4 Estimates of aerodynamic roughness and friction speed

Tables 2.5 and 2.6 give the mean values of friction speed ratio and aerodynamic roughness obtained for each major directional sector at each site.

Comparisons between the values of aerodynamic roughness obtained for each site are shown in Figure 2.31. They indicate that aerodynamic roughness estimates increase from the smoothest site, Confidence Mill playa, to the roughest site, Golden Canyon Fan, in parallel with the visual estimates of topographic roughness at each site.

There are some differences in the estimates of z_o for different wind directions, suggesting that local site conditions may strongly affect aerodynamic roughness estimates. The largest difference is at Trail Canyon, where the z_o estimate for northerly winds is an order of magnitude less than that for southerly and westerly directions. At sites where two masts were used, there are also some differences between z_o values for each mast. At Golden Canyon, estimates of z_o for the mast in the more distal location are consistently lower than those for the main mast upfan, suggesting perhaps that the site was not as homogeneous as was thought. At Kit Fox, values for the two masts are almost identical for northerly winds, but diverge significantly for southerly winds.

2.4 Site Characterization

Site characterization involved two main components: assessment of surface particle size and arrangement, and measurements of microtopography. In addition, each site was described in terms of its geologic setting, overall slope, and vegetation cover. Site characteristics were fully documented by photographs.

2.4.1 Surface particle size

The sizes of surface particles were assessed by estimating the proportions of clay/silt, sand, gravel, cobbles and boulders in a 1 m square area at 4 or 5 locations within a 24 x 24 m square centered on the anemometer mast (Fig. 2.32). The sub-site locations were chosen to represent the range of materi-

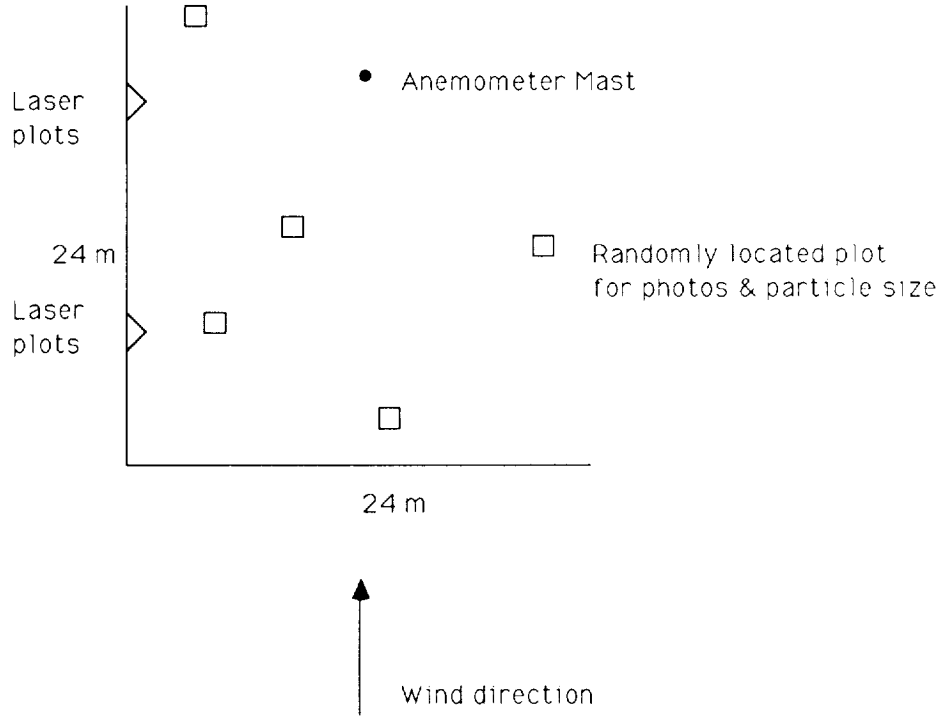

Fig. 2.32. Schematic diagram (not to scale) of the layout of site characterization procedures.

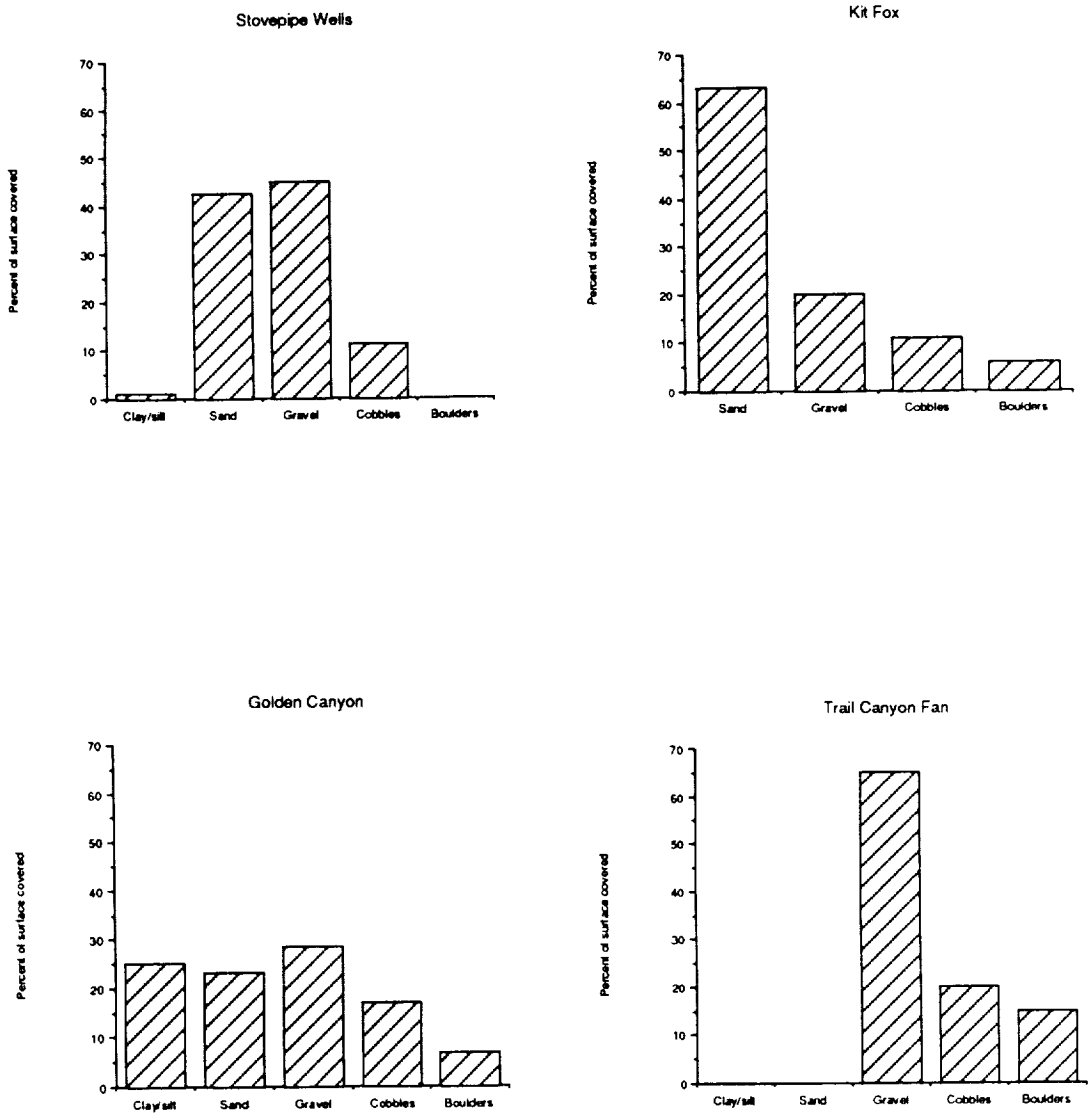

Figure 2.33. Estimates of mean particle size composition for study sites. Confidence Mill is 100% silt and clay sized material.

Table 2.7 Particle-size distribution for sites

Site and sub-site	Particle Size classes				
	Clay/silt	Sand	Gravel	Cobbles	Boulders
Kit Fox Fan					
1. bar 4 m S of mast		55		15	30
2. adjacent to channel 12 m S of mast			50	50	
3. swale 4 m W of mast		60		40	
4. swale 5 m NW of mast		70	30		
5. channel 3 m NW of mast		80	20		
Stovepipe Wells					
1. 10 m NE of mast	5	30	60	5	
2. 10 m S of mast		45	50	5	
3. 15 m SW of mast		45	35	20	
4. 10 m WNW of mast		50	35	15	
Golden Canyon Fan					
1. channel 10 m SW of mast	60	15	20	5	
2. swale 8 m SW of mast	5	25	30	25	15
3. gravel bar 2 m SSW of mast	20	10	40	30	
4. channel 8 m NW of mast	30	58	10	2	
5. bar 10 m NW of mast	15	20	30	30	5
6. bar 1 m NW of mast	20	10	40	10	20
Trail Canyon Fan					
1. 10 m S of mast			90	10	
2. 2 m NW of mast			30	20	50
3. 12 m NE of mast			90	10	
4. 12 m N of mast			75	20	5
5. 12 m S of mast			40	40	20
Confidence Mill Playa					
1. "flat" surface 4 m WSW of mast	100				
2. "puffy" surface 20 m W of mast	100				
3. "flat" surface 10 m S of mast	100				

Table 2.8 Estimates of average particle sizes

Site	Mean Particle Size Composition (% of surface covered)				
	Clay/silt	Sand	Gravel	Cobbles	Boulders
Stovepipe Wells	1.3	42.5	45.0	11.25	
Kit Fox Fan		63.0	20.0	11.0	6.0
Golden Canyon Fan	25.0	23.0	28.3	17.0	6.7
Trail Canyon Fan			65.0	20.0	15.0
Confidence Mill Playa	100.0				

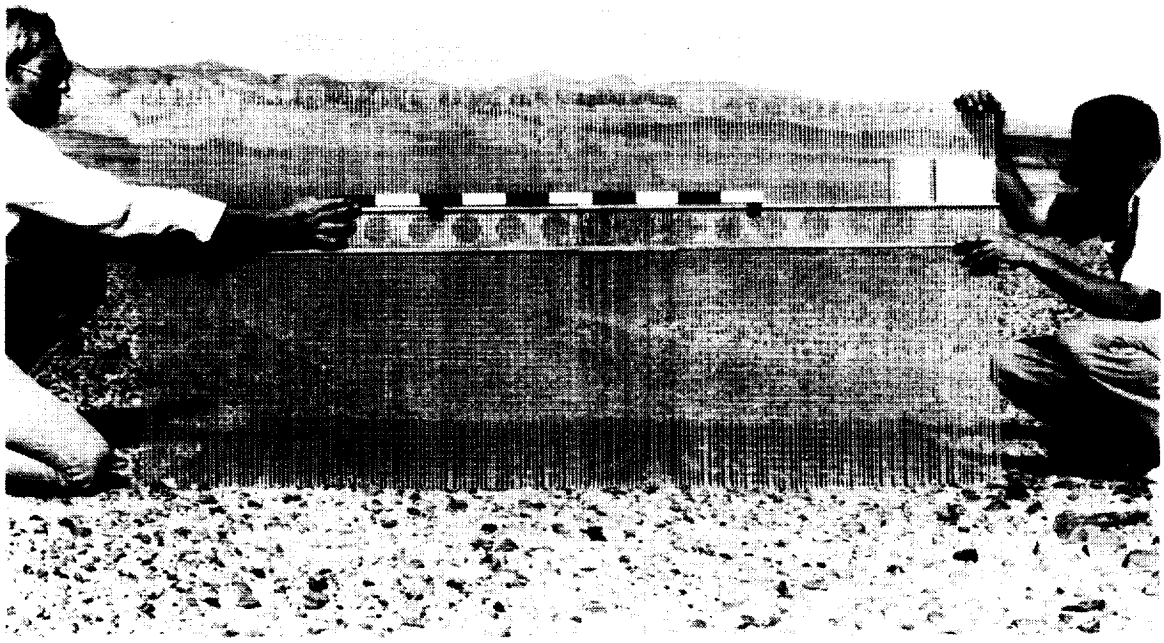

Figure 2.34. Template in use at Stovepipe Wells. Data were digitized from a photograph similar to this, scaled using the scale bar in the center of the photograph.

als at each site. Each sub-site was also photographed from an oblique and near vertical view.

The relative proportions (% of surface covered) of different-sized materials at each site are given in Table 2.7. The average composition of each site is summarized in Table 2.8 and Figure 2.33.

Of the rougher sites studied, Trail Canyon was the "best sorted", with the most uniform particle sizes. This reflects its well-developed desert pavement and relatively greater age and geomorphic stability. The most variable site was Golden Canyon, which is on a recently active alluvial fan/debris flow.

2.4.2 Microtopographic measurements

Procedures

Micro-topographic measurements were made using two devices, both of which provided data. From these data a detailed profile of the ground surface could be reconstructed: a template (Fig. 2.34) and a laser-photo device. The template consisted of a 2 m long bar through which 200 1 m-long by 0.5 cm-diameter aluminum rods protruded, giving a horizontal resolution of 1 cm. These rods were allowed to slide to contact the ground surface when the bar was held horizontal. The positions of the rods were recorded photographically. The height of the bar above the ground surface was also measured at each end so that adjacent template measurements could be linked together. In this manner two profiles 24 m long were obtained approximately parallel to and perpendicular to the major wind directions. In the laboratory, each photograph was printed to the same scale, and the position of the tops of each rod was digitized. This method was employed at all the rougher sites. At sites where the ground surface was composed of soft silt or sand (Stovepipe Wells and Confidence Mill) it was found that the rods penetrated the ground surface and gave erroneous measurements.

The laser profiling device (Fig. 2.35) was designed and constructed at ASU. It consists of a triangle with sides 1.2 m long and raised above the ground by about 50 cm. A small laser was mounted vertically on a traversing stage that was moved by a small motor along the rails that formed each side of the device. The traverse time was set to approximately 45 seconds. To operate the device and produce a record of microtopography, a camera was mounted on the vertice opposite the laser stage and a time exposure of ~ 45 seconds was made as the laser traversed the opposite side. A small electronic flash was used to illuminate a scale and the ground surface. This produced an image of the ground surface with a red profile line imaged across it by the laser (Fig. 2.36). This procedure was repeated for each side of the triangle and the images were then digitized to produce a topographic profile with a 1 mm vertical resolution.

Figure 2.35. Laser photographic profile device. Note traversing stage with laser on left and camera in center.

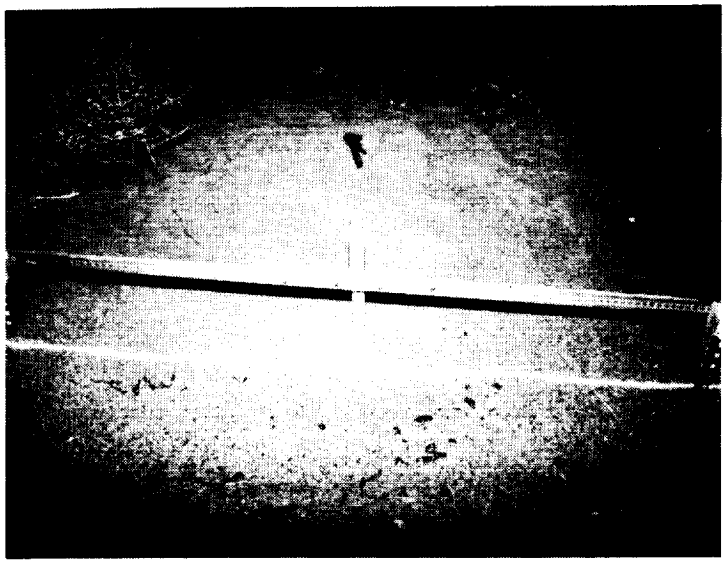

Figure 2.36. Black and white photograph from slide taken of laser profiling device. Slides similar to this were used for digitizing ground profile.

Table 2.9 Terrain statistics from template profiles at study sites

Site	l	Rms Height (m)	Estimated z_o (m) (RMS/30)	Correlation length (m)
Kit Fox Fan				
S-N		0.0615	0.00205	2.12
W-E		0.0329	0.00110	1.74
Trail Canyon Fan				
S-N		0.0660	0.00220	2.84
W-E		0.0256	0.00085	1.62
Golden Canyon Fan				
S-N		0.0772	0.00257	1.17
W-E		0.0394	0.00131	1.47

Table 2.10 Geometric mean values of template rms height at study sites (unfiltered data)

Site	RMS height (m)
Kit Fox	0.04204
Golden Canyon	0.05709
Trail Canyon	0.03642

Table 2.11 Mean values of terrain statistics obtained with laser device

Site	Rms height (m)	Correlation length (m)
Stovepipe Wells	0.0056	0.120
Kit Fox Fan	0.0097	0.125
Golden Canyon Fan	0.0150	0.112
Trail Canyon Fan	0.0076	0.037
Confidence Mill Playa	0.0066	

The digital terrain data produced by both techniques were then analyzed to produce terrain statistics, including rms height (standard deviation of the changes in elevation), correlation length and an estimate of z_o based on the assumption that it is 1/30 of the rms height. For each transect, the linear trend in the data due to overall surface slope was removed. The rms height and correlation length were then calculated from the unfiltered data, for which the longest possible wavelength (l) will be half the transect distance (12 m). Rms height was also calculated for data filtered with a square filter with cut-off for l equal to 2 m and 1 m. This removes low period fluctuations in the data. The template results are given in Table 2.9 and the laser results in Table 2.11. Comparison of the data shows that the rms height of the laser data is about an order of magnitude less than that of the template data, suggesting that it is measuring particle roughness.

These data show that roughness, as measured by rms height derived from both systems, increases in the same sense as that suggested by visual inspection of the surface. Both the template and site characterization data suggest that Golden Canyon Fan was the roughest site studied. Kit Fox Fan and Trail Canyon Fan differ only slightly from each other. The E-W roughness is less in all cases than the N-S values. This is probably a result of the E-W orientation of the bar and swale topography and small washes that occur at all sites. As the winds cross this topography at an oblique angle, a further index of the surface roughness is the geometric mean of the N-S and E-W RMS heights (Table 2.10).

2.5 Comparisons Between Estimates of Aerodynamic Roughness and Microtopography and Particle Size Data

The aerodynamic roughness of a surface is a function of its roughness characteristics. These can be sub-divided into two components: particle roughness, which is a function of surface particle size and spacing, and topographic roughness, which is a function of the microtopography of the site. Figure 2.37 shows that there is a good correlation between the mean particle size at each site and aerodynamic roughness.

In addition, at the alluvial fan sites that were studied, particle roughness is superimposed on the microtopography of the bars and swales developed on the fan surface. The template data can be analyzed to provide a measure of roughness at both scales. In this experiment, the rms height of the surface is a good index of its roughness. The rms height was compared to the aerodynamic roughness estimates for both northerly and southerly wind directions at each site. The plots of these data (Fig. 2.38) show that there is a good relationship between unfiltered rms height and aerodynamic roughness. However, the wind crosses the surface at an oblique angle to the template profiles. The geometric mean of the rms height for both profiles

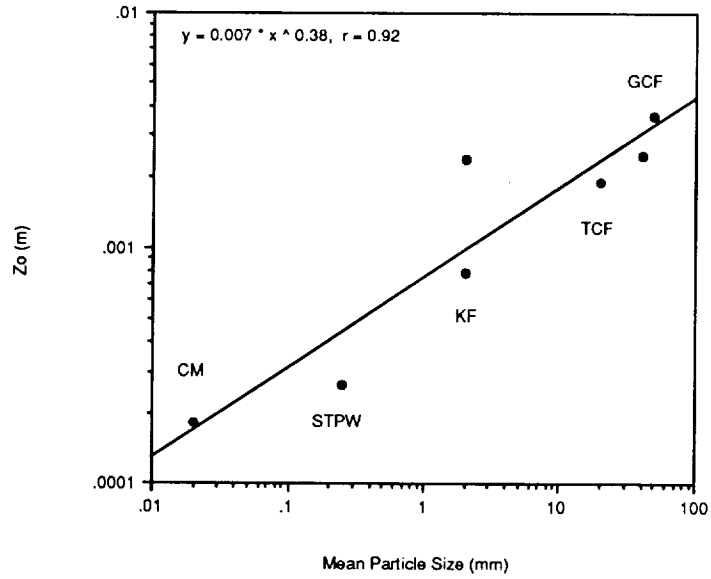

Figure 2.37. Relationship between aerodynamic roughness (southerly wind data) and estimated mean particle size at study sites.

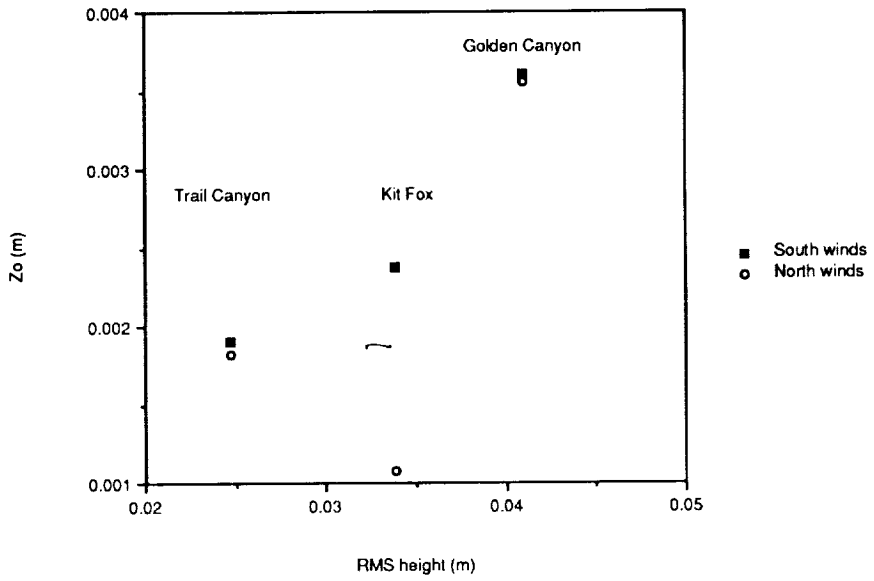

Figure 2.38a. Relationship between aerodynamic roughness and rms height (unfiltered data) for E-W transects.

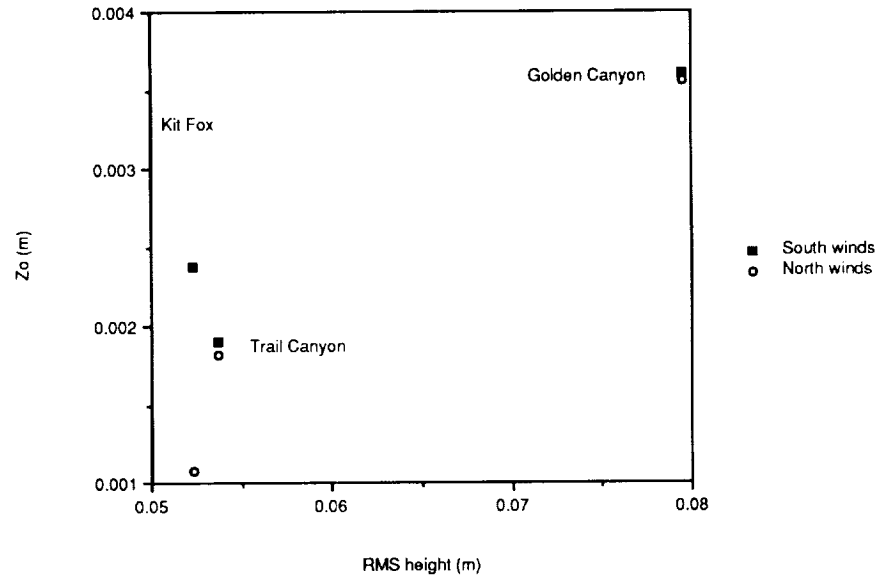

Figure 2.38b. Relationship between aerodynamic roughness and rms height (unfiltered data) for N-S transects.

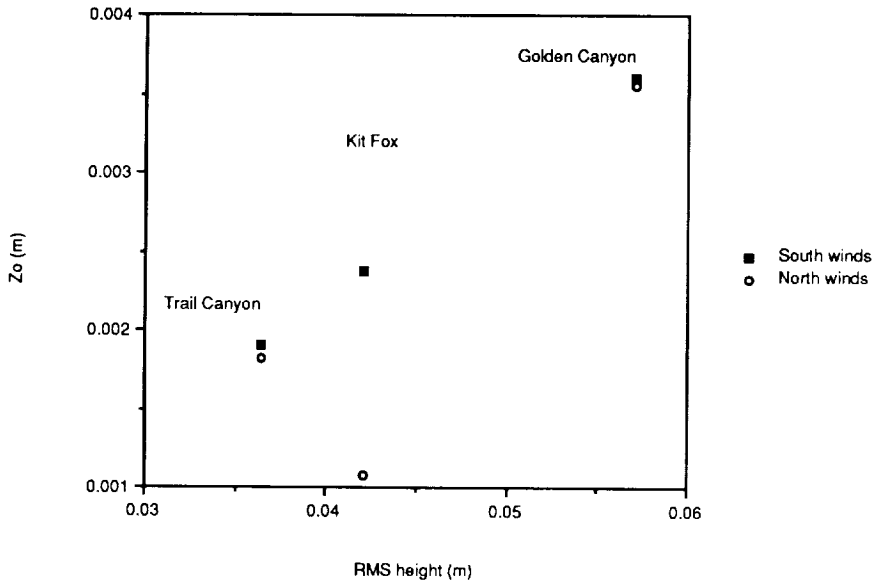

Figure 2.39. Relationship between aerodynamic roughness and geometric mean rms of height (unfiltered data) for E-W and N-S template transects.

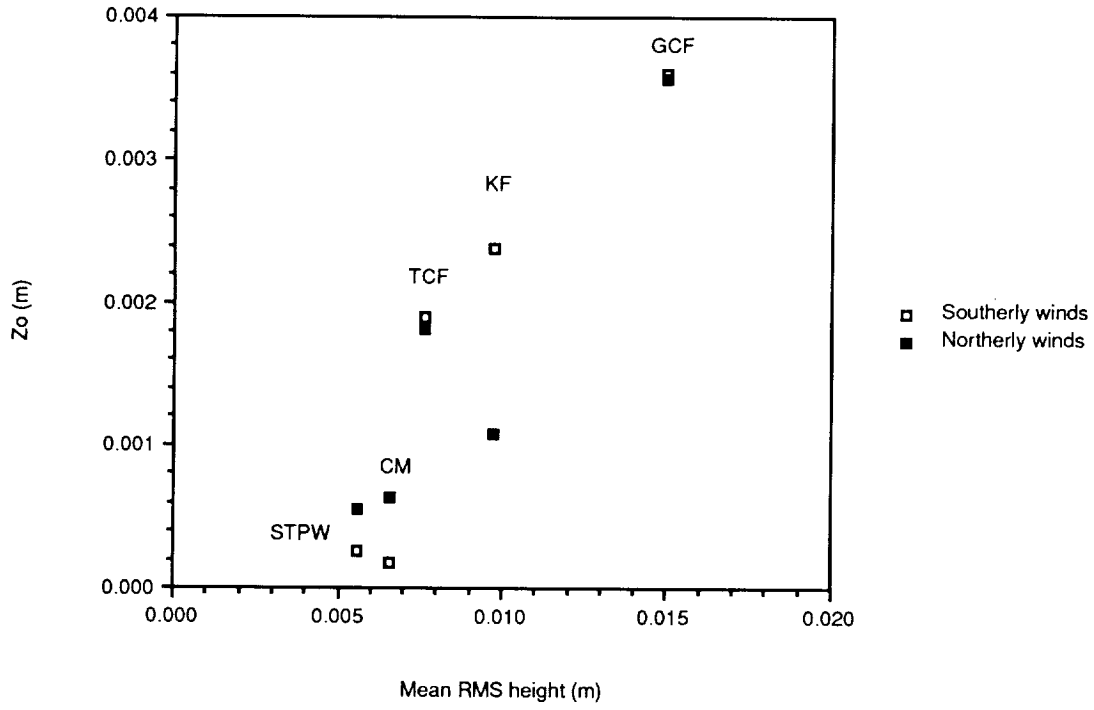

Figure 2.40. Relationship between mean rms height derived from laser data and aerodynamic roughness for all study sites.

gives a better "3-D" characterization of the surface, which correlates well with aerodynamic roughness estimates (Fig. 2.39).

Data for the laser profiles at each site provide a measure of particle roughness. There is a similarly good correlation between mean rms height for each site and aerodynamic roughness (Fig. 2.40).

2.6 Acknowledgements

This research was conducted in Death Valley National Monument with permission from the Superintendent. We thank the National Park Service for their assistance and support. We thank Gary Beardmore for his technical assistance, D. Ball for photographic services and advice, and Judith Lancaster for field support. This investigation was supported by the National Aeronautic and Space Administration through Ames Research Center Grant NCC 2-346 and Jet Propulsion Laboratory Contract 88-04070.

3.0 ANALYSIS OF MOJAVE FIELD EXPERIMENT RADAR DATA FOR RARP

L. Gaddis and R. Greeley

3.1 Introduction

The purpose of this analysis is to establish further a quantitative relationship between radar backscatter and aerodynamic roughness through analyses of calibrated airborne radar data and field measurements of aerodynamic roughness. Determination of optimal radar imaging parameters (such as incidence angle, wavelength, and polarization) for correlation with aerodynamic roughness will be made from these analyses of aircraft radar data in preparation for the multiparameter, third Shuttle Imaging Radar (SIR-C) experiment to be launched in two phases in 1992 and 1993. Target sites for this investigation include areas of geologic interest in desert terrains with the following characteristics: subject to aeolian activity; relatively free of vegetation; at least 10 km² in size; a range of roughnesses, with each site having homogeneous roughness; and accessible for field measurements. At this time, radar backscatter coefficients (σ°) and aerodynamic roughness values (z_o) exist for lava flows, alluvial fans, and playas in the vicinity of Pisgah and Amboy Volcanic Fields of the Mojave Desert in southern California (Fig. 3.1). Aerodynamic roughness values were measured for the playa at Lucerne Dry Lake, three lava flow surfaces at Pisgah (Fig. 3.2) and 2 lava flow surfaces and an alluvial fan at Amboy (Fig. 3.3, Table 3.1; Greeley and Iversen, 1987; Greeley et al., 1988). Because of limited accessibility of areas surrounding the Pisgah and Amboy fields due to military activities, the z_o measurement of the playa at Lucerne will serve as a surrogate for that of the Lavic Dry Lake playa at Pisgah for these analyses.

3.2 Radar Data

Radar images of the Pisgah and Amboy Volcanic Fields, Mojave Desert, California (Fig. 3.4) were acquired in June, 1988 by the airborne NASA/JPL Imaging Radar Polarimeter during the Mojave Field Experiment (MFE; Wall et al., 1988). These radar data were acquired with a resolution of about 10 m, at 3 wavelengths simultaneously

Table 3.1 Aerodynamic roughness values (z_o) for Mojave sites (from Greeley et al., 1987)

Site	z_o (m)
Amboy	
alluvial fan (Tower 1)	0.00173
mantled pahoehoe (Tower 2)	0.00847
pahoehoe (Tower 3)	0.1007*
Pisgah	
aa (Tower 1)	0.0199
pahoehoe (Tower 2)	0.0042
mantled pahoehoe (Tower 3)	0.0169
Lucerne	
playa	0.00014

*z_o values for this site are included for completeness only. Tower 3 was located in the wake of the Amboy cinder cone and thus did not have adequate fetch for accurate measurement of wind speed. See Figures 3.2 and 3.3 for location of wind tower sites at Pisgah and Amboy.

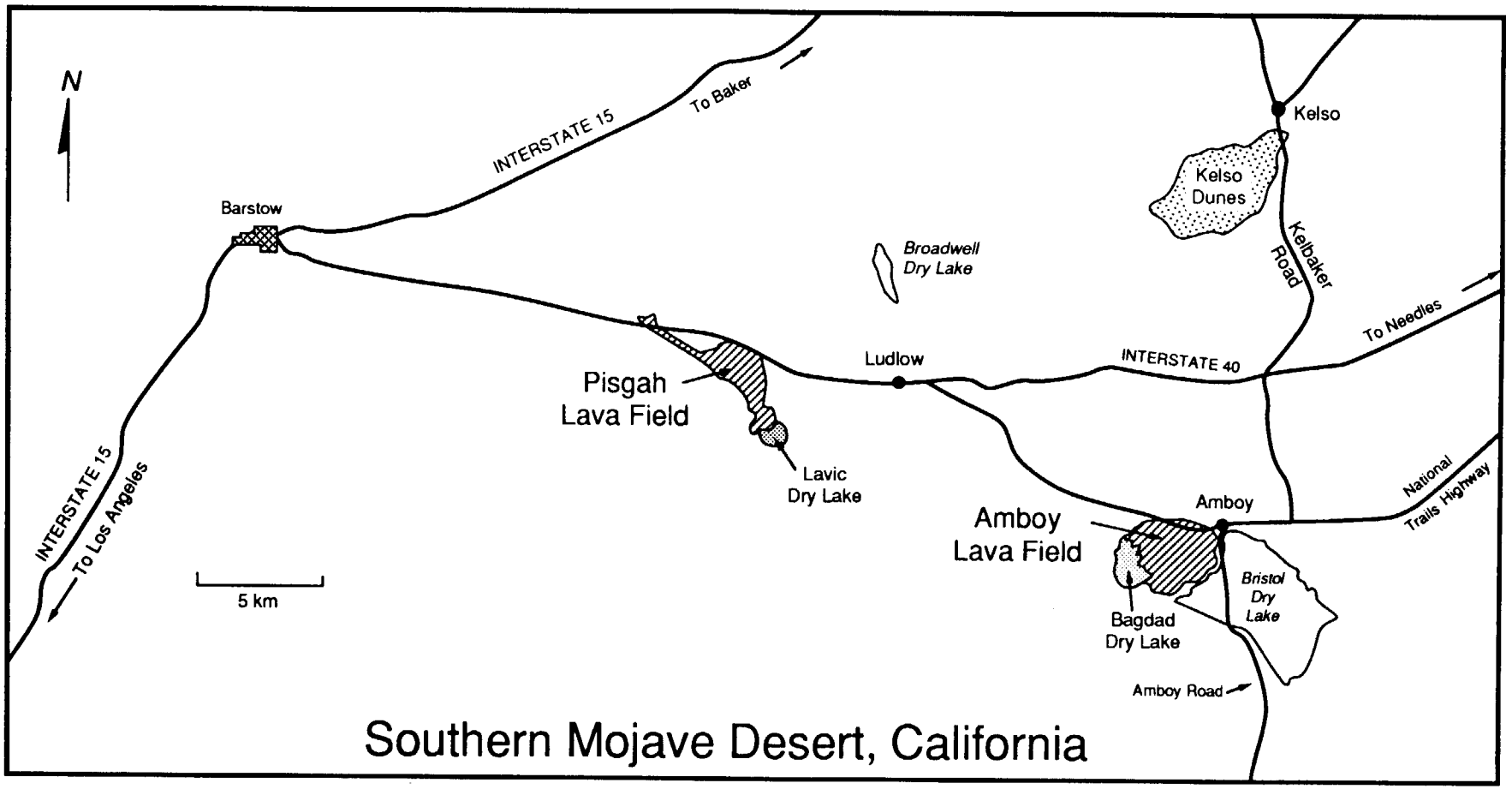

Figure 3.1. Sketch map of the southern Mojave Desert, CA, showing the locations of the Pisgah and Amboy lava fields.

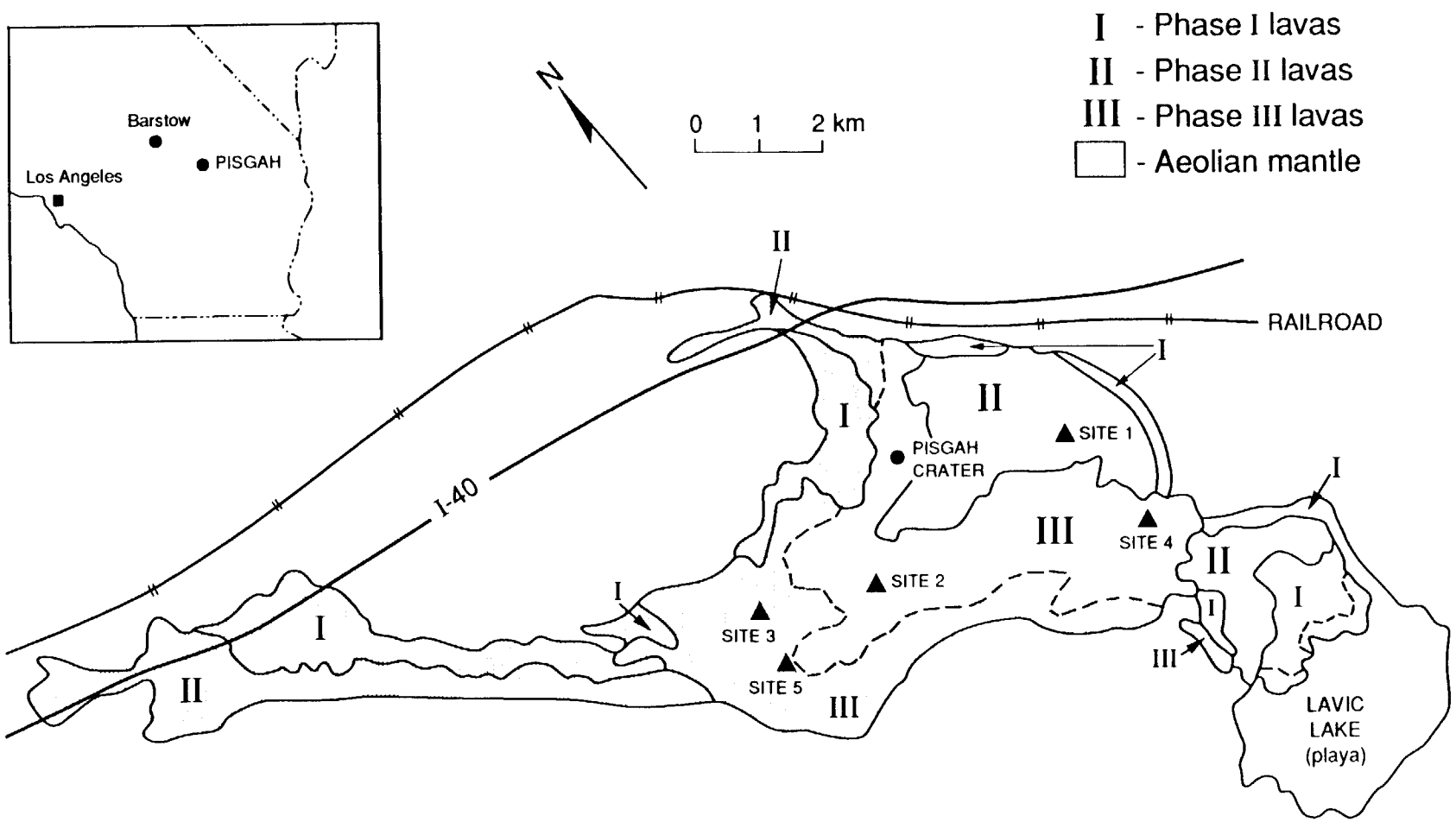

Figure 3.2. Sketch map of the Pisgah lava field showing the major geologic units and the five sites for aerodyanmic roughness measurements (triangles).

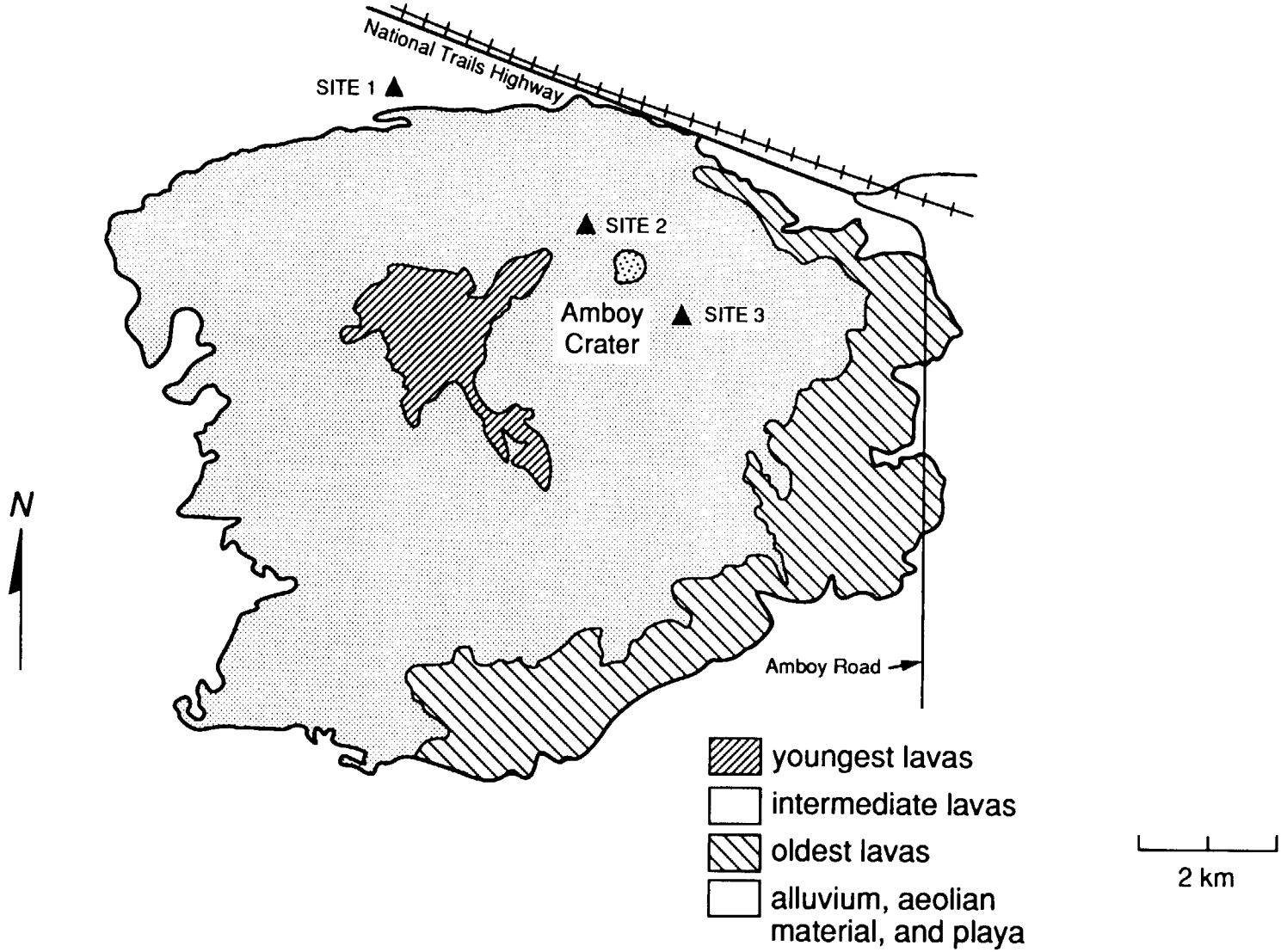

Figure 3.3. Sketch map of the Amboy volcanic field showing the sites for aerodynamic roughness measurements.

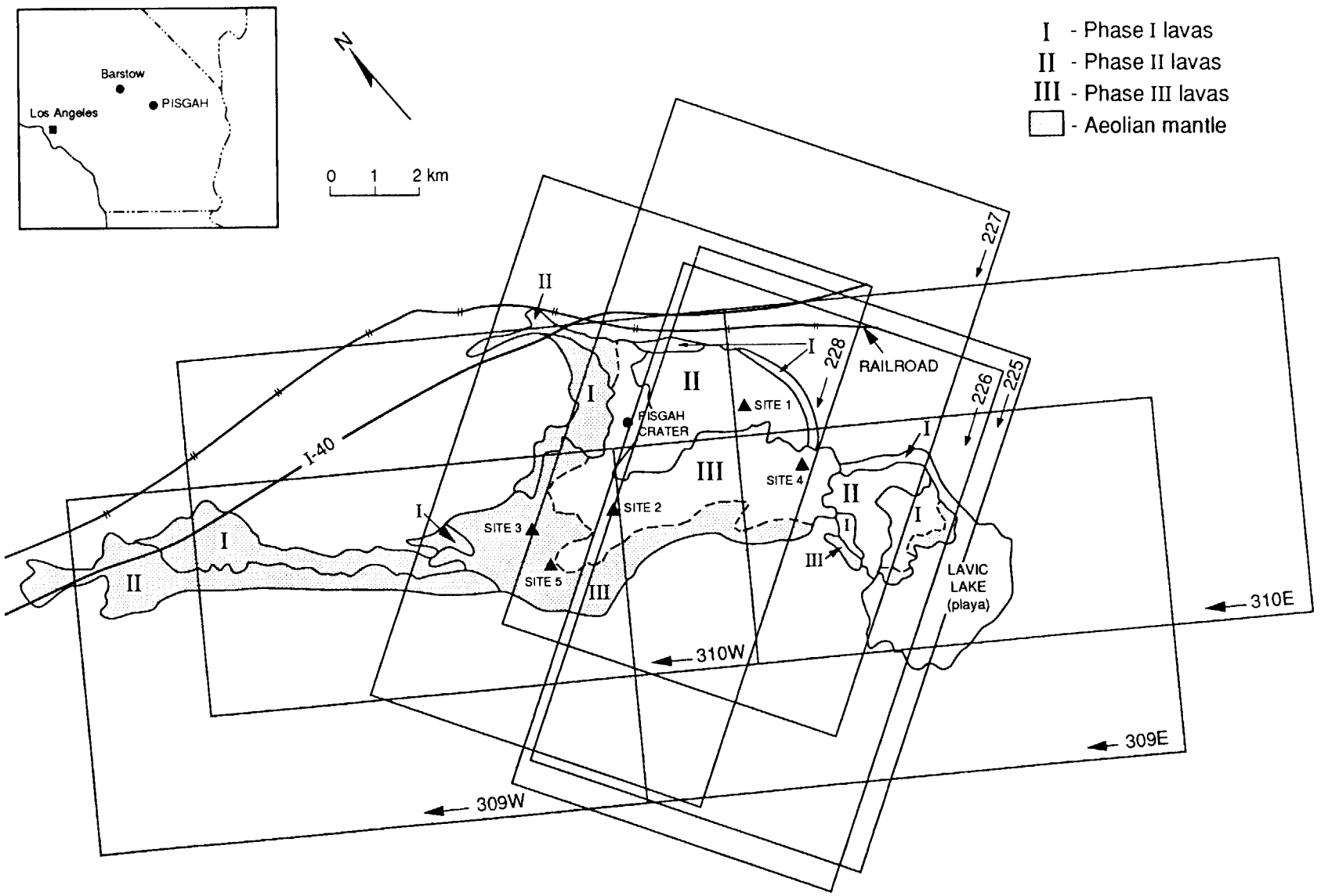

Figure 3.4. Sketch map of the southern Mojave Desert showing the ground tracks (10 km wide) of aircraft radar data for the Pisgah and Amboy lava fields during the MFE; arrows indicate the flight direction of the left-looking aircraft radar instrument.

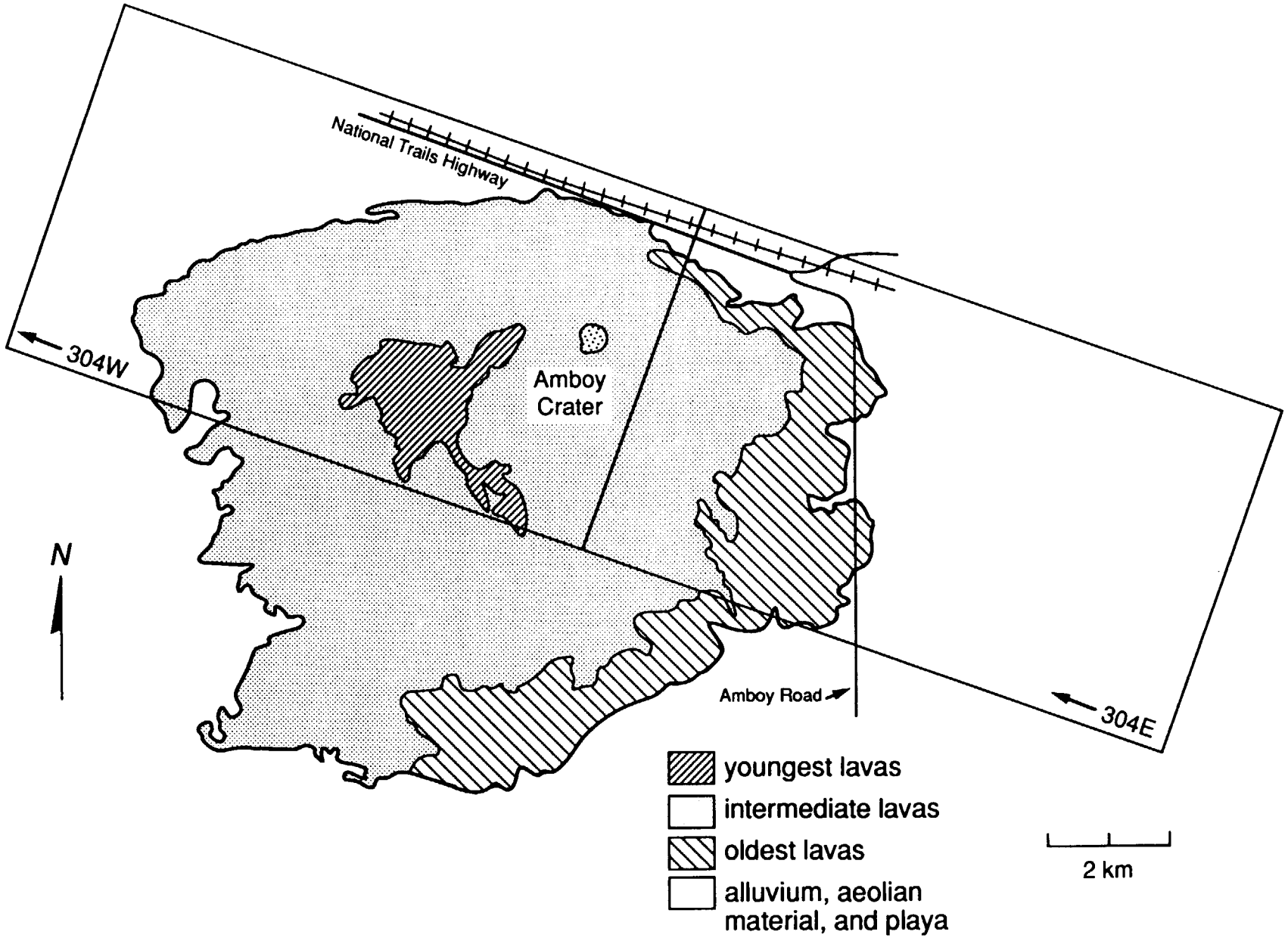
National Trails Highway
304W
Amboy Crater
N
Amboy Road
304E
youngest lavas
intermediate lavas
oldest lavas
alluvium, aeolian material, and playa
2 km

Figure 3.4b.

Calculation of Incidence Angle for AIRSAR Data

$$\cos \theta = A/D_s$$
$$\theta = \text{acos}(A/D_s)$$

where

incidence angle = θ
aircraft altitude* = A
slant range distance = D_s

EX: D_s, total slant range = 756 pixels across an image x slant range pixel size (m)
= 756 x 6.662
= 5036.472 m

EX: D_s, half slant range = (756/2) pixels across half an image x slant range pixel size (m)

* Note that these parameters can be read from the tape header or from the hardcopy header. Although their values are similar from image to image, subtle differences may exist and should be accounted for.

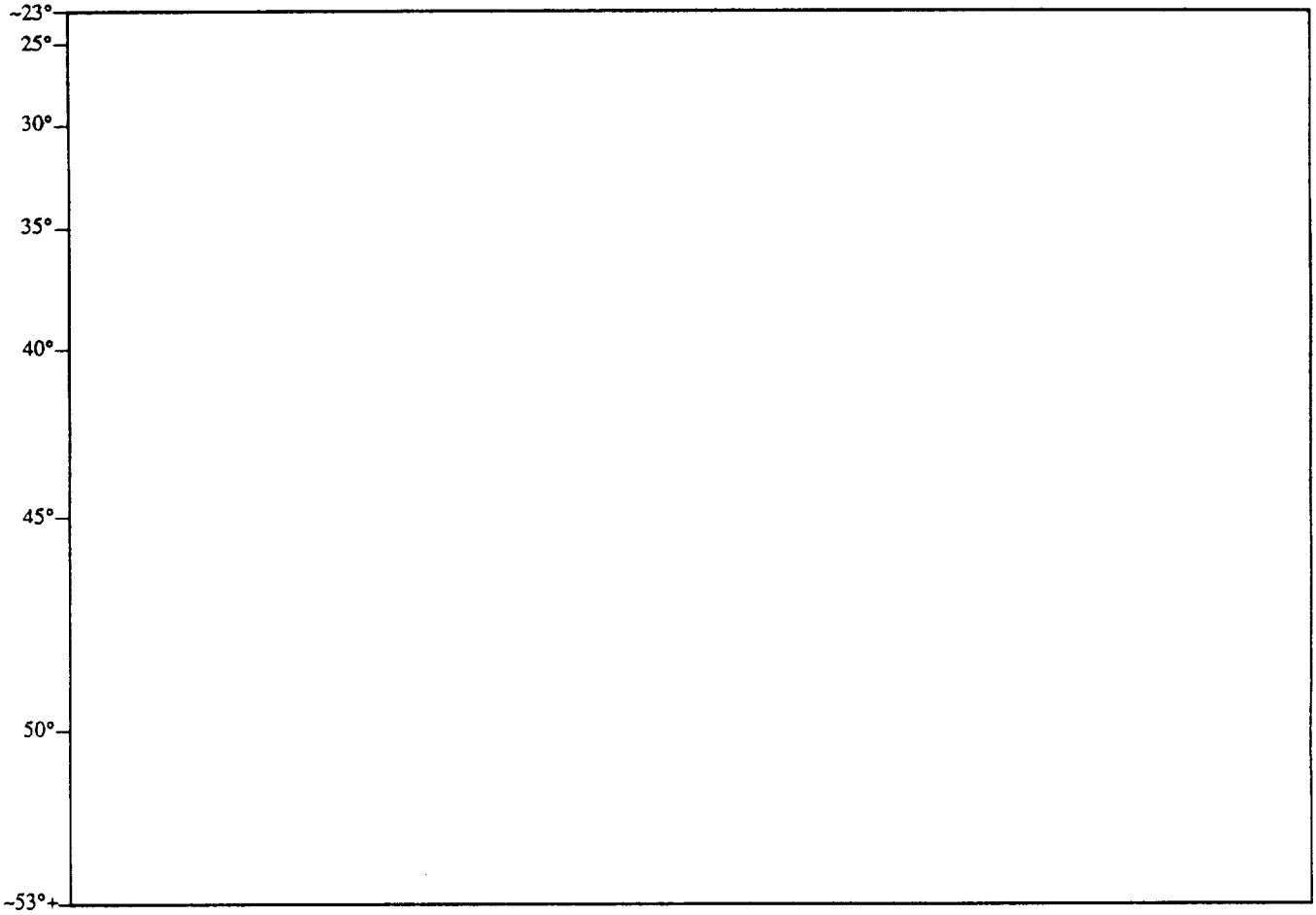

Figure 3.5. A template showing the variation in incidence angle from near- to far-range (top to bottom) in a typical aircraft radar image; image dimensions are 750 lines, 1024 columns. The parameters and equations used to calculate incidence angle at any given line in a radar image are included.

Table 3.2 Aircraft radar data acquired during the Mojave Field Experiment

We have received the following complete set of full-resolution digital radar images from the Mojave Field Experiment. These radar data consist of C-, L-, and P-band images at four polarizations for each site. Except where noted (* denotes calibrated data), digital radar data are uncalibrated and are delivered in compressed format.

Site	Image Center Incidence Angle
Amboy-304* (from J. Plaut, 9/89)	40.66°
Amboy-303* (")	40.66°
Cima-1-070	42.98°
Kelso Dunes-064	41.79°
Kelso Dunes-065	40.20°
Kelso Dunes-062	43.76°
Pisgah-2-225	41.93°
Pisgah-2-226	43.67°
Pisgah-2-227	44.04°
Pisgah-1-308* (from F. Burnette, 4/89)	44.22°
Pisgah-1-309* (")	43.90°
Pisgah-1-309(west)	42.84°
Pisgah-1-310* (from F. Burnette, 4/89)	43.27°
Pisgah-1-310*(west) (")	43.07°
Pisgah-2-228	43.67°

As of 10/6/89, we have requested of Jakob van Zyl that the following images from the Mojave Field Experiment be calibrated at the current level of capability:

Priority	Site
1	Pisgah-1-310
1	Pisgah-1-310(west)
1	Pisgah-2-228
1	Pisgah-2-226
2	Pisgah-2-225
2	Pisgah-2-227
2	Pisgah-1-309
2	Pisgah-1-309(west)
3	Amboy-304
3	Amboy-303
3	Pisgah-1-308

(P-band: 68 cm; L-band: 24 cm; and C-band: 5.6 cm), and at multiple polarizations. Although any combination of transmitted and received polarization states may be simulated utilizing the complete polarimetric capabilities of the instrument (Zebker et al., 1987; van Zyl et al., 1987), only direct- and cross-polarized data (HH, HV, VV, VH, comparable to those of the SIR-C experiment) were produced for this analysis. The acquisition of multiple incidence-angle data for a single target was made possible by altering the ground track of the airborne instrument. Images of portions of the Pisgah volcanic field were obtained at center incidence angles of about 30°, 40°, and 50° and of the Amboy field at about 40°. An example of the variation in incidence angle across an aircraft radar image is shown in Figure 3.5. A list of the radar data acquired during the Mojave Field Experiment over the Pisgah and Amboy fields is presented in Table 3.2. Stereo photographs obtained from a helicopter were also acquired for 6 sites on the Pisgah lava field by Tom Farr, Eilene Theilig, Jakob van Zyl, and Steve Wall, and photogrammetrically analyzed by Franz Leberl. The locations and rms heights for these sites are illustrated in Figure 3.6.

Relative radiometric calibration of the MFE data was achieved through the analysis of the backscattered signal from a series of calibrated

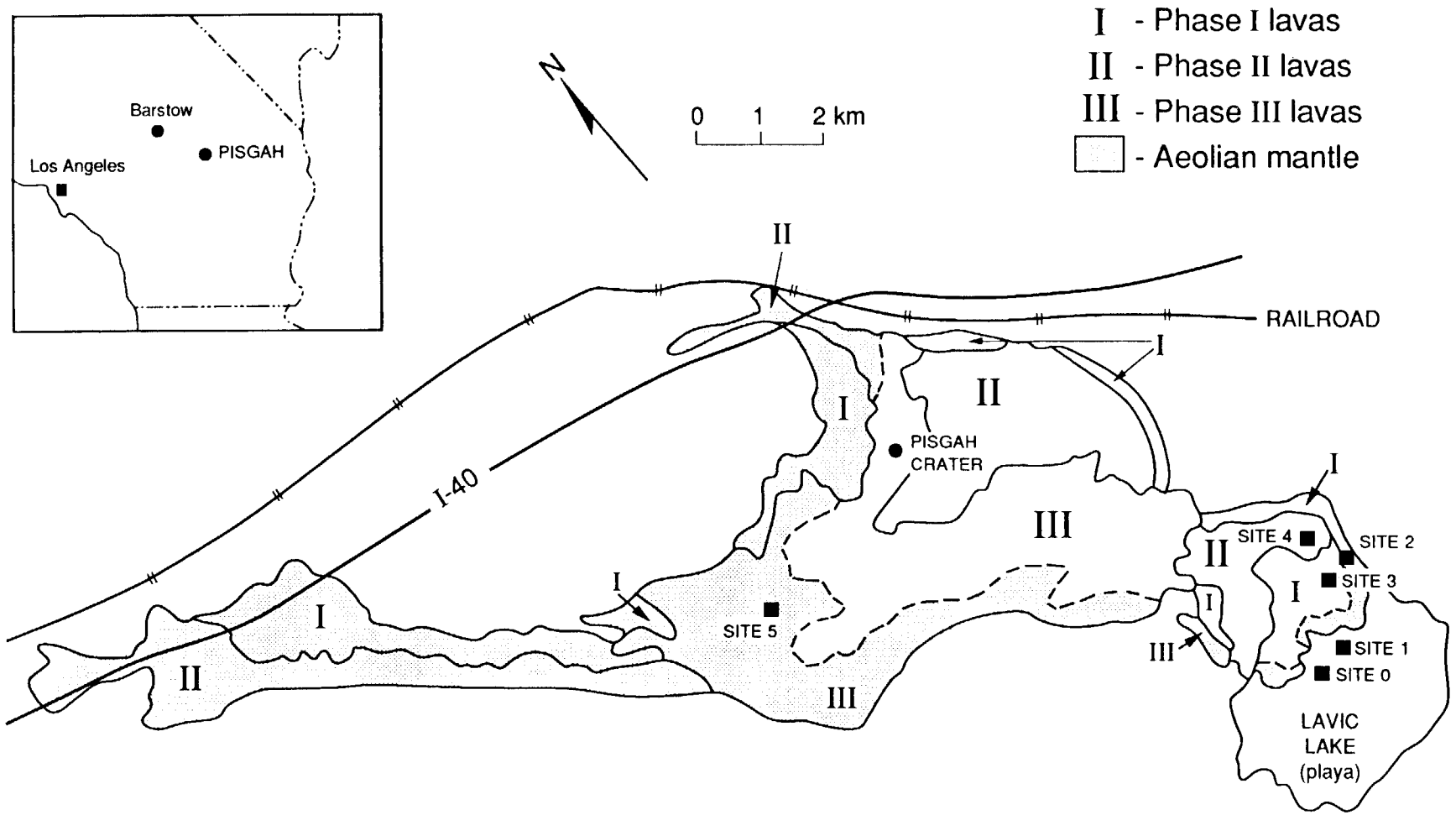

Figure 3.6. Schematic map of the Pisgah lava field showing the six locations at which stereo photographs were acquired to determine terrain roughness. RMS heights (cm) calculated for each of these sites are also indicated.

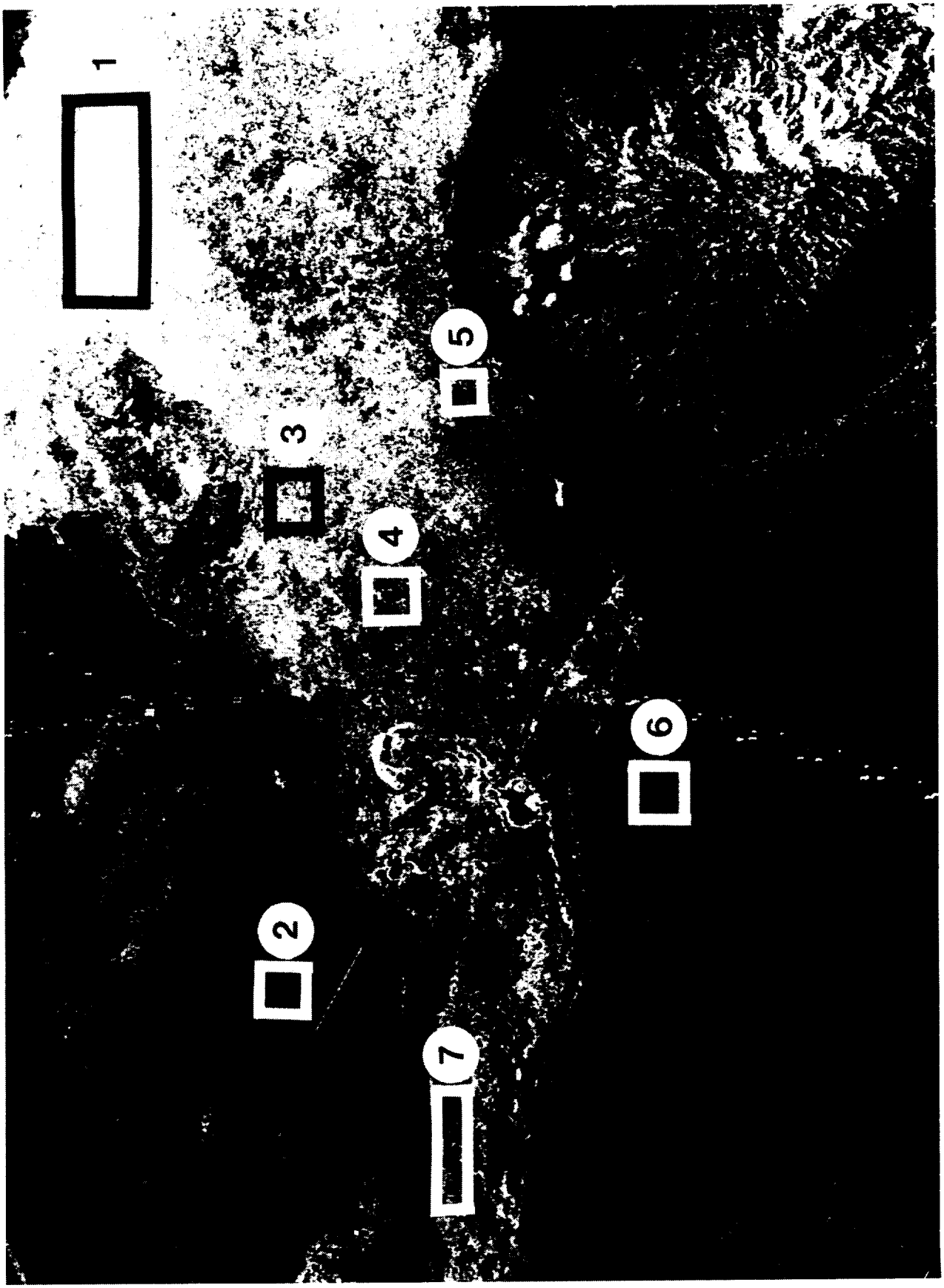

Figure 3.7. Calibrated radar images (a) "Pisgah-310W", (b) "Pisgah-310E", and (c) "Amboy-304" showing areas where backscatter coefficients were calculated. Numbers correspond to sites listed in Table 3.3.

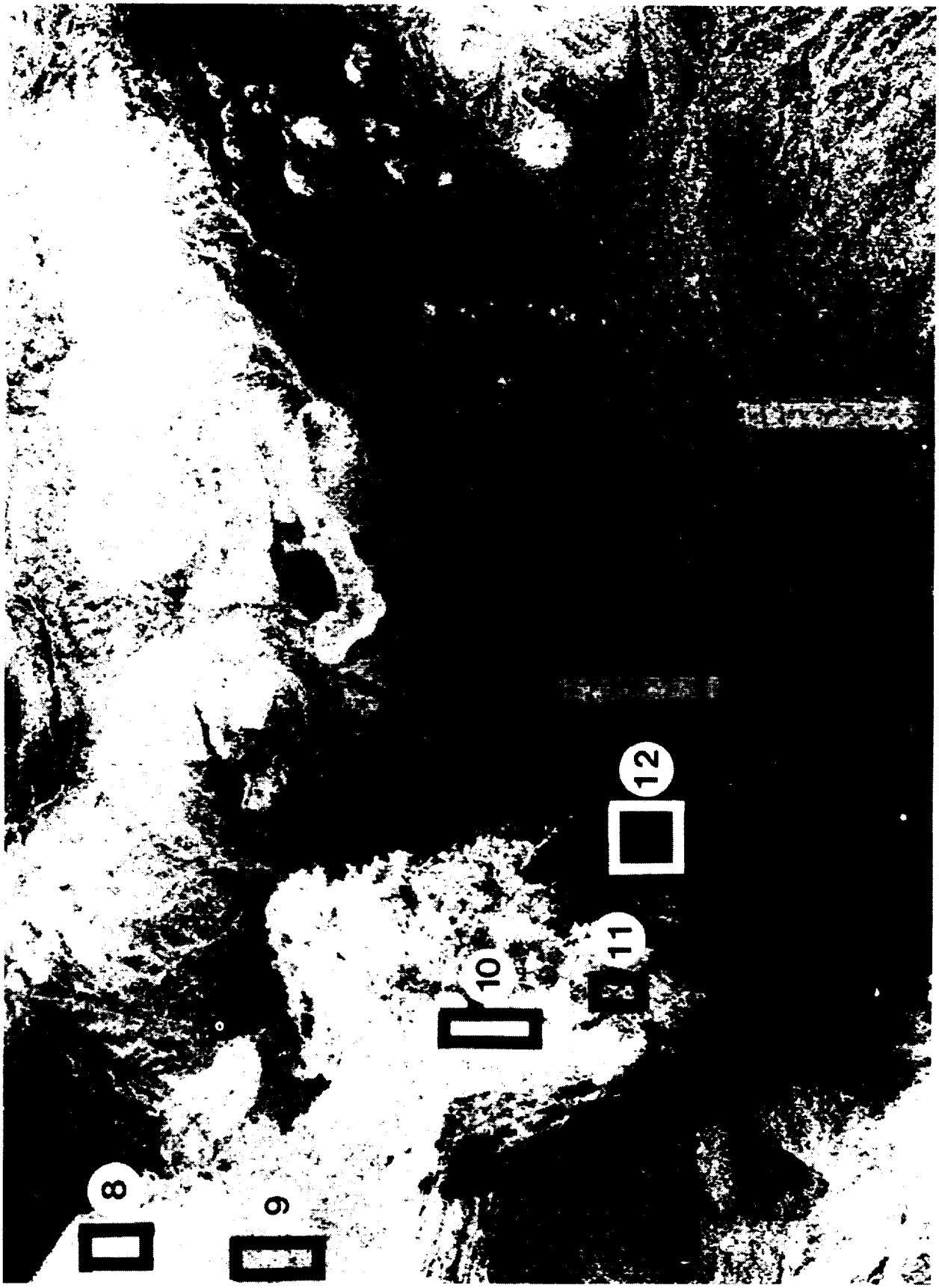

Figure 3.7b.

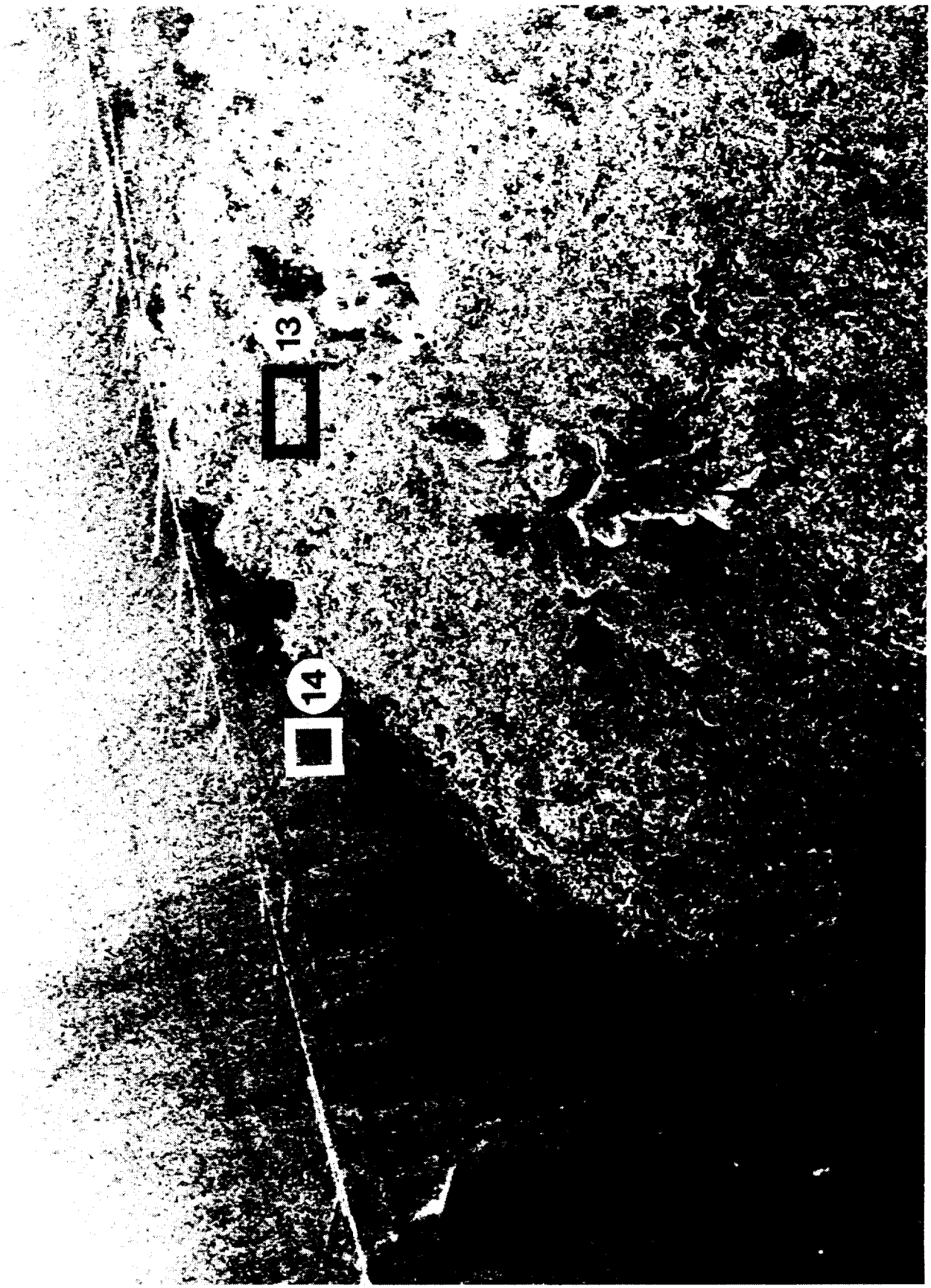

Figure 3.7c

Table 3.3. Backscatter coefficients (σ°) for geologic units, Pisgah and Amboy lava fields

Site*	Unit**	P			L			C		
		σ°HH	σ°HV/VH	σ°VV	σ°HH	σ°HV/VH	σ°VV	σ°HH	σ°HV/VH	σ°VV
1	aa (II)	-9.88	-21.30	-11.14	-4.37	-14.68	-5.97	-5.08	-14.40	-5.98
2	alluvium	-30.10	-42.52	-29.61	-22.42	-34.12	-22.51	-14.20	-24.68	-13.60
3	pahoehoe (P2, III)	-11.42	-23.99	-12.01	-7.60	-19.22	-8.61	-6.68	-16.20	-6.94
4	mantled pahoehoe (P3, III)	-15.79	-29.86	-15.77	-11.63	-24.81	-12.17	-9.30	-19.14	-9.55
5	mantled pahoehoe (III)	-18.59	-32.39	-18.25	-14.59	-26.80	-14.83	-11.07	-20.12	-10.90
6	alluvium	-29.66	-39.06	-29.24	-25.63	-35.95	-24.93	-16.58	-25.69	-15.83
7	mantled pahoehoe (I?)	-20.95	-33.98	-20.38	-15.22	-27.27	-14.75	-11.09	-20.67	-11.64
8	aa (~P1, II)	-10.93	-25.55	-12.19	-4.96	-15.13	-6.43	-5.51	-17.36	-6.29
9	pahoehoe (III?)	-13.77	-30.86	-14.10	-9.24	-22.22	-10.07	-8.09	-21.29	-7.92
10	aa (II)	-12.18	-26.62	-12.32	-8.72	-18.41	-9.12	-6.94	-18.25	-7.24
11	mantled pahoehoe (I)	-21.79	-36.50	-20.16	-16.53	-27.63	-15.55	-10.45	-22.40	-9.81
12	playa	-28.72	-44.74	-27.15	-23.06	-40.03	-21.56	-18.31	-32.55	-16.01
13	mantled pahoehoe (A2)	-13.5	-25.9	-9.8	-9.7	-22.3	-9.0	-6.2	-17.6	-6.2
14	alluvium (A1)	-25.7	-38.5	-20.6	-15.2	-28.2	-13.7	-6.7	-16.9	-6.4

*Site locations are shown in Figure 7. **Roman numerals correspond to lava flow eruptive phase of Wise, 1966.

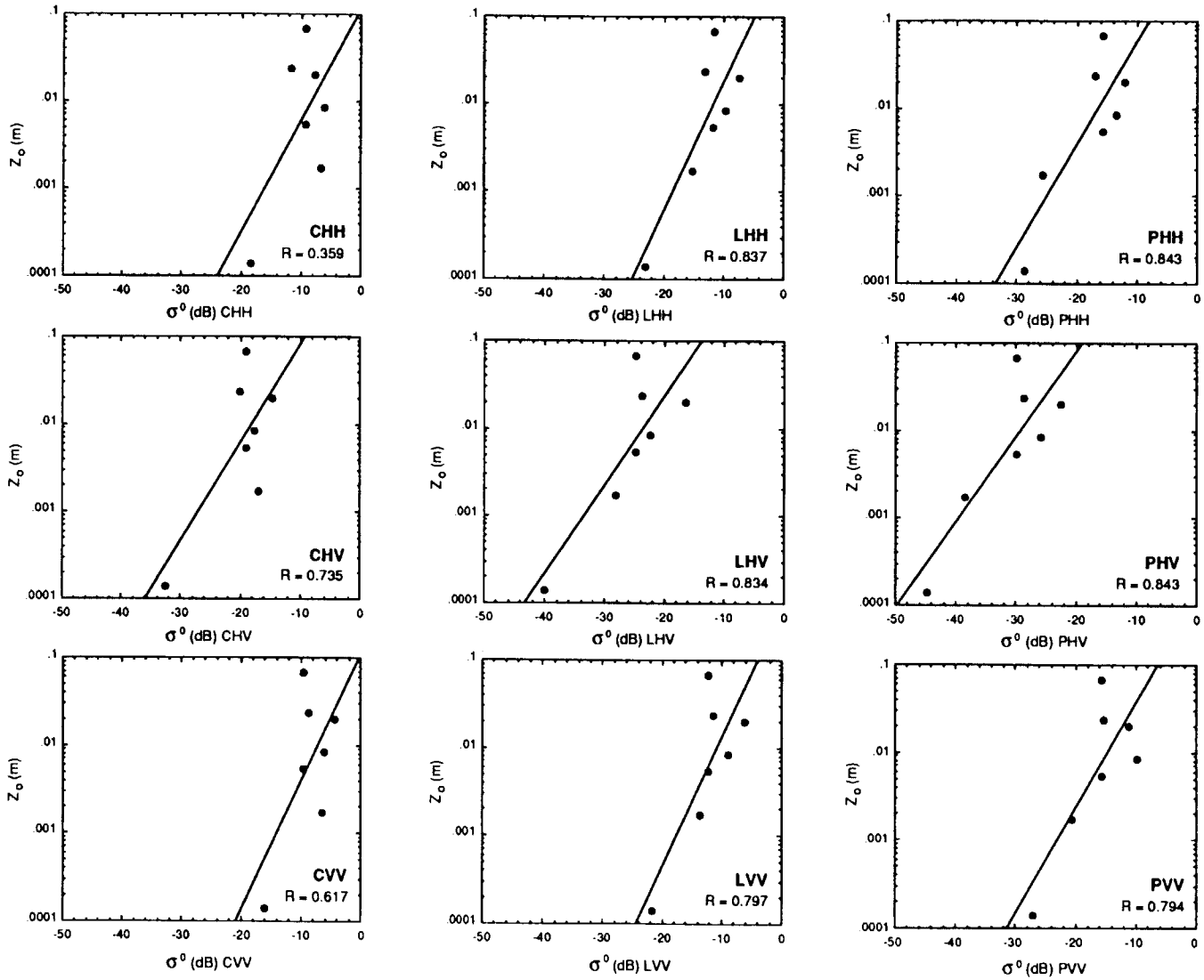

Figure 3.8. Plots showing the correlation between radar backscatter coefficient (σ^o) versus aerodynamic roughness (z_o) for six geologic units (from high to low): aa from Pisgah Wind Tower 1 site (incidence angle = 32°); pahoehoe from Pisgah Wind Tower 2 (incidence angle = 38°); mantled pahoehoe from Pisgah Wind Tower 3 (incidence angle = 42°); mantled pahoehoe from Amboy Wind Tower 2 (incidence angle = 34°); alluvium from Amboy Wind Tower 1 (incidence angle = 35°); and playa from Lake Lucerne. The locations of each site (except Lucerne) are shown in Figures 3.2 and 3.3. Note that highest degree of correlation (as indicated by the highest value of the correlation coefficient, R) is observed for the L-band radar data and the aerodynamic roughness values.

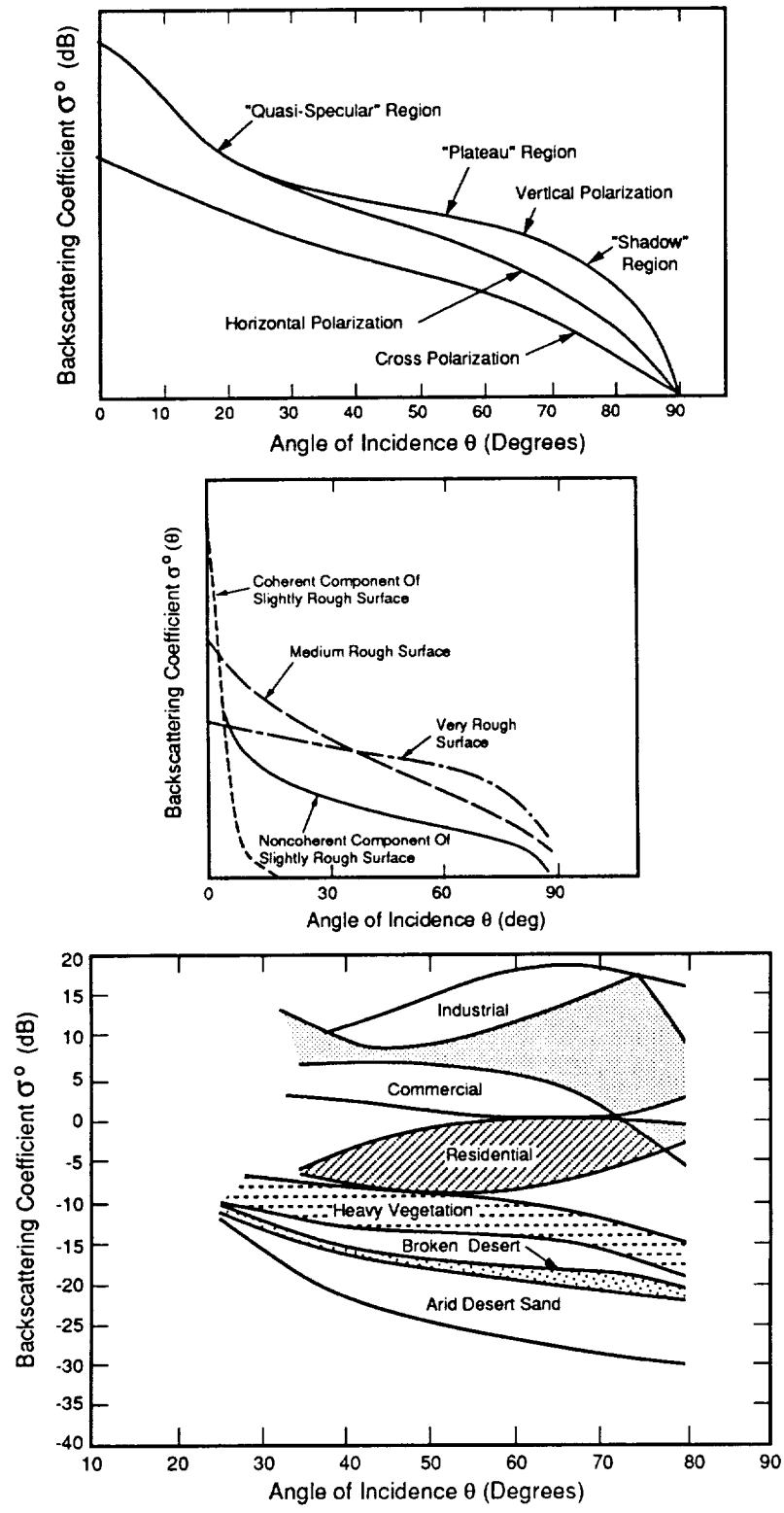

Figure 3.9. Theoretical backscatter curves (after Ulaby et al., 1986) showing variation of backscatter coefficient with angle of incidence at (a) different polarizations, (b) with different surface roughnesses, and (c) measurements for natural surfaces.

trihedral corner reflectors (van Zyl, 1989). Each corner reflector was deployed about 2 km apart on the smooth surface of the Lavic Lake playa, with 5 reflectors spanning the width of the 10-km radar ground swath. Comparison of the polarization signatures of the observed and an ideal corner reflector show good agreement (van Zyl, 1989), permitting the calculation of backscatter coefficients for geologic units within these calibrated areas. Backscatter coefficients (σ°) have been determined for several areas at Pisgah and Amboy from three calibrated radar images (Table 3.3, Fig. 3.7). Calculation of backscatter coefficients for this analysis was made possible through the efforts of Jakob van Zyl, Fred Burnette, and Howard Zebker of the Radar Geology Group at the Jet Propulsion Laboratory.

Our goal in the analyses of these radar data is to assess the correlation between calibrated backscatter coefficients (σ°) and aerodynamic roughness values (z_o) measured at 6 sites at Pisgah and Amboy. Data for these correlations are listed in Tables 3.1 and 3.3 and the locations of these measurement sites are shown in Figure 3.7. Plots of σ° and z_o illustrating the correlation between these parameters at C-, L-, and P-band wavelengths and at direct (HH, VV) and cross (HV/VH) polarizations are presented in Figure 3.8. The general trend of increasing aerodynamic roughness corresponding to increasing (i.e., smaller dB) backscatter coefficients is observed in all cases. It is expected that the stronger direct-polarized backscatter is due to single scattering (reflection) from facets or planes on the surface, and that cross-polarized backscatter is a result of either multiple scattering on or volume scattering within a surface. Direct-polarized data thus give an indication of surface roughness at the scale of the observing wavelength, while cross-polarized data reflect the geometry of the scattering surface at that scale. The highest degree of correlation is observed for the L-band backscatter values and the aerodynamic roughness measurements (correlation coefficients, R~0.89-0.91). The next highest degree of correlation between σ° and z_o is observed at P-band wavelengths (R~0.84-0.87), and the lowest degree of correlation is observed at C-band wavelengths (R~0.77-0.82). The relatively high degree of correlation between σ° and z_o at L-band wavelengths is likely to be due to the combined sensitivity of these parameters to surface roughness on the order of 25 cm, but the influence of subsurface scattering cannot be ruled out at this wavelength. Note that at C-band wavelengths the spread of the data points is primarily in the vertical (z_o) direction, indicating that most of the geologic units in this study (except the playa) are approximately equally radar-rough at a scale of ~ 6 cm. At the longer P-band wavelength, the spread among the data points is better in both the vertical (z_o) and horizontal (σ°) directions, but distinction between portions of the backscatter due to surface and subsurface (volume) scattering is difficult. Thus, the longer wavelength radar data may be influenced by surface scatterers ~70 cm in size as well as subsurface scatterers up to ~70 cm deep, and a correlation between the surface roughnesses reflected in the σ° and z_o may not be valid at this wavelength. Because of these uncertainties and the small range of correlation coefficients between the direct and cross-polarized backscatter at each wavelength, evaluation of polarization as a factor in these determinations would be premature. Additional data, particularly for rougher surfaces, are expected to improve the correlations and to provide greater separation among the radar imaging parameters.

For the wavelengths planned for the SIR-C mission (X-, C- and L-bands), discrimination among geologic units with a wide range of surface roughnesses is expected to be best at L-band wavelengths, in which the widest variation in radar backscatter is expected to be observed. Backscatter from targets with surface roughness elements greater than about 1 cm (X-band) and 6 cm (C-band) in size is expected to be almost uniformly high, with little separation between geologic targets. By contrast, backscatter from smoother targets (playas, alluvial fans) should show some measurable variation at smaller wavelengths, particularly C-band. At the X-band wavelength, most geologic targets are expected to be rough and thus to exhibit high (bright) radar backscatter values. Although radar incidence angle is not yet a factor in our determinations due to a lack of calibrated radar data for the same target at multiple incidence angles, theoretical backscatter curves (Fig. 3.9) suggest that the greatest degree of discrimination among geologic units with a range of roughnesses is observed for incidence angles in the range of 30° to 50°, depending upon the radar wavelength.

3.3 References Cited

Dellwig, L.F., 1969. An Evaluation of Multifrequency Radar Imagery of the Pisgah Crater area, California. *Modern Geology, 1*, 65-73.

Gaddis, L.R. and R. Greeley, 1989. Radar Observations of Flow Textures and Aeolian Mantling Deposits at Pisgah Volcanic Field, CA (abstract). *Eos, Trans. Amer. Geophys. Union, 70*, 1183.

Greeley, R., N. Lancaster, R.J. Sullivan, R.S. Saunders, E. Theilig, S. Wall, A. Dobrovolskis, B.R. White, and J.D. Iversen, 1988. A relationship between radar backscatter and aerodynamic roughness: Preliminary results. *Geophys. Res. Lett., 15*, 565-568.

Greeley, R. and J.D. Iversen, 1987. Measurements of wind friction speeds over lava surfaces and assessment of sediment transport. *Geophys. Res. Lett., 14*, 925-928.

van Zyl, J.J., H.A. Zebker, and C. Elachi, 1987. Imaging radar polarization signatures: Theory and observation. *Radio Sci., 22*, 529-543.

Wall, S., J.J. van Zyl, R.E. Arvidson, E. Theilig, and R.S. Saunders, 1988. The Mojave field experiment: Precursor to the planetary test site (abstract). *Bull. Amer. Astrol. Soc., 20*, 809.

Wise, W.S., 1966. Geologic map of the Pisgah and Sunshine Cone lava fields. *NASA Tech. Lett., 11*, 8 pp.

Zebker, H.A., J.J. van Zyl, and D.N. Held, 1987. Imaging radar polarimetry from wave synthesis. *J. Geophys. Res., 92*, 683-701.

4.0 THE EFFECT OF A ROUGHNESS ELEMENT ON LOCAL SALTATION TRANSPORT

J. Iversen, R. Leach, and R. Greeley

Abstract

Wind tunnel tests of rectangular prisms and circular cylinders have been initiated to determine the effects of such boundary layer obstacles on local aeolian saltation erosion and deposition. Preliminary results show that the drift topography adjacent to the rectangular or cylindrical roughness element is a strong function of the element's geometry. Variation of drift topography with cylindrical element aspect ratio is illustrated.

4.1 Introduction

The presence of non-erodible roughness elements in the midst of a bed of saltatable particles creates two primary effects on the saltation process, i.e., (1) it increases the value of threshold shear stress and (2) it decreases the mass transport for a given value of shear stress (Chepil, 1950; Lyles et al., 1974; Greeley and Iversen, 1987). Both of these effects occur because the portion of the mean surface shear stress due to the roughness elements themselves (primarily due to pressure drag) is greater than the mean value. The average shear stress on the erodible particle bed portion of the surface is thus less than the mean value. The mean value of shear stress at initiation of movement is thus higher than the normal threshold value.

Observation of the saltation pattern surrounding a single roughness element (located sufficiently far from any other elements so as to be relatively unaffected by them) shows, however, that the shear stress on the surface of the erodible bed is far from uniform. Indeed, motion of particles occurs just upwind of a tall bluff-shaped object at values of surface shear stress far upwind which are below general threshold. That is, erosion can occur just upwind of the object while the surface is quiescent elsewhere. A complex pattern of net surface erosion and deposition exists surrounding the object whether or not the surface shear stress on the bed upwind is above general threshold.

4.2 Dimensionless Parameters

It is expected that for a given roughness element geometric shape (e.g., a right circular cylinder), that the erosional-depositional pattern surrounding the element would be primarily a function of the following dimensionless parameters (Iversen, 1984, 1986, 1988; Kind, 1976, 1986):

γ/ρ	ratio of particle to fluid density
U_h^2/gD	Froude number
u_*/u_{*_t}	Threshold speed ratio
U_h/u_*	Reference speed ratio
U_t/u_*	Terminal speed ratio
$u_*^3/g\nu$ or u_*D/ν	Reynolds number
u_*t/D	Dimensionless time
H/D	Element aspect ratio

Experiments have been performed in three wind tunnels. Tests involving circular cylinders of diameters from 3 to 10 cm have been performed in the University of Aarhus wind tunnel (the wind tunnel, 35 cm x 50 cm, is described by Rasmussen and Mikkelsen, 1989). Tests with rectangular prisms (widths of 4 to 16 cm) and circular cylinders (3 to 60 cm diameter) have been tested in the Iowa State University (ISU) environmental wind tunnel (described in Iversen, 1982; the cross section is 1.1 m x 1.1 m). Tests of circular cylinders of diameter 1 to 6 cm have been tested in the high pressure (35 atmospheres) aeolian wind tunnel at NASA Ames Research Center (described in Greeley et al., 1984; cross section is a 20 cm diameter cylinder).

4.3 Experimental Results

Example photographs of experiments from the three wind tunnels are shown in Figures 4.1-4.3. Figure 4.1 illustrates the results of experiments in the ISU wind tunnel. In Figure 4.1a, the strong effect of the windward vortex is evidenced by the eroded area on the windward and lateral sides of the prism. There appears to be evidence of a secondary vortex just upwind of the primary vortex. In figure 4.1b, a similar result is shown for the circular cylinder. The primary deposition regions for both the prism and the cylinder occur downwind of the element. The drift pattern in each case is a complex function of the shear stress pattern around the element. The net rate of erosion or deposition at a

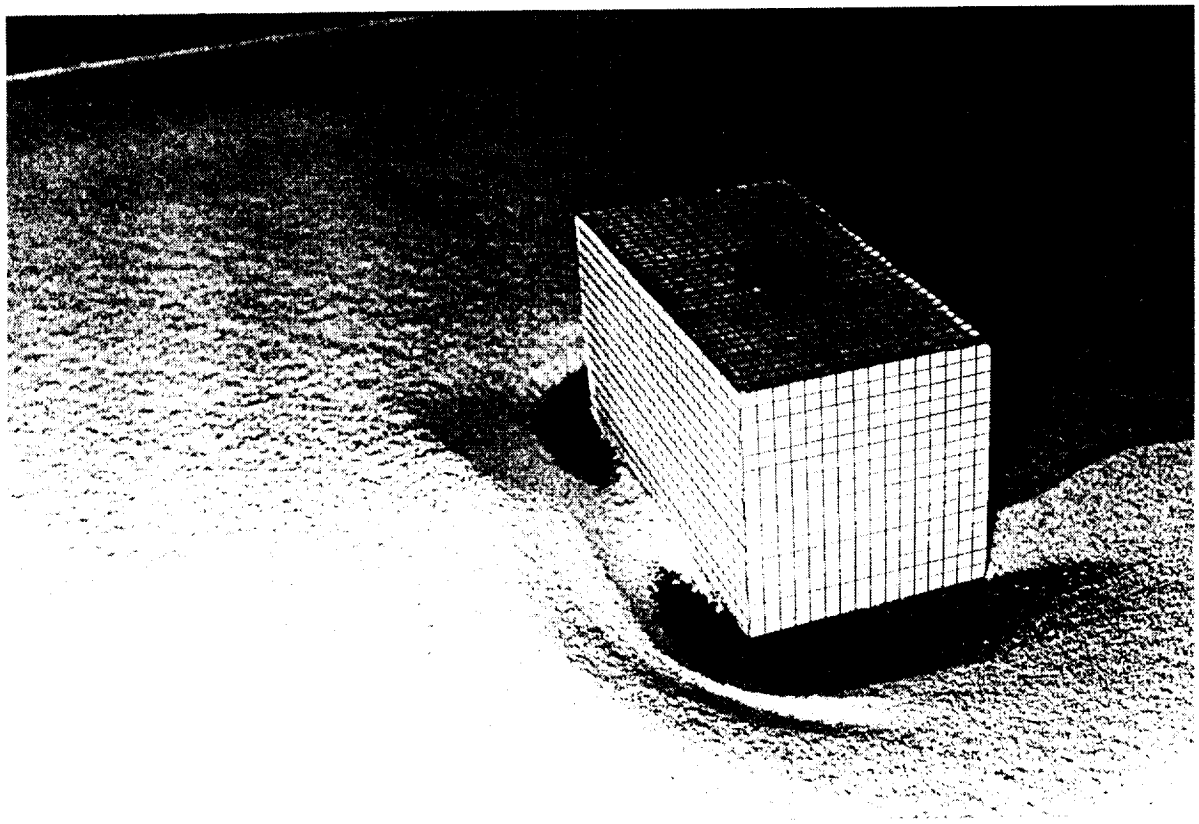

Figure 4.1a. Rectangular Prism Drift Experiment, ISU Wind Tunnel, Height H = 8 cm, Breadth D = 16 cm, D/H = 2, Windwise Dimension = 8 cm, u_* = 0.83 m/s, U_h = 9.3 m/s, U_hD/ν= 98000, $u_*^3/g\nu$= 3850, U_ht/D =, U_h^2/gD = 54.6.

Figure 4.1b. Circular Cylinder, ISU Wind Tunnel, Height H = 10 cm, Diameter D = 15 cm, D/H = 1.5, u_* = 0.80 m/s, U_h = 9.5 m/s, U_hD/ν= 97600, $u_*^3/g\nu$= 3440, U_ht/D = 16700, U_h^2/gD = 61.3.

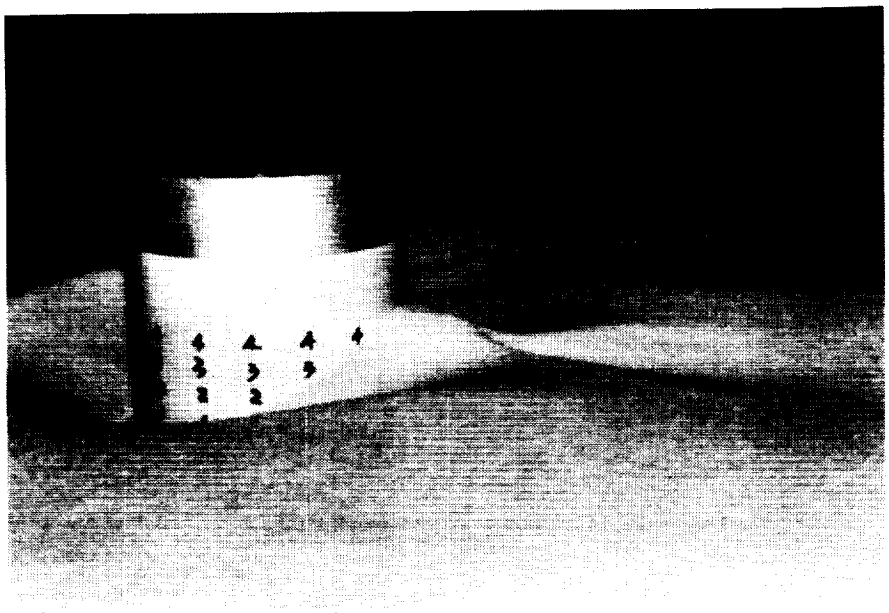

Figure 4.1c. Circular Cylinder, ISU Wind Tunnel, Height H = 10 cm, Diameter D = 10 cm, D/H = 1, $u_* = 0.73$ m/s, $U_h = 7.9$ m/s, $U_hD/\nu = 52600$, $u_*^3/g\nu = 2570$, $U_ht/D = 33100$, $U_h^2/gD = 63.4$.

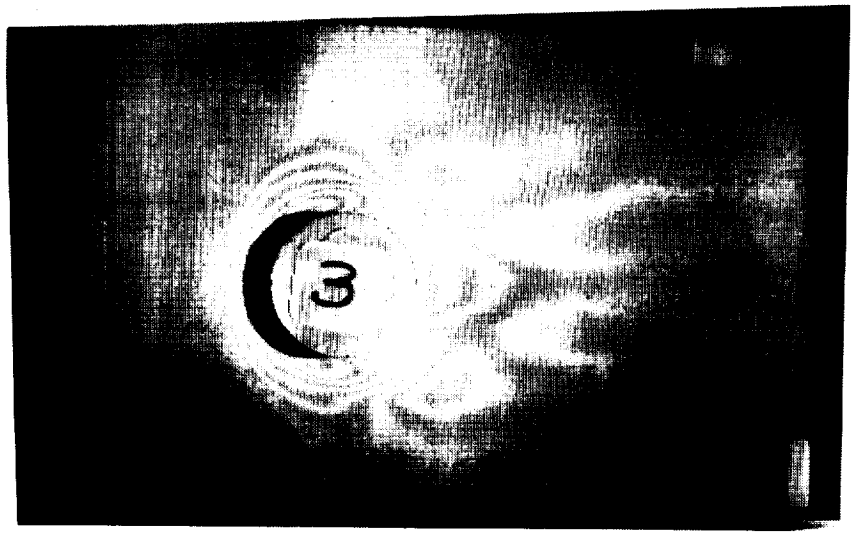

Figure 4.1d. Circular Cylinder, ISU Wind Tunnel, Height H = 8.6 cm, Diameter D = 13 cm, D/H = 1.5, $u_* = 0.73$ m/s, $U_h = 7.1$ m/s, $U_hD/\nu = 75400$, $u_*^3/g\nu = 2570$, $U_ht/D = 17200$, $U_h^2/gD = 31.9$. This figure illustrates the moiré fringe pattern.

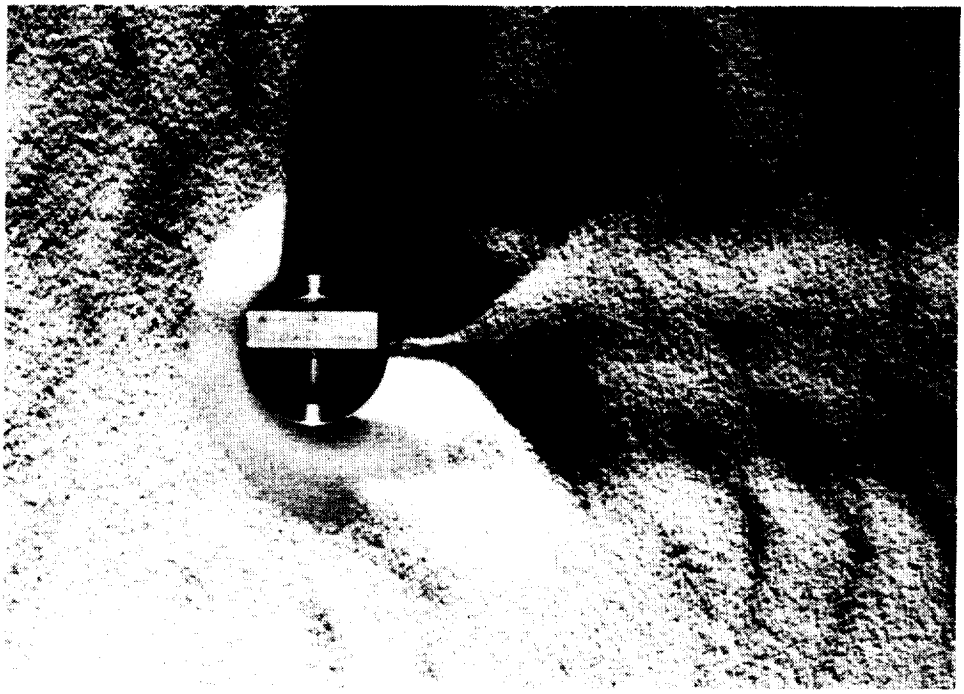

Figure 4.2a. Circular Cylinder, Aarhus Wind Tunnel, Height H = 5 cm, Diameter D = 5 cm, D/H = 1, $u_* = 0.44$ m/s, $U_h = 5.7$ m/s, $U_hD/\nu = 19400$, $u_*^3/g\nu = 596$, $U_ht/D = 40750$, $U_h^2/gD = 65.3$.

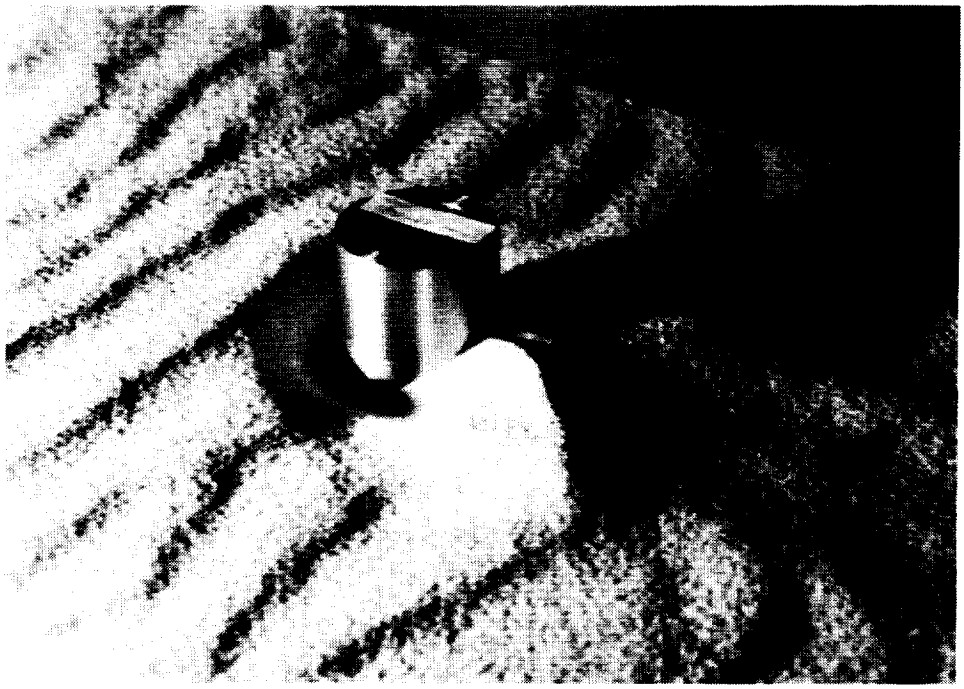

Figure 4.2b. Same experiment as Fig. 4.2a.

given location is a function of not only the stress at that point but also of the rate of transport of material into that point due to the stress pattern upwind. Figure 4.1c illustrates the pattern which evolved when a cylinder is emplaced in a thicker layer of particles (4 cm instead of 1 cm). The interference fringe pattern shown in Figure 4.1d is from a similar experiment. The moiré photographic technique has been used to determine local rates of erosion and deposition as a function of time.

Figure 4.2 illustrates the result of an experiment in the wind tunnel at the Department of Geology at the University of Aarhus, Aarhus, Denmark. The topographic surface contour is similar to the results of the ISU experiment (Fig. 4.1c). The primary difference in the dimensionless parameters between the two experiments is the value of the Reynolds number.

Figure 4.3 illustrates the results of experiments in the high-pressure wind tunnel. For this wind tunnel, the density ratio is far different from the experiments at one atmosphere (see Iversen et al., 1987). Results from two experiments with the same model are shown in Figures 4.3b,c. The striking difference between the two erosional patterns is probably due to the differences in Froude number, although there is also a significant difference in density ratio (it should be noted that the values of densimetric Froude number ru_*^2/ggH are about the same for the two experiments). Figure 4.3d illustrates the erosional pattern for a cylinder similar to that in Figure 4.1c. Again, the patterns of deposition and erosion, as well as the values of Froude number and density ratio, are quite different between the two experiments. Continued experimentation and analysis are needed in order to explain these differences.

Some of the preliminary data collected from these experiments are illustrated in Figures 4.4 and 4.5. Values of the stand-off distance and erosion depth for the windward moat are illustrated in Figures 4.4a,b. Seven cylinders were tested in the Aarhus wind tunnel and 7 in the ISU wind tunnel under similar conditions. The values of H/D for the Aarhus cylinders ranged from 0.33 to 3.33 and for the ISU cylinders from 0.33 to 3.67. For very shallow cylinders ($H/D \ll 1$), the windward erosional moat disappears and net deposition occurs (thus, the negative $\Delta z/D$ values in Figs. 4.4a for small H/D).

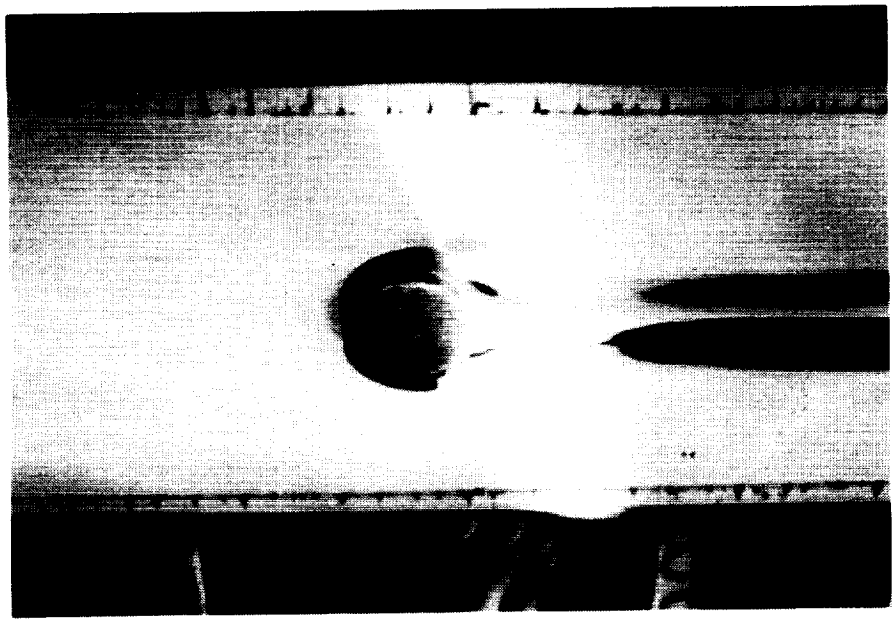

Figure 4.3a. Circular Cylinder, High Pressure Wind Tunnel, p = 29.8 atmospheres, $\gamma/\rho = 42$, Height H = 0.6 cm, Diameter D = 4.2 cm, D/H = 7, $u_* = 0.045$ m/s, $U_h = 0.86$ m/s, $U_hD/\nu = 129000$, $u_*^3/g\nu = 32$, $U_ht/D = ?$, $U_h^2/gD = 10.95$.

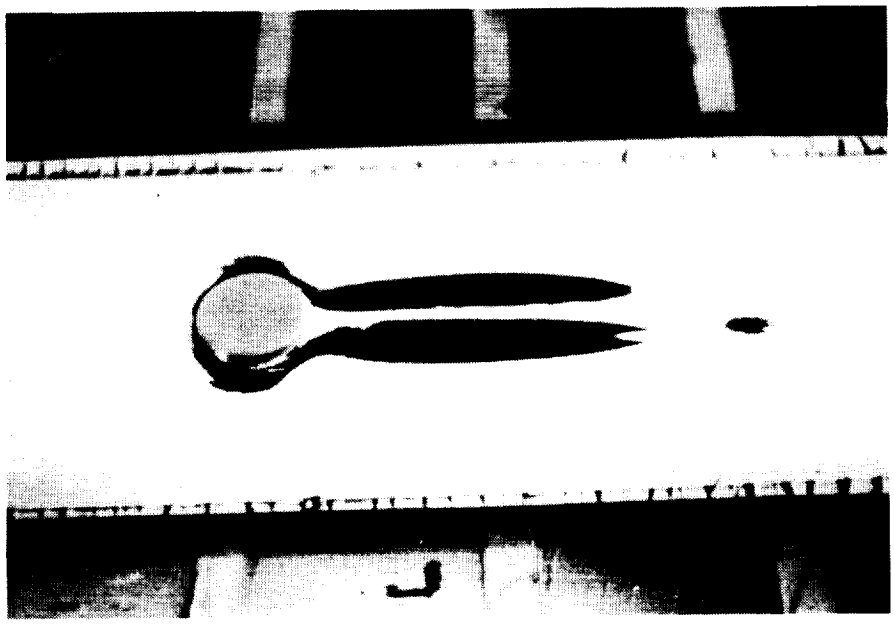

Figure 4.3b. Circular Cylinder, High Pressure Wind Tunnel, p = 18.1 atmospheres, $\gamma/\rho = 73.5$, Height H = 0.6 cm, Diameter D = 6 cm, D/H = 10, $u_* = 0.058$ m/s, $U_h = 1.05$ m/s, $U_hD/\nu = 128000$, $u_*^3/g\nu = 41$, $U_ht/D = 994$, $U_h^2/gD = 18$.

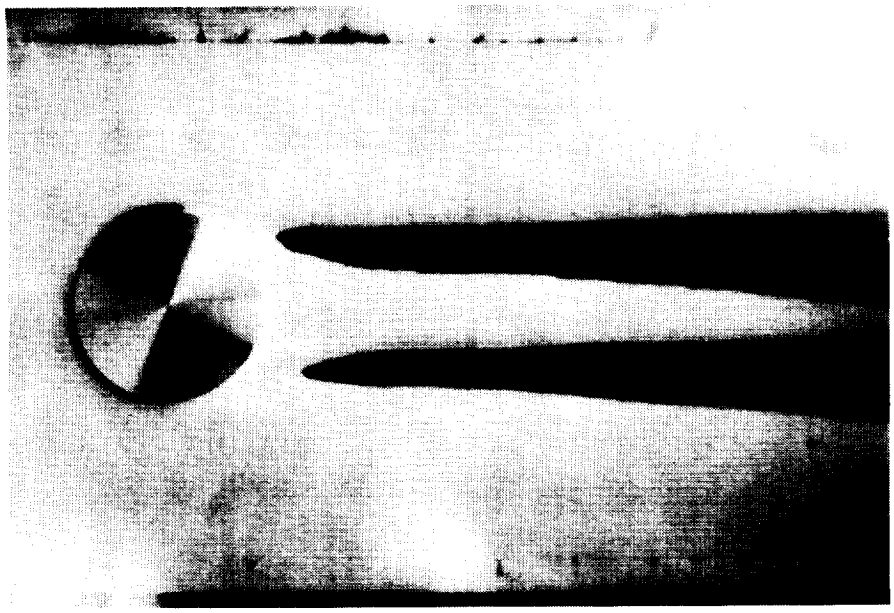

Figure 4.3c. Circular Cylinder, High Pressure Wind Tunnel, p = 4.1 atmospheres, $\gamma/\rho = 42$, Height H = 0.6 cm, Diameter D = 6 cm, D/H = 10, $u_* = 0.121$ m/s, $U_h = 1.73$ m/s, $U_hD/\nu = 47000$, $u_*^3/g\nu = 82$, $U_ht/D = 8700$, $U_h^2/gD = 66$.

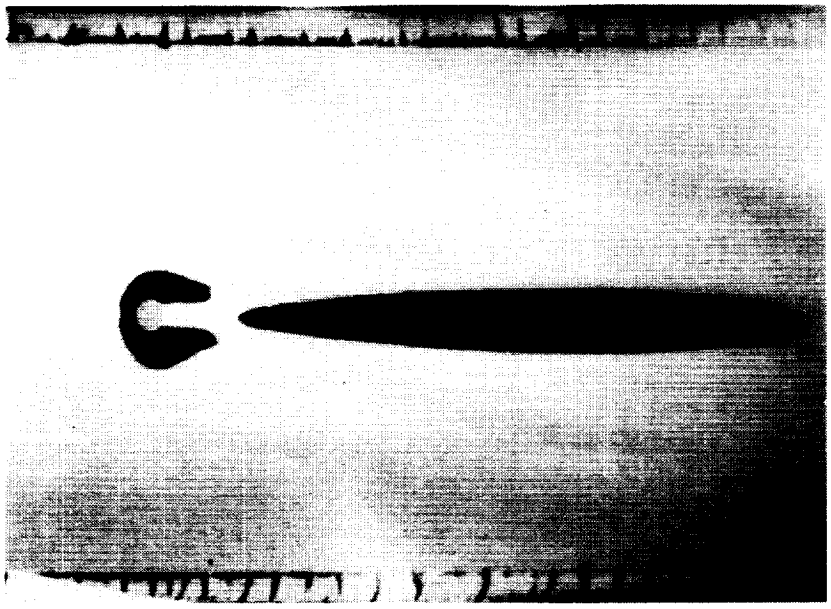

Figure 4.3d. Circular Cylinder, High Pressure Wind Tunnel, p = 18.1 atmospheres, γ/ρ = 73, Height H = 1 cm, Diameter D = 1 cm, D/H = 1, $u_* = 0.065$ m/s, $U_h = 1.21$ m/s, $U_hD/\nu = 24800$, $u_*^3/g\nu = 56.5$, $U_ht/D = 6900$, $U_h^2/gD = 13$.

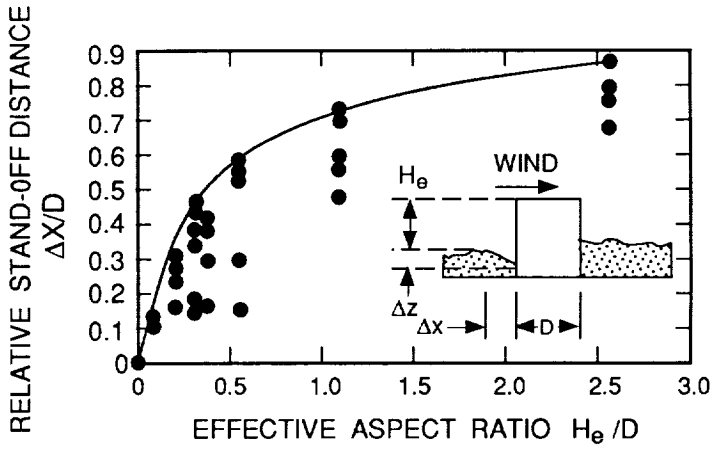

Figure 4.4a. Data for windward moat standoff distance, ISU Wind Tunnel, right circular cylinders. The solid curve is the upper envelope of the data. Data falling below the solid line probably indicate experiments of too short duration to approach equilibrium topography.

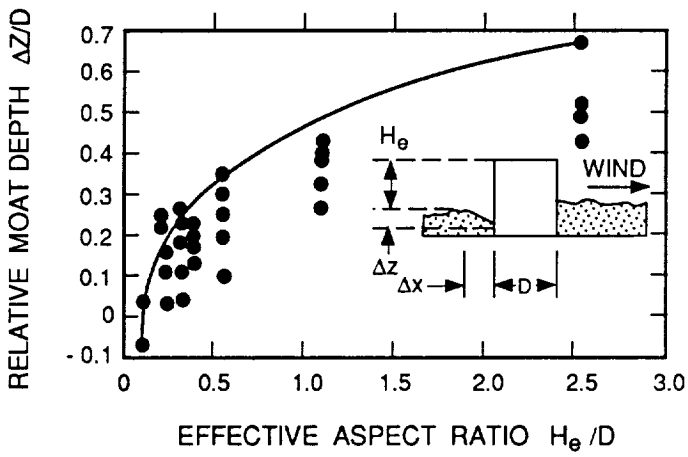

Figure 4.4b. Data for windward moat depth, ISU Wind Tunnel, right circular cylinders. The solid curve is the upper envelope of the data. Data falling below the solid line probably indicate experiments of too short duration to approach equilibrium topography.

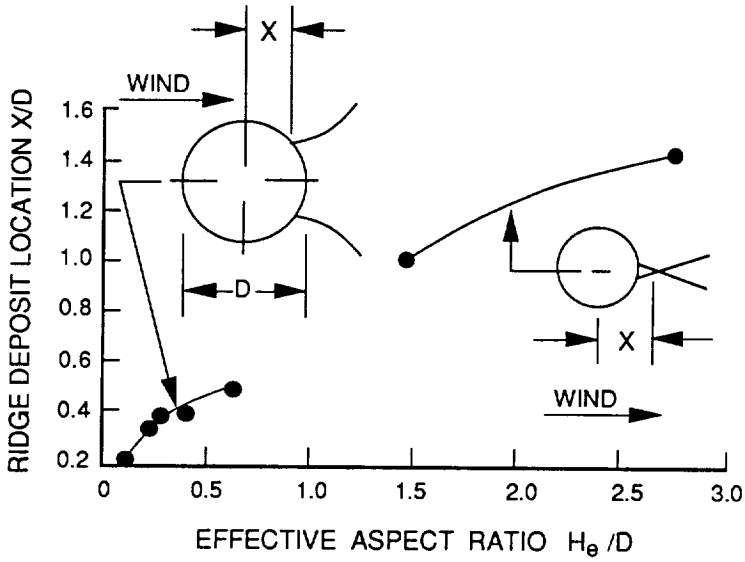

Figure 4.5. Data for location of the maximum deposition ridge points adjacent or near to the cylinder, Aarhus Wind Tunnel.

In general, the relative erosional moat size increases with relative cylinder height. The solid curves in Figure 4.4 represent the upper envelope of the data. Experiments which fall below these lines (including the Aarhus data) were most likely of too short duration and thus equilibrium topography was not approached (data analyses to determine the degree of approach to equilibrium are under way). Data for the maximum deposition point adjacent or just to the leeward of the cylinders are illustrated for the Aarhus tests in Figure 4.5. For shorter cylinders (smaller H/D), the ridge points are at the lateral edges of the cylinders. For taller cylinders, these points have coalesced and the ridge points plotted are on the wake centering downwind of the cylinder.

4.4 Conclusions

A leeward vortex system exists (which may be shed from the top of the cylinder) which persists for a long distance downwind. For a tall cylinder, this vortex system might never come close enough to the surface to much affect particle transport. For the broad, short cylinder, however, this vortex system is relatively closer to the surface and causes alternate rows of deposition and erosion. This phenomenon has been observed to continue for many diameters downwind (Figs. 4.2, 4.3). The erosion capability downwind of the cylinder increases with decrease in H/D, in opposite trend to the windward erosion capability. There seems to be a deposition region between the windward erosion moat and the leeward vortex erosion streaks. The maximum depth of this deposition appears to move to the leeward with increase in H/D (Fig. 4.5).

4.5 References Cited

Chepil, W.S., 1950. Properties of soil which influence wind erosion: I. The governing principle of surface roughness. *Soil Sci., 69*, 149-162.

Greeley, R. and J.D. Iversen, 1987. Measurements of wind friction speeds over lava surfaces and assessment of sediment transport. *Geophys. Res. Lett., 14*, no. 9, 925-928.

Greeley, R., J.D. Iversen, R.N. Leach, J. Marshall, B. White, and S. Williams, 1984. Windblown sand on Venus: Preliminary results of laboratory simulations. *Icarus, 57*, 112-124.

Iversen, J.D., 1982. Small-scale modeling of snow-drift phenomena. *Wind Tunnel Modeling for Civil Engineering Applications*, T. Reinhold, ed., Cambridge University Press, Cambridge, England, 522-545.

Iversen, J.D., 1984. Comparison of snowdrift modeling criteria. *Cold Regions Sci. Tech., 9*, 259-265.

Iversen, J.D., 1986. Small-scale wind tunnel modeling of particle transport. *Aeolian Geomorphology*, W. Nickling, ed., Allen & Unwin, Boston, 19-33.

Iversen, J.D., 1988. Modeling drift geometry in wind tunnels. *Proc. Snow Engineering Conf.*, Santa Barbara, CA, 5 pp.

Iversen, J.D., R. Greeley, J. Marshall, and J. Pollack, 1987. Aeolian saltation threshold: The effect of density ratio. *Sedimentology, 34*, no. 4, 699-706.

Kind, R.J., 1986. A critical examination of the requirements for model simulation of wind-induced erosion/deposition phenomena such as snow-drifting. *Atmos. Environ., 10*, 219-277.

Kind, R.J., 1986. Snowdrifting; a review of modelling methods. *Cold Regions Sci. Tech., 12*, 217-228.

Lyles, L., R.L. Schrandt, and N.F. Schneidler, 1974. How aerodynamic roughness elements control sand movement. *Trans. Amer. Soc. Agricultural Engineering, 17*, 134-139.

Rasmussen, K.R. and H.E. Mikkelsen, 1989. Development of a boundary layer wind tunnel for acolian studies. Report, Dept. of Geology, University of Aarhus, Aarhus, Denmark.

5.0 THEORY AND PLANETARY APPLICATIONS

A. Dobrovolskis

The preliminary relation between aeolian roughness height and radar backscattering properties (Greeley et al., 1988) promises a diagnostic tool for remote sensing of the Earth's boundary layer. If such a relation could be applied to other planets, it would prove very valuable in probing surface conditions on Venus, Mars, and possibly Titan (see, for example, Muhleman et al., 1989b).

5.1 Ground Truth

In order to extend the radar-aeolian roughness relation to another planet, both the roughness height and radar characteristics must be known at several sites. Although micrometeorologic data for Venus and Mars are available from only two locations on each planet, we may draw some tentative conclusions about roughness heights on these planets.

On Earth, z_o is usually obtained from vertical profiles of the wind near the ground. Unfortunately, the anemometers on the Venera and Viking landers were mounted at a single height above the surface. In principle, it is possible to recover z_o from time series of the wind fluctuations at a fixed point. Under conditions of neutral stability, the friction speed u_* is roughly 43% of the root-mean-square variation in the horizontal wind speed (Monin and Yaglom, 1971). Since the mean wind speed u is also known at the height z of the measurements, the logarithmic law for the wind profile can then be inverted for the roughness height:

$$\bar{u}(z) = 2.5\bar{u}_* \ln\left(\frac{z}{z_0}\right); \quad z_0 \Rightarrow z \exp\left[-\frac{0.4\,\bar{u}(z)}{u_*}\right] \qquad (5.1)$$

Of all the U.S. and Soviet missions to Venus, only the Venera 9 and 10 landers carried anemometers to the surface. The Venera 9 anemometer measured a mean wind speed of 40 cm/s and an RMS variation of 10 cm/s, while Venera 10 measured 90 cm/s and 15 cm/s, respectively (Golitsyn, 1978). Because both anemometers were mounted at a height of 130 cm above the surface of Venus, the corresponding roughness lengths from eq. (5.1) are ~3 cm at the Venera 9 landing site and ~0.5 cm at the Venera 10 site. However, these should be regarded as upper limits because flow past the landers themselves may have generated additional turbulence (Golitsyn, 1978).

The anemometers on the Viking Mars landers were less subject to lander interference, but the characteristics of turbulence in the martian boundary layer are strongly influenced by non-neutral or transitional stability effects (Hess et al., 1977; Sutton et al., 1979). From the published mean winds and variances (Hess et al., 1977), eq. (5.1) suggests that z_o lies between 1 cm and 10 cm at the Viking 1 landing site. Based on the lander images, however, Sutton et al. (1979) assumed a roughness height between 0.1 cm and 1.0 cm at both landing sites.

5.2 Rock Distributions

The roughness height can be estimated from images as follows. Lettau (1969) gives the roughness height of a surface strewn with obstacles of height h and frontal area s as

$$z_0 \approx \frac{1}{2} h\, s\, N, \qquad (5.2)$$

where N is the number of such roughness elements per unit area. Lettau (1969) also implies (but does not make explicit) that the contributions from different classes of obstacles combine additively:

$$z_0 = \Sigma \frac{1}{2} h_i\, s_i\, N_i \qquad (5.3)$$

If the exposed portions of the martian blocks are modeled as hemispheres of diameter D, height $h = D/2$, and cross-section $s = \pi D^2/8$, formula (3) gives

$$z_0 = \frac{\pi}{32} \Sigma\, D^3\, N(D) \qquad (5.4)$$

where N(D) is the number density of rocks in the bin for diameter D. The size distribution of rocks at the Viking lander sites is shown in Figure 5.1, from Moore et al. (1979). Applying (5.4) above to this population yields the results shown in Figure 5.2. Here the histograms represent the contribution to z_o from each size bin, while the polygonal curves indicate the cumulative roughness height, added up from the smallest cobbles.

Figure 5.2 shows that the roughness height at the Viking 1 lander site is at least 0.1 cm, while that at the V-2 site is over 0.3 cm. These values are only lower limits, since they do not include the contributions from blocks larger than ~25 cm and ~50 cm in diameter, respectively. However, the form of the histograms suggests that the peak has been passed, so that the total roughness height should not exceed twice the above limits.

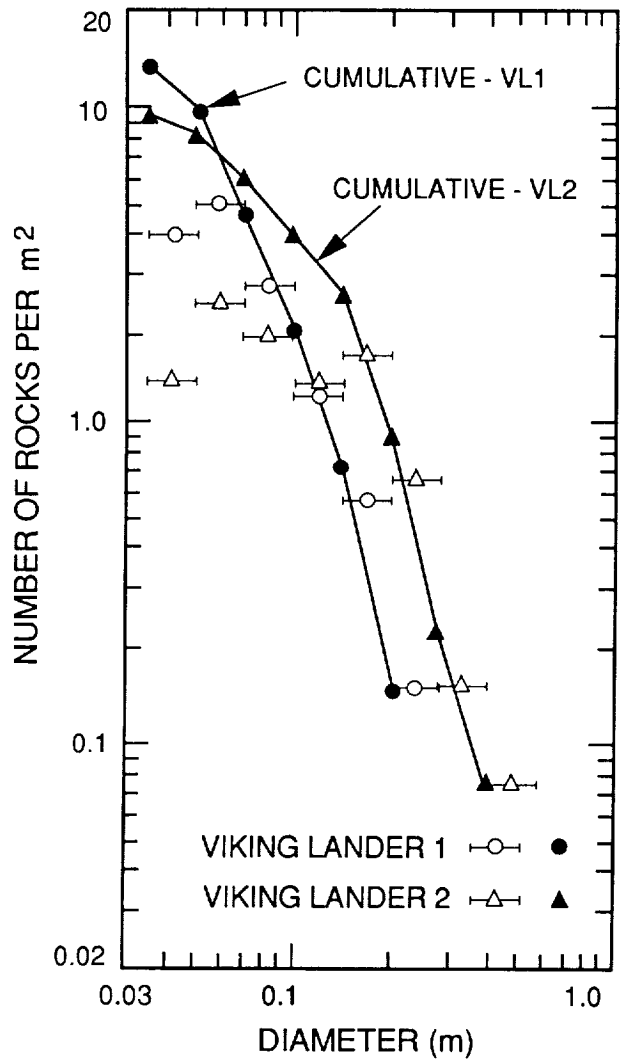

Figure 5.1. Size distribution N(D) and its integral for rocks surrounding the Viking Mars landers (from Moore et al., 1979).

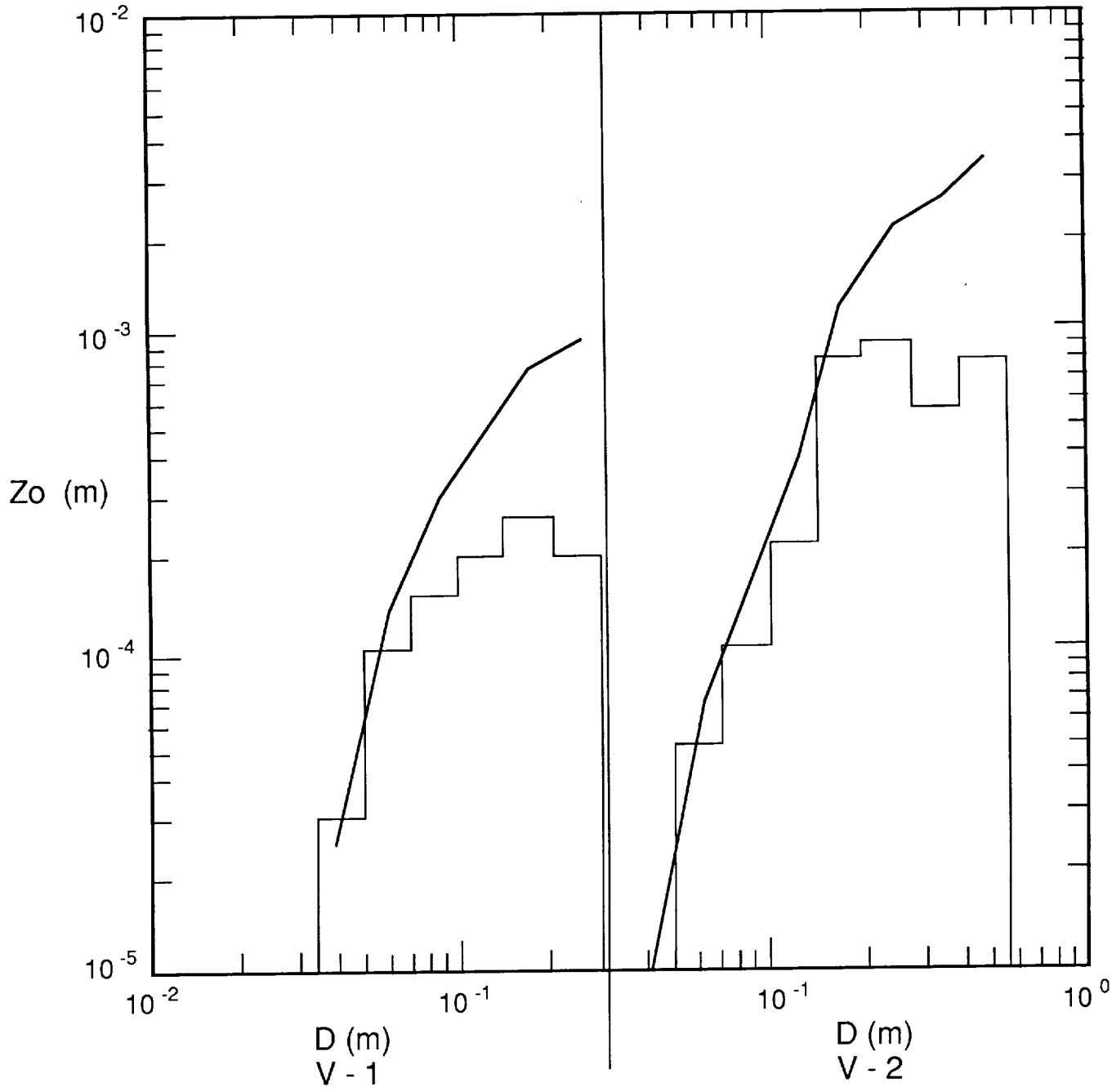

Figure 5.2. The histograms represent the contribution of each size bin to the total roughness height at the Viking lander sites. The polygonal curves show its cumulative value, starting from the smallest diameters.

Corresponding rock distributions have not been published for the Venus landing sites, but the limited statistics available on fragments up to ~4 cm in diameter (Garvin et al., 1983) imply roughness heights of at least ~0.02 cm and ~0.01 cm at the Venera 13 and Venera 14 sites, respectively.

5.3 Radar Correlations

Garvin and Head (1986) tabulated the mean reflectivity r and RMS slope β_0 from the Pioneer Venus radar altimeter for the nine Vega and Venera landing sites. Figure 5.3 plots the corresponding backscattering cross section at vertical incidence $\sigma_\circ = 10 \log (1/2\ \rho/\beta_0^2)$ (in decibels) versus the four roughness heights z_0 for Venus estimated above. This graph indicates that $\sigma_\circ$ and z_0 are inversely correlated, i.e., that $\sigma_\circ$ decreases with increasing z_0. This is not surprising, since backscattering at normal incidence is primarily due to specular reflection, unlike the diffuse reflection at the large incidence angles used in synthetic aperture radars.

Figure 5.4 shows that z_0 increases with increasing β_0, as expected. However, the RMS slope β_0 refers to roughness at scales between the radar wavelength and the horizontal resolution (~17 cm and 100 km for Pioneer Venus). In comparison, the diffuse component of radar scattering is primarily due to the surface roughness on the scale of a wavelength, say 5 to 50 cm. Texture at these scales is more directly related to the aeolian roughness height z_0.

Ford and Pettengill (1984) have combined Pioneer Venus synthetic aperture radar images with altimeter data to derive the fraction α of diffuse to total reflectivity. The resulting values generally increase with increasing RMS slope β_0 (Bindschadler and Head, 1988). Bindschadler and Head (1988) have mapped over most of Venus' surface, although they do not tabulate its numerical value. Like z_0, α seems to be greatest at the Venera 9 landing site and least at the Venera 13 and Venera 14 sites. Therefore α may turn out to be the radar-observable most diagnostic of the aeolian roughness.

Because of technical difficulties, radar data for Mars are quire limited. The area within ~40 km of the Viking 1 landing site has an RMS slope $\beta_0 \approx 5.4°$ (Simpson et al., 1978) and a mean reflectivity $\rho \approx 0.074$ (Moore and Jakosky, 1989). The Viking 2 landing site and indeed, most of the planet, has been inaccessible to Earth-based radar until recently, but it should soon become possible to correlate z_0 with radar characteristics at both Viking sites. Muhleman et al. (1989a) have now succeeded in mapping Mars with the Very Large Array. The resulting images bear a strong resemblance to model predictions based on global geologic maps and infrared thermal inertias (Thompson and Moore, 1989).

5.4 Thermal Inertia

The thermal inertia I is related to the diffuse scattering fraction α because both depend upon the abundance of exposed rocks (Calvin et al., 1988; Thompson and Moore, 1989). This relation is not simple, however, because subsurface scattering also contributes to α in areas where the rocks are covered by up to several meters of fine sediment. Because the thermal inertia is only sensitive to the uppermost few centimeters of the ground, I may be even more diagnostic than α of the rock abundance on the surface of Mars.

The thermal inertia may be divided into separate contributions from exposed rocks and from the fine component of the martian soil; their relative proportions then give the fraction f of the local surface area covered by rocks (Christensen, 1986a,b). The results imply rock fractions of ~14% and ~17% near the Viking 1 and Viking 2 landing sites (Christensen, 1986b), while direct rock counts from the Viking lander images give 8% and 14% respectively (Moore et al., 1979). If the rocks at a given site were all hemispheres of diameter D, the roughness height z_0 from eqs. (5.2) - (5.4) would just be f D/8.

Considering the broad database of thermal inertias available, and the potential for future infrared remote sensing from Mars Observer and other spacecraft (see, for example, Waldrop, 1989, and Selivanov et al., 1989), I and f should prove to be very valuable additions to the radar parameters as predictors of aeolian roughness on Mars.

5.5 References Cited

Bindschadler, D.L. and J.W. Head, 1988. Diffuse scattering of radar on the surface of Venus: Origin and implications for the distribution of soils. *Earth, Moon, and Planets*, *42*, 133-149.

Calvin, W.M., B.M. Jakosky, and P.R. Christensen, 1988. A model of diffuse radar scattering from Martian surface rocks. *Icarus*, *76*, 513-524.

Christensen, P.R., 1986a. Regional dust deposits on Mars: Physical properties, age, and history. *J. Geophys. Res.*, *91*, 3533-3545.

Christensen, P.R., 1986b. The spatial distribution of rocks on Mars. *Icarus*, *68*, 217-238.

Ford, P.G. and G.H. Pettengill, 1984. Venus radar reflectivity—A re-analysis. *Bull. Amer. Astron. Soc.*, *16*, 697.

Garvin, J.B. and J.W. Head, 1986. Characteristics of the Venera and Vega landing sites from Pioneer Venus radar data. *Lunar Planet. Sci.*, *17*, 253-254.

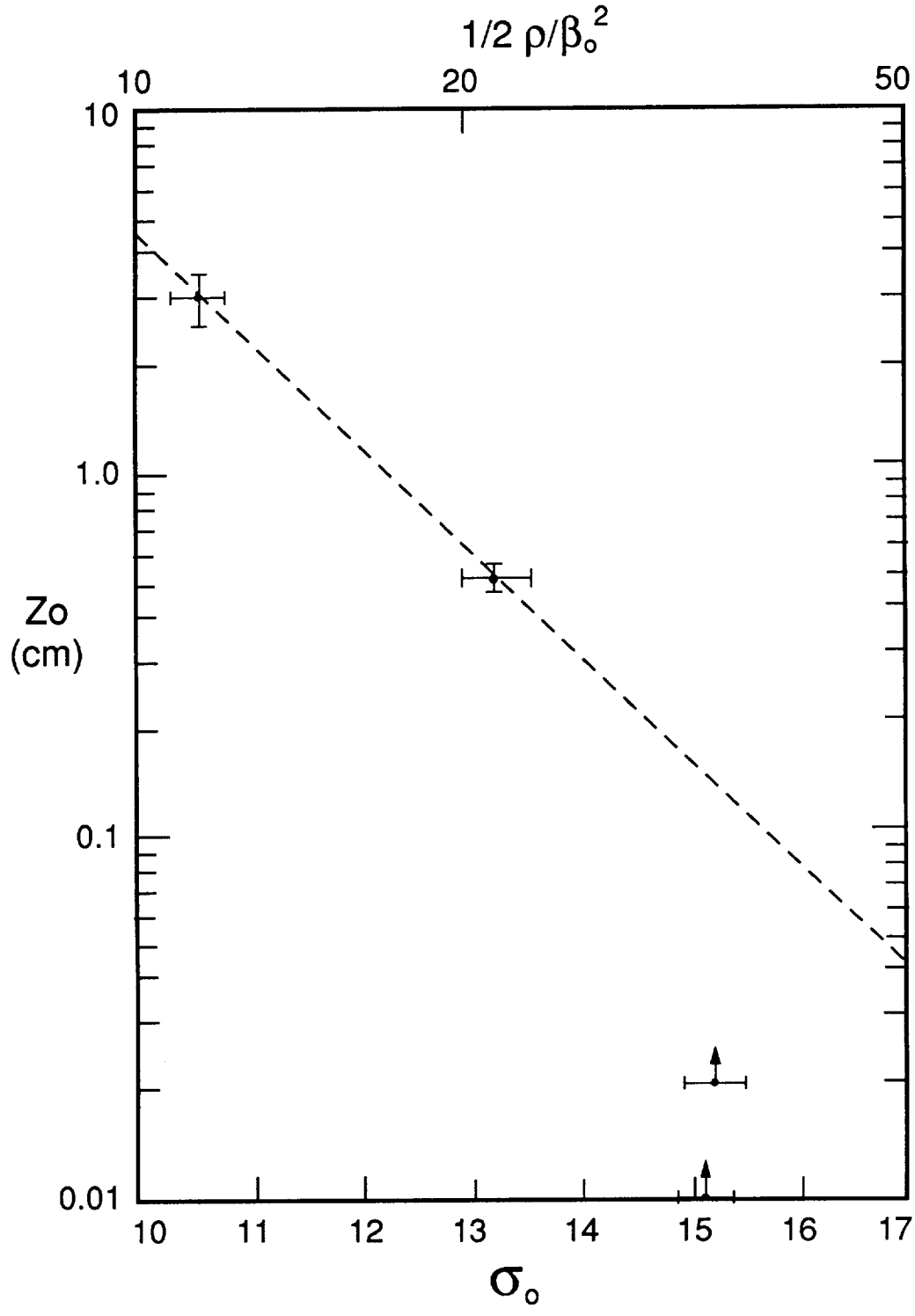

Figure 5.3. Estimated roughness height versus the radar backscattering cross-section for vertical incidence at four Venus landing sites.

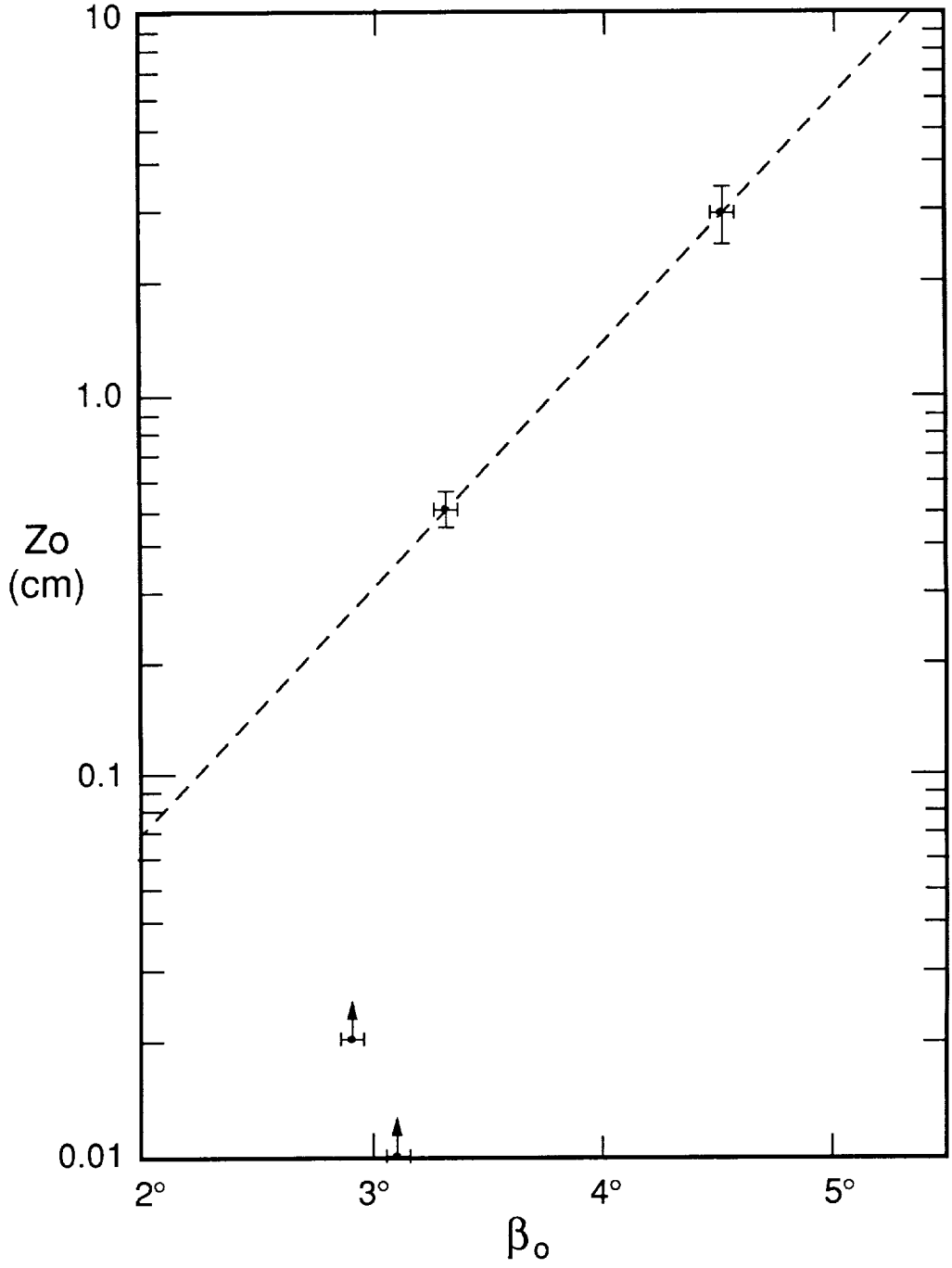

Figure 5.4. Estimated roughness height versus the root-mean-square slope of the surface near the Venera landing sites.

Greeley, R., N. Lancaster, R.J. Sullivan, R.S. Saunders, E. Theilig, S. Wall, A. Dobrovolskis, B.R. White, and J.D. Iversen, 1988. A relationship between radar backscatter and aerodynamic roughness: Preliminary results. *Geophys. Res. Lett., 15*, 565-568.

Golitsyn, G.S., 1978. Estimates of the turbulent state of the atmosphere near the surface of Venus from the data of Venera 9 and Venera 10. *Cosmic Res., 16*, 125-127.

Hess, S.L., R.M. Henry, C.B. Leovy, J.A. Ryan, and J.E. Tillman, 1977. Meteorological results from the surface of Mars: Vikings 1 and 2. *J. Geophys. Res., 82*, 4559-4574.

Lettau, H., 1969. Note on aerodynamic roughness-parameter estimation on the basis of roughness-element description . *J. Applied Meteorology , 8*, 828-832.

Monin, A.S. and A.M. Yaglom, 1971. *Statistical Fluid Mechanics*. The M.I.T. Press, Cambridge, Massachusetts.

Moore, H.J., C.R. Spitzer, K.Z. Bradford, P.M. Cates, R.E. Hutton, and R.W. Shorthill, 1979. Sample fields of the Viking landers, physical properties, and aeolian processes. *J. Geophys. Res., 84*, 8365-8377.

Moore, H.J., and B.M. Jakosky, 1989. Viking landing sites, remote-sensing observations, and physical properties of Martian surface materials. *Icarus, 81*, 164-184.

Muhleman, D.O., et al., quoted by J. Eberhart, 1989a. A different view of Mars. *Science News, 135*, 75.

Muhleman, D.O., et al., quoted by J. Eberhart, 1989b. Titan: No global ocean, maybe some seas. *Science News, 136*, 5.

Selivanov, A.S., M.K. Naraeva, A.S. Panfilov, Uy. M. Gektin, V.D. Kharlamov, A.V. Romanov, D.A. Fomin, and Ya. Ya. Miroshnichenko, 1989. Thermal imaging of the surface of Mars. *Nature, 341*, 593-595.

Simpson, R.A., G.L. Tyler, and D.B. Campbell, 1978. Arecibo radar observations of Mars surface characteristics in the northern hemisphere. *Icarus, 36*, 153-173.

Sutton, J.L., C.B. Leovy, and J.E. Tillman, 1979. Diurnal variations of the Martian surface layer meteorological parameters during the first 45 sols at two Viking lander sites. *J. Atmos. Sci., 35*, 2346-2355.

Thompson, T.W. and H.J. Moore, 1989. A model for depolarized radar echoes from Mars. *Proc. 19th Lunar Planet. Sci. Conf.*, pp. 409-422.

Waldrop, M.M., 1989. Phobos at Mars: A dramatic view—and then failure. *Science, 245*, 1044-1045.

APPENDIX I. CALIBRATION OF ANEMOMETERS AND TEMPERATURE SENSORS

All instruments were calibrated to provide a relationship between their electric output and measured wind speed or temperature conditions, using the following procedures, which follow those suggested by Rasmussen and Lancaster in March, 1989.. The calibrations were conducted at the Planetary Geology Wind Tunnel facility at Arizona State University.

Anemometers

Procedures

1. A 1/8" pitot tube is placed in the wind tunnel 0.8 m upwind of the anemometer calibration site and connected to a high resolution (0.1 mV) SETRA pressure gauge. The gauge is read by a Tandy computer and the mV output converted to wind velocity using the manufacturer's standard conversion.
2. The first anemometer is placed in the tunnel and connected to the Tandy computer.
3. The wind tunnel is turned on and adjusted to a velocity of ± 4 m/sec, as measured by the SETRA. When it is stable, the computer program is started and two 3 minute averages of tunnel wind speed and anemometer output (mV) are obtained. This procedure is repeated for the following additional tunnel wind speeds: ± 6 m/sec, ±9 m/sec, and ±11 m/sec.
4. The tunnel is turned off and the anemometer replaced by the next instrument.

Results

The calibrations are based on the mean of the two 3 minute averages of wind tunnel speed and anemometer output. With the exception of instrument #6, which gave erratic readings at tunnel speeds greater than 6 m/sec, all instruments gave a good linear response. The gain and offset for the calibrations is given below in Table 1.

Table 1: Anemometer calibrations July 1989.

Anemometer #	Offset	Gain
1	0.31378	0.13781
2	0.23780	0.13587
3	0.05484	0.14593
4	0.10015	0.14089
5	0.03850	0.14012
6	0.23534	0.14456
7	0.04200	0.14036
8	0.25737	0.13988
9	0.01230	0.14141
10	0.04736	0.14005
11	0.17283	0.13904
12	0.14849	0.13656
13	0.20170	0.13746
14	0.03379	0.14017
15	0.75645	0.12658
16	0.81963	0.12458
17	0.75624	0.12853
18	0.62215	0.12805
19	0.55801	0.12757
20	0.60508	0.12995
21	0.66913	0.12763
22	0.65452	0.12873
23	0.81959	0.12744
24	0.68395	0.13102
25	0.61799	0.13259
26	0.82949	0.12965
27	0.74152	0.12998
28	0.65217	0.12970

Discussion

The results obtained by using the high resolution SETRA differ in one important respect from the previous calibrations in which wind tunnel speeds were obtained by reading the water manometer (e.g., March, 1989). The slope of the regression lines (gain in table 1) is comparable (and within the calibration accuracy) in both instances, but the gain (approximately equivalent to the calculated stall speed of the anemometers) is much less than those obtained by Rasmussen and Lancaster in March, 1989. This clearly illustrates the problems of using the manometer, which is difficult to read, and has a low resolution compared to the SETRA.

TEMPERATURE SENSORS

Results

Generally, all sensors showed a good linear response, with a gain close to 1.00. However, the offset from absolute zero is considerable and highly variable from one sensor to another, and varies from -2° C to as much as + 30° C. It will probably be necessary to recheck some of these sensors in the near future to discover if the changes are due to problems with the sensors or the wiring to the Tandy. This may help to understand why drifting and other inconsistencies in temperature sensor readings have occurred in the field. The gain and offset for each sensor is shown below in Table 2.

Table 2: Temperature sensor calibrations, July 1989.

Sensor #	Gain	Offset
1	-271.19	0.9938
2	-271.71	0.9954
3	-304.89	1.1134
4	-275.36	1.0107
5	-279.64	1.0255
6	-294.19	1.0763
7	-272.76	1.0096
8	-272.91	1.0011
9	-280.00	1.0343
10	-277.88	1.0185
11	-278.22	1.0195
12	-288.33	1.0569
13	-282.46	1.0322
14	-271.40	0.9949
15	-276.74	1.0125
16	-273.37	1.0046
17	-279.53	1.0267

APPENDIX II. WIND DATA

STOVEPIPE WELLS
DATA FOR NORTHERLY WIND DIRECTIONS

		Wind Speeds						Temperatures		Wind			
Date	Time	U(0.75)	U(1.25)	U(2.07)	U(3.44)	U(5.72)	U9(.5)	TL1	TU2	Dir	Ri	U*	Zo
1-Apr	0:05-0:26	4.41	4.53	4.79	5.20	5.56	5.87	27.05	26.95	353	0.024	0.267	0.0009206
1-Apr	0:26-0:46	6.67	7.09	7.41	7.84	8.43	9.07	26.61	26.50	353	0.008	0.351	0.0028424
1-Apr	0:46-1:06	7.03	7.45	7.79	8.36	8.84	9.45	26.77	26.66	2	0.005	0.365	0.0031903
1-Apr	1:06-1:26	6.53	6.90	7.13	7.64	8.18	8.72	26.44	26.34	7	0.005	0.332	0.0035052
1-Apr	1:26-1:46	6.08	6.41	6.59	7.11	7.68	8.13	26.45	26.35	21	0.008	0.328	0.0021292
1-Apr	1:46-2:07	6.33	6.72	6.86	7.39	7.83	8.39	25.68	25.58	358	0.005	0.303	0.0059107
1-Apr	2:07-2:27	7.44	7.93	8.19	8.78	9.37	9.97	25.57	25.47	353	0.004	0.382	0.0034128
1-Apr	2:27-2:47	6.94	7.39	7.73	8.30	8.91	9.48	25.06	24.96	347	0.004	0.392	0.0016529
1-Apr	2:47-3:07	6.46	6.96	7.14	7.77	8.26	8.73	24.56	24.46	353	0.005	0.361	0.0018152
1-Apr	3:07-3:27	5.40	5.86	5.99	6.46	6.93	7.37	24.32	24.22	1	0.006	0.302	0.0018369
1-Apr	3:27-3:48	5.63	6.01	6.19	6.60	7.11	7.63	24.18	24.09	353	0.009	0.295	0.0028697
1-Apr	3:48-4:08	5.38	5.80	5.91	6.47	6.96	7.43	24.16	24.06	11	0.008	0.322	0.0010969
1-Apr	4:08-4:28	5.61	6.05	6.23	6.74	7.25	7.61	23.87	23.77	18	0.005	0.326	0.0013861
1-Apr	4:28-4:48	6.28	6.82	6.98	7.52	8.07	8.43	23.63	23.54	14	0.005	0.350	0.0018916
1-Apr	4:48-5:08	6.31	6.81	7.04	7.56	8.09	8.58	23.39	23.30	10	0.006	0.352	0.0018825
1-Apr	5:08-5:29	5.23	5.66	5.80	6.36	6.85	7.37	23.08	22.98	10	0.010	0.331	0.0007763
1-Apr	5:49-6:09	4.80	5.25	5.37	5.83	6.29	6.58	22.94	22.84	356	0.009	0.297	0.0009220
1-Apr	6:09-6:29	5.46	5.93	6.10	6.60	7.10	7.50	22.55	22.45	360	0.006	0.325	0.0011917
1-Apr	6:29-6:49	5.84	6.32	6.52	7.01	7.55	7.96	22.47	22.37	354	0.005	0.335	0.0015285
1-Apr	6:49-7:10	5.31	5.75	5.88	6.36	6.80	7.20	22.53	22.43	12	0.006	0.297	0.0018228
1-Apr	7:10-7:30	5.29	5.65	5.76	6.31	6.73	7.08	22.58	22.47	11	0.003	0.293	0.0018573
1-Apr	7:50-8:10	4.28	4.64	4.77	5.21	5.62	5.64	23.01	22.89	357	-0.021	0.281	0.0000349
1-Apr	8:10-8:30	5.01	5.43	5.52	5.89	6.26	6.48	23.77	23.62	5	-0.027	0.258	0.0002014
1-Apr	8:51-9:11	4.52	4.88	4.97	5.27	5.57	5.64	25.38	25.12	350	-0.092	0.231	0.0002345
9-Apr	2:04	4.39	4.59	4.72	5.25	5.58	6.03	27.27	27.18	335	0.033		
9-Apr	3:00	4.03	4.24	4.63	5.30	5.81	6.28	24.35	24.28	0	0.022	0.411	0.0000636
9-Apr	3:31	4.01	4.17	4.38	4.85	5.37	5.69	26.58	26.49	363	0.038	0.293	0.0002782
9-Apr	4:19	4.47	4.69	4.97	5.54	6.19	6.80	30.06	29.95	350	0.037	0.423	0.0000852
9-Apr	4:42	4.30	4.49	4.80	5.16	5.62	6.33	30.42	30.32	345	0.030	0.303	0.0003799
9-Apr	6:22	4.32	4.55	4.81	5.11	5.55	5.99	30.88	30.74	369	0.034	0.282	0.0006320
9-Apr	7:05	4.08	4.19	4.27	4.64	4.94	5.08	24.29	24.19	352	0.036	0.219	0.0020754
9-Apr	15:27	4.05	4.08	4.28	4.46	4.64	4.49	39.21	38.78	0	-0.848	0.217	0.0001852
10-Apr	0:16	4.53	4.77	5.32	5.88	6.19	6.60	26.21	26.12	0	0.011	0.369	0.0001838
10-Apr	0:36	4.78	5.07	5.39	5.82	6.24	6.62	25.95	25.82	0	0.014	0.307	0.0007053
10-Apr	1:44	6.41	6.74	6.99	7.69	8.19	9.07	26.65	26.58	343	0.012	0.383	0.0010469
10-Apr	1:58	5.43	5.69	6.20	6.60	7.14	7.94	33.12	33.05	305	0.020	0.373	0.0004624
10-Apr	2:02	4.77	4.99	5.28	5.73	6.23	6.66	32.88	32.76	10	0.032	0.341	0.0003516
10-Apr	2:22	6.63	6.87	7.25	7.77	8.35	8.93	33.30	33.17	386	0.014	0.369	0.0016811
10-Apr	2:42	6.39	6.69	7.06	7.46	7.95	8.58	32.91	32.76	362	0.012	0.322	0.0038316
10-Apr	3:02	5.13	5.40	5.74	6.03	6.51	7.05	32.06	31.90	329	0.018	0.290	0.0016540
10-Apr	3:04	4.53	4.74	4.88	5.41	5.72	6.05	27.01	26.93	15	0.038	0.298	0.0005632
10-Apr	3:11	4.98	5.16	5.38	5.92	6.50	6.99	26.73	26.66	382	0.029	0.362	0.0002940
10-Apr	3:20	4.70	4.95	5.19	5.73	6.16	6.58	24.57	24.46	0	0.022	0.327	0.0004059
10-Apr	3:22	4.62	4.83	5.13	5.42	5.81	6.22	32.09	31.95	311	0.031	0.270	0.0013078
10-Apr	3:24	6.26	6.56	6.72	7.28	7.80	8.42	26.39	26.30	381	0.011	0.325	0.0027981
10-Apr	3:41	4.83	5.09	5.29	5.79	6.25	6.57	24.42	24.30	0	0.020	0.311	0.0006435
10-Apr	3:44	5.97	6.23	6.46	7.06	7.52	8.13	26.02	25.93	366	0.011	0.335	0.0016016
10-Apr	4:02	4.82	5.08	5.32	5.69	6.23	6.89	30.74	30.61	7	0.024	0.307	0.0007008
10-Apr	4:04	4.90	5.13	5.20	5.73	6.18	6.65	25.65	25.56	13	0.019	0.289	0.0010706
10-Apr	4:24	5.90	6.12	6.28	6.81	7.28	7.90	25.64	25.54	368	0.012	0.300	0.0032269
10-Apr	4:39	4.54	4.74	5.10	5.62	6.14	6.97	30.36	30.26	329	0.028	0.372	0.0001692
10-Apr	4:44	5.38	5.66	5.80	6.36	6.81	7.39	25.41	25.32	354	0.015	0.310	0.0013181
10-Apr	4:59	5.36	5.64	5.98	6.52	7.02	7.85	31.09	30.97	356	0.024	0.371	0.0004332
10-Apr	5:02	5.79	6.10	6.37	6.87	7.43	8.15	30.79	30.66	337	0.017	0.349	0.0010032
10-Apr	5:04	6.28	6.67	6.85	7.40	7.96	8.69	24.78	24.69	355	0.008	0.342	0.0020706
10-Apr	5:19	4.55	4.71	5.01	5.51	5.94	6.38	30.69	30.57	358	0.032	0.335	0.0002885
10-Apr	5:22	5.69	5.99	6.31	6.73	7.32	8.07	30.73	30.60	347	0.017	0.343	0.0010153
10-Apr	5:24	5.47	5.78	5.97	6.52	6.98	7.65	24.39	24.30	329	0.011	0.318	0.0012842
10-Apr	5:42	5.88	6.24	6.52	6.88	7.51	8.14	30.65	30.52	354	0.015	0.334	0.0015611
10-Apr	5:44	6.03	6.35	6.63	7.12	7.55	8.40	24.50	24.45	316	0.009	0.314	0.0030066
10-Apr	6:02	5.16	5.47	5.76	6.21	6.85	7.57	31.44	31.31	359	0.022	0.366	0.0003710
10-Apr	7:03	4.73	4.86	5.13	5.41	5.84	6.25	30.37	30.23	395	0.028	0.255	0.0021235
10-Apr	7:25	6.64	7.05	7.26	7.84	8.32	9.00	24.66	24.55	333	0.005	0.339	0.0035043
10-Apr	7:45	4.83	5.09	5.22	5.65	5.99	6.36	24.71	24.59	360	-0.010	0.245	0.0001978
10-Apr	8:05	5.39	5.63	5.73	6.23	6.61	6.99	25.37	25.23	20	-0.021	0.270	0.0002100
10-Apr	17:08	4.47	4.60	4.81	5.02	5.18	5.23	40.02	39.72	0	-0.267	0.188	0.0012496
20-Apr	1:25	4.09	4.24	4.42	4.88	5.28	5.46	33.44	33.20	0	0.022	0.274	0.0004778
20-Apr	4:25	4.86	5.11	5.27	5.76	6.18	6.51	31.99	31.74	0	0.011	0.280	0.0013247
21-Apr	8:48	4.59	4.78	4.85	5.10	5.51	5.72	29.59	29.37	0	-0.025	0.198	0.0007596
21-Apr	10:08	4.10	4.27	4.20	4.54	4.85	4.93	30.77	30.56	0	-0.147	0.199	0.0002747

STOVEPIPE WELLS
DATA FOR SOUTH EASTERLY WIND DIRECTIONS

		Wind Speeds						Temperatures		Wind			
Date	Time	U(0.75)	U(1.25)	U(2.07)	U(3.44)	U(5.72)	U9(.5)	TL1	TU2	Dir	Ri	U*	Zo
30-Mar	18:08-18:28	4.15	4.27	4.49	4.75	4.93	5.06	32.70	31.77	121	-0.121	0.191	0.0000906
30-Mar	18:28-18:48	4.01	4.12	4.39	4.66	4.89	5.16	31.84	31.41	116	-0.032	0.200	0.0000423
31-Mar	9:52-10:12	4.00	4.04	4.25	4.45	4.59	4.59	26.55	25.40	147	-0.352	0.178	0.0001306
9-Apr	4:17	4.24	4.53	4.65	5.04	5.39	5.80	21.85	22.09	109	0.014	0.240	0.0001486
9-Apr	4:37	4.11	4.42	4.60	4.94	5.25	5.70	21.38	21.55	120	0.011	0.231	0.0001650
9-Apr	5:21	4.31	4.48	4.58	5.12	5.47	5.89	22.32	22.73	125	0.022	0.274	0.0000583
9-Apr	7:58	4.11	4.37	4.49	4.83	5.14	5.28	21.45	20.95	101	-0.038	0.222	0.0000242
9-Apr	8:39	4.12	4.17	4.42	4.71	4.77	4.92	30.54	29.86	153	-0.110	0.179	0.0001415
9-Apr	9:16	4.10	4.20	4.41	4.65	4.75	4.86	30.66	29.60	145	-0.197	0.175	0.0001942
9-Apr	9:56	4.37	4.44	4.62	4.87	4.98	5.00	31.17	29.93	124	-0.338	0.180	0.0002716
9-Apr	9:59	4.25	4.28	4.45	4.72	4.76	4.76	33.36	32.12	130	-0.512	0.181	0.0002092
9-Apr	10:16	4.33	4.41	4.57	4.84	4.94	4.86	31.79	30.55	138	-0.477	0.193	0.0001374
9-Apr	10:56	4.28	4.32	4.48	4.69	4.86	4.84	33.47	31.99	126	-0.511	0.184	0.0001823
9-Apr	11:07	4.13	4.20	4.40	4.58	4.71	4.66	36.42	35.00	165	-0.541	0.183	0.0001571
9-Apr	11:16	4.21	4.26	4.37	4.58	4.74	4.63	34.18	32.81	137	-0.836	0.193	0.0001144
9-Apr	11:36	4.03	4.06	4.22	4.45	4.55	4.39	34.99	33.55	133	-1.196	0.230	0.0000232
9-Apr	12:27	4.20	4.32	4.48	4.62	4.80	4.68	38.17	36.42	116	-0.815	0.197	0.0001057
9-Apr	12:47	4.12	4.21	4.40	4.60	4.75	4.65	38.63	36.86	127	-0.676	0.206	0.0000568
9-Apr	13:27	4.31	4.41	4.59	4.80	4.94	4.80	39.37	37.47	129	-0.848	0.221	0.0000500
9-Apr	13:47	4.21	4.27	4.45	4.67	4.82	4.70	39.65	37.88	98	-0.788	0.216	0.0000464
9-Apr	16:28	4.33	4.41	4.60	4.81	4.94	4.89	41.50	39.86	121	-0.554	0.192	0.0001514
9-Apr	16:35	4.30	4.41	4.54	4.81	4.97	4.93	32.73	31.21	129	-0.416	0.197	0.0001072
9-Apr	16:48	4.22	4.32	4.51	4.73	4.92	4.88	41.56	40.01	108	-0.376	0.199	0.0000851
9-Apr	17:15	4.28	4.37	4.53	4.85	4.97	4.91	32.36	31.09	117	-0.345	0.206	0.0000674
9-Apr	17:28	4.28	4.39	4.59	4.86	5.05	5.09	41.41	40.23	146	-0.188	0.199	0.0000843
9-Apr	18:56	4.12	4.35	4.48	4.87	5.11	5.20	30.80	30.45	132	-0.028	0.218	0.0000277
10-Apr	1:57	6.30	6.68	6.94	7.42	7.96	8.41	23.96	24.07	104	0.004	0.330	0.0002579
10-Apr	2:17	6.69	7.18	7.47	7.86	8.44	9.02	23.74	23.83	114	0.003	0.337	0.0003773
10-Apr	2:37	6.15	6.68	6.94	7.33	7.80	8.22	23.31	23.36	118	0.003	0.317	0.0003286
10-Apr	2:57	5.43	5.93	6.16	6.55	6.95	7.40	22.73	22.82	112	0.005	0.296	0.0002214
10-Apr	3:17	4.87	5.27	5.38	5.79	6.17	6.56	22.41	22.50	107	0.006	0.257	0.0002589
10-Apr	3:37	5.42	5.89	6.10	6.52	7.02	7.58	22.22	22.42	95	0.007	0.313	0.0001363
10-Apr	3:57	4.71	5.09	5.29	5.68	6.18	6.64	22.02	22.33	93	0.012	0.296	0.0000751
10-Apr	4:01	5.36	5.62	5.83	6.34	6.85	7.30	23.69	24.06	104	0.013	0.318	0.0000977
10-Apr	4:21	5.71	5.99	6.17	6.64	7.16	7.56	23.37	23.62	105	0.011	0.302	0.0002224
10-Apr	4:41	5.10	5.32	5.49	5.89	6.31	6.72	23.07	23.32	99	0.014	0.257	0.0003257
10-Apr	5:01	4.56	4.73	4.87	5.30	5.69	6.11	22.82	23.17	111	0.020	0.255	0.0001432
10-Apr	8:59	4.85	4.98	5.25	5.56	5.61	5.83	31.46	30.54	127	-0.102	0.200	0.0002573
10-Apr	9:19	5.15	5.29	5.57	5.85	6.01	6.26	31.84	30.73	122	-0.097	0.211	0.0002724
10-Apr	9:36	4.48	4.60	4.81	5.08	5.18	5.25	30.80	29.72	138	-0.196	0.175	0.0004305
10-Apr	9:39	4.53	4.60	4.81	5.08	5.08	5.23	32.80	31.62	138	-0.258	0.171	0.0006390
10-Apr	10:36	4.50	4.61	4.74	5.00	5.16	5.20	32.56	31.06	125	-0.333	0.185	0.0002778
10-Apr	10:47	4.66	4.84	4.99	5.27	5.47	5.54	35.94	34.45	121	-0.207	0.204	0.0001549
10-Apr	12:07	4.62	4.75	4.90	5.10	5.24	5.26	37.67	36.14	142	-0.400	0.174	0.0007435
10-Apr	14:07	4.77	4.89	5.11	5.31	5.49	5.45	40.03	38.21	102	-0.421	0.206	0.0001887
10-Apr	14:27	4.67	4.77	5.01	5.22	5.43	5.40	40.38	38.44	112	-0.389	0.217	0.0000950
10-Apr	14:47	4.80	4.91	5.11	5.31	5.49	5.51	40.32	38.67	97	-0.348	0.191	0.0004022
10-Apr	15:07	4.66	4.75	4.97	5.18	5.35	5.33	40.85	39.05	118	-0.427	0.203	0.0001705
10-Apr	16:55	4.63	4.77	4.90	5.16	5.34	5.41	32.48	31.01	130	-0.262	0.188	0.0003259
10-Apr	17:35	4.58	4.72	4.87	5.15	5.28	5.40	32.12	30.95	126	-0.187	0.181	0.0004039
10-Apr	17:48	4.48	4.60	4.84	5.10	5.36	5.41	41.35	40.31	127	-0.125	0.214	0.0000639
10-Apr	17:55	4.84	5.01	5.20	5.56	5.72	5.86	31.83	30.84	139	-0.101	0.216	0.0001208
10-Apr	18:16	4.78	4.98	5.21	5.54	5.72	5.91	31.66	30.78	144	-0.073	0.220	0.0000930
10-Apr	18:36	4.77	4.94	5.20	5.57	5.81	6.00	31.29	30.65	133	-0.044	0.239	0.0000426
18-Apr	15:40	4.00	4.09	4.15	4.33	4.53	4.43	40.80	39.27	118	-0.876	0.187	0.0000998
18-Apr	16:20	4.22	4.27	4.38	4.63	4.83	4.85	41.09	39.58	114	-0.402	0.186	0.0001388
18-Apr	16:40	4.80	4.94	5.12	5.35	5.60	5.65	41.14	39.54	124	-0.235	0.204	0.0001967
18-Apr	17:00	5.31	5.51	5.67	5.95	6.26	6.46	40.51	39.11	143	-0.112	0.220	0.0002360
18-Apr	17:20	5.28	5.46	5.64	6.03	6.19	6.32	40.26	39.12	134	-0.110	0.226	0.0001776
18-Apr	17:40	4.81	4.97	5.05	5.44	5.65	5.75	40.37	39.25	121	-0.132	0.213	0.0001233
18-Apr	18:00	4.50	4.61	4.67	5.07	5.32	5.34	40.29	39.22	124	-0.158	0.220	0.0000493
18-Apr	18:20	4.52	4.65	4.72	5.08	5.31	5.39	39.84	38.96	119	-0.120	0.200	0.0001194
18-Apr	18:40	4.43	4.56	4.70	5.11	5.33	5.41	39.77	39.04	130	-0.077	0.221	0.0000412
18-Apr	19:00	4.25	4.35	4.51	4.93	5.22	5.40	39.06	38.71	121	-0.024	0.226	0.0000224
19-Apr	12:43	4.07	4.11	4.22	4.54	4.76	4.60	39.69	37.78	155	-0.728	0.253	0.0000107
19-Apr	13:03	4.39	4.41	4.52	4.82	5.00	4.90	39.89	38.11	127	-0.731	0.230	0.0000355

		Wind Speeds						Temperatures		Wind			
Date	Time	U(0.75)	U(1.25)	U(2.07)	U(3.44)	U(5.72)	U9(.5)	TL1	TU2	Dir	Ri	U*	Zo
30-Mar	18:08-18:28	4.15	4.27	4.49	4.75	4.93	5.06	32.70	31.77	121	-0.121	0.191	0.0000906
21-Apr	11:08	4.78	4.97	5.02	5.26	5.53	5.75	32.30	31.12	131	-0.135	0.177	0.0007700
21-Apr	11:28	4.50	4.64	4.65	4.93	5.19	5.30	33.55	32.08	146	-0.249	0.186	0.0002359
21-Apr	11:48	4.84	5.02	5.05	5.32	5.63	5.72	33.82	32.36	125	-0.204	0.200	0.0002438
21-Apr	12:08	5.58	5.82	5.95	6.29	6.59	6.81	34.08	32.58	127	-0.107	0.234	0.0002126
21-Apr	12:28	6.90	7.22	7.44	7.85	8.14	8.41	35.27	33.50	133	-0.084	0.283	0.0002798
21-Apr	12:48	7.80	8.19	8.50	8.95	9.37	9.77	36.29	34.33	130	-0.055	0.344	0.0001371
21-Apr	13:08	8.81	9.22	9.68	10.24	10.67	11.20	36.66	34.63	138	-0.039	0.410	0.0000828
21-Apr	13:28	9.44	9.91	10.38	11.02	11.62	12.10	36.90	34.94	130	-0.030	0.469	0.0000462

		Wind Speeds						Temperatures		Wind			
Date	Time	U(0.75)	U(1.25)	U(2.07)	U(3.44)	U(5.72)	U9(.5)	TL1	TU2	Dir	Ri	U*	Zo
30-Mar	18:08-18:28	4.15	4.27	4.49	4.75	4.93	5.06	32.70	31.77	121	-0.121	0.191	0.0000906
19-Apr	13:23	4.91	4.99	5.00	5.37	5.57	5.64	40.33	38.48	135	-0.371	0.211	0.0001624
19-Apr	13:43	5.04	5.20	5.33	5.66	5.87	5.96	39.68	38.10	126	-0.199	0.214	0.0001991
19-Apr	14:03	5.29	5.42	5.58	5.90	6.11	6.23	40.27	38.64	154	-0.196	0.213	0.0003154
19-Apr	14:23	5.00	5.08	5.16	5.53	5.73	5.76	40.85	39.14	93	-0.315	0.219	0.0001403
19-Apr	14:43	4.49	4.52	4.63	4.91	5.11	5.03	41.32	39.59	128	-0.630	0.218	0.0000631
19-Apr	15:03	4.55	4.67	4.70	5.03	5.17	5.13	41.33	39.77	145	-0.491	0.198	0.0001648
19-Apr	16:23	4.11	4.22	4.32	4.68	4.93	4.85	40.92	39.93	112	-0.187	0.218	0.0000268
19-Apr	16:43	5.52	5.69	5.87	6.31	6.61	6.77	40.66	39.89	161	-0.050	0.254	0.0000818
19-Apr	17:04	6.57	6.84	7.15	7.66	8.01	8.38	40.41	39.80	151	-0.019	0.314	0.0000601
19-Apr	17:24	6.48	6.78	6.99	7.52	7.85	8.18	40.29	39.74	142	-0.019	0.298	0.0000850
19-Apr	17:44	5.96	6.19	6.42	6.90	7.30	7.62	40.32	39.79	156	-0.019	0.292	0.0000468
19-Apr	18:04	4.92	5.12	5.27	5.66	5.95	6.10	40.28	39.76	157	-0.036	0.230	0.0000722
20-Apr	0:05	4.79	4.98	5.10	5.60	6.12	6.51	33.70	34.30	99	0.025	0.311	0.0000512
20-Apr	0:25	4.83	5.02	5.21	5.63	6.13	6.51	33.62	34.12	107	0.022	0.292	0.0000842
20-Apr	0:45	5.52	5.79	5.92	6.38	6.94	7.30	34.03	34.39	113	0.015	0.304	0.0001625
20-Apr	1:05	5.47	5.78	6.00	6.40	6.88	7.28	33.78	34.03	92	0.011	0.288	0.0002502
20-Apr	2:45	5.40	5.65	6.03	6.57	7.01	7.42	32.54	32.71	97	0.006	0.339	0.0000699
20-Apr	3:05	5.34	5.59	5.77	6.20	6.68	6.88	32.21	32.31	105	0.008	0.277	0.0002621
20-Apr	3:25	5.55	5.85	6.01	6.46	6.92	7.36	32.03	32.19	107	0.008	0.280	0.0003348
20-Apr	3:45	5.27	5.51	5.69	6.21	6.65	7.08	31.90	32.09	98	0.009	0.293	0.0001534
20-Apr	4:05	5.32	5.55	5.74	6.21	6.69	7.04	31.93	32.12	102	0.010	0.289	0.0001789
20-Apr	4:45	4.46	4.67	4.85	5.30	5.71	5.97	31.64	31.91	103	0.016	0.273	0.0000800
20-Apr	5:05	4.33	4.48	4.61	5.05	5.41	5.63	31.19	31.38	137	0.017	0.244	0.0001327
20-Apr	5:45	4.71	4.89	5.01	5.43	5.85	6.26	31.05	31.33	113	0.016	0.251	0.0001977
20-Apr	6:05	4.90	5.14	5.34	5.78	6.18	6.60	31.16	31.41	112	0.012	0.271	0.0001663
20-Apr	6:26	5.51	5.78	5.90	6.33	6.74	7.25	31.12	31.28	120	0.008	0.254	0.0007006
20-Apr	6:46	5.33	5.63	5.78	6.28	6.53	7.03	31.06	31.21	125	0.008	0.253	0.0005700
20-Apr	7:06	5.34	5.55	5.77	6.23	6.49	6.98	30.88	30.93	133	0.005	0.244	0.0007701
20-Apr	7:26	6.32	6.64	6.85	7.41	7.66	8.14	31.18	31.13	125	0.000		
20-Apr	7:46	6.36	6.69	6.92	7.41	7.65	8.17	31.37	31.26	133	-0.002	0.268	0.0001877
20-Apr	8:06	6.24	6.55	6.75	7.28	7.53	8.02	31.76	31.44	135	-0.009	0.278	0.0001127
20-Apr	8:26	6.21	6.44	6.68	7.22	7.41	7.94	32.39	31.83	131	-0.019	0.274	0.0001180
20-Apr	8:46	6.53	6.79	7.03	7.57	7.80	8.22	32.98	32.22	131	-0.028	0.289	0.0001208
20-Apr	9:06	6.66	6.94	7.18	7.74	8.03	8.41	33.30	32.36	155	-0.032	0.309	0.0000780
20-Apr	9:26	7.28	7.59	7.93	8.44	8.77	9.29	33.73	32.66	137	-0.028	0.328	0.0001043
20-Apr	9:46	7.27	7.65	7.89	8.41	8.79	9.22	34.51	33.14	138	-0.039	0.331	0.0000976
20-Apr	17:46	6.59	7.30	8.00	7.42	9.63	9.58	38.87	38.55	143	-0.003	0.684	0.0000005
20-Apr	18:06	5.11	5.30	5.41	5.75	6.08	6.45	38.83	38.50	178	-0.017	0.208	0.0002429
20-Apr	18:26	5.78	6.06	6.21	6.62	7.00	7.40	39.04	38.62	169	-0.015	0.256	0.0001142
20-Apr	18:46	5.79	6.01	6.23	6.63	7.01	7.42	38.69	38.36	151	-0.011	0.259	0.0001039
20-Apr	19:06	5.33	5.57	5.74	6.15	6.55	6.90	38.22	38.04	166	-0.005	0.253	0.0000589
20-Apr	19:26	7.19	7.53	7.81	8.32	8.80	9.40	37.64	37.54	155	-0.001	0.325	0.0000935
20-Apr	19:46	6.29	6.63	6.92	7.34	7.82	8.28	37.11	37.15	142	0.003	0.303	0.0005134
20-Apr	20:06	6.11	6.42	6.70	7.11	7.49	7.97	36.55	36.61	152	0.004	0.277	0.0008724
20-Apr	20:26	6.55	6.90	7.20	7.56	8.08	8.64	36.03	36.11	160	0.004	0.300	0.0007907
20-Apr	20:46	5.91	6.18	6.38	6.82	7.22	7.71	35.78	35.88	166	0.006	0.268	0.0008355
20-Apr	21:06	7.47	7.83	8.15	8.68	9.23	9.75	35.53	35.61	174	0.003	0.353	0.0005843
20-Apr	21:26	7.19	7.51	7.76	8.23	8.78	9.40	35.15	35.27	179	0.004	0.320	0.0009761
20-Apr	21:46	6.50	6.89	7.11	7.54	8.04	8.54	34.80	34.92	186	0.005	0.304	0.0006694
20-Apr	22:06	7.13	7.54	7.80	8.22	8.72	9.29	34.81	34.94	167	0.005	0.312	0.0012144
20-Apr	22:26	6.68	7.03	7.28	7.77	8.24	8.75	34.30	34.37	142	0.003	0.312	0.0006497
20-Apr	22:46	6.23	6.46	6.75	7.21	7.62	8.17	33.96	34.02	128	0.004	0.287	0.0007056
20-Apr	23:06	5.85	6.10	6.31	6.72	7.16	7.72	33.85	33.93	98	0.005	0.266	0.0007875
20-Apr	23:26	7.05	7.49	7.75	8.18	8.77	9.21	33.28	33.32	101	0.002	0.334	0.0005965
20-Apr	23:46	7.18	7.65	7.90	8.36	8.98	9.60	32.87	32.91	93	0.002	0.349	0.0004889
21-Apr	0:06	7.01	7.38	7.66	8.07	8.63	9.19	32.60	32.67	100	0.003	0.318	0.0008508
21-Apr	0:27	6.13	6.46	6.68	7.05	7.62	8.11	32.45	32.55	95	0.005	0.295	0.0005039
21-Apr	0:47	6.61	6.94	7.19	7.64	8.15	8.68	32.29	32.34	121	0.003	0.307	0.0006869
21-Apr	1:07	6.76	7.11	7.36	7.80	8.28	8.76	31.87	31.87	114	0.002	0.300	0.0010461
21-Apr	1:27	6.59	6.94	7.16	7.64	8.16	8.66	31.54	31.56	132	0.002	0.312	0.0005767
21-Apr	1:47	5.85	6.12	6.34	6.86	7.24	7.85	31.27	31.30	139	0.003	0.286	0.0004241
21-Apr	2:07	5.75	5.97	6.14	6.59	7.00	7.53	30.96	30.98	129	0.003	0.258	0.0008597
21-Apr	2:27	5.33	5.59	5.71	6.14	6.54	6.98	30.59	30.62	138	0.004	0.247	0.0006731
21-Apr	8:28	4.24	4.38	4.44	4.70	5.08	5.27	29.74	29.51	107	-0.018	0.184	0.0001196
21-Apr	9:08	4.73	5.09	5.26	5.60	5.95	6.17	30.63	30.15	93	-0.023	0.252	0.0000283
21-Apr	9:28	4.02	4.16	4 10	4.43	4.72	4.78	30.76	30.11	104	-0.116	0.154	0.0003575
21-Apr	10:28	4.11	4.27	4.23	4.53	4.84	4.87	32.15	31.07	98	-0.200	0.196	0.0000615
21-Apr	10:48	4.53	4.68	4.74	5.00	5.26	5.47	32.04	30.97	103	-0.130	0.176	0.0004277

KIT FOX FAN: MAST 1
DATA FOR NORTHERLY WIND DIRECTIONS

		Wind Speeds						Temperatures		Wind			
Date	Time	U(0.75)	U(1.25)	U(2.07)	U(3.44)	U(5.72)	U9(.50)	TL2	TU1	Dir	Ri	U*	Zo
7-May	1:36	4.15	4.45	4.86	5.27	5.69	5.89	34.73	35.38	0	0.0264	0.26406963	0.0005408
9-May	12:49	7.12	7.63	8.16	8.59	9.05	9.36	38.44	36.90	54	-0.0328	0.39559786	0.0015743
9-May	13:09	6.41	6.86	7.34	7.83	8.19	8.48	37.49	36.42	54	-0.0263	0.36603807	0.0012699
9-May	13:49	8.04	8.48	9.10	9.69	10.08	10.59	38.25	37.03	53	-0.0198	0.44123173	0.0015823
9-May	14:09	7.70	8.15	8.79	9.36	9.87	10.30	38.62	37.38	54	-0.0194	0.45489816	0.0009397
9-May	14:29	8.39	8.88	9.53	10.22	10.56	10.91	38.73	37.45	54	-0.0213	0.45210494	0.0018795
9-May	14:49	9.74	10.28	10.88	11.75	12.25	12.55	38.88	37.53	53	-0.0181	0.51070738	0.0022234
9-May	15:09	10.43	11.19	11.85	12.73	13.35	13.71	38.63	37.36	55	-0.0125	0.57296546	0.0016394
9-May	15:30	10.06	10.71	11.36	12.25	12.75	13.36	38.20	37.02	53	-0.0114	0.56189952	0.0013889
9-May	15:50	9.71	10.31	10.83	11.78	12.26	12.77	38.03	36.96	53	-0.0120	0.53119008	0.0015834
9-May	16:10	9.34	9.86	10.45	11.33	11.82	12.28	38.01	37.16	53	-0.0102	0.51336828	0.0015071
9-May	16:30	8.22	8.71	9.30	10.13	10.52	10.85	38.33	37.75	53	-0.0084	0.46562609	0.0012392
9-May	16:50	8.10	8.51	9.16	9.91	10.32	10.75	37.88	37.38	53	-0.0070	0.46125559	0.0011536
9-May	17:10	6.86	7.40	8.03	8.62	8.97	9.29	37.36	36.81	53	-0.0092	0.41929882	0.0007959
9-May	17:30	6.87	7.36	8.11	8.66	9.11	9.42	35.41	35.07	54	-0.0048	0.4393239	0.0005724
9-May	17:50	7.76	8.37	9.01	9.62	10.16	10.56	34.52	34.35	54	-0.0016	0.46139566	0.0009148
9-May	18:10	7.77	8.44	9.00	9.74	10.24	10.49	34.44	34.25	54	-0.0020	0.46217993	0.0009335
9-May	18:30	8.21	8.93	9.45	10.28	10.92	11.07	33.94	33.67	54	-0.0029	0.49913721	0.0007954
9-May	18:50	7.98	8.67	9.31	10.08	10.59	10.91	32.95	33.04	54	0.0020	0.4796299	0.0008529
9-May	19:10	9.34	9.91	10.64	11.57	12.08	12.48	31.92	32.11	54	0.0029	0.52181898	0.0013140
9-May	19:30	9.45	10.18	10.85	11.85	12.38	12.78	30.88	30.95	54	0.0013	0.55078956	0.0010153
9-May	19:50	10.07	10.85	11.59	12.65	13.25	13.75	29.91	29.96	54	0.0009	0.60408178	0.0008286
9-May	20:10	8.60	9.31	10.02	10.81	11.38	11.76	29.24	29.32	55	0.0016	0.51530866	0.0008611
9-May	20:30	8.13	8.77	9.45	10.05	10.71	11.21	28.64	28.74	55	0.0019	0.48796607	0.0008278
9-May	20:50	7.68	8.31	9.02	9.65	10.28	10.59	28.07	28.17	54	0.0022	0.47520853	0.0006923
9-May	21:10	7.51	7.96	8.66	9.24	9.71	10.33	27.71	27.84	55	0.0027	0.44461823	0.0008586
9-May	21:30	6.98	7.56	8.18	8.64	9.09	9.64	27.28	27.40	55	0.0029	0.409267	0.0009975
9-May	21:50	6.62	7.10	7.71	8.37	8.71	9.11	26.60	26.71	55	0.0032	0.40288324	0.0007535
9-May	22:51	6.18	6.60	7.12	7.63	8.09	8.56	25.34	25.43	56	0.0031	0.3752778	0.0007305
9-May	23:11	7.44	8.00	8.57	9.24	9.64	10.17	24.72	24.80	56	0.0022	0.4306854	0.0010568
9-May	23:31	7.90	8.44	9.12	9.80	10.27	10.77	24.34	24.42	55	0.0020	0.46015668	0.0009997
9-May	23:51	8.39	9.06	9.70	10.23	10.93	11.48	23.75	23.81	55	0.0015	0.48353428	0.0010932
10-May	0:11	6.91	7.44	8.02	8.56	9.07	9.75	23.34	23.41	56	0.0019	0.43893574	0.0005486
10-May	0:31	6.78	7.26	7.87	8.45	8.98	9.58	23.06	23.13	56	0.0019	0.44103827	0.0004667
10-May	0:51	6.16	6.76	7.42	7.93	8.27	8.91	22.83	22.92	56	0.0023	0.42200833	0.0003758
10-May	1:11	7.30	8.01	8.74	9.36	9.99	10.52	22.68	22.76	56	0.0016	0.50820311	0.0003390
10-May	1:31	7.83	8.48	9.23	9.91	10.39	10.92	22.33	22.35	56	0.0010	0.49319167	0.0006191
10-May	1:51	7.83	8.48	9.06	9.81	10.26	10.79	22.14	22.16	56	0.0011	0.47025944	0.0008345
10-May	2:11	6.97	7.48	8.14	8.77	9.13	9.69	22.12	22.17	56	0.0017	0.43102326	0.0006741
10-May	2:31	6.75	7.23	7.76	8.33	8.71	9.09	22.16	22.23	56	0.0028	0.37388134	0.0014545
10-May	2:51	6.20	6.69	7.30	7.83	8.19	8.76	21.91	22.00	56	0.0027	0.39830634	0.0005306
10-May	3:11	5.71	6.18	6.69	7.21	7.53	8.04	21.71	21.81	57	0.0035	0.361003	0.0005907
10-May	3:31	4.83	5.20	5.72	6.11	6.37	6.83	21.60	21.71	57	0.0050	0.30837089	0.0005530
10-May	3:51	5.03	5.40	5.85	6.34	6.55	7.07	21.45	21.55	57	0.0045	0.31448957	0.0006143
10-May	4:11	4.98	5.34	5.88	6.30	6.56	7.00	21.25	21.33	57	0.0040	0.31612332	0.0005697
10-May	4:31	5.39	5.84	6.41	6.86	7.20	7.70	21.45	21.48	57	0.0020	0.36041108	0.0004194
10-May	4:52	5.89	6.36	6.92	7.39	7.82	8.22	21.61	21.63	57	0.0017	0.36985548	0.0006206
10-May	5:12	5.26	5.71	6.26	6.71	7.03	7.43	21.64	21.65	57	0.0017	0.34334179	0.0004967
10-May	5:32	5.16	5.64	6.19	6.61	6.94	7.33	21.56	21.55	57	0.0012	0.34238276	0.0004586
10-May	5:52	5.48	5.95	6.49	6.96	7.19	7.63	21.40	21.39	56	0.0013	0.33848271	0.0007159
10-May	6:12	5.30	5.68	6.19	6.64	7.00	7.35	21.24	21.24	57	0.0017	0.32906968	0.0006540
10-May	6:32	5.42	5.87	6.41	6.81	7.16	7.59	21.18	21.17	57	0.0012	0.34005742	0.0006335
10-May	6:52	5.08	5.52	6.05	6.37	6.67	7.15	21.26	21.14	57	-0.0016	0.32701184	0.0005521
10-May	7:12	5.33	5.72	6.22	6.61	6.88	7.37	21.81	21.54	57	-0.0059	0.33128921	0.0006749
10-May	7:32	5.40	5.84	6.35	6.82	7.14	7.72	21.78	21.50	57	-0.0048	0.37393614	0.0003419
10-May	7:52	5.56	6.00	6.53	7.03	7.37	7.80	21.50	21.36	57	-0.0019	0.36531192	0.0004729
10-May	8:12	5.33	5.81	6.30	6.64	6.98	7.37	22.49	22.14	57	-0.0082	0.33334863	0.0006931
10-May	8:32	5.62	6.12	6.59	7.02	7.33	7.73	23.24	22.58	56	-0.0157	0.35301072	0.0006812
10-May	8:52	5.45	5.97	6.44	6.88	7.13	7.57	23.80	22.99	56	-0.0194	0.35469991	0.0005555
10-May	9:12	5.28	5.66	6.12	6.54	6.77	7.18	23.80	23.08	57	-0.0213	0.32399296	0.0007654
10-May	9:32	5.52	5.85	6.39	6.88	7.10	7.43	23.74	23.13	57	-0.0176	0.33764109	0.0007604
10-May	9:52	5.32	5.68	6.09	6.54	6.65	6.87	24.65	23.78	56	-0.0392	0.28648121	0.0020254
10-May	10:52	4.55	4.90	5.27	5.45	5.65	5.87	26.30	25.06	56	-0.0782	0.24116774	0.0024759
10-May	11:12	4.01	4.32	4.58	4.84	5.06	5.23	26.57	25.46	56	-0.0814	0.22698584	0.0014738
10-May	11:33	4.50	4.79	5.12	5.30	5.49	5.79	27.07	25.84	56	-0.0810	0.23144429	0.0029393
10-May	11:53	4.75	5.04	5.42	5.70	5.86	6.23	27.47	26.05	56	-0.0715	0.26617784	0.0014897

		Wind Speeds						Temperatures		Wind			
Date	Time	U(0.75)	U(1.25)	U(2.07)	U(3.44)	U(5.72)	U9(.50)	TL2	TU1	Dir	Ri	U*	Zo
10-May	12:13	4.68	5.02	5.39	5.65	5.79	5.99	27.85	26.55	56	-0.0831	0.24614771	0.0026197
10-May	12:33	4.78	5.13	5.54	5.80	6.00	6.25	28.41	27.03	56	-0.0701	0.26927035	0.0015292
10-May	12:53	4.33	4.61	4.89	5.20	5.44	5.68	29.16	27.63	55	-0.0923	0.25414443	0.0010839
10-May	13:13	4.56	4.83	5.16	5.49	5.66	5.86	29.36	27.82	55	-0.1002	0.25226694	0.0016911
10-May	13:33	4.93	5.31	5.65	5.99	6.22	6.46	29.50	28.07	55	-0.0669	0.27961907	0.0014393
10-May	13:53	5.58	5.99	6.32	6.78	7.02	7.23	29.93	28.31	55	-0.0654	0.30880803	0.0016879
10-May	14:13	6.16	6.59	7.01	7.62	7.89	8.04	30.42	28.92	55	-0.0464	0.36068585	0.0010878
10-May	14:33	6.75	7.49	7.99	8.56	8.90	8.97	31.08	29.46	55	-0.0360	0.41626612	0.0008565
10-May	14:53	6.88	7.44	7.97	8.50	8.78	9.05	30.43	29.04	55	-0.0322	0.38897551	0.0014539
10-May	15:13	8.10	8.83	9.39	10.05	10.50	10.83	30.67	29.43	55	-0.0180	0.47274266	0.0011398
10-May	15:33	8.93	9.69	10.24	10.92	11.55	11.92	31.01	29.66	55	-0.0164	0.51380478	0.0012143
10-May	15:53	8.20	8.86	9.48	10.11	10.66	10.97	31.13	29.92	55	-0.0170	0.48363701	0.0010238
10-May	16:13	9.42	10.27	10.93	11.64	12.21	12.53	31.14	30.22	55	-0.0101	0.53188529	0.0014281
10-May	16:33	9.93	10.70	11.23	12.18	12.74	13.12	30.82	30.23	54	-0.0059	0.54585308	0.0016015
10-May	16:53	9.75	10.53	11.25	12.21	12.77	13.15	30.97	30.39	54	-0.0051	0.58480392	0.0008774
10-May	17:13	9.91	10.74	11.42	12.28	12.91	13.44	30.21	29.69	56	-0.0042	0.58528921	0.0009745
10-May	17:33	10.26	10.98	11.66	12.62	12.94	13.44	29.58	29.17	55	-0.0040	0.5382355	0.0022812
10-May	17:53	8.80	9.49	10.22	10.96	11.39	11.96	28.96	28.49	55	-0.0047	0.52231693	0.0009447
20-May	10:53	5.27	6.74	5.73	5.67	6.85	7.07	33.93	35.23	0	0.0473	0.40404087	0.0001126
20-May	11:13	4.73	5.46	5.90	6.38	6.77	7.21	33.52	34.80	0	0.0246	0.34942637	0.0002711
20-May	11:33	5.48	6.20	6.72	7.25	7.72	8.29	32.88	34.13	42	0.0188	0.40219378	0.0002646
20-May	11:53	5.51	6.00	6.52	6.97	7.40	7.90	32.12	33.33	35	0.0252	0.34015474	0.0006951
20-May	12:18	4.33	4.51	4.94	5.15	5.27	5.42	36.08	35.63	36	-0.0367	0.20601109	0.0051516
20-May	14:13	6.71	7.24	7.79	8.31	8.74	9.27	30.38	31.68	0	0.0237	0.36721061	0.0015991
20-May	14:33	4.64	4.90	5.35	5.68	6.04	6.37	30.77	32.04	0	0.0506	0.23724395	0.0024913
20-May	17:35	4.61	4.82	5.28	5.73	6.08	6.35	27.95	29.34	56	0.0550	0.24681728	0.0016641
20-May	23:45	4.90	5.33	5.79	6.14	6.64	6.98	32.60	33.66	42	0.0293	0.29739005	0.0007729
21-May	0:05	4.21	4.44	4.93	5.26	5.63	5.91	32.21	33.25	0	0.0431	0.24287792	0.0010094
21-May	2:25	4.20	4.38	4.65	5.08	5.41	6.15	30.25	31.53	43	0.0402	0.27016484	0.0003874
21-May	2:45	4.33	4.52	4.81	5.27	5.57	6.26	30.19	31.45	0	0.0404	0.26690331	0.0005290
21-May	3:25	4.19	4.32	4.40	4.80	4.99	6.10	29.43	30.66	0	0.0404	0.27938223	0.0002351
21-May	4:26	4.11	4.27	4.35	4.80	5.13	5.85	28.73	29.97	0	0.0492	0.24241042	0.0006008
21-May	5:06	4.08	4.26	4.56	4.90	5.16	5.96	28.50	29.75	42	0.0425	0.2545711	0.0004705
21-May	23:28	4.90	5.27	5.66	6.10	6.47	6.94	32.89	33.98	0	0.0312	0.28609234	0.0009504
22-May	0:08	5.70	6.15	6.36	6.99	7.43	7.82	32.69	33.78	0	0.0289	0.30775895	0.0016245
23-May	1:54	4.04	4.37	4.66	5.18	5.40	5.87	29.60	30.66	43	0.0382	0.25295556	0.0005874
23-May	2:14	4.28	4.70	5.12	5.57	5.83	6.36	29.33	30.37	0	0.0291	0.28915993	0.0003937
23-May	4:55	4.24	4.75	5.12	5.50	6.02	6.51	27.62	28.67	0	0.0248	0.31918302	0.0002128
23-May	5:55	4.28	4.70	5.00	5.43	5.83	6.16	27.58	28.62	0	0.0358	0.26257018	0.0007184
23-May	6:15	4.48	4.90	5.02	5.53	5.91	6.56	27.60	28.58	0	0.0277	0.29044684	0.0004338
23-May	6:55	4.21	4.42	4.68	5.08	5.35	5.84	28.17	29.00	0	0.0385	0.22571753	0.0015275
23-May	7:55	4.01	4.28	4.56	4.87	5.15	5.41	29.69	30.35	0	0.0420	0.19352034	0.0041240

KIT FOX : MAST 1
DATA FOR SOUTHERLY WINDS

		Wind Speeds						Temperatures		Wind			
Date	Time	U(0.75)	U(1.25)	U(2.07)	U(3.44)	U(5.72)	U9(.50)	TL2	TU1	Dir	Ri	U*	Zo
5-May	16:07	4.02	4.20	4.49	4.64	5.01	5.15	42.01	41.33	163	-0.0533	0.21233052	0.0017633
6-May	14:34	4.12	4.33	4.73	4.95	5.07	5.24	42.04	41.17	123	-0.0709	0.21549779	0.0021491
6-May	15:34	4.21	4.49	4.89	5.14	5.26	5.51	42.59	41.84	132	-0.0447	0.2334543	0.0013960
6-May	15:54	4.22	4.46	4.84	5.16	5.28	5.48	42.58	41.85	135	-0.0462	0.23451151	0.0013262
6-May	16:54	4.12	4.33	4.74	5.13	5.26	5.51	41.84	41.48	140	-0.0171	0.24917748	0.0006754
6-May	17:34	4.28	4.54	4.97	5.35	5.57	5.78	41.74	41.65	157	-0.0015	0.25583262	0.0007211
6-May	17:54	4.88	5.26	5.69	6.13	6.38	6.67	42.02	41.88	142	-0.0027	0.29762824	0.0006600
6-May	18:14	5.11	5.47	5.94	6.33	6.67	6.93	42.28	42.10	145	-0.0040	0.30649698	0.0007276
6-May	18:34	4.91	5.25	5.69	6.13	6.38	6.74	42.11	42.15	164	0.0033	0.28983426	0.0007746
6-May	18:54	4.71	5.06	5.54	5.89	6.10	6.52	41.49	41.79	144	0.0121	0.27089831	0.0009530
6-May	19:14	4.17	4.51	4.93	5.28	5.57	6.03	40.90	41.35	135	0.0162	0.27136964	0.0004068
7-May	2:36	4.05	4.32	4.79	5.13	5.50	5.77	33.08	33.70	97	0.0260	0.25644768	0.0004741
7-May	19:21	5.25	5.61	6.13	6.63	7.06	7.33	41.89	42.37	167	0.0137	0.32759722	0.0005255
8-May	2:23	4.27	4.49	5.01	5.42	5.75	6.09	33.87	34.55	95	0.0252	0.27440212	0.0004112
8-May	15:05	4.15	4.36	4.71	4.95	5.07	5.29	42.08	40.92	153	-0.0929	0.21800298	0.0020790
8-May	17:25	4.58	4.89	5.32	5.64	5.85	6.15	42.82	42.64	153	-0.0053	0.2607176	0.0010583
8-May	17:45	4.27	4.46	4.87	5.21	5.38	5.59	42.98	42.68	158	-0.0151	0.23707704	0.0012099
9-May	8:08	4.68	5.03	5.58	5.89	6.23	6.74	31.75	32.03	120	0.0091	0.30980119	0.0003648
9-May	8:49	4.26	4.50	4.97	5.28	5.62	5.87	32.84	33.04	96	0.0113	0.25383215	0.0006997
9-May	9:49	4.62	4.96	5.42	5.82	6.12	6.56	34.42	34.37	138	0.0003	0.30614487	0.0003610
9-May	10:09	5.60	6.04	6.56	6.99	7.24	7.59	34.01	33.70	151	-0.0071	0.3327001	0.0008149
9-May	10:29	5.60	5.93	6.40	6.85	7.08	7.31	35.05	34.31	144	-0.0261	0.3102823	0.0013139
9-May	10:49	5.46	5.86	6.25	6.62	6.79	7.02	35.71	34.80	151	-0.0391	0.27970239	0.0025916
9-May	11:09	4.70	5.01	5.40	5.59	5.85	6.16	36.29	35.17	133	-0.0556	0.25750051	0.0014970
9-May	11:29	4.71	4.99	5.37	5.60	5.89	6.15	36.88	35.71	118	-0.0597	0.26092497	0.0013517
9-May	11:49	5.35	5.74	6.15	6.51	6.77	7.09	37.07	35.78	142	-0.0453	0.30787917	0.0010562
9-May	12:09	6.06	6.51	6.96	7.44	7.59	7.88	37.56	36.26	111	-0.0417	0.32922772	0.0016414
9-May	12:29	5.83	6.17	6.71	7.02	7.20	7.59	38.17	36.83	142	-0.0459	0.3130894	0.0017166
9-May	13:29	7.72	8.14	8.70	9.34	9.75	10.10	38.36	37.01	166	-0.0253	0.42836595	0.0012455
20-May	10:16	4.00	4.23	4.58	4.82	4.94	5.12	32.65	32.63	128	0.0036	0.18125964	0.0063830
20-May	12:33	5.59	6.16	6.68	7.09	7.50	8.04	31.54	32.77	168	0.0244	0.34367122	0.0006317
20-May	12:53	6.42	6.93	7.44	7.90	8.46	8.86	31.00	32.18	123	0.0237	0.35542346	0.0012320
20-May	13:13	6.60	7.27	7.83	8.30	8.84	9.30	30.20	31.36	110	0.0191	0.39216234	0.0008038
20-May	13:33	6.78	7.37	7.89	8.42	8.97	9.44	29.96	31.15	131	0.0202	0.38822805	0.0009854
20-May	13:53	7.16	7.69	8.34	8.79	9.42	10.04	29.80	31.02	139	0.0176	0.42125126	0.0007749
20-May	20:44	4.95	5.28	5.85	6.28	6.58	7.04	35.28	36.43	140	0.0311	0.2991721	0.0006484
20-May	21:04	5.46	5.88	6.42	6.83	7.30	7.76	34.87	35.96	125	0.0244	0.33210639	0.0006281
20-May	21:24	5.78	6.30	6.89	7.33	7.73	8.27	34.37	35.42	132	0.0201	0.35897925	0.0005764
20-May	22:45	5.05	5.80	6.33	6.80	7.16	7.62	33.07	34.12	118	0.0190	0.3700696	0.0002419
20-May	23:05	5.28	5.95	6.41	6.77	7.33	7.78	32.88	33.95	126	0.0204	0.35585602	0.0003664
20-May	23:25	5.83	6.49	6.95	7.39	8.01	8.34	32.57	33.63	123	0.0201	0.36818276	0.0005386
21-May	2:05	4.26	4.30	4.57	4.97	5.11	6.19	30.60	31.81	91	0.0388	0.28112472	0.0002214
21-May	5:26	4.15	4.52	4.96	5.30	5.70	6.12	28.37	29.65	115	0.0396	0.26939252	0.0004177
21-May	5:46	4.69	5.11	5.66	6.04	6.57	7.10	28.80	30.26	135	0.0300	0.33931592	0.0002151
21-May	15:07	4.27	4.45	4.83	5.08	5.22	5.33	38.53	37.92	173	-0.0543	0.20736812	0.0037177
21-May	15:27	4.03	4.25	4.59	4.79	4.92	5.09	38.27	37.65	149	-0.0554	0.19591263	0.0038579
21-May	15:47	4.30	4.47	4.84	5.04	5.17	5.27	38.35	37.98	164	-0.0366	0.18528545	0.0105375
21-May	16:07	4.03	4.19	4.56	4.81	4.92	5.13	38.59	38.22	125	-0.0284	0.19969222	0.0029801
21-May	21:48	4.20	4.55	5.02	5.43	5.87	6.31	35.21	36.42	133	0.0320	0.29912697	0.0002321
21-May	22:08	4.52	4.88	5.37	5.75	6.23	6.59	34.50	35.64	138	0.0315	0.29724843	0.0003772
21-May	22:28	4.83	5.19	5.71	5.99	6.50	6.81	34.20	35.32	133	0.0339	0.28289995	0.0008134
21-May	22:48	5.32	5.63	6.14	6.57	7.12	7.45	33.84	34.96	119	0.0293	0.3157553	0.0006891
21-May	23:08	5.22	5.67	6.07	6.53	6.99	7.35	33.39	34.50	121	0.0291	0.30514481	0.0008367
21-May	23:48	6.01	6.23	6.35	7.00	7.30	8.12	32.88	33.92	114	0.0279	0.31053695	0.0014413
22-May	0:29	5.64	6.11	6.48	7.02	7.57	7.84	32.17	33.24	97	0.0265	0.32688612	0.0008691
22-May	0:49	5.49	6.10	6.55	7.01	7.53	7.79	31.93	33.02	95	0.0247	0.33715518	0.0006550
22-May	1:09	5.41	6.04	6.50	6.95	7.48	7.63	31.51	32.59	91	0.0263	0.33151119	0.0006798
22-May	1:29	5.17	5.73	6.23	6.58	7.03	7.30	31.17	32.24	93	0.0283	0.30652116	0.0008465
22-May	1:49	4.98	5.57	6.01	6.44	6.95	7.25	30.70	31.76	99	0.0248	0.32907543	0.0004109
22-May	2:09	5.29	5.88	6.35	6.81	7.22	7.63	30.39	31.45	120	0.0233	0.33528367	0.0005329
22-May	2:29	5.04	5.54	5.97	6.45	6.86	7.40	29.97	31.09	130	0.0242	0.33367596	0.0003756
22-May	2:49	4.77	5.23	5.62	6.05	6.40	6.87	29.89	31.02	104	0.0308	0.29078224	0.0006445
22-May	3:09	4.33	4.73	5.16	5.52	5.83	6.29	29.47	30.59	128	0.0351	0.26799619	0.0005823
22-May	3:29	4.06	4.38	4.76	5.07	5.43	5.95	29.55	30.77	109	0.0410	0.25317442	0.0005067
22-May	3:49	4.47	4.83	5.32	5.68	6.10	6.52	29.69	30.92	116	0.0351	0.28674836	0.0004438
22-May	9:10	4.12	4.37	4.72	4.97	5.21	5.38	31.89	31.75	158	-0.0057	0.21431357	0.0020470

		Wind Speeds						Temperatures		Wind			
Date	Time	U(0.75)	U(1.25)	U(2.07)	U(3.44)	U(5.72)	U9(.50)	TL2	TU1	Dir	Ri	U*	Zo
22-May	9:30	4.48	4.79	5.12	5.52	5.77	5.95	32.25	31.99	140	-0.0105	0.25660331	0.0010127
22-May	9:50	4.64	4.91	5.23	5.55	5.76	5.98	32.69	32.36	133	-0.0170	0.23197884	0.0028313
22-May	10:10	4.19	4.40	4.76	4.99	5.15	5.36	33.09	32.71	145	-0.0264	0.20696008	0.0031622
22-May	10:30	4.32	4.56	4.87	5.13	5.29	5.51	33.69	33.30	114	-0.0263	0.20756141	0.0040169
22-May	13:30	4.01	4.17	4.45	4.58	4.78	4.99	37.25	36.57	177	-0.0720	0.17968941	0.0072339
22-May	17:52	5.97	6.32	6.96	7.36	7.72	7.86	40.40	40.74	168	0.0124	0.31077448	0.0019703
22-May	18:12	4.39	4.73	5.12	5.48	5.77	5.97	39.74	40.21	178	0.0235	0.23721407	0.0015234
22-May	18:32	4.22	4.55	5.00	5.35	5.58	5.88	39.07	39.71	151	0.0282	0.24105471	0.0010180
22-May	18:52	4.37	4.80	5.20	5.56	5.90	6.23	38.61	39.44	161	0.0286	0.26364706	0.0007159
22-May	19:12	4.67	5.34	5.84	6.23	6.62	6.88	38.02	39.01	159	0.0239	0.322673	0.0003426
22-May	19:32	5.09	5.83	6.35	6.76	7.20	7.56	37.50	38.50	140	0.0194	0.35889634	0.0003019
22-May	19:52	6.01	6.82	7.48	7.97	8.41	9.03	36.50	37.47	141	0.0126	0.4405538	0.0002334
22-May	20:12	5.51	6.15	6.70	7.23	7.66	8.00	35.92	36.97	150	0.0200	0.36948119	0.0003816
22-May	20:34	4.71	5.12	5.54	5.95	6.38	6.80	35.29	36.43	137	0.0308	0.29439516	0.0005288
22-May	20:54	5.69	6.32	6.78	7.16	7.83	8.31	34.52	35.57	132	0.0182	0.37906222	0.0003695
22-May	21:14	6.64	7.29	7.91	8.48	9.02	9.36	33.88	34.85	142	0.0157	0.41360451	0.0005841
22-May	21:34	8.64	9.31	10.10	10.68	11.46	12.00	33.48	34.43	151	0.0101	0.51578913	0.0007235
22-May	21:54	7.73	8.43	9.03	9.63	10.31	10.85	33.04	34.00	144	0.0118	0.46892521	0.0006628
22-May	22:14	7.44	8.20	8.83	9.30	10.05	10.47	32.80	33.78	137	0.0128	0.45547302	0.0006518
22-May	22:34	6.30	6.89	7.52	8.01	8.52	8.92	32.35	33.31	130	0.0168	0.39180939	0.0005838
22-May	22:54	6.89	7.56	8.16	8.72	9.28	9.75	32.12	33.09	141	0.0143	0.42707267	0.0005947
22-May	23:14	5.47	5.97	6.51	6.98	7.37	7.73	31.93	32.94	129	0.0238	0.33110738	0.0006964
22-May	23:34	5.26	5.74	6.26	6.63	7.14	7.55	31.64	32.64	124	0.0229	0.33102585	0.0005228
22-May	23:54	4.87	5.30	5.83	6.26	6.69	7.02	30.95	31.93	91	0.0256	0.31563338	0.0004353
23-May	2:34	4.42	4.88	5.38	5.82	6.20	6.54	29.28	30.31	96	0.0277	0.30670171	0.0002974
23-May	5:15	4.29	4.81	5.17	5.58	6.02	6.34	27.54	28.58	93	0.0301	0.28946259	0.0003574
23-May	5:35	4.09	4.57	4.95	5.30	5.75	6.06	27.58	28.63	100	0.0329	0.27585649	0.0003557
23-May	6:35	4.26	4.71	5.04	5.34	5.71	6.05	27.97	28.86	99	0.0341	0.24495124	0.0010048
23-May	8:15	4.15	4.57	4.99	5.31	5.56	5.85	30.16	30.48	110	0.0150	0.2532775	0.0006876
23-May	8:35	4.67	5.28	5.78	6.16	6.44	6.70	30.70	30.74	102	0.0028	0.32120479	0.0003479
23-May	8:55	4.36	4.85	5.24	5.60	5.87	6.10	31.34	31.26	123	-0.0008	0.28163227	0.0004946
23-May	9:15	4.34	4.83	5.28	5.48	5.67	5.97	32.07	31.89	135	-0.0051	0.26330242	0.0007835
23-May	9:35	4.69	5.26	5.70	6.00	6.17	6.55	32.27	32.10	150	-0.0036	0.29533118	0.0006120
23-May	9:57	4.79	5.34	5.75	6.06	6.25	6.67	32.66	32.50	154	-0.0032	0.29465802	0.0006935
23-May	10:17	4.95	5.40	5.88	6.33	6.42	6.82	33.12	32.79	129	-0.0087	0.3119499	0.0005691
23-May	10:37	4.81	5.35	5.74	6.13	6.30	6.69	33.44	33.13	127	-0.0080	0.30384138	0.0005857
23-May	11:57	4.49	4.93	5.31	5.69	5.83	6.04	34.75	34.67	161	-0.0009	0.25613483	0.0011321
23-May	12:17	5.61	6.19	6.80	7.26	7.57	7.83	34.86	34.69	153	-0.0025	0.37237689	0.0004176
23-May	12:37	6.00	6.52	7.23	7.56	7.93	8.10	34.76	34.71	179	0.0003	0.35259307	0.0008876
23-May	12:57	5.42	5.95	6.52	6.90	7.20	7.46	34.79	34.84	149	0.0030	0.32670235	0.0007578
23-May	13:17	7.01	7.60	8.25	8.69	9.17	9.56	35.00	35.16	135	0.0038	0.3998667	0.0010525
23-May	13:37	7.63	8.33	8.99	9.47	10.03	10.40	35.82	35.78	139	0.0003	0.44130632	0.0009725
23-May	13:57	8.07	8.75	9.34	9.97	10.43	10.73	37.27	36.65	146	-0.0088	0.45458181	0.0012068
23-May	14:17	6.58	7.06	7.60	8.12	8.50	8.73	38.08	37.48	165	-0.0130	0.3777387	0.0010302
23-May	14:57	7.06	7.66	8.20	8.87	9.27	9.53	38.50	37.69	153	-0.0136	0.43401039	0.0006577
23-May	15:17	6.30	6.84	7.38	7.81	8.25	8.33	38.45	37.82	145	-0.0154	0.36659824	0.0009847
23-May	15:57	5.40	5.89	6.33	6.65	6.98	7.07	39.72	39.16	181	-0.0198	0.29927496	0.0014498

KIT FOX: MAST 2
DATA FOR NORTHERLY WINDS

		Wind Speeds				Temperatures		Wind			
Date	Time	U(1.0)	U(2.11)	U(4.49)	U(9.50)	TL2	TU1	Dir	Ri	U*	Zo
7-May	1:36	4.60	5.18	5.52	6.23	34.73	35.38	0	0.0264	0.25647176	0.0006397
9-May	12:49	7.24	8.19	8.59	9.31	38.44	36.90	54	-0.0328	0.40531522	0.0007556
9-May	13:09	6.44	7.22	7.60	8.37	37.49	36.42	54	-0.0263	0.37227744	0.0005680
9-May	13:49	8.40	9.42	9.94	10.80	38.25	37.03	53	-0.0198	0.45827377	0.0008743
9-May	14:09	7.92	8.99	9.33	10.10	38.62	37.38	54	-0.0194	0.41734567	0.0011701
9-May	14:29	8.44	9.46	9.93	10.93	38.73	37.45	54	-0.0213	0.47549935	0.0006762
9-May	14:49	9.86	10.98	11.45	12.73	38.88	37.53	53	-0.0181	0.54551634	0.0007388
9-May	15:09	10.51	11.77	12.54	14.01	38.63	37.36	55	-0.0125	0.65827348	0.0003125
9-May	15:30	10.18	11.44	12.07	13.37	38.20	37.02	53	-0.0114	0.59580115	0.0005027
9-May	15:50	10.05	11.19	11.89	13.06	38.03	36.96	53	-0.0120	0.56482113	0.0006665
9-May	16:10	9.76	10.95	11.49	12.71	38.01	37.16	53	-0.0102	0.54862801	0.0006654
9-May	16:30	8.49	9.52	9.91	11.05	38.33	37.75	53	-0.0084	0.47408274	0.0006813
9-May	16:50	8.29	9.24	9.43	10.84	37.88	37.38	53	-0.0070	0.48208816	0.0004622
9-May	17:10	7.23	8.21	8.40	9.60	37.36	36.81	53	-0.0092	0.44512565	0.0003376
9-May	17:30	7.01	7.96	8.33	9.21	35.41	35.07	54	-0.0048	0.40169895	0.0005855
9-May	17:50	8.14	9.17	9.65	10.67	34.52	34.35	54	-0.0016	0.45442776	0.0006832
9-May	18:10	8.31	9.29	10.00	11.07	34.44	34.25	54	-0.0020	0.50112495	0.0003907
9-May	18:30	8.53	9.56	10.14	11.17	33.94	33.67	54	-0.0029	0.47902181	0.0006565
9-May	18:50	8.28	9.36	9.88	10.97	32.95	33.04	54	0.0020	0.46803791	0.0006103
9-May	19:10	9.64	10.81	11.36	12.65	31.92	32.11	54	0.0029	0.52160279	0.0008196
9-May	19:30	9.74	11.03	11.65	12.99	30.88	30.95	54	0.0013	0.56732493	0.0004918
9-May	19:50	10.40	11.70	12.48	13.80	29.91	29.96	54	0.0009	0.59658868	0.0005477
9-May	20:10	8.73	9.81	10.38	11.73	29.24	29.32	55	0.0016	0.52514061	0.0003773
9-May	20:30	8.45	9.53	9.99	11.28	28.64	28.74	55	0.0019	0.49362451	0.0004649
9-May	20:50	8.30	9.44	9.99	11.06	28.07	28.17	54	0.0022	0.47999825	0.0005287
9-May	21:10	7.57	8.60	9.12	10.24	27.71	27.84	55	0.0027	0.46311609	0.0003499
9-May	21:30	7.09	8.06	8.56	9.56	27.28	27.40	55	0.0029	0.4280074	0.0003868
9-May	21:50	6.68	7.67	8.03	9.13	26.60	26.71	55	0.0032	0.42406692	0.0002742
9-May	22:51	6.50	7.45	7.80	8.82	25.34	25.43	56	0.0031	0.40146617	0.0003298
9-May	23:11	7.59	8.51	9.08	10.26	24.72	24.80	56	0.0022	0.46706031	0.0003228
9-May	23:31	7.97	8.95	9.64	10.64	24.34	24.42	55	0.0020	0.46801351	0.0004634
9-May	23:51	8.75	9.76	10.30	11.57	23.75	23.81	55	0.0015	0.49412188	0.0005813
10-May	0:11	7.46	8.33	8.96	10.02	23.34	23.41	56	0.0019	0.44935507	0.0003756
10-May	0:31	6.98	7.80	8.11	9.30	23.06	23.13	56	0.0019	0.40920105	0.0004271
10-May	0:51	6.43	7.23	7.55	8.71	22.83	22.92	56	0.0023	0.40108764	0.0002837
10-May	1:11	7.89	8.87	9.13	10.43	22.68	22.76	56	0.0016	0.4480299	0.0005441
10-May	1:31	8.41	9.41	9.70	10.96	22.33	22.35	56	0.0010	0.44932962	0.0008624
10-May	1:51	8.20	9.30	9.57	10.86	22.14	22.16	56	0.0011	0.46785707	0.0005460
10-May	2:11	7.27	8.19	8.55	9.70	22.12	22.17	56	0.0017	0.42515637	0.0004550
10-May	2:31	6.81	7.65	8.04	9.09	22.16	22.23	56	0.0028	0.39659036	0.0004692
10-May	2:51	6.59	7.38	7.80	8.82	21.91	22.00	56	0.0027	0.38867959	0.0004268
10-May	3:11	5.92	6.66	6.97	7.87	21.71	21.81	57	0.0035	0.33774662	0.0005448
10-May	3:31	4.97	5.74	5.98	6.79	21.60	21.71	57	0.0050	0.31220343	0.0002971
10-May	3:51	5.05	5.81	6.02	6.73	21.45	21.55	57	0.0045	0.28901934	0.0005696
10-May	4:11	5.26	5.95	6.31	7.12	21.25	21.33	57	0.0040	0.32105168	0.0003484
10-May	4:31	5.78	6.47	6.85	7.61	21.45	21.48	57	0.0020	0.3189755	0.0007090
10-May	4:52	6.23	7.03	7.39	8.31	21.61	21.63	57	0.0017	0.36278271	0.0004803
10-May	5:12	5.64	6.41	6.77	7.66	21.64	21.65	57	0.0017	0.35236249	0.0003008
10-May	5:32	5.47	6.13	6.47	7.27	21.56	21.55	57	0.0012	0.3153164	0.0005081
10-May	5:52	5.65	6.45	6.81	7.67	21.40	21.39	56	0.0013	0.35270598	0.0003081
10-May	6:12	5.43	6.09	6.39	7.28	21.24	21.24	57	0.0017	0.32475743	0.0003832
10-May	6:32	5.74	6.49	6.81	7.58	21.18	21.17	57	0.0012	0.32113209	0.0006545
10-May	6:52	5.19	5.85	6.09	6.90	21.26	21.14	57	-0.0016	0.30876076	0.0004156
10-May	7:12	5.41	6.10	6.41	7.16	21.81	21.54	57	-0.0059	0.32121793	0.0004439
10-May	7:32	5.58	6.27	6.64	7.38	21.78	21.50	57	-0.0048	0.32930101	0.0004618
10-May	7:52	5.83	6.51	6.99	7.77	21.50	21.36	57	-0.0019	0.35178193	0.0003852
10-May	8:12	5.82	6.52	6.89	7.53	22.49	22.14	57	-0.0082	0.31674081	0.0008551
10-May	8:32	5.82	6.54	6.82	7.50	23.24	22.58	56	-0.0157	0.31678491	0.0008662
10-May	8:52	5.84	6.61	6.92	7.59	23.80	22.99	56	-0.0194	0.33299981	0.0006351
10-May	9:12	5.55	6.29	6.52	7.08	23.80	23.08	57	-0.0213	0.29349387	0.0011334
10-May	9:32	5.69	6.38	6.61	7.33	23.74	23.13	57	-0.0176	0.31093782	0.0008247
10-May	9:52	5.54	6.20	6.39	6.88	24.65	23.78	56	-0.0392	0.26546288	0.0025516
10-May	10:52	4.77	5.36	5.46	5.97	26.30	25.06	56	-0.0782	0.25072574	0.0012289
10-May	11:12	4.35	4.84	4.96	5.41	26.57	25.46	56	-0.0814	0.22122739	0.0015761
10-May	11:33	4.65	5.22	5.36	5.83	27.07	25.84	56	-0.0810	0.24636583	0.0011745
10-May	11:53	4.88	5.37	5.63	6.16	27.47	26.05	56	-0.0715	0.26407045	0.0009412

		Wind Speeds				Temperatures		Wind			
Date	Time	U(1.0)	U(2.11)	U(4.49)	U(9.50)	TL2	TU1	Dir	Ri	U*	Zo
10-May	12:13	4.96	5.48	5.67	6.19	27.85	26.55	56	-0.0831	0.25658819	0.0013601
10-May	12:33	5.06	5.60	5.76	6.32	28.41	27.03	56	-0.0701	0.25941444	0.0014279
10-May	12:53	4.73	5.27	5.46	6.01	29.16	27.63	55	-0.0923	0.26989338	0.0006630
10-May	13:13	5.00	5.51	5.69	6.24	29.36	27.82	55	-0.1002	0.26403486	0.0011585
10-May	13:33	5.36	5.90	6.10	6.63	29.50	28.07	55	-0.0669	0.25986535	0.0022596
10-May	13:53	5.85	6.41	6.69	7.27	29.93	28.31	55	-0.0654	0.29043412	0.0018369
10-May	14:13	6.27	6.99	7.32	7.85	30.42	28.92	55	-0.0464	0.31646871	0.0016798
10-May	14:33	7.09	7.84	8.26	8.96	31.08	29.46	55	-0.0360	0.36761229	0.0012865
10-May	14:53	7.04	7.92	8.20	9.01	30.43	29.04	55	-0.0322	0.38389079	0.0008823
10-May	15:13	8.42	9.50	10.00	11.00	30.67	29.43	55	-0.0180	0.48941582	0.0005469
10-May	15:33	9.43	10.64	11.21	12.21	31.01	29.66	55	-0.0164	0.52663451	0.0007374
10-May	15:53	8.54	9.64	10.16	11.21	31.13	29.92	55	-0.0170	0.50535725	0.0004801
10-May	16:13	9.84	11.02	11.55	12.66	31.14	30.22	55	-0.0101	0.52433417	0.0010021
10-May	16:33	9.97	11.17	11.81	13.01	30.82	30.23	54	-0.0059	0.55844838	0.0006771
10-May	16:53	10.43	11.65	12.44	13.50	30.97	30.39	54	-0.0051	0.56592367	0.0008686
10-May	17:13	10.27	11.44	12.35	13.68	30.21	29.69	56	-0.0042	0.62785039	0.0003571
10-May	17:33	10.06	11.21	12.04	13.25	29.58	29.17	55	-0.0040	0.58528609	0.0005063
10-May	17:53	9.05	10.31	10.96	12.13	28.96	28.49	55	-0.0047	0.5631441	0.0003358
20-May	10:53	5.21	5.92	6.08	6.88	33.93	35.23	0	0.0473	0.24588021	0.0023848
20-May	11:13	5.48	6.21	6.47	7.19	33.52	34.80	0	0.0246	0.26985874	0.0017515
20-May	11:33	5.82	6.74	7.04	7.83	32.88	34.13	42	0.0188	0.32523169	0.0006895
20-May	11:53	5.70	6.47	6.85	7.61	32.12	33.33	35	0.0252	0.30107777	0.0010088
20-May	12:18	4.41	4.98	5.04	5.53	36.08	35.63	36	-0.0367	0.22284303	0.0015927
20-May	14:13	6.78	7.76	8.22	9.20	30.38	31.68	0	0.0237	0.38340177	0.0006107
20-May	14:33	4.49	5.16	5.41	6.13	30.77	32.04	0	0.0506	0.23820236	0.0009561
20-May	17:35	4.18	4.82	5.01	5.72	27.95	29.34	56	0.0550	0.22133066	0.0009583
20-May	23:45	5.25	6.02	6.28	6.90	32.60	33.66	42	0.0293	0.25747164	0.0018995
21-May	0:05	4.72	5.34	5.51	6.21	32.21	33.25	0	0.0431	0.22161207	0.0024986
21-May	2:25	4.72	5.39	5.69	6.46	30.25	31.53	43	0.0402	0.26059571	0.0006987
21-May	2:45	4.85	5.43	5.75	6.51	30.19	31.45	0	0.0404	0.24932074	0.0011492
21-May	3:25	4.73	5.43	5.57	6.46	29.43	30.66	0	0.0404	0.2613155	0.0006637
21-May	4:26	4.47	5.21	5.37	6.06	28.73	29.97	0	0.0492	0.23310586	0.0011279
21-May	5:06	4.43	4.93	5.24	6.04	28.50	29.75	42	0.0425	0.24239117	0.0006739
21-May	23:28	5.16	5.95	6.27	7.11	32.89	33.98	0	0.0312	0.30044956	0.0004907
22-May	0:08	5.99	6.85	7.17	7.91	32.69	33.78	0	0.0289	0.29915782	0.0016158
23-May	1:54	4.40	5.08	5.31	6.00	29.60	30.66	43	0.0382	0.24107939	0.0007643
23-May	2:14	4.59	5.25	5.44	6.19	29.33	30.37	0	0.0291	0.24899446	0.0007938
23-May	4:55	5.00	5.73	5.95	6.57	27.62	28.67	0	0.0248	0.24853061	0.0016833
23-May	5:55	4.67	5.35	5.51	6.12	27.58	28.62	0	0.0358	0.22120567	0.0024712
23-May	6:15	4.93	5.57	5.82	6.55	27.60	28.58	0	0.0277	0.25292041	0.0012154
23-May	6:55	4.47	5.14	5.29	5.94	28.17	29.00	0	0.0385	0.2221652	0.0016272
23-May	7:55	4.40	4.97	5.19	5.72	29.69	30.35	0	0.0420	0.19684453	0.0040344

KIT FOX: MAST 2
DATA FOR SOUTHERLY WIND DIRECTIONS

		Wind Speeds				Temperatures		Wind			
Date	Time	U(1.0)	U(2.11)	U(4.49)	U(9.50)	TL2	TU1	Dir	Ri	U*	Zo
5-May	16:07	4.02	4.42	4.55	5.00	42.01	41.33	163	-0.0533	0.19778580	0.0012821
6-May	14:34	4.34	4.80	4.88	5.41	42.04	41.17	123	-0.0709	0.22281900	0.0009162
6-May	15:34	4.11	4.71	4.74	5.29	42.59	41.84	132	-0.0447	0.23917224	0.0003725
6-May	15:54	4.26	4.82	4.89	5.40	42.58	41.85	135	-0.0462	0.22948855	0.0006541
6-May	16:54	4.22	4.76	4.85	5.47	41.84	41.48	140	-0.0171	0.23931908	0.0004086
6-May	17:34	4.47	5.18	5.43	6.11	41.74	41.65	157	-0.0015	0.29422833	0.0001555
6-May	17:54	4.96	5.65	5.96	6.61	42.02	41.88	142	-0.0027	0.29847085	0.0002778
6-May	18:14	5.18	5.92	6.21	6.89	42.28	42.10	145	-0.0040	0.31111435	0.0002846
6-May	18:34	5.10	5.78	6.00	6.77	42.11	42.15	164	0.0033	0.28925798	0.0003874
6-May	18:54	4.92	5.61	5.87	6.51	41.49	41.79	144	0.0121	0.26387925	0.0006126
6-May	19:14	4.22	4.84	5.10	5.84	40.90	41.35	135	0.0162	0.26454266	0.0001954
7-May	2:36	4.22	4.79	5.09	5.75	33.08	33.70	97	0.0260	0.24059893	0.0003719
7-May	19:21	5.68	6.38	6.73	7.58	41.89	42.37	167	0.0137	0.31383050	0.0004595
8-May	2:23	4.36	5.00	5.17	5.93	33.87	34.55	95	0.0252	0.24829978	0.0003695
8-May	15:05	4.24	4.83	4.85	5.30	42.08	40.92	153	-0.0929	0.22954124	0.0006762
8-May	17:25	4.80	5.46	5.70	6.29	42.82	42.64	153	-0.0053	0.27271912	0.0004209
8-May	17:45	4.29	4.87	5.03	5.52	42.98	42.68	158	-0.0151	0.23223296	0.0006181
9-May	8:08	4.96	5.63	5.88	6.65	31.75	32.03	120	0.0091	0.28455085	0.0003566
9-May	8:49	4.65	5.27	5.50	6.26	32.84	33.04	96	0.0113	0.26889124	0.0003311
9-May	9:49	4.77	5.45	5.80	6.54	34.42	34.37	138	0.0003	0.31090667	0.0001570
9-May	10:09	5.99	6.67	7.11	7.80	34.01	33.70	151	-0.0071	0.33516795	0.0004558
9-May	10:29	5.74	6.42	6.75	7.36	35.05	34.31	144	-0.0261	0.31258410	0.0005941
9-May	10:49	5.48	6.19	6.43	6.99	35.71	34.80	151	-0.0391	0.29822819	0.0006242
9-May	11:09	4.98	5.57	5.81	6.27	36.29	35.17	133	-0.0556	0.26088216	0.0008459
9-May	11:29	4.74	5.36	5.51	6.07	36.88	35.71	118	-0.0597	0.27045129	0.0004423
9-May	11:49	5.41	6.08	6.30	6.79	37.07	35.78	142	-0.0453	0.27581603	0.0010453
9-May	12:09	6.04	6.76	7.06	7.70	37.56	36.26	111	-0.0417	0.32834007	0.0006167
9-May	12:29	5.95	6.78	7.04	7.75	38.17	36.83	142	-0.0459	0.35858568	0.0003039
9-May	13:29	7.89	8.83	9.28	10.12	38.36	37.01	166	-0.0253	0.42959538	0.0005947
20-May	10:16	4.05	4.60	4.61	5.03	32.65	32.63	128	0.0036	0.17462012	0.0038490
20-May	12:33	6.04	6.91	7.26	8.08	31.54	32.77	168	0.0244	0.32231503	0.0006345
20-May	12:53	6.64	7.48	7.80	8.69	31.00	32.18	123	0.0237	0.32449533	0.0012266
20-May	13:13	6.72	7.71	8.14	9.12	30.20	31.36	110	0.0191	0.38679082	0.0003628
20-May	13:33	7.09	8.11	8.58	9.54	29.96	31.15	131	0.0202	0.39360805	0.0004738
20-May	13:53	7.47	8.53	9.06	10.04	29.80	31.02	139	0.0176	0.41754200	0.0004522
20-May	20:44	5.22	5.97	6.21	7.15	35.28	36.43	140	0.0311	0.29883260	0.0003511
20-May	21:04	5.88	6.77	7.12	8.07	34.87	35.96	125	0.0244	0.34571734	0.0003075
20-May	21:24	6.19	7.07	7.48	8.49	34.37	35.42	132	0.0201	0.36942835	0.0002726
20-May	22:45	5.74	6.60	6.97	7.70	33.07	34.12	118	0.0190	0.31701591	0.0005034
20-May	23:05	5.82	6.61	7.01	7.86	32.88	33.95	126	0.0204	0.32729312	0.0004180
20-May	23:25	6.27	7.15	7.56	8.38	32.57	33.63	123	0.0201	0.33914400	0.0005741
21-May	2:05	4.82	5.46	5.61	6.74	30.60	31.81	91	0.0388	0.29813028	0.0001819
21-May	5:26	4.46	5.03	5.43	6.13	28.37	29.65	115	0.0396	0.25216318	0.0003867
21-May	5:46	4.82	5.54	6.00	6.96	28.80	30.26	135	0.0300	0.33335322	0.0001042
21-May	15:07	4.50	4.99	5.01	5.51	38.53	37.92	173	-0.0543	0.20794203	0.0021774
21-May	15:27	4.29	4.74	4.82	5.25	38.27	37.65	149	-0.0554	0.19486189	0.0026105
21-May	15:47	4.37	4.80	4.90	5.29	38.35	37.98	164	-0.0366	0.18109978	0.0060417
21-May	16:07	4.09	4.56	4.54	5.05	38.59	38.22	125	-0.0284	0.19287407	0.0017160
21-May	21:48	4.61	5.29	5.48	6.30	35.21	36.42	133	0.0320	0.26082763	0.0003852
21-May	22:08	4.77	5.44	5.78	6.51	34.50	35.64	138	0.0315	0.26816411	0.0004175
21-May	22:28	5.25	6.01	6.30	7.13	34.20	35.32	133	0.0339	0.28715205	0.0005087
21-May	22:48	5.46	6.28	6.68	7.60	33.84	34.96	119	0.0293	0.33222483	0.0002412
21-May	23:08	5.46	6.32	6.64	7.65	33.39	34.50	121	0.0291	0.34040107	0.0002030
21-May	23:48	6.26	7.12	7.51	8.57	32.88	33.92	114	0.0279	0.36084140	0.0003383
22-May	0:29	5.84	6.63	6.93	7.64	32.17	33.24	97	0.0265	0.28255791	0.0013885
22-May	0:49	5.67	6.43	6.79	7.43	31.93	33.02	95	0.0247	0.27899384	0.0012222
22-May	1:09	5.85	6.62	7.07	7.88	31.51	32.59	91	0.0263	0.31933384	0.0005199
22-May	1:29	5.70	6.43	6.85	7.56	31.17	32.24	93	0.0283	0.29072711	0.0008860
22-May	1:49	5.49	6.20	6.55	7.24	30.70	31.76	99	0.0248	0.27637074	0.0009859
22-May	2:09	5.51	6.33	6.67	7.42	30.39	31.45	120	0.0233	0.30319952	0.0005092
22-May	2:29	5.28	6.08	6.41	7.36	29.97	31.09	130	0.0242	0.32912723	0.0002028
22-May	2:49	4.96	5.72	6.01	6.92	29.89	31.02	104	0.0308	0.30295174	0.0002305
22-May	3:09	4.59	5.24	5.50	6.33	29.47	30.59	128	0.0351	0.26551397	0.0003258
22-May	3:29	4.32	5.06	5.17	6.03	29.55	30.77	109	0.0410	0.25800944	0.0002653
22-May	3:49	4.69	5.42	5.58	6.49	29.69	30.92	116	0.0351	0.27607027	0.0002880
22-May	9:10	4.29	4.84	4.97	5.40	31.89	31.75	158	-0.0057	0.20473972	0.0016540

		Wind Speeds				Temperatures		Wind			
Date	Time	U(1.0)	U(2.11)	U(4.49)	U(9.50)	TL2	TU1	Dir	Ri	U*	Zo
22-May	9:30	4.83	5.45	5.53	6.07	32.25	31.99	140	-0.0105	0.23338009	0.0014684
22-May	9:50	4.68	5.30	5.38	5.96	32.69	32.36	133	-0.0170	0.24472434	0.0007805
22-May	10:10	4.20	4.77	4.84	5.34	33.09	32.71	145	-0.0264	0.22238591	0.0007315
22-May	10:30	4.39	4.95	5.06	5.43	33.69	33.30	114	-0.0263	0.20378575	0.0022402
22-May	13:30	3.99	4.45	4.37	4.87	37.25	36.57	177	-0.0720	0.19450931	0.0013286
22-May	17:52	6.10	6.91	7.16	8.09	40.40	40.74	168	0.0124	0.33061779	0.0005349
22-May	18:12	4.63	5.26	5.42	6.17	39.74	40.21	178	0.0235	0.24526129	0.0006251
22-May	18:32	4.37	4.91	5.19	5.90	39.07	39.71	151	0.0282	0.23934906	0.0004778
22-May	18:52	4.53	5.14	5.42	6.09	38.61	39.44	161	0.0286	0.24271599	0.0005918
22-May	19:12	5.14	5.74	6.04	6.84	38.02	39.01	159	0.0239	0.27025857	0.0006452
22-May	19:32	5.52	6.13	6.40	7.33	37.50	38.50	140	0.0194	0.29521147	0.0005428
22-May	19:52	6.84	7.73	8.12	9.15	36.50	37.47	141	0.0126	0.38278990	0.0004245
22-May	20:12	6.31	7.14	7.44	8.57	35.92	36.97	150	0.0200	0.36563349	0.0003153
22-May	20:34	5.04	5.78	6.16	7.07	35.29	36.43	137	0.0308	0.31401052	0.0002015
22-May	20:54	6.03	6.83	7.35	8.21	34.52	35.57	132	0.0182	0.35440349	0.0003062
22-May	21:14	7.09	7.94	8.54	9.39	33.88	34.85	142	0.0157	0.37903052	0.0006099
22-May	21:34	9.07	10.17	10.83	12.10	33.48	34.43	151	0.0101	0.50899781	0.0004162
22-May	21:54	8.30	9.41	9.92	11.19	33.04	34.00	144	0.0118	0.48046835	0.0003358
22-May	22:14	7.92	8.98	9.50	10.72	32.80	33.78	137	0.0128	0.46371440	0.0003101
22-May	22:34	6.25	7.08	7.51	8.51	32.35	33.31	130	0.0168	0.36842116	0.0002924
22-May	22:54	7.23	8.15	8.48	9.53	32.12	33.09	141	0.0143	0.37849954	0.0006966
22-May	23:14	5.52	6.18	6.52	7.45	31.93	32.94	129	0.0238	0.30773430	0.0004117
22-May	23:34	5.98	6.78	7.24	8.12	31.64	32.64	124	0.0229	0.34062225	0.0003791
22-May	23:54	5.47	6.18	6.58	7.47	30.95	31.93	91	0.0256	0.31556006	0.0003351
23-May	2:34	4.83	5.45	5.71	6.42	29.28	30.31	96	0.0277	0.24814837	0.0008054
23-May	5:15	4.65	5.36	5.60	6.23	27.54	28.58	93	0.0301	0.24500529	0.0007091
23-May	5:35	4.59	5.25	5.43	6.12	27.58	28.63	100	0.0329	0.23487365	0.0008497
23-May	6:35	4.37	5.05	5.22	5.86	27.97	28.86	99	0.0341	0.22820641	0.0007469
23-May	8:15	4.51	5.05	5.27	5.68	30.16	30.48	110	0.0150	0.19308097	0.0042024
23-May	8:35	5.12	5.79	6.05	6.56	30.70	30.74	102	0.0028	0.25080908	0.0012918
23-May	8:55	4.94	5.56	5.80	6.25	31.34	31.26	123	-0.0008	0.23525909	0.0016654
23-May	9:15	4.82	5.42	5.63	6.05	32.07	31.89	135	-0.0051	0.22676532	0.0018979
23-May	9:35	5.03	5.63	5.92	6.40	32.27	32.10	150	-0.0036	0.24994321	0.0011683
23-May	9:57	5.12	5.79	6.00	6.51	32.66	32.50	154	-0.0032	0.25328040	0.0012266
23-May	10:17	5.35	6.02	6.16	6.79	33.12	32.79	129	-0.0087	0.26779599	0.0010837
23-May	10:37	5.13	5.76	6.00	6.55	33.44	33.13	127	-0.0080	0.26242412	0.0009290
23-May	11:57	4.65	5.31	5.44	6.12	34.75	34.67	161	-0.0009	0.26418806	0.0003962
23-May	12:17	6.08	6.85	7.04	7.78	34.86	34.69	153	-0.0025	0.30785586	0.0009649
23-May	12:37	6.53	7.34	7.53	8.33	34.76	34.71	179	0.0003	0.31681713	0.0013188
23-May	12:57	5.83	6.60	6.85	7.51	34.79	34.84	149	0.0030	0.29125370	0.0010783
23-May	13:17	7.08	7.96	8.32	9.19	35.00	35.16	135	0.0038	0.36355495	0.0008401
23-May	13:37	7.80	8.69	9.23	10.18	35.82	35.78	139	0.0003	0.41901893	0.0005828
23-May	13:57	8.28	9.24	9.79	10.79	37.27	36.65	146	-0.0088	0.46612167	0.0004375
23-May	14:17	7.03	7.82	8.06	8.94	38.08	37.48	165	-0.0130	0.35902023	0.0008987
23-May	14:57	7.57	8.37	8.79	9.75	38.50	37.69	153	-0.0136	0.41084077	0.0005586
23-May	15:17	6.85	7.60	7.98	8.83	38.45	37.82	145	-0.0154	0.37406112	0.0005433
23-May	15:57	5.78	6.42	6.69	7.26	39.72	39.16	181	-0.0198	0.28179537	0.0013933

GOLDEN CANYON: MAST 1
DATA FOR NORTHERLY WINDS

		Wind Speeds								Wind			
Date	Time	U(0.75)	U(1.25)	U(2.07)	U(3.44)	U(5.72)	U(9.5)	TL1	TU2	Dir	Ri	U*	Zo
1-Apr	30-3:50	4.88	5.36	5.97	6.42	6.71	7.00	26.63	26.28	17	-0.007	0.3631709	0.0034523
4-Apr	21:38	4.45	4.78	5.33	5.81	6.18	6.46	31.65	31.47	19	-0.003	0.3449121	0.0025065
4-Apr	23:40	4.20	4.45	4.97	5.33	5.63	5.84	29.57	29.42	37	-0.004	0.2856504	0.0051657
5-Apr	0:00	4.59	4.89	5.43	5.92	6.37	6.45	29.29	29.14	50	-0.003	0.3381664	0.0032176
5-Apr	0:20	4.88	5.14	5.75	6.20	6.52	6.62	29.10	28.89	56	-0.006	0.3226048	0.0061234
5-Apr	0:40	4.78	4.96	5.62	6.03	6.32	6.62	28.94	28.71	41	-0.006	0.3275813	0.0046819
5-Apr	1:20	4.02	4.09	4.77	5.15	5.43	5.68	28.52	28.36	49	-0.004	0.3062774	0.0024305
7-Apr	2:14	4.27	4.54	5.05	5.48	5.83	6.13	28.72	28.93	50	0.009	0.3211229	0.0027777
9-Apr	21:54	4.46	4.87	5.45	6.00	6.32	6.47	35.06	35.28	49	0.008	0.3586732	0.0021324
9-Apr	22:14	4.45	4.79	5.39	5.88	6.27	6.44	34.69	34.84	49	0.006	0.3512855	0.0022540
9-Apr	22:34	5.26	5.63	6.26	6.78	7.20	7.40	34.48	34.55	49	0.003	0.3705666	0.0041610
9-Apr	22:54	4.14	4.54	5.03	5.53	5.78	5.83	34.66	35.15	57	0.022	0.3292454	0.0023058
10-Apr	22:02	4.22	4.56	5.09	5.62	5.83	6.09	34.84	35.00	51	0.007	0.3253425	0.0025863
11-Apr	4:24	4.33	4.66	5.26	5.81	6.22	6.32	31.24	31.68	62	0.014	0.3751348	0.0014117
11-Apr	5:04	4.53	4.89	5.43	6.03	6.47	6.65	30.94	31.31	53	0.011	0.3834633	0.0015599
11-Apr	5:24	4.28	4.63	5.18	5.68	6.01	6.09	30.86	31.35	59	0.019	0.3474518	0.0019953
11-Apr	5:44	4.87	5.23	5.82	6.27	6.79	6.95	30.55	30.77	55	0.007	0.3670256	0.0028345
12-Apr	4:10	4.75	5.11	5.73	6.21	6.58	6.76	33.15	33.06	56	-0.001	0.3491820	0.0033770
12-Apr	4:30	5.02	5.39	5.98	6.36	6.69	7.01	32.76	32.58	21	-0.003	0.3336989	0.0061781
12-Apr	4:52	6.01	6.60	7.38	7.87	8.33	8.71	32.69	32.45	26	-0.003	0.4499954	0.0032705
12-Apr	5:12	5.54	5.99	6.62	7.19	7.52	7.71	32.34	32.09	17	-0.005	0.3834892	0.0049595
12-Apr	9:12	4.82	5.24	5.77	6.18	6.48	6.69	31.68	30.54	2	-0.035	0.3413242	0.0046907
12-Apr	9:32	4.19	4.55	5.00	5.29	5.62	5.79	32.24	30.88	22	-0.058	0.2984313	0.0046168
12-Apr	9:52	4.25	4.55	5.00	5.38	5.71	5.86	32.57	31.06	5	-0.064	0.3114379	0.0037602
12-Apr	10:12	4.05	4.35	4.76	5.05	5.32	5.50	32.81	31.23	0	-0.082	0.2778344	0.0057202
12-Apr	10:32	4.22	4.51	4.92	5.24	5.53	5.74	33.32	31.61	15	-0.081	0.2904531	0.0054669
12-Apr	11:54	4.04	4.31	4.72	5.11	5.33	5.62	35.05	32.99	38	-0.091	0.3032283	0.0033121
12-Apr	22:56	4.18	4.48	5.00	5.61	5.99	6.08	31.06	31.47	53	0.015	0.3634212	0.0013536
12-Apr	23:16	4.22	4.51	4.94	5.40	5.58	5.80	31.73	31.87	0	0.009	0.2771119	0.0063594
13-Apr	11:20	4.27	4.62	5.02	5.40	5.72	5.93	33.45	31.24	19	-0.089	0.3192523	0.0035079
13-Apr	12:20	4.64	5.07	5.56	5.97	6.25	6.49	34.22	31.88	49	-0.076	0.3496649	0.0034710
14-Apr	2:24	4.22	4.53	5.04	5.58	5.92	6.22	27.34	27.28	54	0.000		
14-Apr	2:44	4.45	4.76	5.19	5.71	6.01	6.21	27.91	28.12	0	0.010	0.3125978	0.0041538
25-Apr	21:39	4.13	4.58	5.14	5.52	5.86	6.11	21.19	20.20	15	-0.028	0.3523064	0.0017922

GOLDEN CANYON: MAST 1
DATA FOR SOUTHERLY WINDS

		Wind Speeds						Temperatures		Wind			
Date	Time	U(0.75)	U(1.25)	U(2.07)	U(3.44)	U(5.72)	U(9.50)	TL1	TU2	Dir	Ri	U*	Zo
2-Apr	23:46	4.54	4.78	5.31	5.76	6.29	6.58	26.17	26.07	130	-0.001	0.36306112	0.0018976
3-Apr	0:06	4.27	4.50	4.97	5.52	6.03	6.50	25.82	25.72	150	-0.001	0.36926039	0.0012690
3-Apr	0:26	6.10	6.53	7.14	7.77	8.43	8.85	25.98	25.74	140	-0.003	0.47859990	0.0022065
3-Apr	0:46	6.96	7.35	8.11	8.89	9.55	9.90	25.56	25.21	140	-0.004	0.55027931	0.0020709
3-Apr	1:06	7.20	7.59	8.39	9.03	9.85	10.19	25.22	24.87	136	-0.004	0.55227084	0.0024097
3-Apr	1:26	6.49	6.83	7.58	8.24	8.88	9.32	24.90	24.54	135	-0.004	0.50794829	0.0021793
3-Apr	1:46	6.32	6.69	7.39	7.99	8.70	9.22	24.58	24.22	141	-0.004	0.49623269	0.0021577
3-Apr	2:06	5.19	5.39	6.01	6.57	7.05	7.54	24.38	24.05	131	-0.006	0.40716363	0.0020859
3-Apr	2:46	5.07	5.25	5.93	6.34	6.94	7.23	23.87	23.56	119	-0.006	0.40370326	0.0019243
3-Apr	3:06	5.66	5.95	6.64	7.17	7.78	8.18	23.42	23.04	133	-0.006	0.45075860	0.0019995
3-Apr	3:26	4.75	4.91	5.57	6.01	6.57	7.03	22.88	22.50	127	-0.007	0.39761943	0.0014967
3-Apr	3:46	4.96	5.05	5.74	6.12	6.70	7.19	22.55	22.20	125	-0.007	0.38613918	0.0020649
3-Apr	4:06	5.66	5.90	6.65	7.10	7.69	8.08	22.41	22.01	129	-0.007	0.43758897	0.0023137
3-Apr	4:26	5.08	5.19	5.87	6.32	6.86	7.34	21.94	21.50	143	-0.009	0.39781861	0.0020377
3-Apr	4:46	4.48	4.56	5.20	5.58	6.16	6.62	21.75	21.36	121	-0.008	0.37416106	0.0014465
3-Apr	7:08	4.00	4.09	4.63	5.09	5.54	5.91	21.57	21.14	135	-0.012	0.34929299	0.0011945
4-Apr	1:32	4.12	4.37	4.90	5.37	5.97	6.60	26.14	26.41	144	0.006	0.38434775	0.0009062
4-Apr	1:52	4.11	4.35	4.87	5.34	5.93	6.30	26.28	26.32	149	0.002	0.37409952	0.0010010
4-Apr	3:34	4.46	4.78	5.26	5.85	6.45	6.96	24.51	24.42	161	-0.001	0.40761861	0.0010129
4-Apr	3:54	5.22	5.50	6.20	6.68	7.29	7.76	24.22	23.94	149	-0.004	0.43679927	0.0015618
4-Apr	4:54	4.13	4.25	4.79	5.25	5.76	6.27	23.44	23.21	140	-0.004	0.35627222	0.0012466
4-Apr	5:14	4.22	4.38	4.97	5.35	5.83	6.29	23.28	23.03	134	-0.005	0.34828573	0.0016183
4-Apr	5:34	4.00	4.07	4.63	5.03	5.43	5.91	23.07	22.80	140	-0.007	0.32344553	0.0017053
8-Apr	10:04	4.66	4.95	5.42	5.81	6.10	6.28	32.14	30.38	170	-0.074	0.33646686	0.0039792
8-Apr	10:24	4.53	4.76	5.21	5.60	5.81	6.02	32.88	31.12	180	-0.087	0.31193110	0.0051639
8-Apr	10:44	4.25	4.47	4.88	5.24	5.39	5.54	33.42	31.58	176	-0.121	0.28875269	0.0057985
11-Apr	9:26	4.45	4.77	5.23	5.64	5.94	6.10	32.70	31.19	175	-0.061	0.34142236	0.0028629
11-Apr	9:46	4.87	5.23	5.65	6.02	6.32	6.50	32.96	31.38	173	-0.065	0.32790476	0.0061339
11-Apr	10:26	4.31	4.61	5.04	5.38	5.53	5.72	34.04	32.26	157	-0.098	0.29833976	0.0053747
11-Apr	14:06	4.03	4.22	4.61	4.87	5.05	5.27	39.85	37.72	168	-0.150	0.25877506	0.0083449
11-Apr	14:46	4.13	4.31	4.72	5.02	5.18	5.36	40.93	38.90	148	-0.144	0.27070928	0.0072152
11-Apr	15:06	4.16	4.37	4.79	5.09	5.30	5.54	41.18	39.20	168	-0.112	0.28021135	0.0060552
11-Apr	15:28	4.34	4.58	5.01	5.28	5.51	5.71	41.59	39.71	148	-0.107	0.28243895	0.0075957
11-Apr	16:48	4.06	4.27	4.62	4.94	5.25	5.42	42.66	41.46	162	-0.068	0.27284381	0.0057563
11-Apr	17:08	4.82	5.06	5.55	5.88	6.26	6.55	42.88	41.57	157	-0.046	0.32430190	0.0056135
11-Apr	17:28	5.17	5.45	6.03	6.40	6.82	7.09	42.67	41.41	141	-0.036	0.36822280	0.0040195
11-Apr	17:48	5.34	5.66	6.24	6.66	7.10	7.47	42.32	41.24	151	-0.025	0.38467791	0.0037431
11-Apr	18:08	5.67	6.03	6.63	7.15	7.64	8.08	42.13	41.25	140	-0.016	0.42374002	0.0029938
11-Apr	18:28	5.78	6.15	6.71	7.17	7.71	7.99	41.65	41.03	122	-0.013	0.40599425	0.0042108
11-Apr	18:48	6.25	6.65	7.28	7.82	8.33	8.81	41.13	40.76	145	-0.005	0.43530220	0.0043637
11-Apr	19:08	5.74	6.15	6.77	7.26	7.78	8.30	40.65	40.49	138	-0.002	0.41763553	0.0034007
11-Apr	19:28	5.86	6.26	6.85	7.35	8.00	8.49	39.99	39.96	118	0.000	0.42487030	0.0032945
11-Apr	19:48	5.43	5.79	6.32	6.79	7.27	7.83	39.38	39.43	132	0.002	0.37243711	0.0046047
11-Apr	20:08	5.66	6.00	6.58	7.02	7.56	8.03	39.02	39.12	135	0.003	0.38587022	0.0046995
11-Apr	20:28	5.85	6.18	6.78	7.14	7.84	8.29	38.82	38.94	134	0.003	0.39939710	0.0045358
11-Apr	20:48	5.10	5.44	6.04	6.45	7.08	7.50	38.50	38.67	123	0.004	0.40097716	0.0021276
11-Apr	21:08	4.66	4.93	5.52	5.98	6.53	7.04	38.11	38.36	148	0.006	0.38944950	0.0015330
11-Apr	22:50	4.09	4.32	4.78	5.20	5.62	6.00	34.77	34.93	144	0.007	0.32068804	0.0021080
11-Apr	23:10	4.84	5.19	5.77	6.19	6.81	7.31	34.69	34.85	142	0.004	0.39757680	0.0017185
21-Apr	8:52	5.30	4.35	5.04	5.74	6.63	7.34	31.19	30.04	174	-0.030	0.61006342	0.0002092
21-Apr	9:32	6.57	6.95	7.67	8.29	8.78	9.47	31.48	30.35	159	-0.015	0.48290239	0.0032485
21-Apr	9:52	5.46	5.73	6.37	6.92	7.30	7.75	32.28	30.90	169	-0.029	0.42021522	0.0025445
21-Apr	10:12	6.17	6.52	7.15	7.79	8.20	8.62	32.70	31.05	177	-0.030	0.45896823	0.0031046
21-Apr	10:32	6.56	7.00	7.63	8.17	8.62	9.19	33.24	31.45	166	-0.028	0.45144512	0.0050201
21-Apr	10:52	7.63	8.19	8.89	9.59	10.27	10.81	33.52	31.81	168	-0.019	0.56069662	0.0033640
21-Apr	11:12	7.80	8.39	9.02	9.74	10.40	10.92	33.50	31.95	164	-0.017	0.54850685	0.0043247
21-Apr	11:32	8.36	8.93	9.70	10.50	11.35	11.82	33.84	32.25	155	-0.014	0.63137411	0.0027960
21-Apr	11:52	8.42	8.95	9.74	10.52	11.31	11.85	34.00	32.43	163	-0.015	0.61466533	0.0033522
21-Apr	12:12	8.28	8.82	9.53	10.21	11.13	11.53	34.13	32.57	154	-0.016	0.59683727	0.0035803
21-Apr	12:32	8.23	8.75	9.40	10.20	11.02	11.32	35.96	33.77	162	-0.025	0.60084692	0.0033596
21-Apr	12:52	9.28	9.98	10.74	11.63	12.44	12.79	36.60	34.09	156	-0.022	0.67349465	0.0036281
21-Apr	13:12	9.19	9.75	10.48	11.29	12.14	12.59	37.00	34.38	151	-0.025	0.63398182	0.0046758
21-Apr	13:32	9.09	9.68	10.43	11.22	12.13	12.42	37.07	34.37	142	-0.027	0.65104312	0.0038038
21-Apr	13:52	7.86	8.36	9.07	9.61	10.44	10.54	37.46	34.82	133	-0.040	0.55800033	0.0041060
21-Apr	14:12	8.23	8.73	9.47	10.00	10.86	11.03	37.88	35.22	111	-0.037	0.56685979	0.0048495
21-Apr	14:32	8.95	9.53	10.26	10.86	11.63	12.01	38.04	35.49	138	-0.030	0.57160440	0.0078204

		Wind Speeds						Temperatures		Wind			
Date	Time	U(0.75)	U(1.25)	U(2.07)	U(3.44)	U(5.72)	U(9.50)	TL1	TU2	Dir	Ri	U*	Zo
21-Apr	14:52	9.83	10.56	11.26	11.98	13.02	13.50	37.97	35.47	160	-0.020	0.66047079	0.0055927
21-Apr	15:12	9.92	10.61	11.33	12.02	13.01	13.36	38.15	35.71	129	-0.023	0.64413010	0.0069043
21-Apr	15:33	9.82	10.44	11.25	11.98	12.90	13.34	38.17	35.75	128	-0.021	0.65108817	0.0059989
21-Apr	15:53	9.29	9.86	10.57	11.18	12.06	12.36	38.58	36.33	136	-0.026	0.58520989	0.0082998
21-Apr	16:13	9.88	10.53	11.37	12.07	13.09	13.27	38.63	36.51	159	-0.020	0.67286444	0.0050970
21-Apr	16:33	10.31	11.06	11.71	12.66	13.74	14.27	38.70	36.67	134	-0.014	0.71102342	0.0046201
21-Apr	16:53	10.42	11.17	11.89	12.63	13.77	14.18	38.39	36.68	154	-0.013	0.68388735	0.0062896
21-Apr	17:13	9.75	10.37	11.23	11.96	13.03	13.32	38.09	36.28	147	-0.015	0.68493656	0.0041514
21-Apr	17:33	9.26	9.79	10.61	11.25	12.28	12.68	37.67	36.01	132	-0.015	0.63246964	0.0048102
21-Apr	17:53	9.12	9.73	10.43	11.15	12.12	12.56	37.17	35.63	137	-0.014	0.62183868	0.0049462
21-Apr	18:13	9.08	9.59	10.44	11.05	12.01	12.34	36.57	35.15	139	-0.014	0.61487033	0.0050891
21-Apr	18:33	8.91	9.48	10.27	10.99	11.96	12.29	36.01	34.69	116	-0.012	0.63548498	0.0037765
21-Apr	18:53	9.83	10.36	11.19	11.98	12.94	13.36	35.14	33.96	134	-0.010	0.65232587	0.0056216
21-Apr	19:13	9.95	10.65	11.48	12.21	13.29	13.62	34.38	33.35	135	-0.008	0.68047500	0.0048651
21-Apr	19:33	9.91	10.54	11.36	12.12	13.14	13.57	33.68	32.74	134	-0.007	0.66296227	0.0054510
21-Apr	19:53	9.02	9.57	10.34	11.01	12.02	12.47	33.06	32.19	133	-0.008	0.61639147	0.0047320
21-Apr	20:13	7.93	8.41	9.13	9.68	10.47	10.87	32.32	31.49	133	-0.010	0.52675278	0.0057577
21-Apr	20:33	7.75	8.18	8.87	9.59	10.30	10.76	31.98	31.21	121	-0.009	0.53948830	0.0042355
21-Apr	20:53	8.85	9.36	10.11	10.76	11.69	12.10	31.81	31.04	145	-0.008	0.58580660	0.0057179
21-Apr	21:13	7.99	8.50	9.26	9.85	10.77	11.20	31.57	30.80	155	-0.008	0.57182073	0.0036642
21-Apr	21:33	7.71	8.24	9.01	9.70	10.61	11.02	31.00	30.22	157	-0.007	0.59924213	0.0023469
21-Apr	21:53	7.75	8.26	9.02	9.60	10.45	10.94	30.48	29.68	134	-0.008	0.55691567	0.0036300
21-Apr	23:14	9.26	9.95	10.72	11.46	12.46	12.99	28.74	27.87	134	-0.007	0.64979010	0.0041997
21-Apr	23:34	8.82	9.43	10.22	10.91	11.93	12.46	28.38	27.55	136	-0.007	0.63447543	0.0035778
21-Apr	23:54	8.02	8.59	9.30	9.90	10.90	11.36	28.09	27.27	147	-0.008	0.58627461	0.0032709
22-Apr	0:14	7.66	8.19	8.92	9.53	10.37	10.86	27.65	26.82	163	-0.009	0.55849076	0.0033670
22-Apr	0:34	8.68	9.17	9.86	10.53	11.63	12.04	27.07	26.20	149	-0.008	0.60929471	0.0039017
22-Apr	0:54	8.34	8.88	9.59	10.19	11.22	11.74	26.74	25.88	135	-0.008	0.58834290	0.0039306
22-Apr	1:14	8.04	8.47	9.19	9.91	10.72	11.17	26.49	25.63	138	-0.009	0.56574406	0.0039370
22-Apr	1:34	8.11	8.63	9.35	10.02	10.95	11.49	26.31	25.47	139	-0.008	0.58546738	0.0034626
22-Apr	1:54	7.25	7.65	8.24	9.06	9.66	10.14	26.26	25.44	137	-0.011	0.52077341	0.0035056
22-Apr	2:14	7.19	7.65	8.30	8.96	9.85	10.27	25.84	25.01	147	-0.009	0.55302650	0.0024286
22-Apr	2:34	6.60	6.93	7.62	8.26	8.93	9.36	25.83	25.03	149	-0.011	0.50123692	0.0025762
22-Apr	2:54	5.27	5.58	6.24	6.73	7.28	7.76	25.57	24.82	133	-0.013	0.43264457	0.0017941
22-Apr	3:14	5.36	5.61	6.25	6.68	7.28	7.74	25.57	24.84	159	-0.014	0.41415914	0.0023626
22-Apr	3:34	4.72	5.00	5.60	6.03	6.43	6.92	25.02	24.27	134	-0.017	0.37507982	0.0021652
22-Apr	3:54	4.84	5.01	5.66	6.06	6.54	6.98	24.81	24.01	128	-0.019	0.38120654	0.0021256
22-Apr	4:14	4.86	5.03	5.68	6.18	6.58	6.95	24.65	23.85	135	-0.020	0.39424046	0.0018343
22-Apr	4:34	6.42	6.72	7.46	8.10	8.69	9.08	24.48	23.65	149	-0.013	0.49733024	0.0023335
22-Apr	4:55	6.32	6.66	7.41	7.90	8.55	8.99	24.18	23.34	134	-0.013	0.47745998	0.0027342
22-Apr	5:15	6.22	6.57	7.17	7.76	8.47	8.99	23.71	22.84	130	-0.012	0.47746742	0.0024477
22-Apr	5:35	6.69	7.11	7.77	8.36	9.03	9.54	23.64	22.78	140	-0.012	0.49314739	0.0031528
22-Apr	5:55	6.01	6.33	6.98	7.45	8.13	8.55	23.30	22.43	139	-0.015	0.45160590	0.0027814
22-Apr	6:15	5.05	5.33	5.95	6.50	6.95	7.36	23.14	22.31	138	-0.017	0.41991465	0.0016854
22-Apr	6:35	4.87	5.10	5.74	6.18	6.72	7.12	23.02	22.18	117	-0.018	0.40644577	0.0016219
22-Apr	6:55	4.13	4.34	4.88	5.40	5.90	6.23	22.97	22.12	114	-0.021	0.39408410	0.0008744
22-Apr	7:15	4.21	4.39	4.98	5.39	5.87	6.14	22.88	21.95	116	-0.027	0.37408040	0.0012123
22-Apr	8:15	4.04	4.23	4.68	5.03	5.32	5.60	24.74	23.28	118	-0.067	0.30222210	0.0031019
22-Apr	8:35	4.60	4.81	5.25	5.61	6.00	6.39	25.33	23.77	140	-0.055	0.31924186	0.0045929
22-Apr	8:55	5.31	5.49	6.06	6.58	7.02	7.34	25.99	24.30	131	-0.046	0.40047274	0.0027432
22-Apr	9:15	5.81	6.05	6.58	7.16	7.71	8.08	26.65	24.62	139	-0.044	0.43447344	0.0028701
22-Apr	9:35	5.39	5.64	6.14	6.55	7.06	7.27	27.17	24.98	119	-0.070	0.38338403	0.0040227
22-Apr	9:55	4.95	5.19	5.60	6.03	6.43	6.74	27.56	25.29	151	-0.080	0.34513076	0.0045825
22-Apr	10:15	5.50	5.78	6.34	6.87	7.26	7.53	27.85	25.45	162	-0.066	0.41339271	0.0030231
22-Apr	10:35	5.23	5.52	6.08	6.53	6.93	7.18	28.19	25.72	121	-0.073	0.39713482	0.0029347
22-Apr	10:55	4.28	4.47	4.85	5.20	5.49	5.59	28.46	26.11	154	-0.154	0.30270480	0.0044988
22-Apr	11:15	4.66	4.88	5.28	5.69	5.97	6.17	29.16	26.63	169	-0.125	0.32286416	0.0050050
22-Apr	11:36	4.57	4.75	5.13	5.47	5.72	5.91	29.46	26.92	159	-0.159	0.29149716	0.0083877
22-Apr	11:56	4.74	4.88	5.30	5.68	5.97	6.06	30.23	27.65	138	-0.166	0.31899682	0.0058199
22-Apr	12:16	5.36	5.65	6.15	6.56	7.00	7.17	30.64	27.90	161	-0.094	0.38355254	0.0041143
22-Apr	12:36	4.49	4.77	5.13	5.42	5.78	5.93	31.21	28.50	146	-0.147	0.30638600	0.0057962
22-Apr	12:56	4.59	4.76	5.24	5.58	5.84	6.00	31.59	28.82	165	-0.156	0.32174062	0.0047296
22-Apr	13:16	4.34	4.51	4.96	5.24	5.47	5.56	32.05	29.53	122	-0.189	0.29576435	0.0057791
22-Apr	13:36	4.89	5.09	5.56	5.93	6.21	6.43	32.70	30.05	161	-0.125	0.32842852	0.0059958
22-Apr	13:56	5.03	5.22	5.76	6.16	6.49	6.75	33.38	30.57	152	-0.106	0.36043715	0.0039950
22-Apr	14:16	5.56	5.83	6.39	6.82	7.19	7.44	33.84	31.16	163	-0.084	0.38706617	0.0047722
22-Apr	14:36	5.67	5.92	6.45	6.95	7.32	7.60	34.47	31.72	153	-0.082	0.39460274	0.0046605
22-Apr	14:56	7.06	7.44	8.12	8.71	9.26	9.57	35.01	32.23	133	-0.049	0.49779140	0.0042781
22-Apr	15:16	7.77	8.24	8.92	9.57	10.25	10.45	35.18	32.58	167	-0.040	0.54566122	0.0043588

		Wind Speeds						Temperatures		Wind			
Date	Time	U(0.75)	U(1.25)	U(2.07)	U(3.44)	U(5.72)	U(9.50)	TL1	TU2	Dir	Ri	U*	Zo
22-Apr	15:36	8.02	8.56	9.27	10.02	10.70	10.92	35.57	32.99	136	-0.034	0.58636430	0.0034927
22-Apr	15:56	8.43	8.87	9.62	10.17	11.07	11.22	35.51	33.10	133	-0.034	0.57167421	0.0051400
22-Apr	16:16	8.74	9.31	10.09	10.81	11.64	11.72	35.26	32.98	129	-0.028	0.62344858	0.0039522
22-Apr	16:36	8.85	9.40	10.11	10.82	11.72	11.84	35.36	33.29	150	-0.025	0.61136330	0.0046427
22-Apr	16:56	9.97	10.66	11.45	12.25	13.30	13.47	34.99	33.10	163	-0.017	0.69394112	0.0044467
22-Apr	17:16	9.21	9.83	10.59	11.27	12.21	12.62	34.68	32.85	141	-0.017	0.62548010	0.0051675
22-Apr	17:36	9.76	10.32	11.13	11.95	12.99	13.36	33.79	32.18	129	-0.014	0.67944541	0.0042526
22-Apr	17:56	9.36	10.01	10.86	11.52	12.50	12.75	33.15	31.71	141	-0.014	0.65020247	0.0045331
22-Apr	18:17	8.72	9.22	10.00	10.70	11.63	11.91	32.89	31.47	165	-0.015	0.61419328	0.0040154
22-Apr	18:37	9.07	9.75	10.57	11.22	12.33	12.45	32.31	31.00	136	-0.012	0.66815673	0.0032237
22-Apr	18:57	9.22	9.90	10.59	11.40	12.41	12.65	31.45	30.33	140	-0.010	0.65502608	0.0038933
22-Apr	19:17	8.61	9.20	10.06	10.78	11.69	12.04	30.88	29.89	141	-0.009	0.63938445	0.0030514
22-Apr	19:37	8.48	9.04	9.84	10.57	11.48	11.81	30.25	29.33	140	-0.009	0.62277071	0.0032009
22-Apr	19:57	8.45	8.92	9.72	10.41	11.33	11.49	29.87	28.98	139	-0.010	0.60439153	0.0036188
22-Apr	20:17	9.51	10.22	11.00	11.78	12.94	13.19	29.56	28.68	133	-0.007	0.69575655	0.0032620
22-Apr	20:37	8.98	9.58	10.29	11.11	12.08	12.41	29.18	28.33	141	-0.008	0.63928580	0.0037540
22-Apr	20:57	7.96	8.47	9.10	9.82	10.67	11.08	28.76	27.93	142	-0.009	0.56219167	0.0039196
22-Apr	21:17	6.72	7.14	7.89	8.44	9.12	9.61	28.40	27.59	149	-0.010	0.50617701	0.0028175
22-Apr	21:37	7.70	8.18	8.91	9.50	10.24	10.64	27.93	27.07	144	-0.011	0.53068543	0.0046520
22-Apr	21:57	8.44	9.01	9.76	10.59	11.44	11.97	27.44	26.55	153	-0.008	0.62484410	0.0030489
22-Apr	22:17	9.06	9.71	10.47	11.34	12.22	12.73	27.22	26.31	150	-0.007	0.65350171	0.0035682
22-Apr	22:37	9.73	10.35	11.20	12.03	13.10	13.52	26.99	26.06	136	-0.007	0.69479696	0.0036767
22-Apr	22:57	9.82	10.54	11.29	12.17	13.08	13.74	26.76	25.83	149	-0.007	0.66789422	0.0050524
22-Apr	23:17	10.16	10.92	11.78	12.65	13.84	14.32	26.47	25.53	147	-0.006	0.74696273	0.0031806
22-Apr	23:37	10.70	11.50	12.25	13.14	14.24	14.76	26.31	25.38	146	-0.006	0.71602954	0.0055293
22-Apr	23:57	9.95	10.62	11.44	12.27	13.30	13.92	25.86	24.92	149	-0.006	0.68616992	0.0045596
23-Apr	0:17	9.04	9.62	10.40	11.22	12.12	12.60	25.52	24.57	155	-0.008	0.64064751	0.0038815
23-Apr	0:37	9.27	9.97	10.66	11.42	12.37	13.07	25.25	24.28	151	-0.007	0.62939387	0.0051190
23-Apr	0:59	9.49	10.12	10.88	11.66	12.79	13.48	24.96	23.99	147	-0.007	0.67377720	0.0037743
23-Apr	1:19	8.98	9.61	10.38	11.09	12.14	12.74	24.67	23.69	139	-0.008	0.64481754	0.0036190
23-Apr	1:39	8.51	9.11	9.90	10.59	11.63	12.20	24.39	23.42	147	-0.008	0.63881464	0.0028294
23-Apr	1:59	9.01	9.55	10.23	10.99	12.09	12.64	24.16	23.17	145	-0.008	0.63585426	0.0038163
23-Apr	2:19	8.72	9.33	10.11	10.76	11.89	12.38	23.86	22.86	144	-0.008	0.64642215	0.0030078
23-Apr	2:39	8.72	9.35	10.03	10.73	11.72	12.12	23.74	22.74	126	-0.010	0.61292322	0.0041255
23-Apr	2:59	8.23	8.73	9.50	10.25	11.10	11.45	23.59	22.60	139	-0.010	0.60362290	0.0031903
23-Apr	3:19	7.58	8.03	8.73	9.38	10.17	10.66	23.47	22.49	143	-0.011	0.54422022	0.0035937
23-Apr	3:39	6.86	7.33	8.02	8.59	9.36	9.74	23.14	22.17	133	-0.013	0.52229738	0.0026773
23-Apr	3:59	6.90	7.39	7.98	8.61	9.32	9.66	22.88	21.97	146	-0.013	0.50520696	0.0033206
23-Apr	4:19	6.99	7.38	8.09	8.75	9.50	10.12	22.76	21.91	147	-0.009	0.53152523	0.0025762
23-Apr	4:39	7.26	7.52	8.30	8.88	9.67	10.09	22.73	21.88	146	-0.012	0.52231452	0.0033352
23-Apr	4:59	6.90	7.35	7.95	8.55	9.27	9.72	22.52	21.68	125	-0.012	0.49445084	0.0036808
23-Apr	5:19	7.49	7.90	8.56	9.24	10.24	10.72	22.36	21.51	132	-0.009	0.57563579	0.0023447
23-Apr	5:39	6.77	7.24	7.83	8.44	9.18	9.50	22.01	21.14	137	-0.013	0.50251967	0.0030501
23-Apr	5:59	6.90	7.34	7.96	8.61	9.33	9.74	21.83	20.97	145	-0.012	0.51089457	0.0030470
23-Apr	6:19	6.83	7.22	7.96	8.53	9.24	9.71	21.69	20.79	138	-0.012	0.51158999	0.0028587
23-Apr	6:39	5.99	6.26	6.85	7.51	8.07	8.46	21.55	20.65	138	-0.016	0.45927063	0.0024277
23-Apr	6:59	5.80	6.09	6.74	7.27	7.79	8.10	21.58	20.65	141	-0.019	0.43758968	0.0027618
23-Apr	7:19	5.64	5.94	6.54	7.04	7.50	7.79	21.84	20.86	163	-0.023	0.41039664	0.0034407
23-Apr	7:41	6.50	6.87	7.53	8.11	8.75	8.98	22.34	21.17	140	-0.021	0.48695946	0.0029035
23-Apr	8:01	5.60	5.87	6.46	6.98	7.37	7.69	22.90	21.64	157	-0.032	0.40219103	0.0037202
23-Apr	8:21	5.97	6.34	6.97	7.52	7.98	8.36	23.61	22.00	176	-0.032	0.44688976	0.0030587
23-Apr	8:41	6.37	6.73	7.34	8.02	8.56	8.89	24.02	22.36	163	-0.029	0.48772070	0.0026072
23-Apr	9:01	5.83	6.24	6.90	7.42	7.88	8.13	24.44	22.45	152	-0.043	0.45944108	0.0024218
23-Apr	9:21	5.14	5.42	5.96	6.33	6.74	6.98	24.92	22.76	158	-0.073	0.36964837	0.0039647
23-Apr	13:21	4.45	4.72	5.11	5.44	5.69	5.83	30.05	27.25	133	-0.166	0.30793464	0.0054662
23-Apr	14:01	4.47	4.76	5.08	5.46	5.69	5.86	30.53	27.86	181	-0.155	0.30000978	0.0065182
23-Apr	14:23	5.62	5.99	6.42	6.79	7.22	7.52	31.10	28.17	113	-0.091	0.36348211	0.0078051
23-Apr	14:43	6.89	7.26	7.95	8.41	8.94	9.14	31.14	28.38	142	-0.061	0.46685509	0.0055509
23-Apr	15:03	7.54	8.08	8.78	9.39	10.02	10.26	30.95	28.28	139	-0.040	0.54241089	0.0039508
23-Apr	15:23	8.02	8.48	9.26	9.73	10.44	10.71	31.07	28.43	134	-0.041	0.52991718	0.0063422
23-Apr	15:43	8.34	8.98	9.76	10.34	11.12	11.28	31.25	28.61	149	-0.034	0.59440398	0.0041819
23-Apr	16:03	8.53	9.11	9.85	10.41	11.30	11.58	31.46	28.79	142	-0.032	0.58860789	0.0048534
23-Apr	16:23	8.65	9.14	9.94	10.60	11.40	11.75	30.66	28.24	138	-0.028	0.59560355	0.0047688
23-Apr	16:43	8.89	9.47	10.27	11.06	11.83	12.18	29.96	27.86	132	-0.022	0.63121943	0.0040288
23-Apr	17:03	8.86	9.42	10.20	10.93	11.86	12.23	29.56	27.59	146	-0.019	0.63481992	0.0037347
23-Apr	17:23	8.75	9.32	10.06	10.72	11.64	12.03	29.42	27.52	138	-0.020	0.60706614	0.0045328
23-Apr	17:43	8.58	9.14	9.73	10.45	11.27	11.65	29.19	27.41	132	-0.021	0.56717764	0.0060331
23-Apr	18:03	8.39	8.94	9.66	10.36	11.09	11.31	28.72	27.13	149	-0.021	0.57506755	0.0049507
23-Apr	18:23	8.66	9.26	9.95	10.76	11.42	11.80	28.41	26.87	122	-0.017	0.58841693	0.0052308

		Wind Speeds						Temperatures		Wind			
Date	Time	U(0.75)	U(1.25)	U(2.07)	U(3.44)	U(5.72)	U(9.50)	TL1	TU2	Dir	Ri	U*	Zo
23-Apr	18:43	9.69	10.29	11.12	12.10	12.99	13.33	27.69	26.24	121	-0.012	0.70142343	0.0034531
23-Apr	19:03	9.14	9.75	10.54	11.26	12.03	12.43	27.10	25.77	122	-0.014	0.60636125	0.0060012
23-Apr	19:23	8.92	9.45	10.20	11.07	11.89	12.31	26.66	25.42	126	-0.012	0.63058625	0.0039239
23-Apr	19:43	9.18	9.79	10.50	11.41	12.36	12.81	26.22	25.07	135	-0.010	0.66322429	0.0034613
23-Apr	20:03	9.49	10.05	10.91	11.80	12.79	13.12	25.87	24.76	131	-0.009	0.69343927	0.0032153
23-Apr	20:23	8.74	9.36	10.02	10.74	11.70	12.09	25.60	24.52	140	-0.011	0.60757463	0.0043987
23-Apr	20:43	8.96	9.54	10.28	11.16	11.96	12.42	25.35	24.28	132	-0.010	0.63121278	0.0040491
23-Apr	21:05	9.15	9.76	10.51	11.42	12.22	12.69	25.10	24.04	138	-0.009	0.64492644	0.0040557
23-Apr	21:25	7.93	8.43	9.08	9.87	10.53	10.89	24.97	23.93	128	-0.013	0.55396585	0.0042807
23-Apr	21:45	8.18	8.70	9.41	10.06	10.97	11.28	24.79	23.75	130	-0.012	0.57965349	0.0038978
23-Apr	22:05	7.86	8.37	9.05	9.77	10.63	11.04	24.57	23.54	128	-0.011	0.57852942	0.0031374
23-Apr	22:25	7.72	8.20	8.96	9.70	10.40	10.79	24.27	23.23	111	-0.012	0.57106436	0.0031015
23-Apr	22:45	7.12	7.57	8.30	8.92	9.47	9.90	24.06	23.02	136	-0.015	0.50573647	0.0040017
23-Apr	23:05	6.77	7.18	7.80	8.42	9.01	9.52	23.89	22.85	134	-0.015	0.47885218	0.0040064
23-Apr	23:25	6.27	6.60	7.21	7.75	8.30	8.68	23.77	22.74	118	-0.020	0.44071173	0.0041193
23-Apr	23:45	5.94	6.29	6.82	7.47	8.05	8.43	23.72	22.71	122	-0.018	0.45709634	0.0024652
24-Apr	0:05	6.18	6.53	7.21	7.77	8.42	8.71	23.41	22.37	133	-0.018	0.48326143	0.0022925
24-Apr	0:25	6.62	7.01	7.64	8.21	8.88	9.27	23.20	22.17	112	-0.016	0.48093844	0.0034103
24-Apr	0:45	7.74	8.30	9.03	9.76	10.56	10.96	23.17	22.14	131	-0.011	0.58869499	0.0027019
24-Apr	1:05	7.94	8.44	9.14	9.95	10.81	11.30	22.94	21.89	153	-0.010	0.60408079	0.0025903
24-Apr	1:25	7.52	7.98	8.64	9.31	10.03	10.50	22.72	21.67	151	-0.013	0.53004027	0.0040429
24-Apr	1:45	7.33	7.76	8.34	9.03	9.73	10.21	22.42	21.35	135	-0.014	0.50950550	0.0043214
24-Apr	2:05	8.59	9.12	9.89	10.56	11.46	11.75	22.13	21.05	156	-0.012	0.59872454	0.0043070
24-Apr	2:25	9.44	10.08	10.84	11.79	12.67	13.09	21.62	20.51	154	-0.009	0.67618056	0.0036844
24-Apr	2:45	8.96	9.61	10.44	11.22	12.17	12.44	21.40	20.30	150	-0.010	0.66467009	0.0030925
24-Apr	3:05	9.60	10.35	11.11	11.96	13.01	13.32	21.10	19.99	132	-0.009	0.69692090	0.0034849
24-Apr	3:25	8.78	9.39	10.10	10.99	12.06	12.35	20.55	19.42	141	-0.010	0.68162536	0.0023267
24-Apr	3:47	8.36	9.09	9.84	10.61	11.60	12.00	20.16	19.06	136	-0.009	0.66098533	0.0022465
24-Apr	4:07	7.69	8.26	8.95	9.63	10.52	10.90	19.88	18.80	152	-0.012	0.58546489	0.0026772
24-Apr	4:27	7.66	8.29	8.97	9.62	10.40	10.78	19.62	18.55	140	-0.012	0.56492653	0.0033047
24-Apr	4:47	7.52	8.17	8.77	9.49	10.31	10.70	19.45	18.42	133	-0.011	0.57268037	0.0027467
24-Apr	5:07	7.97	8.62	9.30	10.02	10.87	11.24	19.47	18.46	139	-0.011	0.59593974	0.0030155
24-Apr	5:27	8.66	9.45	10.27	11.12	12.02	12.40	19.19	18.17	156	-0.008	0.68884175	0.0022171
24-Apr	5:47	7.93	8.62	9.41	10.19	11.08	11.51	18.74	17.72	155	-0.009	0.64824017	0.0019064
24-Apr	6:07	8.70	9.55	10.35	11.06	11.87	12.19	18.50	17.46	136	-0.010	0.64666118	0.0033020
24-Apr	6:27	8.19	8.87	9.64	10.36	11.18	11.58	18.32	17.26	151	-0.010	0.61671930	0.0029470
24-Apr	6:47	9.54	10.32	11.16	11.99	12.89	13.27	18.16	17.08	136	-0.009	0.68816314	0.0037215
24-Apr	7:07	8.99	9.75	10.53	11.33	12.33	12.77	18.12	17.04	147	-0.009	0.68059398	0.0028185
24-Apr	7:27	9.85	10.65	11.45	12.25	13.33	13.79	18.21	17.00	150	-0.009	0.70667480	0.0037768
24-Apr	7:47	9.23	9.98	10.80	11.62	12.56	13.00	18.59	17.28	149	-0.010	0.68596026	0.0031379
24-Apr	8:07	9.95	10.72	11.43	12.28	13.32	13.80	18.85	17.38	140	-0.011	0.69022650	0.0045492
24-Apr	8:27	10.15	10.97	11.72	12.57	13.59	14.20	19.39	17.83	140	-0.011	0.70268011	0.0046763
24-Apr	8:47	9.58	10.41	11.09	11.92	13.10	13.48	19.94	18.32	140	-0.012	0.71573409	0.0030080
24-Apr	9:07	9.53	10.25	10.93	11.70	12.69	13.21	20.34	18.41	142	-0.016	0.65271371	0.0049531
24-Apr	9:27	10.26	11.15	11.94	12.71	13.76	14.19	20.62	18.52	130	-0.016	0.71582142	0.0046163
24-Apr	9:47	10.74	11.57	12.45	13.42	14.63	14.97	20.76	18.58	154	-0.014	0.80557409	0.0029321
24-Apr	10:07	11.38	12.35	13.15	14.10	15.20	15.65	21.05	18.78	132	-0.014	0.78314259	0.0049521
24-Apr	11:29	11.05	11.87	12.64	13.54	14.48	14.98	22.36	19.74	111	-0.020	0.71733217	0.0070152
24-Apr	11:49	11.40	12.30	13.07	14.02	15.22	15.61	22.63	19.91	143	-0.018	0.78886139	0.0046901
24-Apr	12:09	10.55	11.37	12.19	13.03	13.96	14.28	23.18	20.49	141	-0.022	0.71550807	0.0054588
24-Apr	12:29	10.00	10.78	11.49	12.29	13.21	13.57	23.79	20.92	126	-0.026	0.67393634	0.0056630
24-Apr	12:49	10.32	11.17	11.89	12.74	13.72	14.08	24.27	21.38	121	-0.024	0.70908145	0.0050565
24-Apr	13:09	9.42	10.16	10.75	11.57	12.42	12.83	24.61	21.56	128	-0.030	0.63485085	0.0056565
24-Apr	13:29	9.80	10.52	11.23	11.98	12.94	13.18	24.96	21.97	133	-0.030	0.66305091	0.0054781
24-Apr	13:49	9.79	10.50	11.10	11.91	12.84	13.10	24.97	22.00	138	-0.031	0.64610865	0.0063048
24-Apr	14:09	9.47	10.24	10.86	11.67	12.68	12.90	25.12	22.23	147	-0.028	0.67306596	0.0040967
24-Apr	14:29	10.10	10.87	11.56	12.31	13.45	13.73	24.73	21.90	140	-0.025	0.69640353	0.0048010
24-Apr	14:49	9.38	10.07	10.81	11.59	12.44	12.74	25.02	22.19	133	-0.029	0.65154782	0.0047111
24-Apr	15:09	9.68	10.43	11.15	11.96	12.79	13.13	25.00	22.20	136	-0.027	0.65868114	0.0053755
24-Apr	15:29	8.92	9.49	10.37	11.10	11.83	12.14	25.28	22.54	140	-0.030	0.63575920	0.0040339
24-Apr	15:49	8.99	9.61	10.41	11.11	11.97	12.27	25.13	22.49	141	-0.028	0.63626969	0.0041852
24-Apr	16:09	8.67	9.30	10.05	10.75	11.63	11.77	25.04	22.58	149	-0.029	0.63001049	0.0036150
24-Apr	16:29	8.47	9.17	9.93	10.64	11.51	11.81	25.05	22.65	138	-0.025	0.63983006	0.0029714
24-Apr	16:49	9.36	10.01	10.79	11.52	12.41	12.69	24.82	22.74	142	-0.021	0.64255011	0.0049391
24-Apr	17:11	8.60	9.28	9.91	10.73	11.64	12.00	24.62	22.46	120	-0.021	0.63798691	0.0031659
24-Apr	17:31	8.59	9.29	9.92	10.59	11.44	11.71	24.16	22.27	147	-0.022	0.59183163	0.0049563
24-Apr	17:51	8.24	8.85	9.59	10.29	11.15	11.64	23.85	21.99	112	-0.018	0.61027927	0.0031930
24-Apr	18:11	8.49	9.16	9.83	10.50	11.44	11.73	23.51	21.79	145	-0.019	0.61034812	0.0037872
24-Apr	18:31	8.46	9.21	9.95	10.67	11.47	11.71	23.09	21.52	140	-0.017	0.62500292	0.0033781

		Wind Speeds						Temperatures		Wind			
Date	Time	U(0.75)	U(1.25)	U(2.07)	U(3.44)	U(5.72)	U(9.50)	TL1	TU2	Dir	Ri	U*	Zo
24-Apr	18:51	8.96	9.71	10.45	11.18	12.20	12.62	22.59	21.13	131	-0.012	0.66178818	0.0032469
24-Apr	19:11	8.02	8.58	9.24	10.00	10.97	11.41	22.11	20.83	151	-0.012	0.61394906	0.0025386
24-Apr	19:31	6.80	7.33	7.95	8.63	9.42	9.94	21.53	20.41	139	-0.013	0.54540269	0.0020526
24-Apr	19:51	6.43	6.83	7.42	8.03	8.73	9.13	21.19	20.16	132	-0.016	0.48812346	0.0026654
24-Apr	20:11	6.29	6.85	7.41	7.94	8.59	8.98	21.00	20.01	149	-0.015	0.47447522	0.0029870
24-Apr	20:31	6.50	6.97	7.69	8.24	8.98	9.39	20.71	19.75	146	-0.013	0.51911696	0.0021121
24-Apr	20:51	6.52	6.99	7.64	8.25	8.97	9.40	20.46	19.51	148	-0.013	0.51317027	0.0022580
24-Apr	21:11	6.14	6.59	7.17	7.79	8.40	8.84	20.18	19.22	121	-0.015	0.47773479	0.0024200
24-Apr	21:31	7.12	7.68	8.31	9.05	9.81	10.09	20.03	19.08	116	-0.012	0.56119697	0.0022542
24-Apr	21:51	7.90	8.56	9.28	9.83	10.70	11.15	19.80	18.83	123	-0.010	0.56871764	0.0037853
24-Apr	22:11	7.44	7.95	8.65	9.28	9.99	10.50	19.61	18.64	136	-0.012	0.53328101	0.0037632
24-Apr	22:31	7.28	7.88	8.55	9.17	10.12	10.61	19.41	18.48	135	-0.009	0.57849522	0.0021486
24-Apr	22:51	7.82	8.42	9.08	9.71	10.64	11.18	19.17	18.22	139	-0.009	0.57483463	0.0032366
24-Apr	23:11	6.95	7.54	8.22	8.83	9.70	10.19	18.92	17.99	136	-0.010	0.56239420	0.0019881
24-Apr	23:31	6.68	7.20	7.76	8.36	9.25	9.71	18.56	17.62	144	-0.011	0.52778618	0.0021749
24-Apr	23:53	6.77	7.35	8.00	8.60	9.29	9.78	18.31	17.36	140	-0.012	0.52074071	0.0026524
25-Apr	0:13	7.01	7.43	8.10	8.77	9.56	10.13	18.31	17.41	140	-0.010	0.53686355	0.0024916
25-Apr	0:33	5.62	6.04	6.63	7.16	7.85	8.25	18.12	17.25	123	-0.014	0.46681244	0.0017239
25-Apr	0:53	5.31	5.68	6.29	6.81	7.47	7.92	17.88	17.03	153	-0.014	0.45648117	0.0014453
25-Apr	1:13	5.01	5.35	5.95	6.44	7.08	7.53	17.66	16.83	154	-0.014	0.43912648	0.0013154
25-Apr	1:33	5.45	5.87	6.49	7.06	7.78	8.13	17.56	16.71	164	-0.013	0.48911740	0.0011911
25-Apr	1:53	5.64	6.07	6.73	7.18	7.88	8.23	17.58	16.71	149	-0.014	0.46798034	0.0017617
25-Apr	2:13	6.23	6.66	7.32	7.91	8.55	8.97	17.01	16.10	140	-0.014	0.49127056	0.0022427
25-Apr	2:33	5.59	6.05	6.59	7.10	7.75	8.12	16.98	16.09	147	-0.016	0.44931819	0.0020821
25-Apr	2:53	4.87	5.22	5.70	6.26	6.80	7.23	16.61	15.72	147	-0.018	0.41335149	0.0015454
25-Apr	3:13	5.86	6.40	7.00	7.61	8.30	8.72	16.64	15.75	136	-0.012	0.50531759	0.0014899
25-Apr	3:33	6.61	7.09	7.67	8.35	8.93	9.33	16.70	15.78	109	-0.014	0.49192970	0.0030744
25-Apr	3:53	5.12	5.48	6.02	6.44	6.93	7.29	16.44	15.55	136	-0.021	0.38660700	0.0029096
25-Apr	4:13	4.29	4.57	5.01	5.44	5.90	6.22	16.37	15.48	148	-0.027	0.34968055	0.0019079
25-Apr	4:33	4.56	4.81	5.33	5.77	6.29	6.64	16.06	15.17	128	-0.023	0.37769326	0.0017092
25-Apr	4:53	5.02	5.38	6.03	6.47	7.07	7.52	16.03	15.16	134	-0.016	0.43558373	0.0014163
25-Apr	5:13	4.46	4.85	5.39	5.79	6.20	6.60	15.99	15.10	143	-0.022	0.37326604	0.0017940
25-Apr	5:53	4.01	4.24	4.76	5.19	5.64	6.09	15.47	14.69	139	-0.020	0.35776597	0.0012087
25-Apr	8:15	4.41	4.66	5.12	5.50	5.89	6.13	17.54	15.91	133	-0.064	0.33885741	0.0027105
25-Apr	8:35	4.75	5.10	5.51	5.90	6.33	6.60	18.07	16.48	145	-0.053	0.34764847	0.0036261
25-Apr	8:55	4.26	4.52	4.98	5.32	5.64	5.90	18.36	16.59	153	-0.076	0.32077347	0.0031399
25-Apr	9:15	4.08	4.34	4.69	4.99	5.28	5.47	18.79	16.71	153	-0.125	0.28466273	0.0050503
26-Apr	9:23	4.40	4.73	5.23	5.61	5.94	6.07	20.12	17.87	181	-0.093	0.36167173	0.0020901
27-Apr	17:11	4.46	4.67	5.00	5.41	5.71	5.83	28.85	26.64	175	-0.132	0.30710811	0.0051327
1-May	0:43	4.25	4.60	5.08	5.63	6.17	6.52	28.47	28.10	147	-0.007	0.40118087	0.0009392
1-May	1:43	4.59	4.91	5.40	5.95	6.52	6.88	27.57	27.10	132	-0.009	0.40725795	0.0012134
1-May	2:03	4.88	5.22	5.76	6.23	6.80	7.27	27.47	26.97	144	-0.009	0.40127500	0.0017789
1-May	2:43	4.06	4.40	4.87	5.27	5.87	6.39	26.47	25.96	141	-0.010	0.37317338	0.0010677
1-May	3:04	5.03	5.42	5.97	6.46	7.16	7.62	26.77	26.19	136	-0.009	0.43997738	0.0013216
2-May	4:07	4.05	4.34	4.80	5.25	5.90	6.34	27.47	27.34	122	-0.002	0.37640955	0.0009418

GOLDEN CANYON: MAST 2
DATA FOR NORTHERLY WINDS

		Wind Speeds				Temperatures		Wind			
Date	Time	U(1.0)	U(2.11)	U(4.49)	U(9.50)	TL1	TU2	Dir	Ri	U*	Zo
1-Apr	30-3:50	6.01	6.69	6.88	7.64	26.63	26.28	17	-0.007	0.3020778	0.0021005
4-Apr	21:38	5.21	5.79	6.11	6.82	31.65	31.47	19	-0.003	0.2935187	0.0008665
4-Apr	23:40	4.68	5.30	5.54	6.19	29.57	29.42	37	-0.004	0.2746162	0.0006795
5-Apr	0:00	5.11	5.78	6.08	6.73	29.29	29.14	50	-0.003	0.2933545	0.0008016
5-Apr	0:20	5.47	6.13	6.39	7.05	29.10	28.89	56	-0.006	0.2894259	0.0014547
5-Apr	0:40	5.34	5.99	6.29	6.89	28.94	28.71	41	-0.006	0.2842494	0.0014141
5-Apr	1:20	4.19	4.82	5.00	5.60	28.52	28.36	49	-0.004	0.2570653	0.0005166
7-Apr	2:14	4.51	5.16	5.56	6.42	28.72	28.93	50	0.009	0.3236261	0.0001789
9-Apr	21:54	5.13	5.70	6.14	6.94	35.06	35.28	49	0.008	0.3101159	0.0004993
9-Apr	22:14	4.78	5.39	5.83	6.67	34.69	34.84	49	0.006	0.3259915	0.0002368
9-Apr	22:34	5.50	6.25	6.74	7.59	34.48	34.55	49	0.003	0.3632695	0.0003011
9-Apr	22:54	4.60	5.21	5.57	6.24	34.66	35.15	57	0.022	0.2624851	0.0007884
10-Apr	22:02	4.84	5.50	5.88	6.53	34.84	35.00	51	0.007	0.2876784	0.0006110
11-Apr	4:24	4.83	5.59	5.95	6.72	31.24	31.68	62	0.014	0.3106715	0.0003655
11-Apr	5:04	5.20	5.93	6.35	7.18	30.94	31.31	53	0.011	0.3311896	0.0003771
11-Apr	5:24	4.85	5.46	5.85	6.32	30.86	31.35	59	0.019	0.2404381	0.0024285
11-Apr	5:44	5.37	6.08	6.46	7.28	30.55	30.77	55	0.007	0.3244134	0.0005285
12-Apr	4:10	5.81	6.48	6.73	7.49	33.15	33.06	56	-0.001	0.3004474	0.0016401
12-Apr	4:30	5.47	6.19	6.35	7.12	32.76	32.58	21	-0.003	0.3010413	0.0010535
12-Apr	4:52	7.13	7.90	8.28	9.15	32.69	32.45	26	-0.003	0.3661302	0.0017572
12-Apr	5:12	6.50	7.16	7.59	8.41	32.34	32.09	17	-0.005	0.3510071	0.0011788
12-Apr	9:12	5.69	6.20	6.51	7.13	31.68	30.54	2	-0.035	0.2837508	0.0023308
12-Apr	9:32	4.62	5.13	5.34	5.99	32.24	30.88	22	-0.058	0.2793284	0.0005797
12-Apr	9:52	4.93	5.39	5.63	6.22	32.57	31.06	5	-0.064	0.2649983	0.0013329
12-Apr	10:12	4.79	5.32	5.38	5.97	32.81	31.23	0	-0.082	0.2499794	0.0017238
12-Apr	10:32	4.72	5.15	5.28	5.92	33.32	31.61	15	-0.081	0.2557570	0.0012165
12-Apr	11:54	4.57	5.05	5.19	5.89	35.05	32.99	38	-0.091	0.2840123	0.0004791
12-Apr	22:56	4.83	5.54	5.78	6.55	31.06	31.47	53	0.015	0.2822566	0.0006711
12-Apr	23:16	4.71	5.35	5.62	6.21	31.73	31.87	0	0.009	0.2523186	0.0013020
13-Apr	11:20	5.15	5.66	5.82	6.44	33.45	31.24	19	-0.089	0.2729710	0.0015277
13-Apr	12:20	5.67	6.21	6.45	7.09	34.22	31.88	49	-0.076	0.2949414	0.0017600
14-Apr	2:24	4.62	5.21	5.53	6.43	27.34	27.28	54	0.000		
14-Apr	2:44	4.86	5.54	5.86	6.54	27.91	28.12	0	0.010	0.2813714	0.0007310
25-Apr	21:39	4.99	5.59	5.89	6.54	21.19	20.20	15	-0.028	0.3002342	0.0006006

GOLDEN CANYON: MAST 2
DATA FOR SOUTHERLY WINDS

		Wind Speeds				Temperatures		Wind			
Date	Time	U(1.0)	U(2.11)	U(4.49)	U(9.5)	TL1	TU2	Dir	Ri	U*	Zo
2-Apr	23:46	4.62	5.27	5.71	6.67	35.51	33.10	133	-0.034	0.40711292	0.0004554
3-Apr	0:06	4.64	5.29	5.67	6.80	21.10	19.99	132	-0.009	0.41097150	0.0004037
3-Apr	0:26	6.58	7.43	7.82	9.05	24.97	23.93	128	-0.013	0.46921499	0.0012782
3-Apr	0:46	7.61	8.59	9.14	10.37	38.39	36.68	154	-0.013	0.52035859	0.0016936
3-Apr	1:06	7.60	8.57	9.09	10.45	22.63	19.91	143	-0.018	0.54618623	0.0012505
3-Apr	1:26	7.26	8.17	8.66	9.96	37.97	35.47	160	-0.020	0.52097523	0.0012609
3-Apr	1:46	6.42	7.22	7.66	8.95	32.31	31.00	136	-0.012	0.48331434	0.0009233
3-Apr	2:06	5.56	6.32	6.71	7.69	24.97	22.00	138	-0.031	0.41724307	0.0010330
3-Apr	2:46	5.58	6.40	6.64	7.64	41.59	39.71	148	-0.107	0.44510702	0.0008211
3-Apr	3:06	6.10	6.98	7.35	8.51	42.32	41.24	151	-0.025	0.46733645	0.0009095
3-Apr	3:26	5.10	5.80	6.14	7.24	25.33	23.77	140	-0.055	0.44047364	0.0005017
3-Apr	3:46	5.47	6.21	6.52	7.64	32.96	31.38	173	-0.065	0.45210549	0.0006296
3-Apr	4:06	6.07	6.83	7.25	8.48	35.18	32.58	167	-0.040	0.48628963	0.0007032
3-Apr	4:26	5.47	6.21	6.57	7.74	21.57	21.14	135	-0.012	0.43271307	0.0007153
3-Apr	4:46	5.02	5.75	6.11	7.25	33.84	31.16	163	-0.084	0.47612830	0.0003428
3-Apr	7:08	4.13	4.77	4.98	6.00	22.34	21.17	140	-0.021	0.36659913	0.0004158
4-Apr	1:32	4.37	5.07	5.49	6.71	18.31	17.36	140	-0.012	0.44885254	0.0002184
4-Apr	1:52	4.11	4.82	5.08	6.23	25.87	24.76	131	-0.009	0.40331980	0.0002625
4-Apr	3:34	4.70	5.39	5.75	6.91	24.96	23.99	147	-0.007	0.41638221	0.0004031
4-Apr	3:54	5.54	6.30	6.69	7.77	21.62	20.51	154	-0.009	0.41846659	0.0009316
4-Apr	4:54	4.61	5.29	5.63	6.71	22.88	21.97	146	-0.013	0.40160924	0.0004503
4-Apr	5:14	4.65	5.25	5.57	6.53	29.96	27.86	132	-0.022	0.36680395	0.0007401
4-Apr	5:34	4.44	5.06	5.28	6.20	22.72	21.67	151	-0.013	0.33593992	0.0009136
8-Apr	10:04	5.13	5.66	5.85	6.49	24.51	24.42	161	-0.001	0.24308272	
8-Apr	10:24	4.98	5.54	5.71	6.26	38.11	38.36	148	0.006	0.23231240	
8-Apr	10:44	4.75	5.23	5.38	5.85	38.82	38.94	134	0.003	0.19673815	
11-Apr	9:26	5.12	5.66	5.86	6.44	39.02	39.12	135	0.003	0.23588473	
11-Apr	9:46	5.32	5.92	6.12	6.79	39.99	39.96	118	0.000	0.25940275	0.0172714
11-Apr	10:26	4.55	5.06	5.16	5.78	33.68	32.74	134	-0.007	0.22954586	
11-Apr	14:06	4.25	4.70	4.71	5.29	25.98	25.74	140	-0.003	0.19455128	
11-Apr	14:46	4.57	5.06	5.09	5.72	35.14	33.96	134	-0.010	0.22005370	
11-Apr	15:06	4.58	5.12	5.22	5.83	40.65	40.49	138	-0.002	0.22671464	
11-Apr	15:28	4.33	4.85	4.96	5.53	21.40	20.30	150	-0.010	0.22461383	
11-Apr	16:48	4.45	4.99	5.16	5.82	26.76	25.83	149	-0.007	0.25344890	0.0053866
11-Apr	17:08	5.44	6.10	6.37	7.18	25.25	24.28	151	-0.007	0.32219106	0.0041355
11-Apr	17:28	5.52	6.24	6.47	7.31	25.57	24.82	133	-0.013	0.33681329	0.0034784
11-Apr	17:48	5.80	6.51	6.80	7.73	22.36	21.51	132	-0.009	0.36034868	0.0029753
11-Apr	18:08	6.15	6.86	7.17	8.30	20.76	18.58	154	-0.014	0.41284364	0.0017641
11-Apr	18:28	6.05	6.80	7.07	8.14	28.19	25.72	121	-0.073	0.43860516	0.0012678
11-Apr	18:48	6.64	7.45	7.99	9.08	19.45	18.42	133	-0.011	0.46006915	0.0015354
11-Apr	19:08	6.57	7.33	7.80	8.88	42.13	41.25	140	-0.016	0.44099599	0.0018410
11-Apr	19:28	6.71	7.59	8.06	9.13	33.42	31.58	176	-0.121	0.52878013	0.0008886
11-Apr	19:48	5.99	6.77	7.22	8.31	32.28	30.90	169	-0.029	0.45447839	0.0009519
11-Apr	20:08	5.96	6.80	7.22	8.40	38.63	36.51	159	-0.020	0.47008737	0.0007650
11-Apr	20:28	6.29	7.06	7.55	8.73	38.17	35.75	128	-0.021	0.47406636	0.0009514
11-Apr	20:48	5.37	6.08	6.51	7.57	24.74	23.28	118	-0.067	0.45816528	0.0005482
11-Apr	21:08	5.10	5.81	6.15	7.25	18.92	17.99	136	-0.010	0.40678860	0.0006864
11-Apr	22:50	4.35	5.05	5.32	6.34	21.83	20.97	145	-0.012	0.37745298	0.0004662
11-Apr	23:10	5.17	5.98	6.34	7.52	24.27	23.23	111	-0.012	0.44568524	0.0004826
21-Apr	8:52	6.54	6.66	7.80	10.18	39.38	39.43	132	0.002	0.77945847	0.0000862
21-Apr	9:32	7.46	8.29	8.77	9.92	22.55	22.20	125	-0.007	0.45734023	0.0031883
21-Apr	9:52	6.26	7.02	7.29	8.29	25.82	25.72	150	-0.001	0.36584605	0.0043023
21-Apr	10:12	6.73	7.54	7.90	8.91	38.50	38.67	123	0.004	0.39385766	0.0042774
21-Apr	10:32	7.25	8.16	8.57	9.56	25.56	25.21	140	-0.004	0.42049756	0.0048673
21-Apr	10:52	8.50	9.51	10.27	11.44	27.47	27.34	122	-0.002	0.53293001	0.0028108
21-Apr	11:12	8.60	9.67	10.27	11.70	24.90	24.54	135	-0.004	0.56969394	0.0019616
21-Apr	11:32	9.04	10.12	10.78	12.34	24.39	23.42	147	-0.008	0.61707318	0.0016274
21-Apr	11:52	9.45	10.54	11.23	12.63	41.13	40.76	145	-0.005	0.58624363	0.0029955
21-Apr	12:12	9.32	10.33	10.99	12.34	34.38	33.35	135	-0.008	0.56362634	0.0035361
21-Apr	12:32	9.50	10.66	11.25	12.69	23.87	23.56	119	-0.006	0.58862421	0.0030556
21-Apr	12:52	10.11	11.33	11.93	13.49	31.81	31.04	145	-0.008	0.62744202	0.0030125
21-Apr	13:12	9.97	11.15	11.87	13.32	31.98	31.21	121	-0.009	0.62443813	0.0028817
21-Apr	13:32	10.24	11.55	12.17	13.75	19.62	18.55	140	-0.012	0.65904292	0.0024595
21-Apr	13:52	8.63	9.70	10.12	11.42	25.12	22.23	147	-0.028	0.54244649	0.0029283
21-Apr	14:12	8.87	9.87	10.30	11.73	30.23	27.65	138	-0.166	0.65855363	0.0012020
21-Apr	14:32	9.47	10.74	11.18	12.62	23.09	21.52	140	-0.017	0.59729861	0.0028567

		Wind Speeds				Temperatures		Wind			
Date	Time	U(1.0)	U(2.11)	U(4.49)	U(9.5)	TL1	TU2	Dir	Ri	U*	Zo
21-Apr	14:52	10.47	11.83	12.43	14.08	23.07	22.80	140	-0.007	0.66660423	0.0025869
21-Apr	15:12	10.58	11.95	12.63	14.14	30.95	28.28	139	-0.040	0.70425580	0.0021427
21-Apr	15:33	10.08	11.34	11.92	13.41	25.99	24.30	131	-0.046	0.66539081	0.0022313
21-Apr	15:53	10.30	11.49	12.05	13.64	29.42	27.52	138	-0.020	0.64120129	0.0029993
21-Apr	16:13	10.75	12.13	12.87	14.43	28.47	28.10	147	-0.007	0.67911976	0.0027690
21-Apr	16:33	11.07	12.44	13.10	14.83	16.06	15.17	128	-0.023	0.72475648	0.0022342
21-Apr	16:53	10.56	11.84	12.64	14.40	28.09	27.27	147	-0.008	0.71649075	0.0017090
21-Apr	17:13	10.52	11.66	12.47	14.19	23.59	22.60	139	-0.010	0.69450514	0.0019808
21-Apr	17:33	10.11	11.33	12.11	13.78	24.96	21.97	133	-0.030	0.72053357	0.0013490
21-Apr	17:53	10.20	11.53	12.17	13.66	33.50	31.95	164	-0.017	0.65633561	0.0025352
21-Apr	18:13	9.58	10.89	11.34	12.89	21.00	20.01	149	-0.015	0.62629853	0.0022513
21-Apr	18:33	9.55	10.79	11.23	12.66	40.93	38.90	148	-0.144	0.69333807	0.0014067
21-Apr	18:53	10.46	11.86	12.58	14.12	36.60	34.09	156	-0.022	0.70178893	0.0019917
21-Apr	19:13	10.85	12.30	12.97	14.62	22.97	22.12	114	-0.021	0.72094456	0.0020889
21-Apr	19:33	10.32	11.44	12.27	13.98	24.16	22.27	147	-0.022	0.71280315	0.0015496
21-Apr	19:53	9.60	10.78	11.54	12.90	35.96	33.77	162	-0.025	0.63870963	0.0020777
21-Apr	20:13	8.56	9.64	10.35	11.62	35.36	33.29	150	-0.025	0.59297778	0.0016309
21-Apr	20:33	8.28	9.33	9.99	11.37	32.88	31.12	180	-0.087	0.65437540	0.0008371
21-Apr	20:53	9.35	10.56	11.24	12.78	18.56	17.62	144	-0.011	0.64421026	0.0016084
21-Apr	21:13	8.60	9.76	10.32	11.82	27.44	26.55	153	-0.008	0.59813098	0.0015004
21-Apr	21:33	8.68	9.69	10.37	11.76	22.88	22.50	127	-0.007	0.57395028	0.0019894
21-Apr	21:53	8.53	9.52	10.22	11.55	23.18	20.49	141	-0.022	0.58461679	0.0016734
21-Apr	23:14	9.52	10.60	11.40	12.95	15.99	15.10	143	-0.022	0.66559412	0.0014664
21-Apr	23:34	9.39	10.51	11.14	12.73	16.61	15.72	147	-0.018	0.64078125	0.0016766
21-Apr	23:54	8.56	9.63	10.26	11.87	29.87	28.98	139	-0.010	0.62521946	0.0011040
22-Apr	0:14	8.80	9.84	10.52	11.86	23.28	23.03	134	-0.005	0.56436998	0.0024237
22-Apr	0:34	9.69	10.89	11.57	13.17	19.41	18.48	135	-0.009	0.65094835	0.0018342
22-Apr	0:54	9.08	10.19	10.91	12.41	28.72	27.13	149	-0.021	0.64182426	0.0013955
22-Apr	1:14	9.01	10.10	10.83	12.28	20.62	18.52	130	-0.016	0.62313783	0.0015714
22-Apr	1:34	8.28	9.30	9.92	11.37	31.48	30.35	159	-0.015	0.58836836	0.0013201
22-Apr	1:54	7.78	8.81	9.34	10.60	34.68	32.85	141	-0.017	0.53629440	0.0016403
22-Apr	2:14	8.19	9.18	9.78	11.19	18.32	17.26	151	-0.010	0.56499661	0.0015470
22-Apr	2:34	7.33	8.18	8.81	9.93	22.76	21.91	147	-0.009	0.48812464	0.0019386
22-Apr	2:54	5.83	6.62	7.08	8.06	16.37	15.48	148	-0.027	0.43301760	0.0010953
22-Apr	3:14	5.77	6.63	7.00	7.99	22.41	22.01	129	-0.007	0.40932575	0.0013775
22-Apr	3:34	5.14	5.87	6.18	7.24	25.05	22.65	138	-0.025	0.40967465	0.0007226
22-Apr	3:54	5.31	6.05	6.42	7.41	42.88	41.57	157	-0.046	0.42197587	0.0007756
22-Apr	4:14	5.44	6.13	6.45	7.30	24.82	22.74	142	-0.021	0.35688992	0.0022133
22-Apr	4:34	7.22	8.08	8.55	9.70	26.49	25.63	138	-0.009	0.46408899	0.0023978
22-Apr	4:55	7.08	7.89	8.39	9.52	38.15	35.71	129	-0.023	0.47255952	0.0019394
22-Apr	5:15	6.65	7.60	7.97	9.18	42.67	41.41	141	-0.036	0.49961740	0.0010337
22-Apr	5:35	6.82	7.74	8.20	9.43	17.88	17.03	153	-0.014	0.49425639	0.0011983
22-Apr	5:55	6.32	7.13	7.56	8.76	32.89	31.47	165	-0.015	0.46647551	0.0010579
22-Apr	6:15	5.79	6.60	6.98	8.06	23.20	22.17	112	-0.016	0.43232745	0.0010239
22-Apr	6:35	5.03	5.82	6.23	7.31	29.16	26.63	169	-0.125	0.50300700	0.0002956
22-Apr	6:55	4.60	5.33	5.56	6.47	39.85	37.72	168	-0.150	0.42129552	0.0004415
22-Apr	7:15	4.58	5.26	5.54	6.39	31.21	28.50	146	-0.147	0.40565507	0.0005126
22-Apr	8:15	4.76	5.36	5.55	6.27	18.79	16.71	153	-0.125	0.33146817	0.0017351
22-Apr	8:35	4.85	5.45	5.63	6.44	17.66	16.83	154	-0.014	0.30300904	0.0028683
22-Apr	8:55	6.11	6.80	7.17	8.03	35.57	32.99	136	-0.034	0.37737575	0.0032914
22-Apr	9:15	6.21	6.90	7.30	8.09	16.98	16.09	147	-0.016	0.35586288	0.0053903
22-Apr	9:35	5.94	6.62	6.89	7.73	41.18	39.20	168	-0.112	0.38770023	0.0025124
22-Apr	9:55	5.38	6.05	6.21	6.96	18.74	17.72	155	-0.009	0.29442938	0.0073689
22-Apr	10:15	6.08	6.74	7.06	7.71	25.86	24.92	149	-0.006	0.29971312	
22-Apr	10:35	5.77	6.46	6.65	7.31	34.04	32.26	157	-0.098	0.32697518	0.0066645
22-Apr	10:55	4.48	5.03	5.09	5.71	19.19	18.17	156	-0.008	0.23098683	
22-Apr	11:15	5.14	5.83	5.90	6.56	26.17	26.07	130	-0.001	0.25751489	
22-Apr	11:36	5.04	5.55	5.60	6.13	29.56	28.68	133	-0.007	0.20360952	
22-Apr	11:56	5.20	5.75	5.86	6.47	23.14	22.31	138	-0.017	0.24214105	0.0270105
22-Apr	12:16	5.91	6.60	6.74	7.32	28.38	27.55	136	-0.007	0.26090971	
22-Apr	12:36	4.92	5.55	5.64	6.22	23.47	22.49	143	-0.011	0.24479641	0.0160803
22-Apr	12:56	5.06	5.64	5.70	6.27	24.58	24.22	141	-0.004	0.22328453	
22-Apr	13:16	4.45	4.99	4.98	5.52	34.47	31.72	153	-0.082	0.23009708	
22-Apr	13:36	5.13	5.75	5.86	6.37	28.74	27.87	134	-0.007	0.22997910	
22-Apr	13:56	5.66	6.35	6.49	7.12	21.94	21.50	143	-0.009	0.27164965	
22-Apr	14:16	5.92	6.67	6.82	7.56	26.31	25.38	146	-0.006	0.30256926	
22-Apr	14:36	6.06	6.80	7.06	7.80	30.48	29.68	134	-0.008	0.32173293	0.0095290
22-Apr	14:56	7.56	8.43	8.84	9.92	30.66	28.24	138	-0.028	0.45905176	0.0036488
22-Apr	15:16	8.36	9.44	9.87	11.08	25.22	24.87	136	-0.004	0.49515561	0.0041827

		Wind Speeds				Temperatures		Wind			
Date	Time	U(1.0)	U(2.11)	U(4.49)	U(9.5)	TL1	TU2	Dir	Ri	U*	Zo
22-Apr	15:36	8.73	9.90	10.35	11.74	15.47	14.69	139	-0.020	0.57544073	0.0021622
22-Apr	15:56	9.06	10.14	10.64	11.94	25.13	22.49	141	-0.028	0.55936671	0.0032976
22-Apr	16:16	9.42	10.53	11.09	12.38	31.07	28.43	134	-0.041	0.58677532	0.0031985
22-Apr	16:36	9.47	10.65	11.12	12.44	28.76	27.93	142	-0.009	0.55133877	0.0047861
22-Apr	16:56	10.38	11.73	12.41	13.88	24.38	24.05	131	-0.006	0.64229513	0.0031784
22-Apr	17:16	10.18	11.52	12.10	13.48	20.71	19.75	146	-0.013	0.61795111	0.0037205
22-Apr	17:36	10.43	11.80	12.49	14.16	37.46	34.82	133	-0.040	0.73998570	0.0014433
22-Apr	17:56	10.14	11.43	12.11	13.66	24.48	23.65	149	-0.013	0.66177997	0.0022614
22-Apr	18:17	9.59	10.79	11.45	12.91	24.22	23.94	149	-0.004	0.60685311	0.0026630
22-Apr	18:37	9.80	10.95	11.55	13.14	21.58	20.65	141	-0.019	0.64191159	0.0021622
22-Apr	18:57	10.08	11.28	11.79	13.42	17.01	16.10	140	-0.014	0.63299388	0.0027839
22-Apr	19:17	9.52	10.60	11.23	12.96	41.65	41.03	122	-0.013	0.65695825	0.0015023
22-Apr	19:37	8.64	9.73	10.40	11.76	17.56	16.71	164	-0.013	0.58882622	0.0017297
22-Apr	19:57	9.16	10.31	11.01	12.45	20.18	19.22	121	-0.015	0.62321744	0.0017511
22-Apr	20:17	9.87	11.11	11.81	13.54	37.00	34.38	151	-0.025	0.71381745	0.0012259
22-Apr	20:37	9.60	10.84	11.54	13.16	22.11	20.83	151	-0.012	0.67132626	0.0014705
22-Apr	20:57	9.14	10.29	11.00	12.55	16.64	15.75	136	-0.012	0.64377371	0.0013995
22-Apr	21:17	7.78	8.79	9.37	10.63	19.17	18.22	139	-0.009	0.53184581	0.0016834
22-Apr	21:37	8.75	9.65	10.49	11.78	26.66	25.42	126	-0.012	0.57797310	0.0020042
22-Apr	21:57	9.00	9.92	10.82	12.26	25.52	24.57	155	-0.008	0.61765372	0.0015489
22-Apr	22:17	9.61	10.73	11.59	13.18	26.77	26.19	136	-0.009	0.67140339	0.0014350
22-Apr	22:37	10.57	11.82	12.75	14.48	23.72	22.71	122	-0.018	0.75146217	0.0013357
22-Apr	22:57	10.78	12.04	12.90	14.69	20.16	19.06	136	-0.009	0.73471220	0.0016579
22-Apr	23:17	11.28	12.76	13.60	15.47	19.80	18.83	123	-0.010	0.78413909	0.0015259
22-Apr	23:37	11.51	12.91	13.60	15.47	19.39	17.83	140	-0.011	0.74398138	0.0023231
22-Apr	23:57	10.76	12.23	13.03	14.96	25.10	24.04	138	-0.009	0.78488029	0.0011498
23-Apr	0:17	10.31	11.62	12.30	14.00	29.18	28.33	141	-0.008	0.68564153	0.0019523
23-Apr	0:37	9.86	11.12	11.77	13.47	18.16	17.08	136	-0.009	0.67428125	0.0016418
23-Apr	0:59	9.62	10.77	11.52	13.06	31.45	30.33	140	-0.010	0.64626706	0.0018374
23-Apr	1:19	9.61	10.75	11.41	12.93	33.84	32.25	155	-0.014	0.62992159	0.0021539
23-Apr	1:39	9.24	10.46	11.13	12.66	22.94	21.89	153	-0.010	0.63984320	0.0015636
23-Apr	1:59	9.64	10.85	11.52	13.01	22.52	21.68	125	-0.012	0.63230956	0.0021738
23-Apr	2:19	9.83	11.07	11.71	13.16	19.88	18.80	152	-0.012	0.62389285	0.0027018
23-Apr	2:39	9.16	10.36	10.95	12.50	32.70	31.19	175	-0.061	0.68358674	0.0011029
23-Apr	2:59	8.98	10.03	10.82	12.18	23.30	22.43	139	-0.015	0.60926583	0.0017636
23-Apr	3:19	7.96	8.92	9.50	10.82	20.03	19.08	116	-0.012	0.54003530	0.0017285
23-Apr	3:39	8.07	9.02	9.59	11.00	38.58	36.33	136	-0.026	0.57326517	0.0013361
23-Apr	3:59	7.61	8.53	9.14	10.49	25.83	25.03	149	-0.011	0.54501964	0.0012441
23-Apr	4:19	7.63	8.58	9.12	10.45	18.59	17.28	149	-0.010	0.53062461	0.0014830
23-Apr	4:39	7.75	8.63	9.28	10.57	23.17	22.14	131	-0.011	0.53386161	0.0015528
23-Apr	4:59	7.56	8.42	9.12	10.35	27.85	25.45	162	-0.066	0.58072083	0.0009307
23-Apr	5:19	7.53	8.45	9.01	10.27	25.02	22.19	133	-0.029	0.53644800	0.0013487
23-Apr	5:39	7.14	8.02	8.64	9.75	28.41	26.87	122	-0.017	0.49890384	0.0015046
23-Apr	5:59	7.48	8.49	9.04	10.24	23.64	22.78	140	-0.012	0.51723169	0.0016027
23-Apr	6:19	7.60	8.59	9.10	10.21	21.19	20.16	132	-0.016	0.49342445	0.0023901
23-Apr	6:39	6.71	7.56	8.02	9.01	34.13	32.57	154	-0.016	0.43575913	0.0023661
23-Apr	6:59	6.48	7.30	7.68	8.97	24.18	23.34	134	-0.013	0.47574536	0.0010610
23-Apr	7:19	5.91	6.72	7.06	8.10	23.42	23.04	133	-0.006	0.40422891	0.0016440
23-Apr	7:41	6.96	7.94	8.38	9.55	36.57	35.15	139	-0.014	0.48867514	0.0014752
23-Apr	8:01	5.99	6.86	7.15	8.17	27.22	26.31	150	-0.007	0.40338555	0.0018505
23-Apr	8:21	6.61	7.48	7.78	8.78	34.69	34.85	142	0.004	0.39049478	0.0040917
23-Apr	8:41	7.15	8.04	8.43	9.44	26.47	25.53	147	-0.006	0.42066693	0.0043987
23-Apr	9:01	6.26	7.04	7.29	8.15	27.65	26.82	163	-0.009	0.35068476	0.0062721
23-Apr	9:21	5.62	6.34	6.53	7.23	26.99	26.06	136	-0.007	0.29699131	0.0098782
23-Apr	13:21	4.86	5.43	5.44	5.97	33.24	31.45	166	-0.028	0.22024045	0.0358034
23-Apr	14:01	4.87	5.48	5.52	6.07	26.14	26.41	144	0.006	0.22174913	
23-Apr	14:23	6.09	6.78	7.01	7.80	28.46	26.11	154	-0.154	0.38473789	0.0032245
23-Apr	14:43	7.47	8.41	8.75	9.59	36.01	34.69	116	-0.012	0.39666661	0.0098552
23-Apr	15:03	8.25	9.14	9.69	10.79	38.09	36.28	147	-0.015	0.48192166	0.0046335
23-Apr	15:23	8.77	9.72	10.24	11.41	24.73	21.90	140	-0.025	0.51022956	0.0048515
23-Apr	15:43	8.93	9.98	10.74	11.98	25.35	24.28	132	-0.010	0.57160754	0.0025353
23-Apr	16:03	9.25	10.27	10.85	11.98	23.71	22.84	130	-0.012	0.51226518	0.0068759
23-Apr	16:23	9.17	10.16	10.90	11.96	25.02	24.27	134	-0.017	0.53240341	0.0049783
23-Apr	16:43	9.62	10.74	11.48	12.73	25.28	22.54	140	-0.030	0.60763812	0.0029041
23-Apr	17:03	9.46	10.60	11.32	12.94	18.85	17.38	140	-0.011	0.65729076	0.0014895
23-Apr	17:23	9.32	10.45	11.10	12.49	21.55	20.65	138	-0.016	0.60207201	0.0024129
23-Apr	17:43	8.99	10.05	10.71	11.90	24.61	21.56	128	-0.030	0.56782916	0.0029036
23-Apr	18:03	8.80	9.98	10.47	11.78	26.47	25.96	141	-0.010	0.55387782	0.0028687
23-Apr	18:23	9.05	10.27	10.82	12.19	18.36	16.59	153	-0.076	0.65122567	0.0014120

		Wind Speeds				Temperatures		Wind			
Date	Time	U(1.0)	U(2.11)	U(4.49)	U(9.5)	TL1	TU2	Dir	Ri	U*	Zo
23-Apr	18:43	10.13	11.25	12.13	13.60	31.10	28.17	113	-0.091	0.74129917	0.0012584
23-Apr	19:03	9.64	10.77	11.47	12.96	32.14	30.38	170	-0.074	0.69234715	0.0013733
23-Apr	19:23	9.16	10.41	11.00	12.42	31.14	28.38	142	-0.061	0.66425111	0.0013303
23-Apr	19:43	9.75	10.92	11.55	13.09	16.44	15.55	136	-0.021	0.64267999	0.0021156
23-Apr	20:03	10.12	11.36	12.13	13.57	23.61	22.00	176	-0.032	0.67544654	0.0020568
23-Apr	20:23	9.46	10.55	11.29	12.68	27.10	25.77	122	-0.014	0.60975689	0.0024100
23-Apr	20:43	9.61	10.68	11.31	12.82	38.04	35.49	138	-0.030	0.63054586	0.0021694
23-Apr	21:05	9.76	11.21	11.87	13.27	16.03	15.16	134	-0.016	0.66185867	0.0019018
23-Apr	21:25	8.53	9.61	10.21	11.66	26.65	24.62	139	-0.044	0.62776548	0.0011570
23-Apr	21:45	8.42	9.51	10.06	11.40	31.25	28.61	149	-0.034	0.58559634	0.0016001
23-Apr	22:05	8.44	9.50	9.95	11.15	24.44	22.45	152	-0.043	0.53806492	0.0027828
23-Apr	22:25	8.01	9.06	9.65	10.94	29.46	26.92	159	-0.159	0.66373041	0.0007099
23-Apr	22:45	7.72	8.73	9.24	10.42	23.77	22.74	118	-0.020	0.51529510	0.0020149
23-Apr	23:05	7.36	8.29	8.84	10.06	21.84	20.86	163	-0.023	0.52216751	0.0013833
23-Apr	23:25	6.61	7.46	7.86	9.01	32.70	30.05	161	-0.125	0.52904566	0.0008025
23-Apr	23:45	6.50	7.45	7.83	8.89	27.56	25.29	151	-0.080	0.49797137	0.0010122
24-Apr	0:05	6.65	7.47	7.89	8.93	37.07	34.37	142	-0.027	0.44280620	0.0020278
24-Apr	0:25	6.82	7.69	8.24	9.36	30.53	27.86	181	-0.155	0.57519132	0.0006442
24-Apr	0:45	8.09	9.06	9.65	10.95	31.46	28.79	142	-0.032	0.56273681	0.0015613
24-Apr	1:05	8.84	9.87	10.54	11.96	23.86	22.86	144	-0.008	0.58313444	0.0020235
24-Apr	1:25	8.00	9.07	9.68	10.88	27.47	26.97	144	-0.009	0.53523540	0.0019591
24-Apr	1:45	7.89	8.68	9.32	10.42	24.62	22.46	120	-0.021	0.49079879	0.0029977
24-Apr	2:05	8.76	9.83	10.48	11.88	24.67	23.69	139	-0.008	0.58026786	0.0019958
24-Apr	2:25	9.65	10.84	11.59	13.12	31.57	30.80	155	-0.008	0.64578967	0.0018866
24-Apr	2:45	9.57	10.77	11.36	12.98	30.88	29.89	141	-0.009	0.63752414	0.0019178
24-Apr	3:05	9.92	11.15	11.89	13.37	25.04	22.58	149	-0.029	0.67262261	0.0018511
24-Apr	3:25	9.70	10.84	11.50	13.08	20.46	19.51	148	-0.013	0.63958088	0.0020486
24-Apr	3:47	9.51	10.80	11.38	12.97	23.85	21.99	112	-0.018	0.65961275	0.0015815
24-Apr	4:07	8.95	10.01	10.66	12.12	18.12	17.04	147	-0.009	0.59270407	0.0019779
24-Apr	4:27	8.57	9.56	10.17	11.57	37.17	35.63	137	-0.014	0.57042052	0.0019320
24-Apr	4:47	8.48	9.53	10.13	11.46	23.79	20.92	126	-0.026	0.57815009	0.0017616
24-Apr	5:07	8.25	9.34	9.84	11.21	24.06	23.02	136	-0.015	0.56026085	0.0017674
24-Apr	5:27	9.14	10.31	10.87	12.38	31.00	30.22	157	-0.007	0.60140124	0.0020823
24-Apr	5:47	9.48	10.73	11.39	12.79	33.06	32.19	133	-0.008	0.61230295	0.0024216
24-Apr	6:07	9.59	10.93	11.45	13.07	33.52	31.81	168	-0.019	0.66360434	0.0016096
24-Apr	6:27	8.88	9.99	10.59	11.96	18.21	17.00	150	-0.009	0.57335073	0.0023771
24-Apr	6:47	10.35	11.61	12.32	13.94	23.41	22.37	133	-0.018	0.68549013	0.0020559
24-Apr	7:07	10.37	11.64	12.42	13.94	28.40	27.59	149	-0.010	0.66789313	0.0024410
24-Apr	7:27	11.02	12.34	13.14	14.83	27.57	27.10	132	-0.009	0.71125693	0.0023620
24-Apr	7:47	10.33	11.61	12.37	13.95	25.84	25.01	147	-0.009	0.67567003	0.0021982
24-Apr	8:07	10.97	12.30	13.02	14.73	25.57	24.84	159	-0.014	0.71067088	0.0023321
24-Apr	8:27	11.43	12.80	13.53	15.23	33.15	31.71	141	-0.014	0.71698130	0.0028802
24-Apr	8:47	10.55	11.72	12.58	14.15	18.12	17.25	123	-0.014	0.68449862	0.0022870
24-Apr	9:07	10.52	11.71	12.54	14.20	19.94	18.32	140	-0.012	0.69684923	0.0019884
24-Apr	9:27	11.18	12.57	13.32	14.97	37.88	35.22	111	-0.037	0.74777996	0.0020375
24-Apr	9:47	11.79	13.10	13.98	15.63	26.31	25.47	139	-0.008	0.71509125	0.0035164
24-Apr	10:07	11.98	13.48	14.29	15.99	31.19	30.04	174	-0.030	0.78059051	0.0023888
24-Apr	11:29	11.67	12.99	13.92	15.42	30.05	27.25	133	-0.166	0.85548608	0.0013559
24-Apr	11:49	12.05	13.43	14.19	15.94	22.13	21.05	156	-0.012	0.73161288	0.0035260
24-Apr	12:09	11.24	12.62	13.40	14.96	22.01	21.14	137	-0.013	0.69899369	0.0031073
24-Apr	12:29	10.64	11.83	12.59	14.10	17.54	15.91	133	-0.064	0.71153444	0.0020703
24-Apr	12:49	11.14	12.42	13.08	14.52	30.64	27.90	161	-0.094	0.71590957	0.0027897
24-Apr	13:09	10.15	11.38	11.96	13.25	18.07	16.48	145	-0.053	0.62404713	0.0036148
24-Apr	13:29	10.53	11.81	12.32	13.66	22.88	21.95	116	-0.027	0.60486657	0.0055305
24-Apr	13:49	10.67	12.05	12.61	14.09	34.99	33.10	163	-0.017	0.64725231	0.0037332
24-Apr	14:09	10.66	11.82	12.48	13.92	27.93	27.07	144	-0.011	0.61053606	0.0052496
24-Apr	14:29	11.27	12.62	13.21	14.75	21.05	18.78	132	-0.014	0.65564494	0.0048496
24-Apr	14:49	10.08	11.40	11.97	13.26	25.00	22.20	136	-0.027	0.61372068	0.0037859
24-Apr	15:09	10.29	11.51	12.17	13.51	24.65	23.85	135	-0.020	0.61434131	0.0041468
24-Apr	15:29	9.54	10.60	11.16	12.45	17.58	16.71	149	-0.014	0.54973568	0.0051000
24-Apr	15:49	9.83	10.97	11.55	12.82	23.14	22.17	133	-0.013	0.56118242	0.0055426
24-Apr	16:09	9.42	10.59	11.15	12.33	26.22	25.07	135	-0.010	0.54042956	0.0054381
24-Apr	16:29	9.26	10.41	10.92	12.15	20.34	18.41	142	-0.016	0.54633976	0.0044940
24-Apr	16:49	9.87	11.12	11.62	13.05	22.59	21.13	131	-0.012	0.59608265	0.0037456
24-Apr	17:11	9.63	10.80	11.41	12.83	33.38	30.57	152	-0.106	0.68818162	0.0014797
24-Apr	17:31	9.54	10.66	11.26	12.65	25.60	24.52	140	-0.011	0.58200377	0.0034230
24-Apr	17:51	9.13	10.27	10.87	12.22	31.59	28.82	165	-0.156	0.69668846	0.0010809
24-Apr	18:11	9.27	10.38	11.04	12.31	19.61	18.64	136	-0.012	0.56984351	0.0033287
24-Apr	18:31	9.46	10.58	11.28	12.65	22.42	21.35	135	-0.014	0.60363354	0.0025976

		Wind Speeds				Temperatures		Wind			
Date	Time	U(1.0)	U(2.11)	U(4.49)	U(9.5)	TL1	TU2	Dir	Ri	U*	Zo
24-Apr	18:51	9.39	10.54	11.23	12.84	22.90	21.64	157	-0.032	0.68034942	0.0012272
24-Apr	19:11	8.60	9.67	10.29	11.68	30.25	29.33	140	-0.009	0.57479887	0.0019014
24-Apr	19:31	7.18	8.11	8.54	9.75	23.89	22.85	134	-0.015	0.48763810	0.0017516
24-Apr	19:51	6.94	7.73	8.27	9.56	32.70	31.05	177	-0.030	0.52012969	0.0009795
24-Apr	20:11	7.01	7.89	8.41	9.53	18.50	17.46	136	-0.010	0.47102701	0.0018553
24-Apr	20:31	7.18	8.08	8.54	9.56	24.57	23.54	128	-0.011	0.44487358	0.0031697
24-Apr	20:51	6.82	7.76	8.23	9.24	20.55	19.42	141	-0.010	0.45024919	0.0021518
24-Apr	21:11	6.63	7.33	7.88	8.85	20.12	17.87	181	-0.093	0.47625673	0.0013807
24-Apr	21:31	7.83	8.86	9.39	10.55	28.85	26.64	175	-0.132	0.59875612	0.0010632
24-Apr	21:51	8.56	9.59	10.40	11.75	42.66	41.46	162	-0.068	0.66303183	0.0009104
24-Apr	22:11	8.07	9.03	9.74	10.94	24.81	24.01	128	-0.019	0.55095532	0.0017284
24-Apr	22:31	7.45	8.47	9.06	10.38	29.19	27.41	132	-0.021	0.56345734	0.0009746
24-Apr	22:51	8.29	9.38	10.03	11.30	34.00	32.43	163	-0.015	0.56883917	0.0016947
24-Apr	23:11	7.22	8.12	8.65	9.85	23.51	21.79	145	-0.019	0.50382461	0.0015002
24-Apr	23:31	7.42	8.39	8.93	10.13	21.69	20.79	138	-0.012	0.50914284	0.0016611
24-Apr	23:53	7.37	8.37	8.81	9.98	16.70	15.78	109	-0.014	0.49156964	0.0019997
25-Apr	0:13	7.58	8.54	9.07	10.33	33.79	32.18	129	-0.014	0.52004895	0.0016436
25-Apr	0:33	6.41	7.27	7.72	8.87	27.17	24.98	119	-0.070	0.51047816	0.0007884
25-Apr	0:53	6.06	6.96	7.35	8.55	24.16	23.17	145	-0.008	0.46425093	0.0008759
25-Apr	1:13	6.15	6.94	7.35	8.42	26.74	25.88	135	-0.008	0.42308700	0.0015808
25-Apr	1:33	6.39	7.23	7.63	8.78	23.44	23.21	140	-0.004	0.43966955	0.0015531
25-Apr	1:53	6.48	7.33	7.75	8.71	23.74	22.74	126	-0.010	0.41470718	0.0025722
25-Apr	2:13	7.31	8.28	8.63	9.79	38.70	36.67	134	-0.014	0.46797466	0.0025512
25-Apr	2:33	5.89	6.73	7.17	8.07	19.47	18.46	139	-0.011	0.40647567	0.0016577
25-Apr	2:53	5.46	6.13	6.40	7.34	26.26	25.44	137	-0.011	0.35431043	0.0022267
25-Apr	3:13	6.49	7.38	7.86	8.85	29.56	27.59	146	-0.019	0.44996763	0.0016294
25-Apr	3:33	7.48	8.43	8.85	9.94	32.05	29.53	122	-0.189	0.56956464	0.0011225
25-Apr	3:53	5.80	6.65	7.07	7.95	22.36	19.74	111	-0.020	0.40940954	0.0014960
25-Apr	4:13	4.92	5.67	5.97	6.87	32.32	31.49	133	-0.010	0.36394299	0.0010908
25-Apr	4:33	4.77	5.52	5.81	6.68	35.01	32.23	133	-0.049	0.38312201	0.0007634
25-Apr	4:53	5.48	6.22	6.58	7.57	24.27	21.38	121	-0.024	0.40441641	0.0011053
25-Apr	5:13	5.12	5.82	6.18	7.11	27.69	26.24	121	-0.012	0.37505896	0.0011275
25-Apr	5:53	4.26	4.96	5.22	6.17	37.67	36.01	132	-0.015	0.36396628	0.0005156
25-Apr	8:15	5.29	5.93	6.25	6.96	35.26	32.98	129	-0.028	0.32378106	0.0035604
25-Apr	8:35	5.42	6.05	6.26	7.05	22.73	21.88	146	-0.012	0.30650931	0.0057056
25-Apr	8:55	4.69	5.23	5.40	6.00	27.07	26.20	149	-0.008	0.24286640	
25-Apr	9:15	4.21	4.80	4.80	5.32	21.75	21.36	121	-0.008	0.21135285	
26-Apr	9:23	4.99	5.57	5.69	6.33	34.77	34.93	144	0.007	0.24571996	
27-Apr	17:11	4.77	5.34	5.37	5.90	26.28	26.32	149	0.002	0.20498555	
1-May	0:43	4.57	5.28	5.63	6.66	18.31	17.41	140	-0.010	0.39393479	0.0004820
1-May	1:43	4.95	5.62	6.13	7.12	24.02	22.36	163	-0.029	0.42815581	0.0004927
1-May	2:03	5.32	6.07	6.45	7.50	24.79	23.75	130	-0.012	0.41179153	0.0008287
1-May	2:43	4.92	5.65	6.05	7.19	21.53	20.41	139	-0.013	0.43281906	0.0004333
1-May	3:04	5.74	6.53	6.95	7.99	23.02	22.18	117	-0.018	0.43007251	0.0010138
2-May	4:07	4.43	5.15	5.52	6.56	24.92	22.76	158	-0.073	0.44559358	0.0002722

TRAIL CANYON
DATA FOR NORTHERLY WINDS

		Wind Speed						Temperatures		Wind			
Date	Time	U(0.75)	U(1.25)	U(2.07)	U(3.44)	U(5.72)	U(9.50)	TL1	TU1	Dir	Ri	U*	Zo
2-Apr	19:14	4.51	4.76	4.99	5.27	5.35		30.07	30.13	329	0.022	0.1637568	0.0004961
3-Apr	23:18	4.42	4.73	4.92	5.22	5.51		28.71	29.26	326	0.067	0.1592217	0.0005139
3-Apr	23:38	4.58	4.90	5.11	5.37	5.64		28.09	28.55	323	0.060	0.1600505	0.0007553
4-Apr	8:39	5.38	5.72	6.04	6.35	6.69		26.93	26.59	322	-0.021	0.2736381	0.0000221
4-Apr	8:59	5.33	5.61	5.90	6.26	6.59		27.77	27.10	332	-0.050	0.2778363	0.0000180
4-Apr	9:19	5.46	5.66	6.06	6.33	6.60		28.01	27.58	319	-0.037	0.2559234	0.0000415
4-Apr	9:39	5.34	5.60	5.96	6.24	6.44		28.42	27.85	348	-0.055	0.2511130	0.0000436
4-Apr	10:19	5.20	5.45	5.70	5.98	6.18		29.76	28.85	337	-0.115	0.2306709	0.0000762
4-Apr	10:39	5.77	6.11	6.45	6.68	7.05		30.00	28.97	335	-0.077	0.2817309	0.0000329
4-Apr	11:00	5.21	5.45	5.71	6.01	6.27		30.79	29.71	326	-0.118	0.2489098	0.0000388
4-Apr	11:20	4.52	4.69	4.89	5.16	5.31		31.14	30.06	347	-0.212	0.2037158	0.0000669
4-Apr	11:40	4.51	4.66	4.84	5.09	5.23		31.62	30.61	326	-0.237	0.1888047	0.0001326
4-Apr	12:00	4.10	4.20	4.33	4.59	4.74		32.26	31.17	349	-0.325	0.1808271	0.0000789
4-Apr	12:40	4.24	4.40	4.59	4.79	4.91		33.19	31.99	343	-0.327	0.1823470	0.0001115
4-Apr	13:20	4.57	4.73	4.97	5.17	5.38		34.14	32.80	323	-0.250	0.2085133	0.0000611
11-Apr	5:24	5.67	5.98	6.32	6.65	6.86		30.03	30.48	331	0.047	0.2025813	0.0005750
11-Apr	6:24	4.55	4.84	5.02	5.32	5.43		28.64	29.08	330	0.084	0.1233666	
11-Apr	6:44	4.76	5.06	5.32	5.61	5.79		28.47	28.92	321	0.063	0.1605521	0.0011398
11-Apr	7:04	5.03	5.33	5.60	5.92	6.15		28.91	29.35	330	0.052	0.1824627	0.0004828
11-Apr	7:24	5.53	5.89	6.20	6.55	6.85		29.36	29.68	325	0.028	0.2352459	0.0000967
11-Apr	7:44	6.26	6.63	7.03	7.37	7.62		29.67	29.76	320	0.011	0.2651295	0.0001030
11-Apr	8:04	6.20	6.62	6.98	7.29	7.59		30.10	30.03	323	-0.001	0.2763808	0.0000669
11-Apr	8:24	7.27	7.68	8.19	8.41	9.03		30.53	30.30	323	-0.007	0.3529293	0.0000304
11-Apr	8:44	6.90	7.37	7.83	8.07	8.59		31.00	30.54	336	-0.018	0.3449182	0.0000258
11-Apr	9:04	6.79	7.15	7.54	7.77	8.30		31.43	30.89	341	-0.027	0.3129058	0.0000489
11-Apr	9:24	6.32	6.59	6.99	7.28	7.71		31.58	31.18	329	-0.023	0.2944838	0.0000427
11-Apr	9:44	5.60	5.87	6.21	6.49	6.79		32.09	31.36	355	-0.061	0.2652620	0.0000404
11-Apr	10:05	5.23	5.49	5.78	6.02	6.31		32.48	31.70	350	-0.080	0.2419454	0.0000508
11-Apr	10:25	5.58	5.82	6.17	6.46	6.77		33.00	31.99	331	-0.086	0.2738095	0.0000301
11-Apr	10:45	5.61	5.87	6.16	6.42	6.72		33.08	32.00	346	-0.107	0.2548201	0.0000602
11-Apr	11:05	5.49	5.83	6.11	6.37	6.62		33.68	32.49	346	-0.114	0.2593811	0.0000459
11-Apr	11:25	4.97	5.19	5.49	5.76	5.96		33.93	32.79	327	-0.141	0.2159432	0.0000828
11-Apr	11:45	4.99	5.26	5.50	5.79	5.95		34.28	33.04	330	-0.164	0.2356991	0.0000463
11-Apr	12:05	5.42	5.70	5.98	6.21	6.39		34.70	33.44	318	-0.163	0.2356529	0.0000982
11-Apr	12:25	4.95	5.13	5.38	5.64	5.89		34.65	33.49	340	-0.159	0.2294089	0.0000500
11-Apr	12:45	4.73	4.88	5.15	5.31	5.48		35.27	34.03	359	-0.268	0.1980144	0.0001382
11-Apr	13:05	4.25	4.36	4.58	4.80	4.92		35.53	34.42	338	-0.299	0.1868633	0.0000848
11-Apr	13:25	4.69	4.86	5.07	5.32	5.48		36.09	34.87	359	-0.237	0.2051718	0.0000891
11-Apr	13:45	4.85	4.99	5.24	5.51	5.70		36.09	34.79	356	-0.219	0.2223011	0.0000558
11-Apr	14:45	4.48	4.60	4.85	5.15	5.27		36.55	35.33	335	-0.237	0.2179976	0.0000336
11-Apr	15:25	4.51	4.63	4.91	5.16	5.28		36.31	35.42	355	-0.178	0.2038845	0.0000621
11-Apr	16:05	4.08	4.25	4.39	4.59	4.70		37.00	36.15	350	-0.261	0.1609489	0.0002546
12-Apr	4:47	5.52	5.87	6.19	6.49	6.78		27.60	28.11	326	0.047	0.2071246	0.0003427
12-Apr	8:08	5.00	5.28	5.57	5.83	6.17		28.40	28.25	330	-0.009	0.2377659	0.0000364
12-Apr	8:48	6.10	6.44	6.85	7.16	7.48		29.60	28.99	325	-0.038	0.3001609	0.0000295
12-Apr	9:08	6.24	6.59	6.99	7.29	7.69		30.02	29.51	320	-0.028	0.3064348	0.0000292
12-Apr	9:28	5.99	6.38	6.70	7.02	7.33		30.24	29.64	321	-0.039	0.2867427	0.0000382
12-Apr	9:48	5.91	6.23	6.59	6.83	7.12		30.60	29.83	331	-0.063	0.2681405	0.0000613
12-Apr	10:08	5.13	5.38	5.66	5.96	6.19		31.19	30.25	351	-0.101	0.2474710	0.0000359
12-Apr	10:28	4.98	5.23	5.57	5.83	6.02		31.57	30.59	341	-0.110	0.2485802	0.0000280
12-Apr	10:48	5.31	5.53	5.86	6.12	6.39		32.15	31.04	359	-0.116	0.2553658	0.0000365
12-Apr	11:28	5.71	5.97	6.35	6.65	6.89		32.61	31.38	325	-0.108	0.2810479	0.0000307
12-Apr	11:48	5.15	5.40	5.66	5.96	6.16		33.12	31.93	320	-0.143	0.2439978	0.0000433
12-Apr	12:08	5.45	5.77	6.07	6.31	6.56		33.43	32.21	326	-0.121	0.2571042	0.0000464
12-Apr	12:28	5.47	5.68	6.02	6.30	6.47		33.56	32.26	342	-0.159	0.2524066	0.0000540
12-Apr	12:49	4.95	5.15	5.42	5.64	5.81		34.14	32.97	332	-0.193	0.2162146	0.0000913
12-Apr	13:09	4.89	5.14	5.40	5.60	5.79		34.24	32.99	320	-0.188	0.2203444	0.0000714
12-Apr	13:29	5.24	5.48	5.74	5.96	6.12		34.42	33.19	340	-0.194	0.2194544	0.0001398
12-Apr	13:49	4.94	5.15	5.42	5.64	5.67		34.92	33.69	345	-0.281	0.2078458	0.0001398
12-Apr	14:09	5.07	5.35	5.63	5.86	5.92		35.14	33.92	342	-0.205	0.2244824	0.0000870
12-Apr	14:29	5.47	5.78	6.13	6.38	6.59		35.51	34.19	323	-0.128	0.2671615	0.0000348
12-Apr	14:49	4.49	4.68	4.95	5.13	5.29		35.30	34.11	339	-0.226	0.2049953	0.0000631
12-Apr	15:49	4.34	4.61	4.82	5.08	5.32		35.83	34.76	318	-0.134	0.2281728	0.0000190

		Wind Speed						Temperatures		Wind			
Date	Time	U(0.75)	U(1.25)	U(2.07)	U(3.44)	U(5.72)	U(9.50)	TL1	TU1	Dir	Ri	U*	Zo
26-Apr	18:42	4.25	4.50	4.91	5.26	5.29	5.97	26.28	24.40	130	0.133	0.2943180	0.0001539
26-Apr	22:22	4.08	4.23	4.64	4.97	4.97	5.71	22.41	21.03	147	0.137	0.2665050	0.0002059
26-Apr	22:42	4.33	4.58	4.92	5.20	5.19	5.83	22.00	20.57	162	0.119	0.2499473	0.0005085
27-Apr	15:25	4.58	4.75	5.14	5.55	5.64	6.10	25.89	23.28	125	0.108	0.3127773	0.0001621
1-May	0:17	4.02	4.45	4.71	5.10	5.04	5.76	27.61	26.40	159	0.111	0.2767620	0.0001665
1-May	0:37	4.14	4.62	4.88	5.28	5.29	5.85	27.39	26.10	169	0.102	0.2922386	0.0001446
1-May	0:57	4.88	5.59	5.90	6.28	6.34	7.00	27.21	25.88	163	0.068	0.3515795	0.0001317
1-May	1:17	5.03	5.73	6.06	6.48	6.60	7.19	27.02	25.66	169	0.063	0.3658730	0.0001223
1-May	1:37	4.15	4.64	4.88	5.22	5.25	5.81	26.76	25.42	159	0.104	0.2788294	0.0001991
1-May	3:38	6.04	6.80	7.16	7.60	7.77	8.54	25.85	24.50	162	0.041	0.3934223	0.0002302
1-May	3:58	6.04	6.64	7.13	7.47	7.74	8.36	25.60	24.22	164	0.043	0.3821202	0.0002664
1-May	4:18	5.71	6.30	6.77	7.11	7.34	8.00	25.26	23.88	174	0.047	0.3711611	0.0002271
1-May	4:38	5.61	6.18	6.57	6.94	7.11	7.63	25.29	23.93	171	0.051	0.3474861	0.0003118
1-May	4:58	5.38	5.92	6.32	6.59	6.77	7.43	25.03	23.66	149	0.057	0.3248833	0.0003762
1-May	5:18	5.14	5.64	6.00	6.36	6.42	7.08	24.99	23.68	176	0.063	0.3152807	0.0003365
1-May	5:38	5.02	5.54	5.89	6.22	6.34	6.95	24.87	23.55	169	0.066	0.3146210	0.0002950
1-May	5:58	5.24	5.86	6.21	6.56	6.72	7.31	24.73	23.40	160	0.058	0.3423124	0.0002283
1-May	6:18	4.95	5.46	5.79	6.14	6.31	6.89	24.66	23.31	175	0.068	0.3166601	0.0002556
1-May	6:38	4.32	4.77	5.03	5.31	5.31	5.95	24.67	23.28	175	0.098	0.2639969	0.0003689
1-May	7:38	4.66	5.20	5.38	5.71	5.97	6.49	25.80	23.95	153	0.088	0.3018504	0.0002449
1-May	7:58	5.50	6.08	6.40	6.72	6.95	7.48	26.39	24.43	163	0.061	0.3373955	0.0003463
1-May	8:18	5.84	6.44	6.73	7.09	7.29	7.99	26.84	24.71	173	0.054	0.3423352	0.0004730
1-May	8:38	5.81	6.46	6.80	7.10	7.36	7.95	27.38	25.15	161	0.056	0.3591933	0.0003337
1-May	8:58	5.20	5.79	6.06	6.32	6.50	7.05	28.07	25.72	157	0.078	0.3175861	0.0003783
1-May	9:18	4.96	5.42	5.66	5.97	6.16	6.72	28.38	25.97	155	0.091	0.2965793	0.0004228
1-May	9:38	4.13	4.47	4.61	4.79	4.93	5.35	28.85	26.24	137	0.159	0.2266761	0.0008751

		Wind Speed						Temperatures		Wind			
Date	Time	U(0.75)	U(1.25)	U(2.07)	U(3.44)	U(5.72)	U(9.50)	TL1	TU1	Dir	Ri	U*	Zo
24-Apr	12:14	10.02	10.68	11.43	12.11	12.92	13.77	22.81	19.64	132	0.009	0.6321180	0.0002367
24-Apr	12:34	9.20	9.73	10.62	11.28	11.98	12.62	23.18	19.98	148	0.012	0.6266965	0.0001460
24-Apr	12:54	8.46	9.03	9.55	10.17	10.67	11.34	23.77	20.67	125	0.018	0.5016328	0.0003752
24-Apr	13:14	10.63	11.30	11.96	12.74	13.58	14.33	23.54	20.38	127	0.008	0.6418258	0.0003091
24-Apr	13:34	9.38	10.04	10.65	11.25	11.92	12.71	23.49	20.32	158	0.013	0.5577348	0.0003641
24-Apr	13:54	8.22	8.69	9.22	9.88	10.47	11.14	23.93	20.77	164	0.020	0.5149837	0.0002471
24-Apr	14:14	9.16	9.74	10.43	11.07	11.78	12.36	23.93	20.75	133	0.014	0.5810705	0.0002300
24-Apr	14:34	8.09	8.45	9.14	9.69	10.30	10.88	24.14	20.96	157	0.021	0.5155225	0.0002175
24-Apr	14:54	8.06	8.49	9.05	9.63	10.23	10.81	23.92	20.85	139	0.021	0.4973789	0.0002723
24-Apr	15:14	7.28	7.66	8.16	8.64	9.19	9.72	23.89	20.86	145	0.029	0.4441326	0.0002993
24-Apr	15:34	6.05	6.43	6.70	7.11	7.60	7.92	23.57	20.82	120	0.050	0.3628916	0.0003476
24-Apr	15:54	6.16	6.35	6.84	7.30	7.71	8.11	23.97	21.08	179	0.048	0.3930646	0.0002174
24-Apr	16:14	5.01	5.35	5.65	6.04	6.28	6.73	23.82	21.02	182	0.079	0.3222276	0.0002432
24-Apr	16:34	5.39	5.68	6.00	6.42	6.70	7.13	23.83	21.08	121	0.068	0.3324811	0.0003011
24-Apr	16:54	5.19	5.50	5.85	6.23	6.56	6.96	23.65	21.12	123	0.073	0.3352328	0.0002232
24-Apr	17:14	6.44	6.73	7.27	7.74	8.28	8.75	23.35	20.74	127	0.039	0.4336493	0.0001550
24-Apr	17:34	6.29	6.61	7.09	7.54	8.02	8.54	23.22	20.76	145	0.042	0.4060226	0.0002067
24-Apr	19:55	6.48	6.77	7.37	7.85	8.25	8.91	20.11	18.59	143	0.031	0.4125939	0.0002165
24-Apr	20:15	5.88	6.22	6.56	7.04	7.47	8.18	19.80	18.32	158	0.041	0.3607937	0.0002799
24-Apr	20:35	6.00	6.44	6.74	7.21	7.70	8.30	19.53	18.07	135	0.038	0.3725717	0.0002656
24-Apr	20:55	6.41	6.95	7.35	7.81	8.44	8.87	19.15	17.71	130	0.029	0.4301110	0.0001637
24-Apr	21:15	6.66	7.23	7.63	8.17	8.81	9.45	18.72	17.26	118	0.024	0.4556647	0.0001446
24-Apr	21:35	7.27	7.93	8.29	8.85	9.48	10.03	18.29	16.81	124	0.018	0.4642134	0.0002254
24-Apr	21:55	7.63	8.25	8.63	9.22	9.79	10.42	17.99	16.52	123	0.015	0.4594022	0.0003280
24-Apr	22:15	7.53	8.13	8.48	8.94	9.71	10.33	17.68	16.21	140	0.016	0.4547281	0.0003113
24-Apr	22:35	7.55	8.20	8.62	9.12	9.97	10.55	17.28	15.81	142	0.014	0.5007188	0.0001705
24-Apr	22:55	7.87	8.48	8.84	9.37	10.15	10.73	16.87	15.40	138	0.012	0.4764527	0.0003026
24-Apr	23:15	6.67	7.01	7.42	7.92	8.58	9.07	16.45	14.98	130	0.021	0.4223997	0.0002127
24-Apr	23:35	7.23	7.63	8.14	8.65	9.32	9.88	16.02	14.54	141	0.014	0.4556074	0.0002249
24-Apr	23:55	7.01	7.38	7.84	8.34	9.07	9.63	15.75	14.30	126	0.016	0.4494764	0.0001960
25-Apr	0:15	7.29	7.68	8.18	8.70	9.42	9.97	15.55	14.10	138	0.010	0.4633935	0.0002088
25-Apr	0:36	7.21	7.44	8.09	8.59	9.31	9.80	15.41	13.96	146	0.011	0.4752752	0.0001576
25-Apr	0:56	7.58	7.97	8.66	9.14	9.84	10.39	15.22	13.78	129	0.008	0.4937628	0.0001818
25-Apr	1:16	6.63	6.82	7.41	7.85	8.49	9.03	14.97	13.54	138	0.013	0.4280016	0.0001804
25-Apr	1:36	6.65	6.86	7.44	7.95	8.60	9.15	14.83	13.40	141	0.013	0.4466873	0.0001409
25-Apr	1:56	5.86	6.26	6.57	7.01	7.63	8.16	14.61	13.20	136	0.019	0.3853457	0.0001760
25-Apr	2:16	5.12	5.48	5.70	6.19	6.54	7.10	14.31	12.90	139	0.027	0.3264750	0.0002255
25-Apr	2:36	5.28	5.64	5.89	6.35	6.78	7.32	14.24	12.84	134	0.024	0.3380218	0.0002160
25-Apr	2:56	6.97	7.45	7.82	8.36	8.89	9.57	14.39	13.00	150	0.010	0.4166178	0.0003354
25-Apr	3:16	7.42	7.88	8.41	8.95	9.65	10.32	14.47	13.08	145	0.007	0.4789571	0.0001947
25-Apr	3:36	6.18	6.49	6.96	7.43	7.78	8.54	14.36	12.97	140	0.015	0.3712306	0.0003239
25-Apr	3:56	5.97	6.21	6.68	7.11	7.44	8.21	14.28	12.90	151	0.017	0.3496882	0.0003784
25-Apr	4:16	6.00	6.31	6.69	7.18	7.59	8.30	14.14	12.76	149	0.016	0.3640659	0.0002970
25-Apr	4:36	5.72	6.09	6.35	6.86	7.28	7.96	13.88	12.50	131	0.018	0.3522189	0.0002743
25-Apr	4:56	5.56	5.97	6.18	6.62	6.97	7.52	13.93	12.56	153	0.022	0.3176502	0.0004858
25-Apr	5:16	5.23	5.54	5.83	6.28	6.51	7.12	13.82	12.46	150	0.025	0.3062334	0.0004063
25-Apr	5:36	4.88	5.18	5.45	5.83	6.08	6.74	13.83	12.48	150	0.031	0.2848026	0.0004241
25-Apr	5:56	4.52	4.77	5.04	5.49	5.70	6.24	13.77	12.45	153	0.038	0.2908195	0.0002148
25-Apr	7:17	4.74	4.83	5.23	5.58	5.79	6.34	14.38	12.72	130	0.040	0.2877305	0.0003018
25-Apr	7:37	4.62	4.75	5.07	5.40	5.59	6.06	14.99	13.17	155	0.047	0.2672301	0.0004460
25-Apr	7:57	4.95	5.03	5.43	5.85	6.04	6.56	15.62	13.64	126	0.041	0.3096382	0.0002468
25-Apr	8:17	4.67	4.90	5.04	5.41	5.66	6.08	16.16	14.05	136	0.054	0.2619256	0.0005761
25-Apr	8:57	4.00	4.16	4.34	4.59	4.80	5.20	17.26	14.88	133	0.092	0.2334832	0.0004754
26-Apr	2:59	4.14	4.37	4.55	4.82	4.96	5.51	16.47	15.10	148	0.068	0.2136484	0.0011501
26-Apr	5:20	4.19	4.28	4.60	4.87	4.91	5.61	15.93	14.61	156	0.065	0.2247858	0.0007979
26-Apr	5:40	4.30	4.44	4.73	5.09	5.21	5.87	15.85	14.54	160	0.058	0.2491868	0.0004333
26-Apr	6:00	5.07	5.06	5.53	5.96	6.13	6.79	15.64	14.29	152	0.037	0.3085560	0.0002659
26-Apr	6:20	5.62	5.67	6.18	6.59	6.87	7.57	15.30	13.90	148	0.027	0.3307057	0.0003378
26-Apr	6:40	5.08	5.19	5.55	5.96	6.22	6.78	15.07	13.65	149	0.035	0.2964425	0.0003757
26-Apr	7:00	4.97	5.11	5.48	5.87	5.98	6.66	15.25	13.73	144	0.038	0.2806003	0.0005153
26-Apr	7:20	5.55	5.65	6.07	6.48	6.68	7.45	15.72	14.02	159	0.030	0.3081894	0.0005489
26-Apr	7:40	5.59	5.82	6.21	6.62	6.90	7.53	16.18	14.31	139	0.030	0.3259402	0.0004102
26-Apr	8:00	5.89	6.19	6.49	6.89	7.15	7.85	16.70	14.69	155	0.028	0.3101060	0.0009094
26-Apr	8:20	5.54	5.89	6.15	6.51	6.82	7.42	17.43	15.28	134	0.036	0.3069650	0.0006407
26-Apr	8:40	5.22	5.47	5.71	6.09	6.33	6.84	17.95	15.71	143	0.046	0.2870875	0.0006678
26-Apr	9:00	4.88	5.09	5.31	5.65	5.80	6.33	18.59	16.19	122	0.060	0.2610582	0.0008747
26-Apr	9:20	4.28	4.46	4.66	4.93	5.03	5.43	19.19	16.86	124	0 090	0.2317078	0.0008641
26-Apr	14:41	4.01	4.10	4.52	4.76	4.71	5.18	25.97	22.99	136	0.159	0.2944971	0.0001257
26-Apr	16:01	4.01	4.21	4.52	4.72	4.75	5.33	26.66	23.73	118	0.171	0.2561845	0.0003036

		Wind Speed						Temperatures		Wind			
Date	Time	U(0.75)	U(1.25)	U(2.07)	U(3.44)	U(5.72)	U(9.50)	TL1	TU1	Dir	Ri	U*	Zo
23-Apr	7:49	5.67	5.94	6.26	6.69	7.16	7.53	21.06	19.19	131	0.045	0.3492729	0.0002691
23-Apr	8:09	6.29	6.59	6.97	7.33	7.93	8.35	21.67	19.66	135	0.036	0.3742879	0.0003360
23-Apr	8:30	6.19	6.45	6.86	7.36	7.91	8.35	22.24	20.00	139	0.038	0.4055209	0.0001766
23-Apr	8:50	5.04	5.36	5.72	6.05	6.38	6.77	22.95	20.56	133	0.067	0.3246832	0.0002307
23-Apr	9:50	4.62	4.76	5.05	5.37	5.54	5.98	24.72	21.96	116	0.101	0.2745869	0.0004036
23-Apr	13:30	4.53	4.67	4.98	5.13	5.26	5.63	29.30	26.18	128	0.148	0.2477717	0.0008498
23-Apr	13:50	5.77	6.04	6.53	6.81	7.08	7.53	30.20	26.49	131	0.076	0.3506164	0.0003509
23-Apr	14:10	6.00	6.37	6.92	7.21	7.53	7.99	30.13	26.53	119	0.066	0.3852148	0.0002446
23-Apr	14:30	6.59	7.01	7.50	7.87	8.37	8.80	29.97	26.58	129	0.052	0.4164780	0.0002543
23-Apr	14:50	6.87	7.35	7.92	8.30	8.81	9.34	29.89	26.56	120	0.045	0.4474001	0.0002114
23-Apr	15:11	6.95	7.44	7.95	8.33	8.85	9.31	30.03	26.85	130	0.045	0.4339528	0.0002760
23-Apr	15:31	7.38	7.88	8.50	8.91	9.51	10.00	29.82	26.83	114	0.038	0.4788930	0.0002085
23-Apr	15:51	6.84	7.46	8.04	8.45	9.02	9.58	30.25	27.15	110	0.044	0.4841771	0.0001303
23-Apr	16:11	7.22	7.82	8.59	9.15	9.79	10.33	29.83	26.93	128	0.035	0.5697745	0.0000682
23-Apr	16:31	6.94	7.61	8.18	8.70	9.34	9.80	29.61	26.86	111	0.040	0.5210745	0.0000913
23-Apr	16:51	7.08	7.76	8.42	8.87	9.58	10.19	29.00	26.43	119	0.037	0.5371752	0.0000857
23-Apr	17:11	7.33	8.02	8.64	9.14	9.77	10.27	28.58	26.23	128	0.034	0.5253254	0.0001176
23-Apr	17:31	7.40	8.06	8.74	9.28	10.01	10.63	28.42	26.13	141	0.032	0.5588552	0.0000851
23-Apr	17:51	7.75	8.55	9.19	9.72	10.49	11.04	28.18	26.04	120	0.028	0.5739688	0.0000969
23-Apr	18:11	7.86	8.51	9.16	9.79	10.52	11.20	27.64	25.60	120	0.026	0.5681375	0.0001056
23-Apr	18:31	7.15	7.95	8.70	9.32	9.92	10.50	27.31	25.40	114	0.030	0.5925158	0.0000548
23-Apr	18:51	8.18	8.64	9.65	10.30	11.08	11.95	26.28	24.40	120	0.021	0.6408601	0.0000639
23-Apr	19:11	9.31	10.02	11.12	11.86	12.72	13.69	25.51	23.70	122	0.013	0.7300747	0.0000660
23-Apr	19:31	8.95	9.78	10.70	11.36	12.15	13.06	25.12	23.39	131	0.014	0.6734464	0.0000859
23-Apr	19:51	10.15	11.03	12.19	13.05	13.89	14.92	24.60	22.92	114	0.009	0.7938902	0.0000681
23-Apr	20:11	10.71	11.74	12.83	13.82	14.79	15.86	24.10	22.44	117	0.007	0.8491160	0.0000637
23-Apr	20:31	10.31	11.17	12.14	12.90	13.72	14.64	23.81	22.18	116	0.008	0.7165597	0.0001314
23-Apr	20:51	9.92	10.50	11.45	12.02	12.81	13.81	23.52	21.92	105	0.010	0.6208671	0.0002397
23-Apr	21:11	10.08	10.76	11.76	12.44	13.20	14.18	23.37	21.79	115	0.009	0.6684267	0.0001694
23-Apr	21:31	10.43	11.27	12.18	12.92	13.85	14.84	23.14	21.57	115	0.008	0.7103458	0.0001456
23-Apr	22:52	9.66	10.35	11.31	12.02	12.79	13.62	22.03	20.47	111	0.009	0.6681010	0.0001319
23-Apr	23:12	9.56	10.36	11.32	12.07	12.86	13.77	21.82	20.26	133	0.009	0.6970725	0.0000996
23-Apr	23:52	7.74	8.29	9.20	9.91	10.58	11.39	21.43	19.87	119	0.017	0.6206592	0.0000584
24-Apr	0:12	8.58	9.26	10.23	10.95	11.72	12.63	21.35	19.81	119	0.010	0.6712251	0.0000672
24-Apr	0:32	8.67	9.37	10.30	10.93	11.64	12.50	21.16	19.60	105	0.010	0.6347834	0.0000979
24-Apr	0:52	8.52	9.16	9.95	10.64	11.37	12.00	20.88	19.33	113	0.011	0.6079704	0.0001106
24-Apr	1:12	8.60	9.26	10.09	10.77	11.64	12.41	20.60	19.03	119	0.010	0.6409924	0.0000857
24-Apr	1:32	9.34	10.13	10.92	11.59	12.42	13.21	20.29	18.73	131	0.007	0.6418467	0.0001403
24-Apr	1:52	10.46	11.34	12.17	12.85	13.76	14.52	20.02	18.46	122	0.005	0.6806470	0.0001954
24-Apr	2:12	10.22	10.87	11.74	12.45	13.41	14.21	19.62	18.05	144	0.005	0.6714665	0.0001728
24-Apr	2:32	9.66	10.25	11.09	11.73	12.65	13.34	19.25	17.68	130	0.006	0.6328713	0.0001757
24-Apr	2:52	10.23	10.89	11.92	12.66	13.68	14.46	18.93	17.35	132	0.004	0.7285646	0.0001068
24-Apr	3:12	9.82	10.37	11.29	11.95	12.88	13.69	18.66	17.09	132	0.005	0.6532011	0.0001579
24-Apr	3:32	10.26	10.95	11.87	12.61	13.55	14.36	18.36	16.81	124	0.004	0.6924109	0.0001484
24-Apr	3:52	10.20	10.68	11.52	12.18	13.11	13.92	18.13	16.58	107	0.004	0.6251422	0.0002583
24-Apr	4:12	9.95	10.60	11.38	12.08	12.86	13.50	17.79	16.24	149	0.004	0.6175685	0.0002543
24-Apr	4:33	10.16	10.79	11.62	12.19	13.10	14.01	17.53	15.98	138	0.003	0.6178522	0.0002877
24-Apr	4:53	10.06	10.62	11.46	12.10	13.08	13.86	17.36	15.84	125	0.003	0.6388816	0.0002091
24-Apr	5:13	10.19	10.72	11.54	12.29	13.20	14.05	17.00	15.47	120	0.003	0.6446819	0.0002119
24-Apr	5:33	10.80	11.40	12.37	13.10	14.11	14.92	16.80	15.30	119	0.002	0.7010759	0.0001817
24-Apr	5:53	10.66	11.32	12.35	13.12	14.03	14.91	16.55	15.05	130	0.001	0.7165617	0.0001506
24-Apr	6:13	11.23	12.00	13.05	13.76	14.69	15.63	16.37	14.86	130	0.001	0.7266457	0.0001953
24-Apr	6:33	10.45	11.08	12.11	12.82	13.77	14.59	16.18	14.65	144	0.001	0.7052899	0.0001463
24-Apr	6:53	10.70	11.42	12.19	12.84	13.83	14.68	16.13	14.61	143	0.001	0.6486226	0.0002935
24-Apr	7:13	9.24	9.71	10.40	10.99	11.88	12.60	16.24	14.62	118	0.004	0.5664920	0.0002609
24-Apr	7:33	9.98	10.58	11.34	11.97	12.80	13.56	16.64	14.85	143	0.003	0.6009794	0.0003083
24-Apr	7:53	10.00	10.57	11.36	12.04	12.94	13.71	17.10	15.18	117	0.003	0.6297373	0.0002250
24-Apr	8:13	10.49	11.15	11.88	12.57	13.54	14.34	17.50	15.49	129	0.003	0.6438105	0.0002688
24-Apr	8:33	11.28	11.96	12.89	13.48	14.46	15.41	17.87	15.78	130	0.002	0.6729036	0.0003297
24-Apr	8:53	11.36	12.18	13.16	13.95	14.94	15.85	18.40	16.17	118	0.002	0.7546392	0.0001677
24-Apr	9:13	10.96	11.72	12.84	13.72	14.63	15.57	18.95	16.64	133	0.003	0.7898512	0.0001032
24-Apr	9:33	10.91	11.54	12.46	13.11	14.21	14.94	19.40	17.12	133	0.004	0.7008011	0.0001975
24-Apr	9:53	11.76	12.46	13.30	13.86	15.01	15.91	19.71	17.21	129	0.003	0.6829321	0.0003909
24-Apr	10:13	11.38	11.92	13.03	13.77	14.87	15.62	20.14	17.54	142	0.003	0.7597080	0.0001522
24-Apr	10:33	11.68	12.15	13.16	13.90	15.00	15.83	20.55	17.88	136	0.004	0.7285999	0.0002277
24-Apr	10:53	13.05	13.70	14.72	15.59	16.87	17.91	20.70	17.88	144	0.002	0.8175818	0.0002237
24-Apr	11:14	12.83	13.71	14.68	15.66	16.93	17.86	21.05	18.20	130	0.002	0.8605396	0.0001527
24-Apr	11:34	11.78	12.52	13.47	14.30	15.26	16.12	21.45	18.58	121	0.004	0.7479028	0.0002199
24-Apr	11:54	10.74	11.36	12.37	13.12	14.05	14.85	21.92	18.90	114	0.006	0.7238688	0.0001508

		Wind Speed						Temperatures		Wind			
Date	Time	U(0.75)	U(1.25)	U(2.07)	U(3.44)	U(5.72)	U(9.50)	TL1	TU1	Dir	Ri	U*	Zo
22-Apr	5:25	5.64	5.91	6.26	6.74	7.25	7.71	21.95	22.26	153	0.045	0.3030740	0.0005732
22-Apr	5:46	4.97	5.17	5.45	5.79	6.18	6.80	21.72	22.01	164	0.065	0.2157613	0.0033456
22-Apr	6:26	4.01	4.13	4.36	4.71	5.03	5.50	21.37	21.71	173	0.108	0.1726489	0.0032633
22-Apr	6:46	4.27	4.32	4.65	4.92	5.33	5.74	21.28	21.54	178	0.097	0.1939889	0.0019034
22-Apr	7:06	4.15	4.20	4.55	4.89	5.15	5.58	21.57	21.73	176	0.101	0.1973570	0.0013504
22-Apr	8:26	4.33	4.48	4.71	4.98	5.13	5.64	24.07	23.58	181	0.114	0.1921924	0.0034166
22-Apr	8:46	5.24	5.43	5.76	6.10	6.37	6.76	24.61	24.02	168	0.072	0.2593757	0.0012826
22-Apr	9:06	5.14	5.29	5.53	5.93	6.32	6.67	25.37	24.60	135	0.080	0.2767716	0.0006137
22-Apr	9:26	5.64	5.89	6.16	6.57	6.98	7.30	25.72	24.98	151	0.064	0.2981479	0.0007467
22-Apr	9:46	4.23	4.27	4.52	4.83	4.99	5.32	26.31	25.35	142	0.141	0.2144059	0.0010550
22-Apr	10:06	4.64	4.79	5.04	5.32	5.54	5.85	26.80	25.59	127	0.115	0.2287156	0.0014517
22-Apr	10:26	4.40	4.59	4.88	5.17	5.41	5.71	27.38	25.79	121	0.127	0.2555720	0.0004391
22-Apr	11:26	4.39	4.50	4.76	4.99	5.11	5.56	28.85	27.38	162	0.149	0.2093274	0.0020894
22-Apr	11:46	4.40	4.51	4.76	4.98	5.11	5.44	29.09	27.62	103	0.153	0.2054286	0.0025102
22-Apr	12:06	4.29	4.37	4.60	4.83	4.94	5.31	29.43	27.89	139	0.168	0.2018577	0.0023609
22-Apr	12:27	4.67	4.79	5.07	5.33	5.44	5.87	30.06	28.45	127	0.136	0.2246527	0.0019313
22-Apr	12:47	4.81	5.04	5.36	5.66	5.69	6.06	30.54	28.93	132	0.121	0.2506402	0.0010623
22-Apr	13:07	4.47	4.66	4.87	5.17	5.27	5.63	31.37	29.73	150	0.156	0.2239898	0.0014360
22-Apr	13:27	4.63	4.80	5.04	5.33	5.46	5.83	31.74	30.10	141	0.147	0.2290792	0.0015459
22-Apr	13:47	6.14	6.43	6.84	7.18	7.63	8.02	32.51	30.82	133	0.072	0.3416501	0.0005567
22-Apr	14:07	6.86	7.29	7.72	8.17	8.60	9.07	33.09	31.43	126	0.054	0.3878440	0.0005115
22-Apr	14:27	7.12	7.52	7.93	8.37	8.85	9.46	33.58	32.01	135	0.051	0.3829912	0.0007154
22-Apr	14:47	7.19	7.64	8.11	8.61	9.05	9.69	33.87	32.25	147	0.049	0.4131827	0.0004503
22-Apr	15:07	7.64	8.14	8.58	9.07	9.63	10.27	34.00	32.68	143	0.043	0.4252446	0.0005528
22-Apr	15:27	7.97	8.48	9.13	9.67	10.33	10.91	34.24	32.89	154	0.037	0.5046792	0.0002242
22-Apr	15:47	9.49	10.22	11.00	11.62	12.47	13.22	34.14	32.89	128	0.022	0.6162777	0.0001933
22-Apr	16:07	10.13	10.81	11.88	12.59	13.51	14.37	34.17	32.94	110	0.018	0.7113818	0.0001169
22-Apr	16:27	10.21	10.83	11.98	12.72	13.64	14.48	33.89	32.88	137	0.017	0.7263082	0.0001061
22-Apr	16:47	9.86	10.55	11.63	12.32	13.19	13.96	33.63	32.80	130	0.019	0.6958788	0.0001137
22-Apr	17:07	9.38	10.11	10.90	11.65	12.55	13.31	33.40	32.71	129	0.022	0.6472973	0.0001290
22-Apr	17:27	9.99	10.58	11.45	12.13	13.07	13.84	32.69	32.21	138	0.019	0.6317279	0.0002099
22-Apr	17:47	9.47	10.05	10.99	11.69	12.55	13.28	31.85	31.59	123	0.020	0.6317462	0.0001503
22-Apr	18:07	9.40	9.99	10.81	11.50	12.32	13.09	31.13	31.06	130	0.020	0.5804688	0.0002392
22-Apr	18:27	9.43	10.03	10.93	11.56	12.57	13.20	30.70	30.74	115	0.019	0.6171680	0.0001632
22-Apr	18:47	9.85	10.40	11.26	11.89	12.78	13.62	30.32	30.40	141	0.018	0.5783692	0.0003289
22-Apr	19:08	9.64	10.39	11.01	11.60	12.66	13.21	29.66	29.78	139	0.018	0.5731862	0.0003116
22-Apr	19:28	10.05	10.82	11.37	12.02	13.07	13.76	29.07	29.23	155	0.016	0.5719694	0.0004198
22-Apr	19:48	8.84	9.29	9.98	10.47	11.12	12.02	28.71	28.92	144	0.023	0.4439325	0.0010577
22-Apr	20:08	8.68	9.16	9.88	10.40	11.14	11.94	28.08	28.29	156	0.023	0.4783216	0.0005180
22-Apr	20:28	7.01	7.49	8.04	8.56	9.10	9.79	27.54	27.78	160	0.039	0.4016109	0.0004061
22-Apr	20:48	6.43	6.89	7.30	7.78	8.19	8.87	26.85	27.11	158	0.049	0.3321081	0.0008930
22-Apr	21:08	7.89	8.28	8.97	9.58	10.22	10.85	26.20	26.43	111	0.027	0.4617505	0.0003279
22-Apr	21:28	7.97	8.41	8.99	9.48	10.19	10.73	25.91	26.15	138	0.027	0.4252397	0.0006495
22-Apr	21:48	8.04	8.64	9.27	9.79	10.60	11.16	25.46	25.68	136	0.024	0.4870437	0.0002769
22-Apr	22:08	8.27	8.83	9.42	9.92	10.70	11.22	25.24	25.47	149	0.023	0.4611405	0.0004862
22-Apr	22:28	8.03	8.35	9.08	9.54	10.28	10.91	24.96	25.17	145	0.025	0.4441346	0.0004747
22-Apr	22:48	8.13	8.55	9.14	9.69	10.42	10.98	24.54	24.73	160	0.024	0.4448372	0.0005282
22-Apr	23:08	9.21	9.74	10.45	11.02	12.05	12.56	24.18	24.37	154	0.015	0.5490162	0.0002881
22-Apr	23:28	9.53	10.18	10.81	11.31	12.27	12.91	23.97	24.16	159	0.014	0.5187319	0.0005782
22-Apr	23:48	8.27	8.82	9.51	10.06	10.90	11.50	23.65	22.93	144	0.020	0.5419028	0.0001733
23-Apr	0:08	8.12	8.51	9.20	9.69	10.47	11.12	23.38	21.97	137	0.017	0.5090894	0.0002263
23-Apr	0:28	6.16	6.49	6.89	7.29	7.94	8.49	23.14	21.69	136	0.037	0.3918731	0.0002102
23-Apr	0:48	8.08	8.39	9.12	9.59	10.40	11.09	22.61	21.12	127	0.017	0.5115113	0.0002065
23-Apr	1:08	6.79	7.16	7.67	8.16	8.85	9.31	22.52	21.07	106	0.027	0.4497896	0.0001626
23-Apr	1:28	7.65	8.09	8.69	9.14	9.91	10.59	22.64	21.20	142	0.020	0.4837468	0.0002200
23-Apr	1:49	6.74	7.13	7.63	8.06	8.67	9.18	22.44	21.00	145	0.028	0.4208833	0.0002444
23-Apr	2:09	5.76	6.16	6.64	7.10	7.50	8.10	22.08	20.65	113	0.038	0.3906065	0.0001552
23-Apr	2:29	5.46	5.93	6.45	6.92	7.36	7.96	21.85	20.42	119	0.040	0.4188462	0.0000790
23-Apr	2:49	5.80	6.12	6.72	7.19	7.76	8.34	21.70	20.27	112	0.036	0.4384574	0.0000781
23-Apr	3:09	5.42	5.80	6.29	6.80	7.32	7.88	21.53	20.10	112	0.041	0.4213057	0.0000695
23-Apr	3:29	5.13	5.38	5.78	6.20	6.63	7.07	21.35	19.93	125	0.052	0.3473214	0.0001478
23-Apr	3:49	4.67	4.90	5.29	5.66	6.12	6.54	21.11	19.73	131	0.065	0.3348484	0.0001054
23-Apr	4:09	4.44	4.65	4.99	5.36	5.74	6.32	20.89	19.56	122	0.073	0.3066622	0.0001325
23-Apr	4:49	4.59	4.74	5.14	5.50	5.72	6.38	20.63	19.33	125	0.068	0.2878439	0.0002439
23-Apr	5:09	5.28	5.57	5.91	6.34	6.69	7.29	20.32	18.99	135	0.047	0.3261510	0.0002712
23-Apr	5:29	5.26	5.51	5.85	6.22	6.68	7.24	20.11	18.75	142	0.048	0.3255638	0.0002575
23-Apr	5:49	5.43	5.71	6.07	6.44	6.88	7.37	19.85	18.48	125	0.044	0.3300379	0.0002968
23-Apr	6:09	5.66	6.07	6.40	6.81	7.33	7.82	19.81	18.43	133	0.038	0.3640160	0.0002109
23-Apr	6:29	5.02	5.32	5.63	5.94	6.28	6.71	19.60	18.21	141	0.054	0.2903200	0.0004469

		Wind Speed						Temperatures		Wind			
Date	Time	U(0.75)	U(1.25)	U(2.07)	U(3.44)	U(5.72)	U(9.50)	TL1	TU1	Dir	Ri	U*	Zo
17-Apr	2:25	4.16	4.34	4.67	4.84	5.20		30.21	30.64	186	0.174	0.1617656	0.0100290
17-Apr	9:46	4.42	4.64	4.85	5.10	5.02		31.38	30.57	143	0.184	0.1882984	0.0060511
18-Apr	0:08	4.18	4.37	4.71	4.99	5.01		33.70	34.45	164	0.174	0.0663455	
18-Apr	0:28	4.55	4.74	5.12	5.37	5.45		33.28	33.90	183	0.149	0.1155480	
18-Apr	1:28	4.29	4.57	4.97	5.30	5.44		32.74	33.46	178	0.153	0.1763455	0.0062632
18-Apr	1:48	5.07	5.39	5.83	6.16	6.38		32.57	33.16	191	0.113	0.2245716	0.0032045
18-Apr	2:08	5.07	5.31	5.69	6.03	6.26		32.47	33.05	190	0.118	0.1948111	0.0119126
18-Apr	2:29	5.14	5.45	5.89	6.27	6.54		32.31	32.94	170	0.109	0.2416867	0.0018411
18-Apr	2:49	5.24	5.58	5.94	6.23	6.49		31.96	32.45	171	0.110	0.2101375	0.0084814
18-Apr	3:09	4.84	5.15	5.56	5.91	6.09		31.46	31.97	167	0.122	0.2181859	0.0027341
21-Apr	9:43	6.52	6.94	5.80	6.38	7.65	8.78	30.12	30.02	173	0.078	0.9091547	0.0000028
21-Apr	10:03	5.92	6.23	6.70	6.98	7.21	7.86	30.48	30.24	177	0.068	0.2806680	0.0019131
21-Apr	10:23	6.45	6.87	7.33	7.57	7.92	8.41	31.22	30.85	171	0.058	0.3081184	0.0018787
21-Apr	10:43	7.07	7.55	8.03	8.38	8.83	9.45	31.64	31.24	146	0.046	0.3625072	0.0010287
21-Apr	11:03	6.98	7.54	7.93	8.40	8.92	9.48	31.76	31.39	134	0.046	0.3921431	0.0005121
21-Apr	11:23	8.09	8.68	9.22	9.62	10.20	10.90	31.93	31.59	142	0.032	0.4246922	0.0008480
21-Apr	11:43	8.59	9.17	9.71	10.19	10.93	11.75	32.06	31.68	150	0.028	0.4691824	0.0005992
21-Apr	12:03	9.59	10.31	10.89	11.35	12.20	12.92	32.07	31.78	126	0.021	0.5122008	0.0007200
21-Apr	12:23	8.17	8.77	9.35	9.82	10.54	11.23	33.45	32.70	133	0.033	0.4844581	0.0003469
21-Apr	12:43	8.22	8.83	9.41	9.96	10.61	11.25	34.72	33.61	138	0.034	0.4995029	0.0002997
21-Apr	13:03	9.69	10.38	10.96	11.49	12.23	12.99	35.10	33.99	146	0.024	0.5221003	0.0007002
21-Apr	13:23	10.12	10.86	11.55	12.20	13.09	13.74	35.27	34.08	143	0.020	0.6094326	0.0003103
21-Apr	13:43	10.92	11.69	12.34	13.05	14.14	14.99	35.58	34.34	150	0.017	0.6556447	0.0003059
21-Apr	14:03	10.67	11.42	12.18	12.73	13.80	14.46	35.90	34.71	138	0.019	0.6358784	0.0003273
21-Apr	14:23	11.22	11.99	12.79	13.52	14.69	15.45	36.14	34.94	122	0.016	0.7073598	0.0002199
21-Apr	14:43	11.14	12.18	13.28	14.12	15.21	16.11	36.38	35.15	147	0.014	0.8298278	0.0000877
21-Apr	15:03	11.40	12.32	13.17	13.94	15.18	15.95	36.45	35.34	135	0.015	0.7605705	0.0001580
21-Apr	15:23	10.82	11.60	12.47	13.16	14.29	14.99	36.71	35.68	135	0.018	0.7052096	0.0001805
21-Apr	15:43	10.66	11.45	12.29	12.98	13.95	14.76	37.13	36.14	139	0.019	0.6711744	0.0002297
21-Apr	16:03	10.26	11.01	11.67	12.26	13.28	13.93	37.27	36.30	141	0.022	0.6096391	0.0003329
21-Apr	16:24	9.97	10.71	11.34	11.86	12.88	13.47	37.25	36.38	154	0.024	0.5839978	0.0003676
21-Apr	16:44	9.79	10.52	11.19	11.73	12.74	13.27	36.87	36.21	155	0.025	0.5898343	0.0003013
21-Apr	17:04	9.42	10.00	10.73	11.29	12.27	12.96	36.60	36.02	145	0.027	0.5792610	0.0002525
21-Apr	17:24	8.91	9.43	10.09	10.61	11.52	12.08	36.34	35.91	165	0.032	0.5293154	0.0003138
21-Apr	17:44	8.73	9.35	9.91	10.43	11.33	11.89	35.87	35.56	130	0.033	0.5156021	0.0003348
21-Apr	18:04	9.04	9.53	10.20	10.75	11.68	12.36	35.37	35.18	146	0.029	0.5302754	0.0003305
21-Apr	18:24	8.53	9.14	9.68	10.21	11.06	11.69	34.86	34.82	145	0.033	0.4877877	0.0004067
21-Apr	18:44	8.04	8.62	9.12	9.65	10.43	11.09	34.21	34.29	127	0.038	0.4562926	0.0004291
21-Apr	19:04	7.82	8.35	8.79	9.31	10.07	10.53	33.36	33.49	126	0.040	0.4277832	0.0005484
21-Apr	19:24	8.17	8.69	9.17	9.65	10.47	10.96	32.45	32.63	141	0.035	0.4352515	0.0006609
21-Apr	19:44	8.65	9.28	9.80	10.37	11.24	11.80	31.65	31.86	157	0.028	0.4900345	0.0004320
21-Apr	20:04	9.32	9.94	10.53	11.15	12.14	12.84	31.12	31.37	167	0.022	0.5373392	0.0003712
21-Apr	20:24	9.43	10.02	10.75	11.38	12.27	12.93	30.83	31.09	160	0.021	0.5479869	0.0003561
21-Apr	20:44	9.54	10.11	10.88	11.50	12.38	13.21	30.35	30.61	175	0.020	0.5503015	0.0003738
21-Apr	21:04	9.10	9.69	10.30	10.94	11.88	12.69	29.82	30.09	158	0.022	0.5319528	0.0003366
21-Apr	21:24	8.03	8.62	9.12	9.59	10.24	10.99	29.46	29.73	149	0.032	0.4135287	0.0009173
21-Apr	21:44	5.40	5.69	6.09	6.54	6.88	7.47	28.76	29.09	102	0.087	0.2778610	0.0008530
21-Apr	22:04	7.37	7.92	8.59	9.21	9.76	10.48	28.05	28.33	134	0.033	0.4667043	0.0002104
21-Apr	22:24	8.67	9.37	10.36	11.03	11.73	12.43	27.80	28.08	140	0.020	0.6064416	0.0001172
21-Apr	22:44	9.81	10.63	11.68	12.40	13.37	14.32	27.49	27.76	141	0.013	0.6944312	0.0001088
21-Apr	23:05	9.65	10.50	11.27	11.88	12.72	13.53	27.03	27.28	144	0.015	0.5858106	0.0002892
21-Apr	23:25	9.24	9.97	10.62	11.22	12.02	12.88	26.63	26.89	151	0.017	0.5280657	0.0004252
21-Apr	23:45	8.75	9.39	10.02	10.60	11.51	12.25	26.31	26.58	156	0.020	0.5238335	0.0002956
22-Apr	0:05	8.89	9.42	10.02	10.52	11.31	11.99	25.79	26.03	151	0.016	0.4603837	0.0008321
22-Apr	0:25	9.53	10.17	10.76	11.29	12.20	12.95	25.41	25.64	149	0.013	0.5044520	0.0007125
22-Apr	0:45	9.34	9.78	10.47	11.07	12.00	12.64	25.16	25.41	139	0.014	0.5183879	0.0004632
22-Apr	1:05	8.65	9.02	9.66	10.21	11.04	11.73	24.94	25.20	136	0.017	0.4660005	0.0005697
22-Apr	1:25	8.48	8.99	9.62	10.10	10.90	11.43	24.55	24.80	127	0.017	0.4611504	0.0005721
22-Apr	1:45	8.27	8.96	9.46	10.08	10.77	11.42	24.34	24.62	139	0.017	0.4719923	0.0004300
22-Apr	2:05	7.48	8.00	8.50	8.88	9.53	10.18	24.14	24.41	152	0.024	0.3808555	0.0009899
22-Apr	2:25	7.27	7.74	8.17	8.59	9.26	9.75	23.88	24.16	140	0.026	0.3691232	0.0009745
22-Apr	2:45	7.48	7.96	8.52	9.04	9.66	10.28	23.60	23.88	135	0.022	0.4158769	0.0004944
22-Apr	3:05	6.91	7.21	7.68	8.21	8.67	9.38	23.34	23.62	143	0.028	0.3413544	0.0011430
22-Apr	3:25	6.86	7.07	7.61	8.08	8.62	9.31	23.19	23.48	146	0.029	0.3446336	0.0009451
22-Apr	3:45	6.54	6.95	7.35	7.71	8.20	8.77	23.01	23.29	165	0.033	0.3044350	0.0020507
22-Apr	4:05	6.41	6.71	7.09	7.58	8.05	8.64	22.75	23.05	169	0.034	0.3099599	0.0013568
22-Apr	4:25	5.31	5.55	5.89	6.32	6.63	7.31	22.63	22.94	147	0.054	0.2444952	0.0020648
22-Apr	4:45	4.90	5.02	5.41	5.81	6.18	6.73	22.51	22.83	181	0.067	0.2412598	0.0010547
22-Apr	5:05	5.20	5.37	5.73	6.14	6.51	6.96	22.17	22.48	164	0.058	0.2444699	0.0016133

TRAIL CANYON
DATA FOR SOUTHERLY WINDS

		Wind Speed						Temperatures		Wind			
Date	Time	U(0.75)	U(1.25)	U(2.07)	U(3.44)	U(5.72)	U(9.50)	TL1	TU1	Dir	Ri	U*	Zo
1-Apr	21:10	4.42	4.67	4.98	5.27	5.58		29.26	29.69	142	0.198	0.1916323	0.0036910
1-Apr	22:10	4.83	5.13	5.42	5.74	6.17		27.67	28.05	153	0.156	0.2317599	0.0015043
1-Apr	22:30	4.78	5.03	5.37	5.69	6.04		27.10	27.46	176	0.157	0.2209859	0.0020473
1-Apr	22:51	4.42	4.57	4.90	5.19	5.49		26.70	27.05	161	0.195	0.1829474	0.0052019
1-Apr	23:31	4.32	4.54	4.71	5.09	5.40		26.70	27.12	164	0.208	0.1747226	0.0065303
1-Apr	23:51	5.11	5.36	5.62	6.04	6.36		26.47	26.86	162	0.137	0.2193088	0.0038595
2-Apr	0:51	5.27	5.58	5.82	6.25	6.69		24.91	25.27	147	0.085	0.2536034	0.0014209
2-Apr	1:11	5.49	5.76	6.08	6.53	6.97		24.47	24.79	155	0.077	0.2738575	0.0010390
2-Apr	1:31	6.22	6.52	6.86	7.37	7.87		23.96	24.24	165	0.059	0.3128982	0.0009685
2-Apr	1:51	6.15	6.55	6.96	7.37	7.89		23.44	23.69	157	0.059	0.3242921	0.0007314
2-Apr	2:11	5.31	5.60	5.88	6.28	6.66		23.19	23.49	162	0.080	0.2437753	0.0021669
2-Apr	2:31	5.60	5.88	6.25	6.65	7.10		23.22	23.56	145	0.072	0.2748378	0.0012120
2-Apr	2:51	4.86	5.07	5.36	5.71	6.06		23.16	23.50	146	0.098	0.2103163	0.0035113
2-Apr	3:51	4.04	4.20	4.36	4.73	4.97		22.53	22.95	161	0.144	0.1391149	0.0341249
2-Apr	4:31	4.03	4.23	4.48	4.82	5.09		22.21	22.59	173	0.138	0.1746607	0.0034787
2-Apr	8:32	4.01	4.26	4.50	4.82	5.02		21.89	21.67	140	0.147	0.2177922	0.0006440
2-Apr	9:12	4.04	4.24	4.45	4.76	4.94		23.41	22.73	121	0.162	0.2139431	0.0008174
2-Apr	9:32	4.24	4.45	4.64	4.97	5.08		23.87	23.25	153	0.151	0.2052216	0.0016991
2-Apr	9:52	4.20	4.40	4.62	4.94	5.15		24.50	23.53	140	0.158	0.2305487	0.0006322
2-Apr	10:12	4.16	4.39	4.53	4.85	5.00		25.05	24.02	144	0.169	0.2100314	0.0012732
10-Apr	16:42	6.01	6.49	6.90	7.27	7.79		42.35	41.30	124	0.122	0.3753914	0.0002582
10-Apr	17:02	6.11	6.65	7.04	7.56	8.16		42.37	41.38	125	0.113	0.4278222	0.0001245
10-Apr	17:22	6.14	6.65	7.14	7.62	8.24		42.02	41.43	100	0.110	0.4315207	0.0001188
10-Apr	17:42	6.28	6.82	7.24	7.69	8.31		41.70	41.67	111	0.108	0.3890529	0.0002452
10-Apr	18:02	6.12	6.63	7.13	7.59	8.14		41.34	41.36	100	0.111	0.3910786	0.0002020
10-Apr	18:22	5.74	6.23	6.61	7.06	7.47		41.11	41.21	139	0.130	0.3310670	0.0004069
10-Apr	18:42	5.31	5.71	6.05	6.43	6.82		40.72	40.89	145	0.160	0.2824920	0.0007139
10-Apr	19:02	5.20	5.55	5.80	6.14	6.51		39.84	40.08	128	0.175	0.2348743	0.0026703
10-Apr	20:22	4.39	4.68	4.96	5.27	5.54		36.72	37.18	127	0.238	0.1875285	0.0044086
10-Apr	20:43	5.09	5.40	5.68	6.08	6.39		36.51	36.96	126	0.170	0.2245337	0.0031878
10-Apr	21:03	4.78	5.07	5.33	5.67	5.93		35.95	36.37	138	0.199	0.1916282	0.0080833
10-Apr	21:23	5.22	5.55	5.88	6.26	6.57		35.76	36.18	152	0.158	0.2379194	0.0024429
10-Apr	21:43	4.89	5.24	5.57	5.90	6.24		35.49	35.91	171	0.181	0.2342536	0.0016292
10-Apr	22:03	4.92	5.24	5.65	5.98	6.21		35.11	35.59	189	0.175	0.2263202	0.0023058
10-Apr	22:23	4.74	5.02	5.41	5.74	5.98		34.75	35.28	183	0.192	0.2100750	0.0031038
10-Apr	23:03	4.10	4.32	4.66	4.99	5.15		34.42	35.04	155	0.271	0.1563707	0.0126643
10-Apr	23:23	4.01	4.20	4.51	4.75	5.05		33.85	34.41	166	0.304	0.1509594	0.0140712
15-Apr	0:37	4.19	4.37	4.72	4.97	5.00		30.99	31.54	153	0.164	0.0960803	
15-Apr	2:18	4.93	5.16	5.53	5.76	5.88		29.90	30.38	180	0.121	0.1451549	
15-Apr	2:38	5.66	6.02	6.42	6.73	6.99		29.82	30.23	172	0.088	0.2361117	0.0057946
15-Apr	2:58	6.14	6.50	6.99	7.36	7.73		29.51	29.89	188	0.073	0.2950516	0.0015644
15-Apr	3:18	6.14	6.56	7.06	7.47	7.69		29.32	29.70	171	0.071	0.2957975	0.0016038
15-Apr	3:38	5.64	5.97	6.43	6.75	6.99		29.05	29.44	174	0.087	0.2473721	0.0035444
15-Apr	3:58	5.63	6.02	6.53	6.82	7.11		28.82	29.21	156	0.085	0.2736072	0.0014961
15-Apr	4:18	5.23	5.48	5.88	6.16	6.40		28.55	28.93	161	0.104	0.2050830	0.0100343
15-Apr	4:38	5.73	6.08	6.54	6.82	7.21		28.66	29.05	163	0.085	0.2662752	0.0021011
15-Apr	4:58	4.46	4.63	4.98	5.25	5.52		28.34	28.74	173	0.145	0.1758713	0.0086981
15-Apr	5:18	4.05	4.20	4.53	4.77	4.96		28.02	28.44	179	0.177	0.1369392	0.0464951
15-Apr	15:00	4.11	4.36	4.52	4.71	4.67		37.16	35.60	110	0.282	0.1917531	0.0031837
15-Apr	15:20	4.26	4.51	4.69	4.94	5.00		37.32	35.82	108	0.256	0.2057314	0.0021027
15-Apr	15:40	4.04	4.25	4.39	4.59	4.58		37.29	35.98	136	0.305	0.1741571	0.0061989
15-Apr	16:00	4.07	4.28	4.47	4.73	4.69		37.55	36.21	131	0.288	0.1990056	0.0019138
15-Apr	22:01	4.06	4.27	4.55	4.86	5.08		32.88	33.23	167	0.272	0.1706078	0.0048671
15-Apr	22:41	4.43	4.64	4.92	5.15	5.40		32.59	32.98	151	0.237	0.1501037	0.0486980
15-Apr	23:01	4.26	4.48	4.76	5.06	5.33		32.28	32.70	182	0.247	0.1731008	0.0066928
15-Apr	23:21	4.82	5.08	5.42	5.73	5.89		31.83	32.20	178	0.181	0.1850771	0.0126900
15-Apr	23:41	4.09	4.30	4.58	4.81	4.90		31.26	31.62	161	0.276	0.1193529	
16-Apr	1:41	4.19	4.43	4.70	4.96	5.30		29.77	30.18	145	0.162	0.1788244	0.0042123
16-Apr	2:01	4.00	4.19	4.45	4.68	4.94		29.43	29.82	152	0.181	0.1414771	0.0287255
16-Apr	2:21	4.20	4.38	4.67	5.00	5.24		29.31	29.71	170	0.159	0.1716110	0.0060586
16-Apr	8:42	4.12	4.37	4.61	4.89	4.97		28.54	27.79	123	0.182	0.2108705	0.0011647
16-Apr	23:24	4.01	4.24	4.57	4.80	4.94		32.38	32.87	163	0.285	0.1352716	0.0530495
17-Apr	0:45	4.87	5.17	5.56	5.80	5.92		32.28	32.82	158	0.125	0.1667765	0.0467073
17-Apr	1:05	4.24	4.42	4.73	5.00	5.21		32.08	32.61	157	0.168	0.1390452	0.0679214
17-Apr	1:45	4.41	4.69	5.00	5.31	5.72		30.81	31.24	138	0.145	0.2232575	0.0009679
17-Apr	2:05	4.69	4.97	5.27	5.63	6.04		30.51	30.94	167	0.129	0.2338620	0.0010760

CONFIDENCE MILL
DATA FOR NORTHEASTERLY WINDS

		Wind Speeds						Temperatures		Wind			
Date	Time	U(0.75)	U(1.25)	U(2.07)	U(3.44)	U(5.72)	U9(.50)	TL1	TU1	Dir	Ri	U*	Zo
3-May	1:33	5.34	5.55	5.85	6.34	6.52	7.22	29.04	30.08	93	0.0434	0.25546066	0.0001994
3-May	1:53	4.00	4.19	4.50	4.91	5.08	5.68	28.84	30.23	37	0.0686	0.21444243	0.0000834
3-May	2:13	5.24	5.44	5.77	6.11	6.17	6.73	29.37	30.10	93	0.0531	0.19451393	
7-May	1:47	4.52	4.99	5.20	5.62	5.62	6.21	33.15	33.84	46	0.0384	0.22083935	0.0002243
7-May	2:07	4.19	4.57	4.78	5.23	5.25	6.00	32.05	32.79	100	0.0353	0.24022325	0.0000572
7-May	2:27	4.53	4.99	5.22	5.64	5.64	6.28	32.40	32.99	93	0.0322	0.23240476	0.0001474
7-May	2:47	4.34	4.77	4.99	5.39	5.32	5.91	32.22	32.74	45	0.0372	0.20723689	0.0002681
7-May	3:07	4.34	4.75	4.98	5.37	5.48	5.97	32.02	32.58	94	0.0363	0.216145	0.0001886
7-May	3:27	4.58	5.00	5.25	5.64	5.73	6.26	31.83	32.44	49	0.0362	0.22207464	0.0002344
7-May	3:47	4.73	5.22	5.45	5.88	5.96	6.52	31.79	32.41	42	0.0322	0.23850547	0.0001749
7-May	13:29	4.10	4.41	4.48	4.65	4.42	4.95	42.56	40.84	46	-0.2260		
7-May	13:49	4.32	4.73	4.83	5.03	4.67	5.35	42.84	41.15	46	-0.1507	0.22940424	0.0001083
8-May	1:31	4.48	4.84	5.13	5.62	5.72	6.34	32.93	34.24	46	0.0516	0.24087511	0.0000948
8-May	1:51	4.01	4.29	4.62	4.99	5.01	5.67	32.66	33.69	46	0.0538	0.21267008	0.0001009
8-May	2:31	5.04	5.42	5.67	6.06	6.10	6.59	32.66	33.34	47	0.0457	0.20173642	
9-May	5:15	4.73	5.23	5.49	5.89	5.83	6.44	31.12	31.49	91	0.0257	0.23284197	0.0002162
9-May	5:35	5.29	5.86	6.18	6.50	6.70	7.07	31.07	31.27	38	0.0179	0.25241198	0.0003038
9-May	5:55	5.34	5.86	6.22	6.54	6.71	7.09	30.99	31.13	94	0.0163	0.25094379	0.0003383
9-May	6:55	4.57	5.01	5.27	5.63	5.74	6.33	30.05	30.16	94	0.0151	0.24640186	0.0001000

DATA FOR SOUTHERLY WINDS

		Wind Speeds						Temperatures		Wind			
Date	Time	U(0.75)	U(1.25)	U(2.07)	U(3.44)	U(5.72)	U9(.50)	TL1	TU1	Dir	Ri	U*	Zo
3-May	2:33	4.77	4.95	5.20	5.62	5.71	6.31	28.86	29.61	120	0.0512	0.20447573	0.0004080
6-May	13:25	4.41	4.61	4.77	5.02	4.88	5.17	41.40	39.92	118	-0.2361	0.16216725	
6-May	17:46	4.28	4.55	4.68	4.95	4.84	5.17	43.39	42.20	115	-0.1325	0.16867372	
7-May	14:09	4.57	5.01	5.13	5.34	5.14	5.79	43.31	41.50	115	-0.1168	0.22783908	0.0001528
7-May	15:09	4.16	4.48	4.58	4.74	4.52	5.10	43.91	42.39	114	-0.1606	0.19264124	0.0002626
7-May	16:09	4.63	5.09	5.27	5.54	5.36	5.75	44.60	42.86	171	-0.1319	0.21571212	0.0003190
7-May	16:49	4.46	4.94	5.09	5.36	5.09	5.63	44.34	43.11	139	-0.0812	0.21856618	0.0001866
7-May	17:09	4.12	4.42	4.56	4.83	4.64	5.11	44.16	43.16	159	-0.0868	0.18171416	0.0004326
7-May	17:49	4.34	4.75	4.96	5.20	5.09	5.62	44.82	43.09	166	-0.1003	0.22780367	0.0001106
7-May	20:50	4.07	4.45	4.79	5.24	5.09	5.99	37.05	38.03	186	0.0369	0.25716653	0.0000228
7-May	21:10	5.63	6.42	6.86	7.32	7.46	8.13	37.30	37.99	180	0.0168	0.3505508	0.0000324
7-May	21:30	4.25	4.78	5.11	5.52	5.61	6.31	36.46	37.10	199	0.0237	0.27955014	0.0000206
8-May	15:13	4.62	4.86	4.99	5.21	5.06	5.58	43.39	41.88	127	-0.1518	0.18606862	0.0009704
8-May	15:33	4.19	4.42	4.52	4.74	4.43	4.99	43.94	42.31	148	-0.2387	0.19334117	0.0002517
8-May	15:53	4.23	4.43	4.57	4.75	4.55	5.10	43.55	42.20	147	-0.1631	0.17972632	0.0005328
8-May	16:13	5.37	5.85	6.09	6.37	6.24	6.66	44.17	42.51	154	-0.0944	0.23502493	0.0005468
8-May	16:33	5.28	5.66	5.98	6.23	6.02	6.46	44.12	42.47	122	-0.1120	0.22817422	0.0005822
8-May	16:53	5.64	6.01	6.27	6.61	6.48	6.94	43.51	42.23	129	-0.0679	0.23138609	0.0009097
8-May	17:13	5.57	5.88	6.11	6.41	6.21	6.64	43.17	42.18	143	-0.0726	0.19737501	
8-May	17:33	4.98	5.26	5.52	5.82	5.68	6.05	43.13	41.97	126	-0.0898	0.20058543	
8-May	17:53	5.06	5.34	5.56	5.90	5.61	6.12	43.55	42.00	160	-0.1283	0.21430285	0.0006207
8-May	18:13	5.45	5.80	6.11	6.48	6.32	6.79	42.84	41.44	164	-0.0720	0.24442641	0.0003896
8-May	18:33	4.56	4.83	5.14	5.44	5.32	5.78	42.37	41.10	165	-0.0766	0.22200531	0.0001861
8-May	18:53	4.83	5.14	5.46	5.80	5.69	6.23	41.23	40.64	154	-0.0202	0.23320385	0.0001871
8-May	19:13	4.33	4.57	4.84	5.19	5.18	5.64	40.11	40.13	195	0.0161	0.19070094	0.0003759
8-May	19:33	4.05	4.30	4.58	4.92	4.93	5.42	39.10	39.32	192	0.0272	0.19054189	0.0002104
8-May	20:13	4.53	4.82	5.16	5.52	5.52	6.17	37.58	37.97	204	0.0265	0.22641935	0.0001246
9-May	3:14	4.22	4.53	4.80	5.18	5.12	5.73	31.20	31.85	124	0.0474	0.19639735	0.0002326
9-May	6:15	4.10	4.46	4.69	5.02	5.09	5.73	30.23	30.43	103	0.0215	0.22326509	0.0000662
9-May	6:35	4.40	4.76	5.06	5.49	5.71	6.26	29.84	30.19	101	0.0215	0.26271262	0.0000346
9-May	12:56	5.02	5.58	5.73	6.04	5.77	6.26	38.21	35.82	151	-0.1532	0.24855015	0.0001893
9-May	13:16	5.64	6.31	6.61	6.99	6.91	7.27	37.22	35.32	133	-0.0688	0.29683764	0.0001220
9-May	13:36	5.76	6.39	6.70	7.06	6.93	7.30	36.43	35.01	150	-0.0542	0.27887938	0.0002317
9-May	13:56	5.39	5.86	6.18	6.50	6.58	6.84	36.42	34.97	150	-0.0627	0.26062012	0.0002265
9-May	14:16	5.81	6.44	6.77	7.11	7.01	7.42	36.45	34.91	150	-0.0548	0.28597592	0.0002016
9-May	14:36	4.85	5.30	5.55	5.83	5.67	6.05	35.65	34.44	182	-0.0731	0.2196029	0.0003968
9-May	14:56	4.66	5.06	5.31	5.61	5.49	5.79	36.80	35.18	162	-0.1189	0.21867529	0.0002985
9-May	15:16	6.08	6.69	7.08	7.40	7.46	7.82	37.20	35.44	163	-0.0549	0.30553915	0.0001692
9-May	15:36	6.60	7.28	7.74	8.10	8.19	8.48	37.00	35.35	187	-0.0436	0.33540647	0.0001553
9-May	15:56	8.40	9.16	9.73	10.19	10.39	10.69	36.74	35.04	182	-0.0304	0.40362011	0.0002354
9-May	16:16	9.88	10.75	11.43	11.87	12.20	12.61	35.33	33.86	178	-0.0179	0.46084101	0.0002960
9-May	16:36	10.58	11.51	11.67	12.85	13.34	13.83	34.57	32.95	179	-0.0103	0.55817562	0.0000922
9-May	16:56	11.20	12.03	8.65	13.54	14.12	14.59	33.32	31.66	189	-0.0057	1.4426424	0.0000004
9-May	17:17	11.78	12.57	12.86	14.12	14.70	15.24	32.79	30.83	165	-0.0031	0.5897093	0.0001280
9-May	17:37	11.41	12.13	10.66	13.86	14.41	15.00	32.54	29.83	175	-0.0030	0.8950907	0.0000042
9-May	17:57	12.11	12.66	13.49	14.51	15.21	15.76	31.39	28.96	171	0.0001	0.61096367	0.0001148
9-May	18:17	13.05	13.92	17.75	15.75	16.44	17.09	30.17	27.94	180	0.0031	1.02048475	0.0000056

NASA
National Aeronautics and Space Administration

Report Documentation Page

1. Report No.	2. Government Accession No.	3. Recipient's Catalog No.
NASA CR-4378		

4. Title and Subtitle	5. Report Date
Radar-Aeolian Roughness Project	June 1991
	6. Performing Organization Code

7. Author(s)	8. Performing Organization Report No.
R. Greeley, A. Dobrovolskis, L. Gaddis, J. Iversen, N. Lancaster, R. Leach, K. Rasnussen, S. Saunders, J. VanZyl, S. Wall, B. White, and H. Zebker	
	10. Work Unit No.

9. Performing Organization Name and Address	11. Contract or Grant No.
Department of Geology Arizona State University Tempe, AZ 85287-1404	NSG-7415
	13. Type of Report and Period Covered
12. Sponsoring Agency Name and Address	Contractor Report
Office of Space Science and Applications National Aeronautics and Space Administration Washington, DC 20546	14. Sponsoring Agency Code SL

15. Supplementary Notes

R. Greeley, L. Gaddis, and N. Lancaster: Arizona State University, Tempe, Arizona.
A. Dobrovolskis and R. Leach: Arizona State University, Tempe, Arizona (currently at Ames Research Center, Moffett Field, California).
J. Iverson: Department of Aerospace Engineering, Iowa State University, Ames, Iowa.
K. Rasnussen: Institute of Geology, Aarhus University, Aarhus C, Denmark.
S. Saunders, J. VanZyl, S. Wall, and H. Zebker: Jet Propulsion Laboratory, Pasadena, California.
B. White: Department of Mechanical Engineering, University of California, Davis, California.

16. Abstract

The objective of this project is to establish an empirical relationship between measurements of radar, aeolian, and surface roughness on a variety of natural surfaces and to understand the underlying physical causes. This relationship will form the basis for developing a predictive equation to derive aeolian roughness from radar backscatter.

This report gives results from investigations carried out in 1989 on the principal elements of the project, with separate sections on field studies, radar data analysis, laboratory simulations, and development of theory for planetary applications.

17. Key Words (Suggested by Author(s))	18. Distribution Statement
radar sand dust aeolian remote sensing	Unclassified - Unlimited Subject Category 91

19. Security Classif. (of this report)	20. Security Classif. (of this page)	21. No. of pages	22. Price
Unclassified	Unclassified	132	A07

NASA FORM 1626 OCT 86 Available from the National Technical Information Service, Springfield, VA 22161

NASA-Langley, 1991